MULTIPLE-INPUT MULTIPLE-OUTPUT WIRELESS SYSTEM DESIGNS WITH IMPERFECT CHANNEL KNOWLEDGE

by

Minhua Ding

A thesis submitted to the
Department of Electrical and Computer Engineering
in conformity with the requirements
for the degree of Doctor of Philosophy

Queen's University
Kingston, Ontario, Canada
July 2008

ABSTRACT

Employing multiple transmit and receive antennas for wireless transmissions opens up the opportunity to meet the demand of high-quality high-rate services envisioned for future wireless systems with minimum possible resources, e.g., spectrum, power and hardware.

Empowered by linear precoding and decoding, a spatially multiplexed multiple-input multiple-output (MIMO) system becomes a convenient framework to offer high data rate, diversity and interference management. While most of the current precoding/decoding designs have assumed perfect channel state information (CSI) at the receiver, and sometimes even at the transmitter, in this thesis we will design the precoder and decoder with imperfect CSI at both the transmit and the receive sides, and investigate the joint impact of channel estimation errors and channel correlation on system structure and performance. The mean-square error (MSE) related performance metrics will be used as the design criteria.

We begin with the minimum total MSE precoding/decoding design for a single-user MIMO system assuming imperfect CSI at both ends of the link. Here the CSI includes the channel estimate and channel correlation information. The closed-form optimum precoder and decoder are determined for the special case with no receive correlation. For the general case with correlation at both ends, the structures of the precoder and decoder are also determined. It is found that compared to the perfect CSI case, linear filters are added to the transceiver structure to balance the channel noise and the additional noise caused by imperfect channel estimation, which improve system robustness against imperfect CSI.

Furthermore, the effects of channel estimation error and channel correlation are coupled together, and are quantified by simulations.

With imperfect CSI at both ends, the exact capacity expression for a single-user MIMO channel is difficult to obtain. Instead, upper- and lower-bounds on capacity have been derived, and the lower-bound has been used for system design. The closed-form transmit covariance matrix for the lower-bound has not been found in literature, which is referred to as the maximum mutual information design problem with imperfect CSI. Here we transform the transmitter design into a joint precoding/decoding design problem. The closed-form optimum transmit covariance matrix is then derived for the special case with no receive correlation, whereas for the general case with non-trivial correlation at both ends, the optimum structure of the transmit covariance matrix is determined. The close relationship between the maximum mutual information design and the minimum total MSE design is discovered assuming imperfect CSI. The tightness and accuracy of the capacity lower-bound is evaluated by simulation. The impact of imperfect CSI on single-user MIMO ergodic channel capacity is also assessed.

For robust multiuser MIMO communications, minimum average sum MSE transceiver (precoder-decoder pairs) design problems are formulated for both the uplink and the downlink, assuming imperfect channel estimation and channel correlation at the base station (BS). We propose improved iterative algorithms based on the associated Karush-Kuhn-Tucker (KKT) conditions. Under the assumption of imperfect CSI, an uplink–downlink duality in average sum MSE is proved, which is often used to simplify the more involved downlink design. As an alternative for solving the uplink problem, a sequential semidefinite programming (SDP) method is proposed. Simulations are provided to corroborate the analysis and assess the impacts of channel estimation errors and channel correlation at the base station on both the uplink and the downlink system performances.

Acknowledgments

Foremost, I would like to thank my advisor, Prof. Steven D. Blostein, for his guidance, patience, and full support during the past five years. I am grateful to him for his encouragement and patience, especially during the time I needed these most. I am constantly surprised by his technical intuition, and I hope I have learned a bit from him in the way of thinking and carrying out research.

I also want to thank the thesis committee members, Prof. Wei Yu from University of Toronto, Prof. Glen Takahara from Dept. of Mathematics and Statistics, Prof. Il-Min Kim, and Prof. Prof. Alois P. Freundorfer for their taking time to review my thesis.

The kind help received at the early stage of the thesis research from Prof. Norman Rice of Dept. of Mathematics and Statistics is deeply appreciated.

I would like to express sincere thanks to all my lab colleagues, past and present, with whom I have worked and shared my life. They are: Lucien Benacem, Yu Cao, Luis Gurrieri, Leon Lee, Guangping Li, Patrick Li, Hani Mehrpouyan, Wei Sheng, Constantin Siriteanu, Yi Song, Edmund Tam, Neng Wang, Jinsong Wu, and Yi Zheng. I want to thank Yu Cao for many helpful discussions with respect to my thesis, as well as for numerous lifts I received from him. My thanks go to Constantin Siriteanu for reviewing the thesis draft and for his encouragement over these years.

My life here has been an enjoyable journey due to all my friends and all the kind people I have met, at Queen's or outside Queen's. Their characters have enriched my own. In

particular, I want to thank Bei Cai from Dept. of Physics at Queen's for her great friendship.

Last, but not the least, I want to thank all my family members in China, my parents, my sister, and Weilong Qu, for their support.

Contents

List of Tables

List of Figures

Acronyms

ABER	Average Bit Error Rate
AWGN	Additive White Gaussian Noise
BC	Broadcast Channel
BER	Bit Error Rate
BLAST	Bell Laboratories Layered Space-Time
BS	Base Station
CCI	Channel Correlation Information
CDMA	Code Division Multiple Access
CLB	Capacity Lower-Bound
CMI	Channel Mean Information
CSI	Channel State Information
CSIR	Channel State Information at Receiver
CSIT	Channel State Information at Transmitter
CUB	Capacity Upper-Bound
DSL	Digital Subscriber Line
EVD	Eigenvalue Decomposition
i.i.d.	independent and identically-distributed
KKT	Karush-Kuhn-Tucker
LAN	Local Area Network

LMMSE	Linear Minimum Mean-Square Error
MAC	Multiple Access Channel
MIMO	Multiple-Input Multiple-Output
ML	Maximum-Likelihood
MMSE	Minimum Mean-Square Error
MS	Mobile Station
MSE	Mean-Square Error
MSMSE	Minimum Sum Mean-Square Error
OSTBC	Orthogonal Space-Time Block Code
QAM	Quadrature Amplitude Modulation
QoS	Quality of Service
SDP	Semidefinite Programming (Program)
SIC	Successive Interference Cancelation
SINR	Signal-to-Interference-plus-Noise Ratio
SISO	Single-Input Single-Output
SNR	Signal-to-Noise Ratio
STBC	Space-Time Block Code
STTC	Space-Time Trellis Code
SVD	Singular Value Decomposition
TDD	Time-Division Duplex
ZF	Zero-Forcing

List of Important Symbols

$\stackrel{\text{def}}{=}$	Defined as
$\otimes$	Kronecker product
$(\cdot)^T$	Matrix or vector transpose
$(\cdot)^*$	Complex conjugate
$(\cdot)^H$	Matrix or vector conjugate transpose (Hermitian)
$\|x\|$	Absolute value (modulus) of the scalar x
$\det(\cdot)$	Determinant of a matrix
$\log_2(\cdot)$	Logarithm with base 2
$\ln(\cdot)$	Natural logarithm
$\text{diag}(\mathbf{x})$	Diagonal matrix with diagonal entries given by $\mathbf{x}$
$\mathbb{E}(\cdot)$	Expectation of random variables
$\mathbf{I}_m$	Identity matrix of size $m \times m$
$\mathfrak{I}(\cdot)$	Imaginary part of a complex-valued scalar, vector or matrix
n_T	Number of transmit antennas in a single-user MIMO link
n_R	Number of receive antennas in a single-user MIMO link
$\mathfrak{R}(\cdot)$	Real part of a complex-valued scalar, vector or matrix
$\text{tr}(\cdot)$	Trace of a matrix
$vec(\cdot)$	Vectorization operator
$\mathcal{N}_c(\cdot,\cdot)$	Circularly symmetric complex Gaussian distribution

$\min(a,b)$	Minimum of (a,b)
$\max(a,b)$	Maximum of (a,b)
$(a)_+$	$\max(a,0)$
$\{a_i\}_{i=1}^K$	$\{a_1,a_2,\ldots,a_K\}$
$\| \mathbf{x} \|$	Euclidean norm of a vector
$\mathbf{A} \succeq \mathbf{B}$	$\mathbf{A}-\mathbf{B}$ is positive semidefinite, also denoted as $\mathbf{B} \preceq \mathbf{A}$
$\mathbf{A} \succ \mathbf{B}$	$\mathbf{A}-\mathbf{B}$ is positive definite, also denoted as $\mathbf{B} \prec \mathbf{A}$

Chapter 1

Introduction

1.1 MIMO Systems for Future Wireless Communications

The goal of future wireless communications systems is to provide a wide variety of high-quality high-rate services with minimum requirements on spectrum, power consumption and hardware complexity. Toward this end, proper system structures as well as robust system designs are required to meet the challenges in wireless transmissions, such as multipath fading, limited spectrum resource, and interference. Recent research results have unveiled the multiple-input multiple-output (MIMO) system as a potential candidate to play a key role in future wireless [74].

A MIMO wireless system is commonly deployed by using multiple transmit and receive antennas. Early work on multi-antenna systems involves the use of antenna arrays at the receiver to provide spatial diversity against the random destructive effect of fading [9,42,78, 81]. There is a recent rich literature on employing multiple antennas at the transmitter and achieving diversity through space-time coding when there is no channel state information at the transmitter (CSIT) [2,41,99–101,116], or through transmit beamforming when there is perfect CSIT [56]. Clearly, a MIMO system can be designed to fully exploit the transmit

and receive spatial diversity provided by the channel. The improvement in reliability of a MIMO system compared to that of a traditional single-input single-output (SISO) system is typically quantified by the diversity gain and the coding gain [53].

The use of multiple transmit and receive antennas also opens up the spatial domain for boosting data rate. While a flat-fading SISO Gaussian channel provides only a single narrow data pipe, a coherent MIMO channel can be represented as a set of parallel Gaussian channels and thus creates multiple data pipes for data transmission *without additional power or spectrum* [26, 28, 29, 102], an appealing feature to cope with the scarcity of wireless spectrum and the stringent power constraint on terminals. In particular, the ergodic (Shannon) capacity of a coherent MIMO channel scales linearly with the minimum of (n_T, n_R) [denoted as $\min(n_T, n_R)$] in a rich-scattering spatially white environment, where n_T and n_R are the numbers of the transmit and receive antennas, respectively [29, 102]. The gain in terms of ergodic capacity achieved by a coherent MIMO channel over that of a SISO channel is termed the spatial multiplexing gain [129], which can be reaped using the Bell Laboratories Layered Space-Time (BLAST) architecture [26, 27, 117].

Interestingly, MIMO spatial multiplexing systems harness the randomness of the channel, whereas MIMO space-time coded systems combat it [104]. Although both spatial multiplexing and diversity gains can be simultaneously achieved by a MIMO system, there is a basic tradeoff between them [129].

For applications such as in wireless local area network (LAN) as well as in cellular communications, MIMO systems will likely be set up in a multiuser environment, where a multi-antenna base station (BS) simultaneously communicates with several multi-antenna mobile stations (MSs). There are two basic multiuser channels here. One is the multiple-access channel (MAC), also known as the uplink or the many-to-one channel [17, 24].

The other is the broadcast channel (BC), also referred to as the downlink or the one-to-many channel [16, 17]. Recent results from information-theoretic studies have completely characterized the capacity regions of the coherent Gaussian MIMO MAC [31, 54, 124] and BC [11, 107, 115, 123]. It has been found that in a multiuser environment, the use of multiple antennas introduces more flexibility to deal with the multiuser interference and enables simultaneous high-rate, multiuser communications, besides providing spatial multiplexing and diversity gains [104]. Similar to the single-user case, there is a tradeoff among the capabilities of spatial multiplexing, diversity and interference management in multiuser MIMO systems [105].

Thus, MIMO systems have been established as a promising transmission structure to achieve the goal of future wireless systems.

1.2 MIMO System Designs and Channel Knowledge

The promise of a high performance return from using MIMO systems largely relies on the assumption of perfect coherent reception, i.e., perfect channel state information at the receiver (CSIR), and even perfect CSIT with some designs.

In practice, however, perfect coherent reception (perfect CSIR) is unattainable due to channel estimation errors. Consequently, it is necessary to design a system robust to imperfect CSIR.

Some popular MIMO systems, such as space-time coded systems and the BLAST architecture, have considered no CSIT, whereas others, e.g., transmit beamforming [3, 56] or generalized beamforming systems [85, 87, 120], have assumed perfect CSIT. Practical situations indicate that some forms of *partial* CSIT can be available [68, 109]. For example, partial CSIT can be acquired by transferring the CSIR to the transmitter via a feedback

link. Feedback is not an uncommon feature and it is present in most wireless systems, e.g., the power control channel in Code Division Multiple Access (CDMA) systems. If a system operates in the time-division duplex (TDD) mode, the transmitter can infer the CSI by measuring its received signal based on the reciprocity of wireless channels. CSIT obtained this way is usually imperfect due to channel estimation errors, erroneous CSIR, and/or limitation of the feedback link. However incomplete, CSIT, if efficiently used, can yield considerable performance gain in both space-time coded [44, 130, 131] and spatially-multiplexed systems [40], as opposed to the case of no CSIT. Therefore, intelligent MIMO systems designs must exploit the available CSIT.

The uncertainty in CSI can be modeled and dealt with in two different ways. One way is to model the error in channel knowledge as unknown but deterministic and bounded in a certain region. Worst-case optimizations are then employed to guarantee a (certain) minimum reliability level [33, 72, 111] [69, Chapter 7]. However, a worst-case design is rather conservative, since the worst case usually occurs with low probability [112]. Thus, an alternative way, which models the uncertainty by its first-order and second-order statistics [30, 31, 40, 44, 68, 109, 130, 131], is of particular interest and has been widely adopted. A design based on statistical channel information is called a stochastic robust design [69, Chapter 7].

As far as statistical uncertainty models are concerned, the channel mean information (CMI) and channel correlation information (CCI), obtained from channel estimation and propagation geometry measurement, respectively, are extensively used [31]. The CMI and CCI can be conveniently exploited using precoding or joint precoding and decoding. In particular, linear precoding/decoding is often preferred, due to the complexity constraint, especially for mobile terminals.

To make statistical CSI available at the transmitter, feedback is required, albeit infrequent in slow-fading channels. If the feedback link is bandwidth-constrained, it will be more appropriate to employ limited-feedback designs [6, 55, 57, 58, 65, 118]. Nevertheless, the general stochastic robust designs usually lead to solutions that clearly describe system structures, and thus provide direct information on how impairments such as erroneous channel estimation and channel correlation affect system performance. The results from the general designs are also helpful in identifying key channel parameters that should be quantized and transferred back to the transmitter, as well as in assessing the performance of limited-feedback designs. Therefore, it is of great importance to study MIMO system designs with uncertain CSI modeled statistically.

1.3 Motivation and Thesis Overview

With proper linear precoder designs or joint linear precoder-decoder designs, a spatial multiplexing system becomes a convenient framework to improve data rates, enhance link reliability as well as offer a flexible diversity-multiplexing tradeoff for both single-user and multiuser MIMO communications. The joint precoder-decoder design is also known as (joint) transceiver optimization.

For single-user MIMO systems, various performance measures have been considered as the precoder design or joint design criteria, e.g., minimum total mean-square error (MSE) from all data streams [87, 120], minimum weighted MSE [85], maximum mutual information (capacity) [85, 87, 102], minimum Euclidean distance between received signal points [14], and minimum bit error rate (BER) [113, 119]. A comprehensive study of joint precoder-decoder designs under the MSE-based, the signal-to-interference-plus-noise-ratio (SINR)-based, or the BER-based criteria has been presented in [70].

Among the above performance measures, the MSE-related design criteria are of particular interest to us. The minimum total MSE criterion aims at minimizing the trace of a MSE matrix, and balances interference and noise suppression. In addition, minimum sum MSE linear precoding and decoding designs have been applied to multiuser MIMO systems [45, 91, 125]. The maximum mutual information design is also a MSE-related design, since it is equivalent to minimizing the determinant of the MSE matrix [87]. Although the minimum total (sum) MSE criterion does not account for the fairness among data streams (users), it generally leads to tractable analysis and overall good performance.

Most previous work on linear precoder designs or joint linear precoder and decoder designs for single-user MIMO spatial multiplexing systems has assumed perfect CSIR. Only a few studies have considered imperfect CSI at both ends, but these have not considered the effect of channel estimation error when coupled with channel transmit and/or receive correlation. Since these two impairments often coexist, it is important to investigate their joint impacts. Similar observations also apply to existing multiuser MIMO system designs.

In this thesis, we will employ the spatial multiplexing framework with joint linear precoding and decoding for both single-user and multiuser communications in slow, Rayleigh flat-fading MIMO channels. We optimize the transceiver using the MSE-related design criteria. In the single-user case, the imperfect channel estimate as well as both transmit and receive correlation is assumed to be known to both ends of the link. In a multiuser scenario, we consider both channel estimation errors and channel correlation at the BS.

Note that the generic MIMO system model subsumes many other communication channels, e.g., a bundle of twisted pairs in Digital Subscriber Line (DSL) or a frequency-selective channel with transmit and receive filterbanks [70, 80, 85, 86]. Therefore, by considering narrow-band (flat-fading) channels does not necessarily limit our results for other channel conditions and system applications.

In Chapter 2, we briefly introduce basic MIMO communications in slow flat fading. The MIMO channel model used in this thesis is described. Single-user and multiuser MIMO systems with linear precoding and decoding are introduced here.

In Chapter 3, we study the joint linear precoding/decoding design to minimize total MSE from all data streams in a single-user MIMO system, under the assumption of imperfect CSI at both ends. A detailed channel estimation method is introduced, which presents the specific CSI assumptions used thereafter. The minimum total MSE design is formulated as a non-convex optimization problem subject to a total transmit power constraint. The closed-form optimum precoder and decoder are derived for the special with no receive correlation. The optimum transceiver structure for the general case is also determined. Based on the optimum transceiver pair, we investigate the effects of channel estimation error and channel correlation on system structure and average BER performance.

In Chapter 4, we consider maximum mutual information design for a single-user MIMO system under the same CSI assumption as described in Chapter 3. With the assumed CSI, exact capacity expressions are difficult to determine. Instead, tight upper- and lower-bounds on the mutual information are employed for system design. While a capacity lower-bound has been formulated previously, the closed-form optimum transmit covariance matrix remains to be determined, subject to a total transmit power constraint. This is known as the maximum mutual information design, or the capacity lower-bound problem, in the case of imperfect CSI. We relate this problem to that of minimizing the log determinant of the MSE matrix, which is a non-convex problem. We then derive the structure of the optimum transmit covariance matrix by solving this new non-convex problem using the same methodology as in Chapter 3. Through this approach, the relationship between the minimum total MSE design and the maximum mutual information design is also unveiled under the assumption of imperfect CSI. Using Monte Carlo simulations, we examine the tightness

of the ergodic capacity bounds and investigate the effects of channel estimation error and channel correlation.

Chapter 5 focuses on the joint linear precoder/decoder designs to minimize the sum MSE in multiuser MIMO systems. Both the uplink and the downlink are considered. Under similar CSI assumptions as in Chapter 3, we formulate the uplink and downlink minimum average sum MSE transceiver optimization problems. We extend and improve previous Karush-Kuhn-Tucker(KKT)-conditions-based algorithms so that they can be used in our case with reduced complexity. A duality in the average sum MSE between the uplink and the downlink is proved. For the uplink optimization, we also propose a sequential semidefinite programming (SDP) method. Based on optimized transceiver pairs, the effects of channel estimation errors and channel correlation at the BS are assessed.

Chapter 6 concludes this thesis and suggests future work.

1.4 Thesis Contributions

The primary contributions of this thesis are briefly summarized below:

- The minimum total MSE design is studied with imperfect CSI at both ends of a single-user MIMO link. Both channel estimation error and channel correlation are considered. Optimum structures of the linear precoder and decoder are derived. Our results gracefully fit those in the literature as channel estimation error diminishes. Based on analytical and simulation results, the impact of channel estimation error as well as the effect of transmit and receive correlation is assessed.

- When CSI is imperfect at both ends of a single-user MIMO link, the maximum mutual information design relies on a tight lower-bound on capacity. Previously, a numerical search method has been employed to find the optimum transmit covariance

matrix for this lower-bound. Here, the expression for the optimum transmit covariance matrix is determined by using a novel approach which solves an equivalent problem. The analytic solution clearly describes the transmitter structure. The accuracy of using the optimum transmit covariance matrix is shown by comparing it with the uniform power allocation strategy. The effect of imperfect CSI on the ergodic capacity is also investigated.

- Under the imperfect CSI assumption, the relationship between the minimum total MSE design and the maximum mutual information design is discovered. Interestingly, analogous to the perfect CSI case, the two share the same transmitter structure and differ mainly in power allocation with imperfect CSI. Alternatively, the two designs (under imperfect CSI) are connected through the minimum weighted MSE design. Therefore, our results provide a new perspective of the connection between two important quantities in estimation theory and information theory, i.e., the MSE from data estimation and the mutual information between channel input and output.

- Minimum average sum MSE transceiver optimization problems are formulated for multiuser MIMO uplink and downlink considering channel estimation errors and channel correlation at the BS. A duality in average sum MSEs for both links is proved theoretically. Unlike previous methods to prove duality, our method is solely based on the associated Karush-Kuhn-Tucker (KKT) conditions, and thus provides insight into the relation between the dual links. Improved KKT-conditions-based iterative algorithms are proposed for both links. For the uplink optimization, we also propose a sequential SDP method. Effects of imperfect CSI are evaluated by computer simulations.

Chapter 2

Background

2.1 Single-user MIMO Communications over Flat-fading Wireless Channels

2.1.1 MIMO Channel Model and System Model

Consider a wireless communication system with n_T antennas at the transmitter and n_R antennas at the receiver (see Fig. 2.1) [53]. In a flat-fading channel, each signal path is represented by a random complex fading coefficient (channel gain) [78, 81], so that the MIMO channel in Fig. 2.1 is conveniently described by a matrix $\mathbf{H}$, with its (j,i)-th element $h_{j,i}$ denoting the channel gain from transmit antenna i to receive antenna j, $i = 1,\ldots,n_T$, $j = 1,\ldots,n_R$:

$$\mathbf{H} = \begin{pmatrix} h_{1,1} & \ldots & h_{1,n_T} \\ \ldots & \ldots & \ldots \\ h_{n_R,1} & \ldots & h_{n_R,n_T} \end{pmatrix}.$$

The random channel gains are modeled by circularly symmetric complex Gaussian random variables [78,81], denoted as $h_{j,i} \sim \mathcal{N}_c(m_h^{j,i}, 1)$, $\forall i, j$. If the mean of the channel gain ($m_h^{j,i}$)

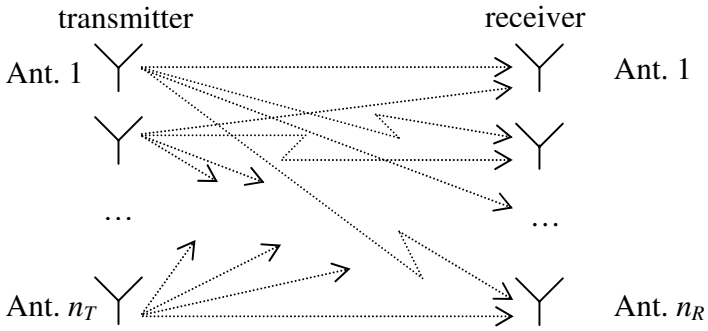

Figure 2.1. A single-user (point-to-point) wireless channel with multiple transmit and receive antennas.

is non-zero, the channel is said to undergo Ricean fading. If $m_h^{j,i} = 0$, the channel undergoes Rayleigh fading. Note that the settings in this thesis are for Rayleigh fading channels.

A Rayleigh fading MIMO channel is said to be spatially white if $\mathbb{E}(h_{j,i}h_{n,m}^*) = 0, i,m = 1,\ldots,n_T, j,n = 1,\ldots,n_R, i \neq m, j \neq n,$ and is denoted by $\mathbf{H}_w$. Here we have used $\mathbb{E}(\cdot)$ to denote the expectation of a random variable. Note that

$$\mathbf{h}_w \stackrel{\text{def}}{=} vec(\mathbf{H}_w) \sim \mathcal{N}_c(0, \mathbf{I}_{n_R \times n_T}),$$

where *vec* denotes the vectorization operation, and $\mathbf{I}_m$ denotes the $m \times m$ identity matrix. When there is spatial correlation, the following nonparametric channel model is commonly used [25, 95]:

$$\mathbf{H} = \mathbf{R}_R^{\frac{1}{2}} \mathbf{H}_w \mathbf{R}_T^{\frac{1}{2}}, \tag{2.1}$$

where $\mathbf{R}_T$ ($n_T \times n_T$) and $\mathbf{R}_R$ ($n_R \times n_R$) denote the transmit and receive correlation matrices, respectively. Thus [53],

$$\mathbf{h} \stackrel{\text{def}}{=} vec(\mathbf{H}) = (\mathbf{R}_T^{\frac{T}{2}} \otimes \mathbf{R}_R^{\frac{1}{2}})\, \mathbf{h}_w \sim \mathcal{N}_c(0, \mathbf{R}_T^T \otimes \mathbf{R}_R), \tag{2.2}$$

where $\otimes$ denotes Kronecker product, and the identity $vec(\mathbf{ABC}) = (\mathbf{C}^T \otimes \mathbf{A})vec(\mathbf{B})$ has been used [10, Table II, T2.13] (Note that this identity holds for complex matrices).

In practical downlink channels, the mobile is likely to be surrounded by a large number of local scatterers. The BS antennas, on the other hand, are often situated at high enough elevation to limit scattering and thus channels arising from the transmit antennas (in the downlink) are correlated. In this case,

$$\mathbf{H} = \mathbf{H}_w \, \mathbf{R}_T^{\frac{1}{2}}. \tag{2.3}$$

For an urban transmission environment, the exponential model has been proposed for transmit and receive correlation [12,30]. This means that the (j,i)-th element of $\mathbf{R}_T$ is given by $\rho_T^{|j-i|}$ for $i, j \in \{1,\ldots,n_T\}$, where ρ_T represents the real-valued transmit correlation for signals on adjacent antennas. The receive correlation matrix $\mathbf{R}_R$ is similarly defined with ρ_T replaced by ρ_R and with the indices ranging from 1 to n_R. In subsequent chapters, the exponential correlation model will be used for Monte Carlo simulations. However, it should be noted that our analytical results can be applied to any correlation model.

At a specific time slot, the received signal at antenna j is given by

$$y_j = \sum_{i=1}^{n_T} h_{j,i} x_i + n_j, j = 1,\ldots,n_R,$$

or, in a vector form,

$$\mathbf{y} = \mathbf{H}\mathbf{x} + \mathbf{n}, \tag{2.4}$$

where $\mathbf{y} = [y_1,\ldots,y_{n_R}]^T$, $\mathbf{n} = [n_1,\ldots,n_{n_R}]^T$ and $\mathbf{x} = [x_1,\ldots,x_{n_T}]^T$ are the received signal vector, the noise vector and the transmitter signal vector, respectively. The noise vector $\mathbf{n}$ is assumed to be spatially white and is distributed as $\mathbf{n} \sim \mathcal{N}_c(0, \sigma_n^2 \cdot \mathbf{I}_{n_R})$.

Further, consider the transmission of a $n_T \times N$ signal matrix composed of N data vectors, $\mathbf{X} = [\mathbf{x}^{t_1},\ldots,\mathbf{x}^{t_N}]$, over N consecutive time slots. In a slow-fading channel, it is often assumed that the channel matrix is constant over a block of N time slots, i.e.,

$$\mathbf{H}^{t_1} = \mathbf{H}^{t_2} = \ldots = \mathbf{H}^{t_N} = \mathbf{H}.$$

Then,

$$\mathbf{Y} = \mathbf{H}\mathbf{X} + \mathbf{N},$$

where $\mathbf{Y}$ and $\mathbf{N}$ denote the received signal matrix and the noise matrix, respectively, $\mathbf{Y} = [\mathbf{y}^{t_1}, \ldots, \mathbf{y}^{t_N}]$ and $\mathbf{N} = [\mathbf{n}^{t_1}, \ldots, \mathbf{n}^{t_N}]$. An equivalent vector signal model here is given by [53]

$$vec(\mathbf{Y}) = (\mathbf{X}^T \otimes \mathbf{I}_{n_R})\, \mathbf{h} + vec(\mathbf{N}).$$

2.1.2 Space-Time Coding for MIMO Systems

For slow-fading narrow-band transmissions, space-time coding is an important technique to extract the spatial diversity provided by the MIMO channel [2, 41, 99–101]. Block transmission is often assumed, as described in Subsection 2.1.1. Here $\mathbf{X}$ is referred to as the codeword matrix and is carefully designed with added redundancy. Two basic space-time codes, the space-time block code (STBC) and space-time trellis code (STTC), have been extensively studied. The orthogonal STBC (OSTBC) and the quasi-orthogonal STBC are two popular STBCs. In particular, the OSTBC is capable of providing full diversity gain $(n_R n_T)$ of the rich-scattering channel with low decoding complexity. Below is an example of the OSTBC with $n_T = N = 2$ (also known as the Alamouti code [2]):

$$\mathbf{X} = \begin{pmatrix} x_1 & -x_2^* \\ x_2 & x_1^* \end{pmatrix}.$$

At each time slot, a column of the codeword matrix is transmitted across different antennas. At the end of a block, the receiver employs maximum-likelihood (ML) decoding to separate different transmitted symbols contained in a codeword.

In the design of a space-time code, several factors are considered: the diversity gain, the coding gain, the decoding complexity, the decoding delay (related to the block length N), and the symbol rate (defined as the ratio of the number of different symbols in a codeword and the block length N; 1 for the Alamouti code).

2.1.3 Spatial Multiplexing

In contrast to the space-time coded system, a spatially multiplexed system transmits different signal vectors across the transmit antennas at different time slots, as described by (2.4). At the receiver, to minimize the error probability, ML detection should be employed. The problem with ML detection is its high complexity, which motivates the use of suboptimum detection schemes. Linear detection methods, such as the zero-forcing (ZF) and minimum MSE (MMSE), are widely used. The non-linear detectors, such as ZF detection with successive interference cancelation (ZF-SIC) and MMSE detection with SIC (MMSE-SIC), generally provide improved performance at the cost of increased complexity [53, 75].

2.1.4 Capacity of Coherent MIMO Channels in Flat Fading

Consider a Gaussian MIMO channel whose input-output relationship is given by (2.4). In coherent communications, the channel $\mathbf{H}$ is perfectly known at the receiver. Given $\mathbf{H}$, the capacity is expressed as [102]

$$C(\mathbf{H}) = \max_{p(\mathbf{x})} I(\mathbf{x};\mathbf{y}) = \max_{\substack{\mathbf{Q}\succeq 0 \\ \mathrm{tr}\{\mathbf{Q}\}\le P_T}} \log_2 \det\left[\mathbf{I}_{n_R} + \frac{1}{\sigma_n^2}\mathbf{H}\mathbf{Q}\mathbf{H}^H\right] \quad (\text{bits/channel use}),$$

where $p(\mathbf{x})$ denotes the input distribution, $I(\cdot\,;\,\cdot)$ denotes the mutual information between channel input and channel output, P_T is the total transmit power, and $\mathbf{Q} \stackrel{\text{def}}{=} \mathbb{E}(\mathbf{x}\mathbf{x}^H)$ is the transmit signal covariance matrix. $\mathbf{Q} \succeq 0$ means that $\mathbf{Q}$ is positive semidefinite. Here the transmitted signal vector is assumed to be zero-mean.

If the channel is unknown to the transmitter, uniform power allocation is used at the transmitter, i.e., $\mathbf{Q} = \frac{P_T}{n_T}\mathbf{I}_{n_T}$, and

$$C_{uni}(\mathbf{H}) = \log_2 \det\left[\mathbf{I}_{n_R} + \frac{P_T}{n_T\sigma_n^2}\mathbf{H}\mathbf{H}^H\right].$$

On the other hand, if the channel is perfectly known at the transmitter, the matrix channel can be decoupled into a set of parallel scalar Gaussian channels by means of singular value

decomposition (SVD) [37]. Specifically, let $\check{r} = \text{rank}(\mathbf{H})$ and let $\mathbf{H}$ be represented by its SVD:

$$\mathbf{H} = \check{\mathbf{U}}\,\check{\mathbf{\Lambda}}^{\frac{1}{2}}\,\check{\mathbf{V}}^H,$$

where $\check{\mathbf{U}}$, $\check{\mathbf{\Lambda}}$ and $\check{\mathbf{V}}$ are $n_R \times \check{r}$, $\check{r} \times \check{r}$ and $n_T \times \check{r}$ matrices, respectively. $\check{\mathbf{\Lambda}} = \text{diag}(\check{\lambda}_1, \ldots, \check{\lambda}_{\check{r}})$ denotes a diagonal matrix composed of the non-zero eigenvalues of $\mathbf{H}\mathbf{H}^H$ arranged in decreasing order. Then we have

$$\check{y}_i = \begin{cases} \sqrt{\check{\lambda}_i}\check{x}_i + \check{n}_i, & i = 1, \ldots, \check{r}, \\ \check{n}_i, & i = \check{r}+1, \ldots, n_R, \end{cases}$$

where $\check{\mathbf{y}} = \check{\mathbf{U}}^H\mathbf{y}$, $\check{\mathbf{x}} = \check{\mathbf{V}}^H\mathbf{x}$, and $\check{\mathbf{n}} = \check{\mathbf{U}}^H\mathbf{n}$. The transmit power is optimally allocated among the effective $\check{r}$ scalar channels using the well-known water-filling procedure [17, Chapter 10, pp. 250-253]. As a result [102],

$$\check{P}_i^{opt} = (\check{\mu} - \sigma_n^2/\check{\lambda}_i)_+, \;\; i = 1, \ldots, \check{r},$$

where $\check{\mu}$ is determined by $\sum_{i=1}^{\check{r}} \check{P}_i^{opt} = P_T$, and $(a)_+$ denotes $\max(a, 0)$. The capacity-achieving input distribution is giving by $\mathbf{x} \sim \mathcal{N}_c(0, \check{\mathbf{Q}})$, where

$$\begin{aligned} \check{\mathbf{Q}} &= \check{\mathbf{V}} \cdot \text{diag}(\check{P}_1^{opt}, \ldots, \check{P}_{\check{r}}^{opt}) \cdot \check{\mathbf{V}}^H \\ &= \check{\mathbf{V}} \cdot (\check{\mu}\mathbf{I}_{\check{r}} - \sigma_n^2\check{\mathbf{\Lambda}}^{-1})_+ \cdot \check{\mathbf{V}}^H, \end{aligned} \tag{2.5}$$

and the capacity is given by

$$C_{wf}(\mathbf{H}) = \sum_{i=1}^{\check{r}} \log_2 \left[1 + \frac{(\check{\lambda}_i\check{\mu} - \sigma_n^2)_+}{\sigma_n^2} \right].$$

It is important to note that, due to CSIT, $C_{wf}(\mathbf{H})$ is usually larger than $C_{uni}(\mathbf{H})$, especially in the low to medium SNR region. For full-rank channels, $C_{uni}(\mathbf{H})$ approaches $C_{wf}(\mathbf{H})$ when P_T goes to infinity.

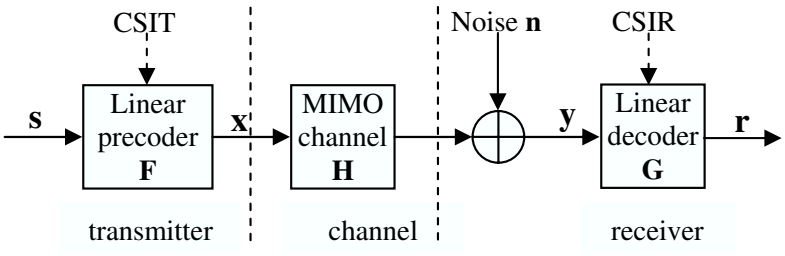

Figure 2.2. A single-user (point-to-point) MIMO system with linear precoding/decoding.

The ergodic capacity of a coherent MIMO fading channel is the capacity $C(\mathbf{H})$ averaged over different channel realizations:

$$C = \mathbb{E}_{\mathbf{H}} \left\{ \max_{\mathbf{Q}, \mathrm{tr}(\mathbf{Q}) \le P_T} \log_2 \det \left[\mathbf{I}_{n_R} + \frac{1}{\sigma_n^2} \mathbf{H}\mathbf{Q}\mathbf{H}^H \right] \right\}.$$

In [26,102], it has been shown that if $\mathbf{H} = \mathbf{H}_w$, then the capacity as expressed in this formula scales linearly with $\min(n_T, n_R)$.

2.1.5 Exploiting CSIT Using Linear Precoding/Decoding in Coherent Spatial Multiplexing

In traditional space-time coded or spatially multiplexed systems, no CSI is needed at the transmitter. However, an efficient use of the available CSIT is beneficial to system performance. A good example has been seen in Subsection 2.1.4, where CSIT is exploited to improve capacity. Through proper designs, it can also ameliorate error rate performance.

To account for CSIT, a simple and general framework employs linear precoding and decoding, as depicted in Fig. 2.2. The information symbols to be sent are denoted by a $B \times 1$ vector $\mathbf{s}$, where the number of data streams, B ($\le n_T$), is properly chosen and fixed. The input signal $\mathbf{s}$ is assumed to be zero-mean and white [$\mathbb{E}(\mathbf{s}\mathbf{s}^H) = \mathbf{I}_B$], and independent of

channel realizations. The data vector is then fed into the precoder, denoted by $\mathbf{F}$, which is a $n_T \times B$ linear matrix processor and takes the available CSIT into account. In the literature, $\mathbf{F}$ is sometimes referred to as a generalized beamformer or a prefilter. After the precoder, the data vector is transmitted across the slow-varying flat-fading MIMO channel $\mathbf{H}$. The $n_R \times 1$ received signal vector at the receive antennas is $\mathbf{y} = \mathbf{HFs} + \mathbf{n}$, where $\mathbf{n}$ is the spatially and temporally white additive Gaussian noise with distribution $\mathcal{N}_c(0, \sigma_n^2 \cdot \mathbf{I}_{n_R})$. In the receiver, a linear decoder described by the $B \times n_R$ matrix $\mathbf{G}$ is employed to recover the original information. The decoder can be interpreted as an equalizer. At the output of the decoder, the signal vector $\mathbf{r}$ is given by

$$\mathbf{r} = \mathbf{Gy} = \mathbf{G}(\mathbf{HFs} + \mathbf{n}).$$

In some system structures, the decoder $\mathbf{G}$ does not appear, or equivalently, $\mathbf{G}$ is represented by an identity matrix. For example, in Subsection 2.1.4, for the perfect CSIT case, $\mathbf{F} = \check{\mathbf{Q}}^{\frac{1}{2}}$ [see (2.5)] and $\mathbf{G}$ is not needed. [Here the input $\mathbf{s}$ is an independent and identically-distributed (i.i.d.) Gaussian vector, distributed as $\mathbf{s} \sim \mathcal{N}_c(0, \mathbf{I}_{n_T})$.]

The framework in Fig. 2.2 subsumes both space-time coded systems [44, 84, 130, 131] and spatially multiplexed systems [1, 14, 40, 50, 70, 85, 87]. With linear precoding/decoding, spatial multiplexing is not only capable of providing high data rate, but also capable of introducing redundancy (diversity) into the precoded data streams, as well as achieving a tradeoff between diversity and multiplexing. Therefore, throughout this thesis, we will concentrate on joint transceiver designs for spatially multiplexed systems.

As mentioned in Section 1.3, various design criteria have been considered, among which the MSE-related ones are most popular. Most of the existing MSE-related designs have assumed *perfect CSIR*, while the CSIT has been assumed to be perfect or partial. In Chapter 3 and Chapter 4, we will consider *imperfect CSIR* (i.e., non-ideal coherent reception) and imperfect CSIT in the transceiver designs, and investigate the joint impact of

channel correlation and erroneous channel estimation on system structure as well as on error rate or data rate performance.

2.2 Multiuser MIMO Communications over Flat-fading Wireless Channels

2.2.1 Multiuser MIMO Uplink and Downlink Systems in Flat Fading

Consider a single cell in a cellular communication system. The BS is equipped with M antennas. There are K users (mobile stations), each with N_i antennas, $i = 1,\ldots,K$. The uplink channels are denoted by $\mathbf{H}_i$, $i = 1,\ldots,K$, whereas the downlink channels are given by $\mathbf{H}_i^H$, $i = 1,\ldots,K$. (In Subsection 2.2.2, we will explain why the uplink and the downlink channels are denoted using the same set of symbols.)

2.2.1.1 The Uplink System Model

Let the $(N_k \times 1)$ transmitted signal vector from the antennas of user k be denoted by $\mathbf{x}_{ul,k}$, $k = 1,\ldots,K$. The signal vector received at the BS antennas is a blend of those from different users contaminated by channel fading and noise, i.e.,

$$\mathbf{y}_{ul} = \sum_{k=1}^{K} \mathbf{H}_k \mathbf{x}_{ul,k} + \mathbf{n}_{ul}.$$

2.2.1.2 The Downlink System Model

In the downlink, the BS broadcasts a mixture of K $(M \times 1)$ signal vectors, each intended for a different user. Different MSs receive different copies of the mixture which have gone through individual fading processes. For user j,

$$\mathbf{y}_{dl,j} = \mathbf{H}_j^H \left[\sum_{k=1}^{K} \mathbf{x}_{dl,k} \right] + \mathbf{n}_{dl,j}, \quad j = 1,\ldots,K.$$

2.2.2 Multiuser MIMO Channels: Capacity Regions, Sum Capacities and Duality

In multiuser communications, it is the simultaneously achievable performances for all users that interest us.

Given perfect knowledge of $\{\mathbf{H}_k\}_{k=1}^K$, the capacity region of a MIMO MAC has been reported in [31,54,124], which characterizes all the simultaneously achievable data rates of individual users. In particular, it has been shown that the sum capacity (i.e., the sum of data rates of all users) of a coherent Gaussian MIMO MAC grows linearly with $\min(M, \sum_{k=1}^K N_k)$ [102].

In cellular systems, the demand of the downlink data transfer is expected to be several times greater than that of the uplink [4]. This makes the MIMO downlink transmission particularly important. On the other hand, it is often harder to find the optimum transmit strategy for the downlink [17, Chapter 14]. In fact, given perfect channel knowledge, the capacity region of a coherent Gaussian MIMO BC has only recently been determined in [115], where it is shown to coincide with the previously found dirty-paper coding (DPC) achievable rate region [11,15,31,107,123].

Interestingly, it has been proved in [107,115] that the capacity regions of the Gaussian MIMO MAC and BC are identical under the same sum power constraint. Furthermore, if a specific set of transmit covariance matrices in MAC/BC achieve a certain set of data rates, then there exists another set of transmit covariance matrices in the BC/MAC that achieve the same set of rates. The explicit transformation between the two sets of covariance matrices is also described in [107]. This relationship between the MAC and the BC is known as the MAC-BC duality [107]. With duality, the capacity region of the MIMO BC can be computed more easily.

Note that to apply the duality, we only need to fabricate a *virtual* dual channel, find

the optimum transmit strategy for the dual channel and then transform it back to the actual channel under investigation. No channel reciprocity is invoked. This explains the notation we have used for the MAC and BC channels in Subsection 2.2.1.

2.2.3 Linear Processing for Multiuser MIMO

Along with the discovery of capacity-achieving transmit strategies for multiuser MIMO, signal processing techniques have been proposed to approach the proposed capacity limits, e.g., Tomlinson-Harashima precoding and vector perturbation techniques for the downlink [36, 123]. In practice, we attempt to approach the limits using signal processing techniques that are easy to implement. As for single-user MIMO systems, linear signal processing plays an important role also for multiuser MIMO.

Various linear processing techniques have been proposed for multiuser MIMO systems, including those for both the uplink [43, 45, 91] and the downlink [13, 43, 47, 76, 89, 96, 103, 125].

The minimum sum MSE (MSMSE) linear precoding/decoding design has been studied in [91] for the uplink, as well as in [47, 89, 103, 125] for the downlink, as a low-complexity and effective signal processing technique to manage both inter-stream and multiuser interferences and to provide high data rate and diversity. A schematic overview of multiuser MIMO systems with linear precoding/decoding is presented in Fig. 2.3.

2.2.3.1 The Uplink System Model with Linear Precoding/Decoding

Suppose that user i has l_i data streams, denoted by the $l_i \times 1$ [$l_i \leq \min(M, N_i)$] vector $\mathbf{s}_{ul,i}$, $i = 1, \ldots, K$. These data vectors are assumed to be zero-mean, white [$\mathbb{E}(\mathbf{s}_{ul,i}\, \mathbf{s}_{ul,i}^H) = \mathbf{I}_{l_i}, \forall i$], and mutually independent among users. Before the data streams are sent into the air, a linear precoder is employed for each user, which is denoted by the $N_i \times l_i$ matrix $\mathbf{F}_i$, $i =$

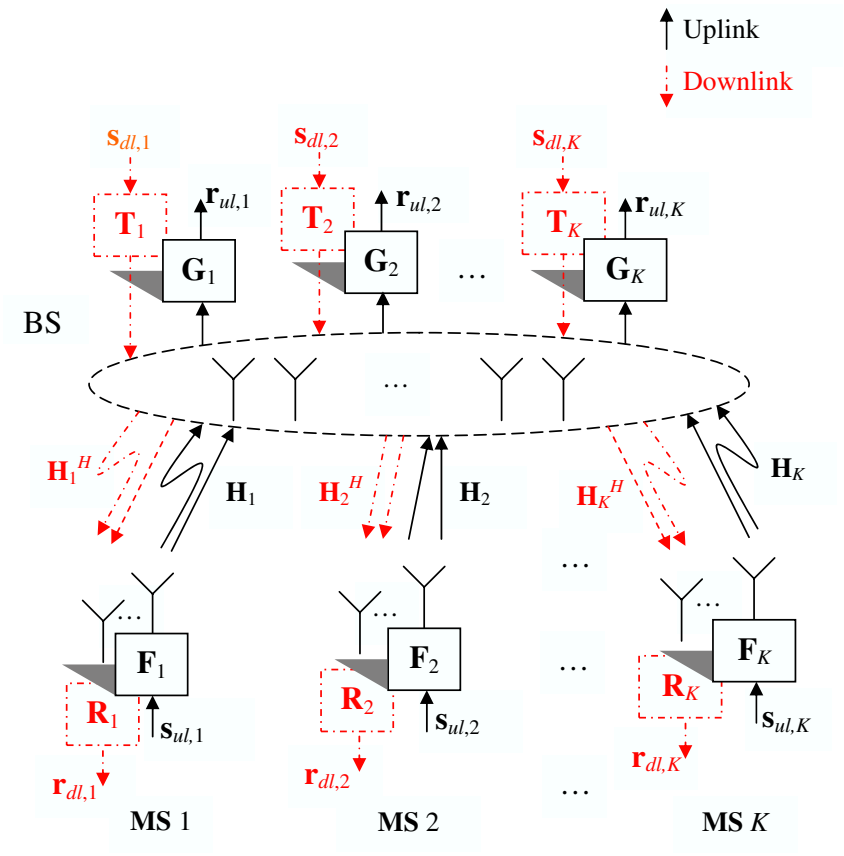

Figure 2.3. Uplink and downlink MIMO transmissions with linear precoders/decoders

$1,\ldots,K$. The signal vector received at the BS antennas is given by

$$\mathbf{y}_{ul} = \sum_{i=1}^{K} \mathbf{H}_i \mathbf{F}_i \mathbf{s}_{ul,i} + \mathbf{n}_{ul}.$$

The noise vector $\mathbf{n}_{ul}$ is assumed to be zero-mean, white, and complex Gaussian, i.e., distributed according to $\mathcal{N}_c(0, \sigma_n^2 \cdot \mathbf{I}_M)$. The data vectors and the noise vector are assumed to be statistically independent. At the BS, to recover the data for the user j, a linear decoder, denoted by the $l_j \times M$ matrix $\mathbf{G}_j$, is used. An estimate of the data vector for user j can thus be expressed as

$$\mathbf{r}_{ul,j} = \mathbf{G}_j \cdot \mathbf{y}_{ul} = \mathbf{G}_j \left[\sum_{i=1}^{K} \mathbf{H}_i \mathbf{F}_i \mathbf{s}_{ul,i} \right] + \mathbf{G}_j \, \mathbf{n}_{ul}, \quad j = 1,\ldots,K.$$

2.2.3.2 The Downlink System Model with Linear Precoding/Decoding

In the downlink, it is assumed that the data streams of user i are denoted by the $l_i \times 1$ vector $\mathbf{s}_{dl,i}$, and the linear precoder for user i at the BS is denoted by the $M \times l_i$ matrix $\mathbf{T}_i$, $i = 1, \ldots, K$. Similar to the uplink, the data vectors are assumed to be zero-mean and white $[\mathbb{E}(\mathbf{s}_{dl,i}\, \mathbf{s}_{dl,i}^H) = \mathbf{I}_{l_i}, \forall i]$. All data vectors are assumed to be mutually independent. The signal received at the antennas of user j is given by:

$$\mathbf{y}_{dl,j} = \mathbf{H}_j^H \left[\sum_{i=1}^{K} \mathbf{T}_i \mathbf{s}_{dl,i} \right] + \mathbf{n}_{dl,j}, \ \ \forall j.$$

It is assumed that the noise vectors are mutually independent and $\mathbf{n}_{dl,j}$ is distributed according to $\mathcal{N}_c(0, \sigma_n^2 \cdot \mathbf{I}_{N_j}), \forall j$. Again, the data and the noise are assumed to be statistically independent. A linear decoder $\mathbf{R}_j$ ($l_j \times N_j$) is employed to recover $\mathbf{s}_{dl,j}$, which gives the following estimate of $\mathbf{s}_{dl,j}$:

$$\mathbf{r}_{dl,j} = \mathbf{R}_j \cdot \mathbf{y}_{dl,j} = \mathbf{R}_j \mathbf{H}_j^H \left[\sum_{i=1}^{K} \mathbf{T}_i \mathbf{s}_{dl,i} \right] + \mathbf{R}_j \cdot \mathbf{n}_{dl,j}, \ \ j = 1, \ldots, K.$$

2.2.3.3 Duality in Linear Precoding/Decoding designs for Multiuser MIMO Uplink and Downlink

Not surprisingly, an uplink–downlink duality also exists in the achievable MSE regions or the signal-to-interference-plus-noise ratio (SINR) regions of both links with linear precoding/decoding [89]. *Perfect* CSI and the same sum power constraint are assumed. Based on the duality, the more involved downlink minimum sum MSE linear precoding/decoding design has been tackled by forming and solving a dual uplink problem [89]. The same idea has also been adopted in [47].

In Chapter 5, we will further study the minimum sum MSE designs for both links and establish the duality in sum MSE with imperfect CSI.

Chapter 3

Minimum Total MSE Design with Imperfect CSI at Both Ends

3.1 Introduction

Previously, the minimum total MSE transceiver designs for single-user MIMO systems have been studied with different assumptions of channel state information (CSI). In [70,85, 87,120], perfect channel state information at the transmitter (CSIT) as well as at the receiver (CSIR) is assumed. Later there have been more practical designs that consider imperfect CSIT. In [49], the minimum total MSE design has been studied with outdated CSIT and perfect CSIR. In [126, 127] [128, Section VII], it is assumed that the CSIT is the channel mean information (CMI) and/or the channel correlation information (CCI), whereas the receiver has perfect CSI. The more important case with imperfect CSIR has also been considered. For example, in [69, Chapter 7], the same imperfect CSI is assumed at both ends, but there the channel correlation has not been accounted for. In [128, Section VI], closed-form robust designs (including the minimum total MSE design) have been derived assuming that the same imperfect CSI, including *channel mean and receive correlation information,* is available to both ends. The same CSI assumption is also used in [92], where

the minimum total MSE design has been specifically studied. However, to the best of our knowledge, little attention has been paid to the joint design where the same imperfect CSI, including the channel mean and *transmit correlation* information, is available at both ends. This case is very interesting, since, as we have mentioned in Subsection 2.1.1 [see (2.3)], in practical downlink systems, the mobile is often surrounded by many local scatterers and channels from different antennas tend to be uncorrelated, whereas the channels from different BS antennas are often correlated due to limited scattering. The more general case, when there is channel estimation error and there is transmit and receive correlation, also remains as an open problem.

In this chapter, we address the problem of linear precoding/decoding to minimize the total MSE with imperfect CSI at both ends of a single-user MIMO link [18, 20]. The CSIR here is composed of the estimated channel (channel mean) as well as transmit (and more generally, transmit and receive) correlation information. To simplify the analysis, we assume the feedback is error-free and instantaneous, as in [66, 92, 121] [128, Section VI], which implies that the CSIT is the same as CSIR[1]. The assumption of instantaneous feedback is partly justified since, as will be shown by our simulations, the system maintains acceptable performance with a reasonably low feedback delay. The design under the above assumption is a step forward from that assuming perfect CSI at both ends [70, 85, 86, 120]. It can also serve as a basis for comparison to future system designs which explicitly take into account the errors and/or delays in the feedback link.

The basic system model used in this chapter has been introduced in Subsection 2.1.5. We consider a slowing-varying flat-fading MIMO channel, which is modeled as in [95], i.e., $\mathbf{H} = \mathbf{R}_R^{\frac{1}{2}} \mathbf{H}_w \mathbf{R}_T^{\frac{1}{2}}$, where $\mathbf{H}_w$ is a spatially white matrix whose entries are independent

[1]One can equivalently assume that the system is implemented offline, and the precoding matrix is calculated at the receiver and then fed back to the transmitter [91].

and identically distributed (i.i.d.) $\mathcal{N}_c(0,1)$ [see Subsection 2.1.1, (2.1)-(2.2)]. The matrices $\mathbf{R}_T$ and $\mathbf{R}_R$ represent normalized transmit and receive correlation (i.e., with unit diagonal entries), respectively. Both $\mathbf{R}_T$ and $\mathbf{R}_R$ are assumed to be *full-rank*.

The rest of this chapter is organized as follows. The imperfect channel estimation is modeled in Section 3.2. Then a mathematical description of the minimum total MSE design with imperfect CSI at both ends is given in Section 3.3. In Section 3.4 the minimum total MSE design problem is solved assuming channel mean and transmit correlation at both ends. In Section 3.5, the analysis is extended to the more general case with both transmit and receive correlation as well as channel mean information at both ends. For wider applications, in Section 3.6, we extend the analysis to the minimum weighted MSE design. Numerical results are presented in Section 3.7. Section 3.8 summarizes this chapter. Detailed derivations and proofs are presented in Section 3.9.

3.2 Modeling Imperfect Channel Estimation

Since $\mathbf{R}_T$ and $\mathbf{R}_R$ are full-rank and assumed to be known, channel estimation is performed on $\mathbf{H}_w$ using the well-established orthogonal training method [34, 66, 92, 122]. At the receive antennas, the signal matrix $\mathbf{Y}_{tr} = \mathbf{H}\mathbf{S}_{tr} + \mathbf{N}_{tr}$ is received in n_T successive time slots, where $\mathbf{S}_{tr}$ is a known $n_T \times n_T$ training signal matrix and $\mathbf{N}_{tr}$ is the collection of channel noise vectors. Thus,

$$\mathbf{Y}_{tr} = \mathbf{R}_R^{\frac{1}{2}}\mathbf{H}_w\mathbf{R}_T^{\frac{1}{2}}\mathbf{S}_{tr} + \mathbf{N}_{tr}. \tag{3.1}$$

Let P_{tr} denote the total training power, i.e., $\mathrm{tr}(\mathbf{S}_{tr}\mathbf{S}_{tr}^H) = P_{tr}$. Choose $\mathbf{S}_{tr} = \mathbf{R}_T^{-\frac{1}{2}}\mathbf{S}_0$, where $\mathbf{S}_0$ is a unitary matrix scaled by $\sqrt{P_{tr}/\mathrm{tr}(\mathbf{R}_T^{-1})}$. Pre-multiplying both sides of (3.1) by $\mathbf{R}_R^{-\frac{1}{2}}$ and then post-multiplying the resultant formula by $\mathbf{S}_0^{-1}$, we obtain

$$\tilde{\mathbf{H}}_w = \mathbf{R}_R^{-\frac{1}{2}}\mathbf{Y}_{tr}\mathbf{S}_0^{-1}$$

$$= \mathbf{H}_w + \mathbf{R}_R^{-\frac{1}{2}} \mathbf{N}_{tr} \mathbf{S}_0^{-1}$$
$$= \mathbf{H}_w + \mathbf{R}_R^{-\frac{1}{2}} \mathbf{N}_0. \tag{3.2}$$

In the above, we have defined $\mathbf{N}_0 = \mathbf{N}_{tr}\mathbf{S}_0^{-1}$, whose entries are i.i.d. $\mathcal{N}_c(0, \sigma_{ce}^2)$ with $\sigma_{ce}^2 = \text{tr}(\mathbf{R}_T^{-1}) \cdot \sigma_n^2 / P_{tr}$. To obtain a better channel estimation performance, the minimum MSE (MMSE) channel estimation of $\mathbf{H}_w$ is performed based on (3.2) [66, 92, 106, 121], which yields

$$\hat{\mathbf{H}}_w = \mathbb{E}[\mathbf{H}_w | \tilde{\mathbf{H}}_w] = [\mathbf{I}_{n_R} + \sigma_{ce}^2 \cdot \mathbf{R}_R^{-1}]^{-1} \tilde{\mathbf{H}}_w. \tag{3.3}$$

Furthermore, $\mathbf{H}_w$ is expressed as the sum of $\hat{\mathbf{H}}_w$ and the estimation error matrix [46, Chapter 12], i.e.,

$$\mathbf{H}_w = \hat{\mathbf{H}}_w + \mathbf{R}_R^{-\frac{1}{2}} [\mathbf{I}_{n_R} + \sigma_{ce}^2 \cdot \mathbf{R}_R^{-1}]^{-\frac{1}{2}} \mathbf{E}_w, \tag{3.4}$$

where the entries of $\mathbf{E}_w$ are i.i.d. $\mathcal{N}_c(0, \sigma_{ce}^2)$, and are independent from those of $\hat{\mathbf{H}}_w$. Detailed derivations of (3.3) and (3.4) are provided in Subsection 3.9.1. Let

$$\mathbf{R}_{e,R} = [\mathbf{I}_{n_R} + \sigma_{ce}^2 \cdot \mathbf{R}_R^{-1}]^{-1}.$$

The CSI model is described by

$$\mathbf{H} = \hat{\mathbf{H}} + \mathbf{E}, \tag{3.5}$$

where $\mathbf{H}$ is the true channel matrix, $\hat{\mathbf{H}} = \mathbf{R}_R^{\frac{1}{2}} \hat{\mathbf{H}}_w \mathbf{R}_T^{\frac{1}{2}}$ is the estimated channel matrix (i.e., the channel mean), and $\mathbf{E} = \mathbf{R}_{e,R}^{\frac{1}{2}} \mathbf{E}_w \mathbf{R}_T^{\frac{1}{2}}$ is the channel estimation error matrix.

In summary, the CSI is given by (3.3)-(3.5). In subsequent sections, we assume that $\hat{\mathbf{H}}$, $\mathbf{R}_R$, $\mathbf{R}_T$, σ_{ce}^2 and σ_n^2 are known to both ends of the link, which is referred to as *the channel mean as well as both transmit and receive correlation information*.

We point out that in [66], a different CSI model for the channel $\mathbf{H} = \mathbf{R}_R^{1/2} \mathbf{H}_w \mathbf{R}_T^{1/2}$ is employed, which is given by $\mathbf{H} = \underline{\hat{\mathbf{H}}} + \underline{\mathbf{E}}$, with $\underline{\hat{\mathbf{H}}} = \mathbf{R}_R^{1/2} \underline{\hat{\mathbf{H}}}_w \mathbf{R}_T^{1/2}$ and $\underline{\mathbf{E}} = \mathbf{R}_R^{1/2} \underline{\mathbf{E}}_w \mathbf{R}_T^{1/2}$,

where the entries of $\underline{\hat{\mathbf{H}}}_w$ and $\underline{\mathbf{E}}_w$ are assumed to be i.i.d.. However, in [66] it is assumed that a genie-provided estimate of $\mathbf{H}_w$ (i.e. $\underline{\hat{\mathbf{H}}}_w$) is available at the receiver. In comparison, this is not required in our channel estimation method or CSI model. Also, in [128, Section VI], it has been assumed that $\mathbf{H} = \underline{\underline{\mathbf{H}}} + \mathbf{R}_R^{1/2} \underline{\underline{\mathbf{E}}}_w \mathbf{R}_T^{1/2}$, where $\underline{\underline{\mathbf{H}}}$ is the channel mean, and $\underline{\underline{\mathbf{E}}}_w$ is spatially white (i.e., with i.i.d. entries). It is important to note that the analysis to be presented in this paper can be applied exactly the same way when using the CSI model in [66] or [128, Section VI].

3.3 A Mathematical Description

With the CSI modeled in previous section, the received signal vector $\mathbf{y}$ can be written as (refer to Subsection 2.1.5):

$$\mathbf{y} = \hat{\mathbf{H}}\mathbf{F}\mathbf{s} + \underbrace{\mathbf{E}\mathbf{F}\mathbf{s} + \mathbf{n}}_{total \quad noise}. \tag{3.6}$$

The system MSE matrix is calculated as

$$\begin{aligned} MSE(\mathbf{F},\mathbf{G}) &= \mathbb{E}\left[(\mathbf{r}-\mathbf{s})(\mathbf{r}-\mathbf{s})^H\right] \\ &= \mathbb{E}\left\{[\mathbf{G}(\hat{\mathbf{H}}+\mathbf{E})\mathbf{F}-\mathbf{I}_B]\,\mathbf{s}\mathbf{s}^H[\mathbf{G}(\hat{\mathbf{H}}+\mathbf{E})\mathbf{F}-\mathbf{I}_B]^H\right\} + \sigma_n^2 \cdot \mathbf{G}\mathbf{G}^H. \end{aligned} \tag{3.7}$$

Using our assumptions on the statistics of the channel (see Subsection 2.1.5), noise and data, with some manipulations, we can simplify (3.7) as

$$\begin{aligned} MSE(\mathbf{F},\mathbf{G}) = {} & \mathbf{G}\hat{\mathbf{H}}\mathbf{F}\mathbf{F}^H\hat{\mathbf{H}}^H\mathbf{G}^H - \mathbf{G}\hat{\mathbf{H}}\mathbf{F} - \mathbf{F}^H\hat{\mathbf{H}}^H\mathbf{G}^H + \mathbf{I}_B \\ & + \left[\sigma_{ce}^2 \cdot \mathrm{tr}(\mathbf{R}_T\mathbf{F}\mathbf{F}^H)\right] \cdot \mathbf{G}\mathbf{R}_{e,R}\mathbf{G}^H + \sigma_n^2 \cdot \mathbf{G}\mathbf{G}^H. \end{aligned} \tag{3.8}$$

In the above, we have used the result $\mathbb{E}\left[\mathbf{E}_w\mathbf{A}\mathbf{E}_w^H\right] = \sigma_{ce}^2 \cdot \mathrm{tr}(\mathbf{A}) \cdot \mathbf{I}_{n_R}$, if the entries of matrix $\mathbf{E}_w$ are i.i.d. $\mathcal{N}_c(0,\sigma_{ce}^2)$, as well as the identity $\mathrm{tr}(\mathbf{A}_1\mathbf{A}_2) = \mathrm{tr}(\mathbf{A}_2\mathbf{A}_1)$.

Our goal is to find a pair of appropriate $\mathbf{F}$ and $\mathbf{G}$, such that the sum of MSEs from

different data streams is minimized subject to a total power constraint P_T, i.e.,

$$\begin{aligned} \min_{\mathbf{F},\,\mathbf{G}} \quad & \mathrm{tr}\,[MSE(\mathbf{F},\mathbf{G})] \\ \text{subject to} \quad & \mathrm{tr}(\mathbf{F}\mathbf{F}^H) \le P_T. \end{aligned} \tag{3.9}$$

This is referred to as the minimum total MSE design with imperfect CSI at both ends. We are also interested in determining the effects of channel correlation and channel estimation error on system performance.

Note that when $\sigma_{ce}^2 = 0$, our problem in (3.9) reduces to those treated in [70,85,87,120]. Also, when $\sigma_{ce}^2 \neq 0$ and $\mathbf{R}_T = \mathbf{I}_{n_T}$, $\mathrm{tr}(\mathbf{F}\mathbf{F}^H)$ is replaced by P_T as in [69, Chapter 7] [92] [128, Section VI], and the problem (3.9) becomes mathematically equivalent to the perfect CSI case. It is when $\sigma_{ce}^2 \neq 0$ and $\mathbf{R}_T \neq \mathbf{I}_{n_T}$ that the problem in (3.9) becomes particularly challenging. No result has been obtained for this case in the literature.

The objective function in (3.9), i.e., $\mathrm{tr}\,[MSE(\mathbf{F},\mathbf{G})]$, is non-convex in $(\mathbf{F},\mathbf{G})$. Thus, the methods designed for convex problems are not applicable here. Fortunately, it can be shown that a global minimum exists for the problem in (3.9) (see Subsection 3.9.2). Furthermore, the objective and constraint functions of (3.9) are *continuously differentiable* (with respect to $\mathbf{G}$ and/or $\mathbf{F}$). Since there is only one inequality constraint and no equality constraints in (3.9), any feasible precoder-decoder pair is regular whether the inequality constraint is active or inactive [5, pp. 309-310][2]. The global-minimum-achieving $(\mathbf{F},\mathbf{G})$ therefore satisfies the first-order Karush-Kuhn-Tucker (KKT) necessary conditions for optimality [5, p. 310, **Proposition 3.3.1**]. Therefore, our method is to find all the solutions which satisfy the KKT conditions and identify the optimum $(\mathbf{F},\mathbf{G})$ among them.

Note that if $(\mathbf{F},\mathbf{G})$ minimizes the total MSE, so does $(\mathbf{F}\mathbf{U},\mathbf{U}^H\mathbf{G})$, with $\mathbf{U}$ being an

[2] According to [5, pp. 309-310], a feasible point is said to be *regular* if either (i) all equality constraint gradients and active inequality constraint gradients at this point are linearly independent, or (ii) in the case of no equality constraints, all the inequality constraints are inactive at this point.

arbitrary $B \times B$ unitary matrix. Below we refer to a specific optimum precoder-decoder pair as the optimum solution *up to a unitary transform* [37].

3.4 Closed-form Optimum Solution for a Special Case

In this section, we consider the special case when $\mathbf{R}_T \neq \mathbf{I}_{n_T}$ and $\mathbf{R}_R = \mathbf{I}_{n_R}$. From (3.2)-(3.4), it can be shown that when $\mathbf{R}_R = \mathbf{I}_{n_R}$, $\mathbf{H}_w = \hat{\mathbf{H}}_{w0} + \mathbf{E}_{w0}$, with both $\hat{\mathbf{H}}_{w0}$ and $\mathbf{E}_{w0}$ being spatially white. The entries of $\hat{\mathbf{H}}_{w0}$ and $\mathbf{E}_{w0}$ are mutually uncorrelated (independent if Gaussian), and are i.i.d. $\mathscr{N}_c(0, 1-\sigma_E^2)$ and $\mathscr{N}_c(0, \sigma_E^2)$, respectively, with $\sigma_E^2 = \sigma_{ce}^2/(1+\sigma_{ce}^2)$. The CSI model is described by

$$\mathbf{H} = (\hat{\mathbf{H}}_{w0} + \mathbf{E}_{w0})\mathbf{R}_T^{\frac{1}{2}} = \hat{\mathbf{H}} + \mathbf{E},$$

where $\hat{\mathbf{H}} = \hat{\mathbf{H}}_{w0}\mathbf{R}_T^{\frac{1}{2}}$ is the channel mean, and $\mathbf{E} = \mathbf{E}_{w0}\mathbf{R}_T^{\frac{1}{2}}$. Here we assume that $\hat{\mathbf{H}}$, $\mathbf{R}_T$, σ_E^2 and σ_n^2 are known to both ends, which is referred to as *the channel mean and transmit correlation information.*

When $\mathbf{R}_R = \mathbf{I}_{n_R}$, the MSE matrix in (3.8) reduces to

$$\begin{aligned} MSE(\mathbf{F}, \mathbf{G}) = {} & \mathbf{G}\hat{\mathbf{H}}\mathbf{F}\mathbf{F}^H\hat{\mathbf{H}}^H\mathbf{G}^H - \mathbf{G}\hat{\mathbf{H}}\mathbf{F} - \mathbf{F}^H\hat{\mathbf{H}}^H\mathbf{G}^H + \mathbf{I}_B \\ & + [\sigma_n^2 + \sigma_E^2 \cdot \mathrm{tr}(\mathbf{R}_T\mathbf{F}\mathbf{F}^H)]\mathbf{G}\mathbf{G}^H. \end{aligned} \tag{3.10}$$

The problem formulation here is the same as (3.9), except that the MSE matrix is given by (3.10). The associated Lagrangian is

$$\mathscr{L}_1(\mathbf{F}, \mathbf{G}, \mu_1) = \mathrm{tr}\,[MSE(\mathbf{F}, \mathbf{G})] + \mu_1 \cdot [\mathrm{tr}(\mathbf{F}\mathbf{F}^H) - P_T],$$

where μ_1 is the Lagrange multiplier. By taking the derivatives of $\mathscr{L}_1(\mathbf{F}, \mathbf{G}, \mu_1)$ with respect to $\mathbf{F}^*$ and $\mathbf{G}^*$ [60], together with the power constraint and the complementary slackness [7], the associated KKT conditions can be obtained as follows:

$$\hat{\mathbf{H}}\mathbf{F} = \left\{\hat{\mathbf{H}}\mathbf{F}\mathbf{F}^H\hat{\mathbf{H}}^H + \left[\sigma_n^2 + \sigma_E^2 \cdot \mathrm{tr}(\mathbf{R}_T\mathbf{F}\mathbf{F}^H)\right] \cdot \mathbf{I}_{n_R}\right\}\mathbf{G}^H, \tag{3.11}$$

$$\mathbf{G}\hat{\mathbf{H}} = \mathbf{F}^H \left[\hat{\mathbf{H}}^H \mathbf{G}^H \mathbf{G}\hat{\mathbf{H}} + \sigma_E^2 \cdot \mathrm{tr}(\mathbf{G}\mathbf{G}^H) \cdot \mathbf{R}_T + \mu_1 \cdot \mathbf{I}_{n_T}\right], \tag{3.12}$$

$$\mu_1 \geq 0,\ \mathrm{tr}(\mathbf{F}\mathbf{F}^H) - P_T \leq 0, \tag{3.13}$$

$$\mu_1 \cdot [\mathrm{tr}(\mathbf{F}\mathbf{F}^H) - P_T] = 0. \tag{3.14}$$

Detailed derivations of the above conditions are presented in Subsection 3.9.3.

Clearly, if $\mathbf{F} = 0$, an obvious solution satisfying the KKT condition is: $\mathbf{F} = 0$, $\mathbf{G} = 0$ and $\mu_1 = 0$. However, this case is not interesting to us in practice. Therefore, we proceed to search for those solutions with $\mathbf{F} \neq 0$ (referred to as the *non-zero* solutions).

Lemma 1 *For any solution satisfying the KKT conditions (3.11)-(3.14),*

$$\mu_1 = \sigma_n^2 \cdot tr(\mathbf{G}\mathbf{G}^H)/P_T. \tag{3.15}$$

Proof. See Subsection 3.9.4. ■

Consider the following eigenvalue decomposition (EVD) [37]:

$$\begin{aligned} &\left[\sigma_E^2 \cdot P_T \cdot \mathbf{R}_T + \sigma_n^2 \cdot \mathbf{I}_{n_T}\right]^{-\frac{1}{2}} \hat{\mathbf{H}}^H \hat{\mathbf{H}} \left[\sigma_E^2 \cdot P_T \cdot \mathbf{R}_T + \sigma_n^2 \cdot \mathbf{I}_{n_T}\right]^{-\frac{1}{2}} \\ &= \left[\mathbf{V}\ \tilde{\mathbf{V}}\right] \begin{pmatrix} \mathbf{\Lambda} & 0 \\ 0 & \tilde{\mathbf{\Lambda}} \end{pmatrix} \left[\mathbf{V}\ \tilde{\mathbf{V}}\right]^H. \end{aligned} \tag{3.16}$$

Let r denote the rank of the estimated matrix $\hat{\mathbf{H}}$ in (3.16), i.e., r = rank($\mathbf{\Lambda}$), the number of non-zero channel eigenmodes. Here the entries of the diagonal matrix $\mathbf{\Lambda}$ are the non-zero eigenvalues and those of $\tilde{\mathbf{\Lambda}}$ are all zero. The $n_T \times (n_T - r)$ matrix $\tilde{\mathbf{V}}$ consists of basis vectors for the null space of (3.16), whereas the $n_T \times r$ matrix $\mathbf{V}$ is composed of the basis eigenvectors corresponding to the non-zero eigenvalues. Without loss of generality, the entries of the diagonal matrix $\mathbf{\Lambda}$ are arranged in *decreasing* order.

Lemma 2 *Assume that the number of data streams B is equal to r. The precoder and decoder satisfying the KKT conditions (3.11)-(3.14) can be expressed as*

$$\mathbf{F} = \left[\sigma_E^2 \cdot P_T \cdot \mathbf{R}_T + \sigma_n^2 \cdot \mathbf{I}_{n_T}\right]^{-\frac{1}{2}} \mathbf{V}\mathbf{\Lambda}_F, \tag{3.17}$$

$$\mathbf{G} = \mathbf{\Lambda}_G \mathbf{V}^H \left[\sigma_E^2 \cdot P_T \cdot \mathbf{R}_T + \sigma_n^2 \cdot \mathbf{I}_{n_T}\right]^{-\frac{1}{2}} \hat{\mathbf{H}}^H, \tag{3.18}$$

where $\mathbf{\Lambda}_F$ and $\mathbf{\Lambda}_G$ are arbitrary $r \times r$ matrices, and $\mathbf{V}$ comes from (3.16).

Proof. See Subsection 3.9.5. ■

Theorem 1 *Assume that the number of data streams B is equal to r. The optimum precoder and decoder for (3.9) have the following general expressions, respectively,*

$$\mathbf{F}_{opt} = \left[\sigma_E^2 \cdot P_T \cdot \mathbf{R}_T + \sigma_n^2 \cdot \mathbf{I}_{n_T}\right]^{-\frac{1}{2}} \mathbf{V} \mathbf{\Lambda}_{Fopt}, \tag{3.19}$$

$$\mathbf{G}_{opt} = \mathbf{\Lambda}_{Gopt} \mathbf{V}^H \left[\sigma_E^2 \cdot P_T \cdot \mathbf{R}_T + \sigma_n^2 \cdot \mathbf{I}_{n_T}\right]^{-\frac{1}{2}} \hat{\mathbf{H}}^H, \tag{3.20}$$

where diagonal $r \times r$ matrices $\mathbf{\Lambda}_{Fopt}$ and $\mathbf{\Lambda}_{Gopt}$ are given by

$$\mathbf{\Lambda}_{Fopt} = \left[\tau_1^{\frac{1}{2}} \mu_1^{-\frac{1}{2}} \sigma_n \cdot \mathbf{\Lambda}^{-\frac{1}{2}} - \tau_1 \cdot \mathbf{\Lambda}^{-1}\right]_+^{\frac{1}{2}}, \tag{3.21}$$

$$\mathbf{\Lambda}_{Gopt} = \left[\mu_1^{\frac{1}{2}} \tau_1^{-\frac{1}{2}} \frac{1}{\sigma_n} \cdot \mathbf{\Lambda}^{-\frac{1}{2}} - \frac{\mu_1}{\sigma_n^2} \cdot \mathbf{\Lambda}^{-1}\right]_+^{\frac{1}{2}} \mathbf{\Lambda}^{-\frac{1}{2}}, \tag{3.22}$$

and

$$\tau_1 = \frac{a_2 \cdot P_T}{P_T \cdot a_3 + a_1 \cdot a_3 - a_2 \cdot a_4}, \tag{3.23}$$

$$\mu_1 = \frac{a_2 \cdot \sigma_n^2 (P_T \cdot a_3 + a_1 \cdot a_3 - a_2 \cdot a_4)}{(P_T + a_1)^2 \cdot P_T}. \tag{3.24}$$

Scalars a_1, a_2, a_3 and a_4 are traces of the $k_0 \times k_0$ top-left submatrices of

$$\mathbf{\Lambda}^{-1},\ \mathbf{\Lambda}^{-\frac{1}{2}},\ \mathbf{\Lambda}^{-\frac{1}{2}} \mathbf{V}^H \left[\sigma_E^2 P_T \mathbf{R}_T + \sigma_n^2 \mathbf{I}_{n_T}\right]^{-1} \mathbf{V},\ \textit{and}\ \mathbf{\Lambda}^{-1} \mathbf{V}^H \left[\sigma_E^2 P_T \mathbf{R}_T + \sigma_n^2 \mathbf{I}_{n_T}\right]^{-1} \mathbf{V},$$

respectively. The integer k_0 denotes the number of the non-zero entries of $\mathbf{\Lambda}_{Fopt}$ ($k_0 \leq r$). The optimum precoder-decoder pair obtained here is unique up to a unitary transform.

Proof. As derived in Subsection 3.9.6, all the non-zero solutions of $(\mathbf{F}, \mathbf{G}, \mu_1)$ satisfying the KKT conditions are given by (3.19)-(3.24) up to a unitary transform. The method

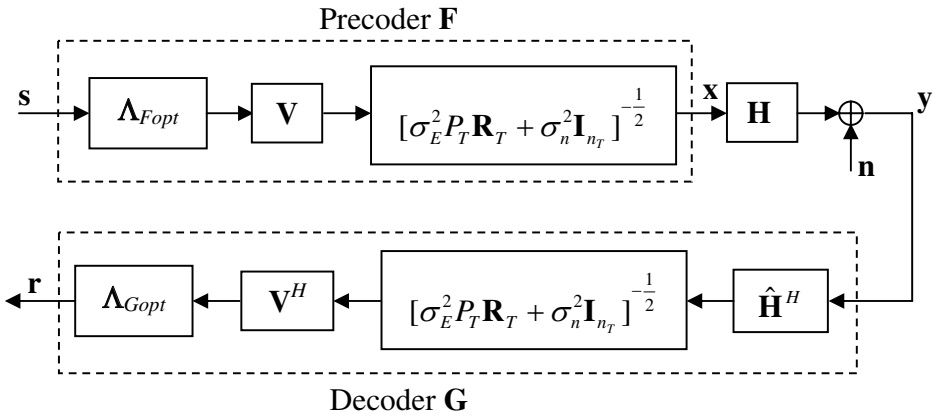

Figure 3.1. Explicit structures of the optimum precoder and decoder.

to determine the number k_0 is also included in Subsection 3.9.6. Thus, we have obtained all the solutions satisfying the KKT conditions (3.11)-(3.14), including ($\mathbf{F} = 0$, $\mathbf{G} = 0$, $\mu_1 = 0$), and the non-zero solutions given by (3.19)-(3.24) up to a unitary transform. It can be readily shown that all the non-zero solutions lead to the same total MSE, which is lower than the MSE yielded by ($\mathbf{F} = 0$, $\mathbf{G} = 0$, $\mu_1 = 0$) (see Subsection 3.9.6 for the comparison). Therefore, we conclude that the non-zero solutions [(3.19)-(3.24), up to a unitary transform] are equivalent global MSE-minimizers. ■

The explicit structures of the optimum precoder and decoder are shown in Fig. 3.1. Let $\mathbf{\Lambda} = \text{diag}\{\lambda_1, \ldots, \lambda_r\}$. The channel diagonalization is illustrated in Fig. 3.2.

Remark 3.1: When $\sigma_E^2 = 0$ ($\sigma_{ce}^2 = 0$), **Theorem 1** reduces to the results in [70, 85, 87, 120]. Compared with the results obtained under the assumption of perfect CSI, from (3.19) and (3.20), a linear filter is added to both the transmitter and receiver here, to balance the suppression of channel noise and the noise from imperfect channel estimation. Furthermore, the estimation error variance σ_E^2 is coupled with the transmit correlation $\mathbf{R}_T$.

Remark 3.2: From (3.16)-(3.18), when $\mathbf{R}_T = \mathbf{I}_{n_T}$, transmission along the eigenmodes of $\hat{\mathbf{H}}^H \hat{\mathbf{H}}$ is optimum, and the channel estimation error simply contributes additional noise

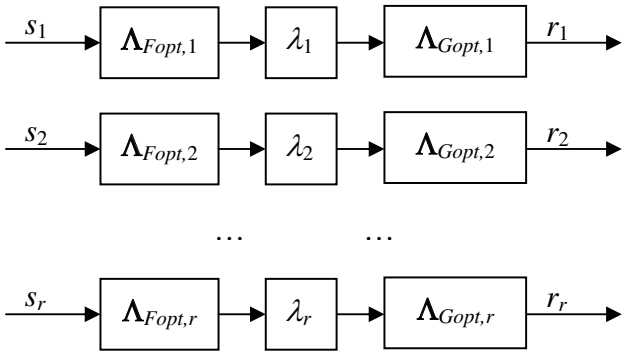

Figure 3.2. Diagonalization of the equivalent channel (3.16).

$(\sigma_E^2 \cdot P_T)$. This result has been mentioned in [69, Chapter 7] and [92]. When $P_T/\sigma_n^2 \to \infty$, the filter $[\sigma_E^2 \cdot P_T \cdot \mathbf{R}_T + \sigma_n^2 \cdot \mathbf{I}_{n_T}]^{-\frac{1}{2}}$ becomes a scaled version of $\mathbf{R}_T^{-\frac{1}{2}}$. This implies that the optimum precoder asymptotically cancels the effect of $\mathbf{R}_T$ and transmits along channel eigenmodes of the white part of the channel estimate ($\hat{\mathbf{H}}_{w0}$).

Remark 3.3: As an alternative, one can verify the results in **Theorem 1** using the Saddle Point Theorem [5, p. 491, **Proposition 5.1.6**]. Basically, the optimum solution obtained here satisfies a necessary and sufficient condition for global optimality.

3.5 Optimum transceiver structure for the General Case

Now we consider the general problem formulated in (3.9) ($\mathbf{R}_T \neq \mathbf{I}_{n_T}$ and $\mathbf{R}_R \neq \mathbf{I}_{n_R}$). We apply the same method as for the special case. The associated Lagrangian is

$$\mathscr{L}_g(\mathbf{F}, \mathbf{G}, \mu_g) = \mathrm{tr}\,[MSE(\mathbf{F}, \mathbf{G})] + \mu_g \cdot [\mathrm{tr}(\mathbf{F}\mathbf{F}^H) - P_T],$$

where μ_g is the Lagrange multiplier. Correspondingly, the KKT conditions associated with (3.9) can be derived (using the same method as in Subsection 3.9.3), as given by (3.25)-(3.28):

$$\hat{\mathbf{H}}\mathbf{F} = \left[\hat{\mathbf{H}}\mathbf{F}\mathbf{F}^H\hat{\mathbf{H}}^H + \sigma_{ce}^2 \cdot \mathrm{tr}(\mathbf{R}_T\mathbf{F}\mathbf{F}^H) \cdot \mathbf{R}_{e,R} + \sigma_n^2 \cdot \mathbf{I}_{n_R}\right]\mathbf{G}^H, \tag{3.25}$$

$$\mathbf{G}\hat{\mathbf{H}} = \mathbf{F}^H\left[\hat{\mathbf{H}}^H\mathbf{G}^H\mathbf{G}\hat{\mathbf{H}} + \sigma_{ce}^2 \cdot \mathrm{tr}(\mathbf{G}\mathbf{R}_{e,R}\mathbf{G}^H) \cdot \mathbf{R}_T + \mu_g \cdot \mathbf{I}_{n_T}\right], \tag{3.26}$$

$$\mu_g \geq 0,\ \mathrm{tr}(\mathbf{F}\mathbf{F}^H) - P_T \leq 0, \tag{3.27}$$

$$\mu_g \cdot [\mathrm{tr}(\mathbf{F}\mathbf{F}^H) - P_T] = 0. \tag{3.28}$$

Similar to the proof for **Lemma 1** in Subsection 3.9.4, it can be shown that

$$\mu_g = \sigma_n^2 \cdot \mathrm{tr}(\mathbf{G}\mathbf{G}^H)/P_T, \tag{3.29}$$

for any solution satisfying the KKT conditions (3.25)-(3.28). Define

$$\tau_2 = \mathrm{tr}(\mathbf{G}\mathbf{R}_{e,R}\mathbf{G}^H) \ \text{ and } \ \tau_3 = \sigma_{ce}^2 \cdot \mathrm{tr}(\mathbf{R}_T\mathbf{F}\mathbf{F}^H). \tag{3.30}$$

Consider the following EVD:

$$\begin{aligned}&[\tau_2 \cdot \sigma_{ce}^2 \cdot \mathbf{R}_T + \mu_g \cdot \mathbf{I}_{n_T}]^{-\frac{1}{2}}\hat{\mathbf{H}}^H[\tau_3 \cdot \mathbf{R}_{e,R} + \sigma_n^2 \cdot \mathbf{I}_{n_R}]^{-1}\hat{\mathbf{H}}[\tau_2 \cdot \sigma_{ce}^2 \cdot \mathbf{R}_T + \mu_g \cdot \mathbf{I}_{n_T}]^{-\frac{1}{2}} \\ &= [\mathbf{V}_g \ \ \tilde{\mathbf{V}}_g]\begin{pmatrix}\mathbf{\Lambda}_g & 0 \\ 0 & \tilde{\mathbf{\Lambda}}_g\end{pmatrix}[\mathbf{V}_g \ \ \tilde{\mathbf{V}}_g]^H,\end{aligned} \tag{3.31}$$

where the subscript "g" means the general case. The matrix $\mathbf{\Lambda}_g$ is a diagonal matrix whose entries are the non-zero eigenvalues of the matrix in (3.31) arranged in decreasing order. The entries of the diagonal matrix $\tilde{\mathbf{\Lambda}}_g$ are all zero. The matrices $\mathbf{V}_g$ and $\tilde{\mathbf{V}}_g$ are composed of eigenvectors corresponding to the non-zero eigenvalues and zero eigenvalues, respectively. Let r_g denote the rank of the matrix in (3.31), i.e., r_g = rank($\mathbf{\Lambda}_g$).

Theorem 2 *Assume that the number of data streams B is equal to r_g. The optimum precoder and decoder for (3.9) can be generally expressed as*

$$\mathbf{F}_{gopt} = [\tau_2 \cdot \sigma_{ce}^2 \cdot \mathbf{R}_T + \mu_g \cdot \mathbf{I}_{n_T}]^{-\frac{1}{2}} \mathbf{V}_g \mathbf{\Lambda}_{F,gopt}, \tag{3.32}$$

$$\mathbf{G}_{gopt} = \mathbf{\Lambda}_{G,gopt} \mathbf{V}_g^H [\tau_2 \cdot \sigma_{ce}^2 \cdot \mathbf{R}_T + \mu_g \cdot \mathbf{I}_{n_T}]^{-\frac{1}{2}} \hat{\mathbf{H}}^H [\tau_3 \cdot \mathbf{R}_{e,R} + \sigma_n^2 \cdot \mathbf{I}_{n_R}]^{-1}, \tag{3.33}$$

where $\mathbf{V}_g$ is from (3.31), $\mathbf{\Lambda}_{F,gopt}$ and $\mathbf{\Lambda}_{G,gopt}$ are $r_g \times r_g$ diagonal matrices, as given below

$$\mathbf{\Lambda}_{F,gopt} = \left[\mathbf{\Lambda}_g^{-\frac{1}{2}} - \mathbf{\Lambda}_g^{-1} \right]_+^{\frac{1}{2}}, \tag{3.34}$$

$$\mathbf{\Lambda}_{G,gopt} = \left[\mathbf{\Lambda}_g^{-\frac{1}{2}} - \mathbf{\Lambda}_g^{-1} \right]_+^{\frac{1}{2}} \mathbf{\Lambda}_g^{-\frac{1}{2}}. \tag{3.35}$$

Inserting (3.32)-(3.35) into the power constraint $tr(\mathbf{F}\mathbf{F}^H) = P_T$, together with the definitions of τ_2 and τ_3 in (3.30), leads to three equations with τ_2, τ_3 and μ_g being the unknowns. By solving these equations numerically, the values of τ_2, τ_3 and μ_g can be determined. The optimum solution obtained using this method is unique up to a unitary transform.

Proof. See Subsection 3.9.7. ■

Theorem 2, hence, provides the structures of the optimum precoder and decoder. However, the scalars τ_2, τ_3 and μ_g need to be determined numerically, which is inconvenient, because the three unknowns are involved together. Alternatively, (3.9) can be solved using an iterative algorithm developed from the KKT conditions, which is given in Table 3.1. This algorithm converges according to [125]. Furthermore, starting from a non-zero feasible **F**, this algorithm obtains a non-zero solution satisfying the KKT conditions. Since all the non-zero solutions satisfying the KKT conditions lead to the same minimum total MSE (see Subsection 3.9.7), we conclude that the iterative algorithm obtains a solution equivalent to the one obtained from **Theorem 2** (up to a unitary transform). Therefore, Table 3.1 presents a convenient method for the general case.

Table 3.1. An iterative algorithm for solving (3.9) in the general case

1)	Initialize $\mathbf{F} = \mathbf{F}_0$; the upper $B \times B$ sub-matrix of $\mathbf{F}_0$ is chosen to be a scaled identity and to satisfy the power constraint with equality, while the remaining entries of $\mathbf{F}_0$ are set to zero.
2)	Update $\mathbf{G}$ using (3.25);
3)	Update μ_g using (3.29);
4)	Update $\mathbf{F}$ using (3.26);
5)	If the termination condition is met, stop; otherwise, go back to 2).

Remark 3.4: We have assumed $B = r$ in **Theorem 1** and $B = r_g$ in **Theorem 2**. If the number of data streams B is chosen to be strictly smaller than the number of non-zero channel eigenmodes, i.e., the B strongest eigenmodes are used, then redundancy is introduced, which can be translated into improved diversity and thus performance improvement [50, 85]. However, the diversity effect is achieved at the cost of a reduced number of data streams (and thus reduced data rate). Therefore, there is a diversity-multiplexing tradeoff here [129]. The choice of B according to channel conditions to guarantee a constant data rate has been studied in [50] assuming perfect CSI at both ends. Also, the optimum choice of B to guarantee that the MSE in every data stream is lower than a given target has been studied in [92] where channel estimation error and receive correlation only are considered. It is possible to extend the method in [92] to the more general setting presented in this section.

3.6 Extension to Minimum Weighted MSE Design

In [85], the minimum weighted MSE transceiver design has been studied with perfect CSI at both ends. It includes several other designs as special cases, e.g., the quality-of-service (QoS)-based designs that achieve different SNRs on different sub-channels by adjusting

the weighting matrix. It is straightforward to extend our analysis in previous sections to the minimum weighted MSE design under imperfect CSI. The impacts of channel estimation error and channel correlation on the QoS-based designs can then be investigated.

To give an example, recall the system model in Subsection 2.1.5 and consider the special case of imperfect CSI as in Section 3.4. The minimum weighted MSE design is formulated as

$$\begin{aligned} \min_{\mathbf{F},\mathbf{G}} \quad & \mathbb{E}\left[\| \mathbf{W}^{\frac{1}{2}} (\mathbf{r}-\mathbf{s}) \|^2 \right] \\ \text{subject to} \quad & \text{tr}(\mathbf{F}\mathbf{F}^H) \leq P_T, \end{aligned} \tag{3.36}$$

where $\mathbf{W}$ is a diagonal positive definite weighting matrix. The weighted MSE matrix is defined as

$$\begin{aligned} MSE_{wt}(\mathbf{F},\mathbf{G}) &\overset{\text{def}}{=} \mathbb{E}\left[\mathbf{W}^{\frac{1}{2}} (\mathbf{r}-\mathbf{s}) (\mathbf{r}-\mathbf{s})^H \mathbf{W}^{\frac{1}{2}} \right] \\ &= \mathbf{W}^{\frac{1}{2}} \cdot MSE(\mathbf{F},\mathbf{G}) \cdot \mathbf{W}^{\frac{1}{2}}, \end{aligned} \tag{3.37}$$

where $MSE(\mathbf{F},\mathbf{G})$ in the second equation is from (3.10). The objective function in (3.36) is simply given by

$$\text{tr}\left[MSE_{wt}(\mathbf{F},\mathbf{G}) \right] = \text{tr}\left[\mathbf{W} \cdot MSE(\mathbf{F},\mathbf{G}) \right].$$

The Lagrangian associated with (3.36) is

$$\mathscr{L}_{wt}(\mathbf{F},\mathbf{G},\mu_{wt}) = \text{tr}\left[MSE_{wt}(\mathbf{F},\mathbf{G}) \right] + \mu_{wt} \cdot \left[\text{tr}\left(\mathbf{F}\mathbf{F}^H \right) - P_T \right],$$

where μ_{wt} is the Lagrange multiplier. Using exactly the same method as in previous sections, we can obtain the following theorem, whose proof is omitted for brevity.

Theorem 3 *Assume that the number of data streams B is equal to r, where r is from (3.16). The optimum precoder and decoder for (3.36) have the following general expressions:*

$$\mathbf{F}_{wt,opt} = \left[\sigma_E^2 \cdot P_T \cdot \mathbf{R}_T + \sigma_n^2 \cdot \mathbf{I}_{n_T} \right]^{-\frac{1}{2}} \mathbf{V}\mathbf{\Lambda}_{Fwt,opt}, \tag{3.38}$$

$$\mathbf{G}_{wt,opt} = \mathbf{\Lambda}_{Gwt,opt}\mathbf{V}^H \left[\sigma_E^2 \cdot P_T \cdot \mathbf{R}_T + \sigma_n^2 \cdot \mathbf{I}_{n_T}\right]^{-\frac{1}{2}} \hat{\mathbf{H}}^H, \tag{3.39}$$

and the diagonal $r \times r$ matrices $\mathbf{\Lambda}_{Fwt,opt}$ and $\mathbf{\Lambda}_{Gwt,opt}$ are given by

$$\mathbf{\Lambda}_{Fwt,opt} = \left[\tau_{wt}^{\frac{1}{2}}\mu_{wt}^{-\frac{1}{2}}\sigma_n \cdot \mathbf{W}^{\frac{1}{2}}\mathbf{\Lambda}^{-\frac{1}{2}} - \tau_{wt} \cdot \mathbf{\Lambda}^{-1}\right]_+^{\frac{1}{2}}, \tag{3.40}$$

$$\mathbf{\Lambda}_{Gwt,opt} = \left[\mu_{wt}^{\frac{1}{2}}\tau_{wt}^{-\frac{1}{2}}\frac{1}{\sigma_n} \cdot \mathbf{W}^{-\frac{1}{2}}\mathbf{\Lambda}^{-\frac{1}{2}} - \frac{\mu_{wt}}{\sigma_n^2} \cdot \mathbf{W}^{-1}\mathbf{\Lambda}^{-1}\right]_+^{\frac{1}{2}} \mathbf{\Lambda}^{-\frac{1}{2}}, \tag{3.41}$$

where $\mathbf{V}$ and $\mathbf{\Lambda}$ are from (3.16),

$$\tau_{wt} = \frac{\tilde{a}_2 \cdot P_T}{P_T \cdot \tilde{a}_3 + \tilde{a}_1 \cdot \tilde{a}_3 - \tilde{a}_2 \cdot \tilde{a}_4}, \tag{3.42}$$

$$\mu_{wt} = \frac{\tilde{a}_2 \cdot \sigma_n^2 (P_T \cdot \tilde{a}_3 + \tilde{a}_1 \cdot \tilde{a}_3 - \tilde{a}_2 \cdot \tilde{a}_4)}{(P_T + \tilde{a}_1)^2 \cdot P_T}. \tag{3.43}$$

Scalars $\tilde{a}_1$, $\tilde{a}_2$, $\tilde{a}_3$ and $\tilde{a}_4$ are traces of the $k_{wt} \times k_{wt}$ top-left submatrices of

$$\mathbf{\Lambda}^{-1},\ \mathbf{W}^{\frac{1}{2}}\mathbf{\Lambda}^{-\frac{1}{2}},\ \mathbf{W}^{\frac{1}{2}}\mathbf{\Lambda}^{-\frac{1}{2}}\mathbf{V}^H\left[\sigma_E^2 P_T \mathbf{R}_T + \sigma_n^2 \mathbf{I}_{n_T}\right]^{-1}\mathbf{V},\ \textit{and}\ \mathbf{\Lambda}^{-1}\mathbf{V}^H\left[\sigma_E^2 P_T \mathbf{R}_T + \sigma_n^2 \mathbf{I}_{n_T}\right]^{-1}\mathbf{V},$$

respectively. The integer k_{wt} denotes the number of the non-zero entries of $\mathbf{\Lambda}_{Fwt,opt}$ ($k_{wt} \leq r$). The optimum precoder-decoder pair obtained here is unique up to a unitary transform.

Remark 3.5: When $\mathbf{W} = \mathbf{I}_B$, **Theorem 3** reduces to **Theorem 1**.

Similar to Section 3.5, we can also extend the weighted minimum total MSE design to the case when $\mathbf{R}_T \neq \mathbf{I}_{n_T}, \mathbf{R}_R \neq \mathbf{I}_{n_R}$.

3.7 Simulation Results and Discussions

1. Simulation Scenario

   Let $n_T = n_R = 4$. The exponential model introduced in Subsection 2.1.1 is used for

transmit and receive channel correlation, i.e.,

$$\mathbf{R}_T = \begin{pmatrix} 1 & \rho_T & \rho_T^2 & \rho_T^3 \\ \rho_T & 1 & \rho_T & \rho_T^2 \\ \rho_T^2 & \rho_T & 1 & \rho_T \\ \rho_T^3 & \rho_T^2 & \rho_T & 1 \end{pmatrix},$$

and $\mathbf{R}_R$ is similarly defined with ρ_T replaced by ρ_R ($0 \leq \rho_T, \rho_R < 1$). 4-QAM is used for each data stream. The optimum matrices $\mathbf{F}_{opt}$ and $\mathbf{G}_{opt}$ or $\mathbf{F}_{gopt}$ and $\mathbf{G}_{gopt}$ are chosen specifically as given by (3.19)-(3.20) or (3.32)-(3.33), respectively. For the minimum total MSE design, a relevant performance measure is the average bit error rate (ABER) per data stream [48, 69, 85], defined as

$$ABER = \frac{1}{B}\sum_{j=1}^{B} BER_j,$$

where BER_j is the BER of data stream j. Define SNR as P_T/σ_n^2. For fair comparisons, we fix P_{tr}/σ_n^2 in the training stage and let $\sigma_{ce}^2 = \text{tr}(\mathbf{R}_T^{-1}) \cdot \sigma_n^2/P_{tr}$ vary with $\mathbf{R}_T$. In our simulations, P_{tr}/σ_n^2 is chosen to be 16.016 dB or 26.016 dB, which corresponds to $\sigma_{ce}^2 = 0.1$ or 0.01 if $\mathbf{R}_T = \mathbf{I}_{n_T}$.

2. Effects of Channel Correlation Alone ($\sigma_{ce}^2 = 0$)

Fig. 3.3 is obtained when there is no channel estimation error ($\sigma_{ce}^2 = 0$). High correlation is observed to have a large impact on system performance. For example, when $B = 4$ and $\rho_R = 0$, as ρ_T increases from 0 to 0.5, the loss in SNR is around 1.67 dB. When ρ_T further increases from 0.5 to 0.9, approximately 6.67 dB loss is incurred in the medium to high SNR range. It is clear that reducing B introduces diversity and thus compensates for the loss caused by channel correlation. Therefore, the number of data streams, B, should be chosen carefully according to channel correlation information.

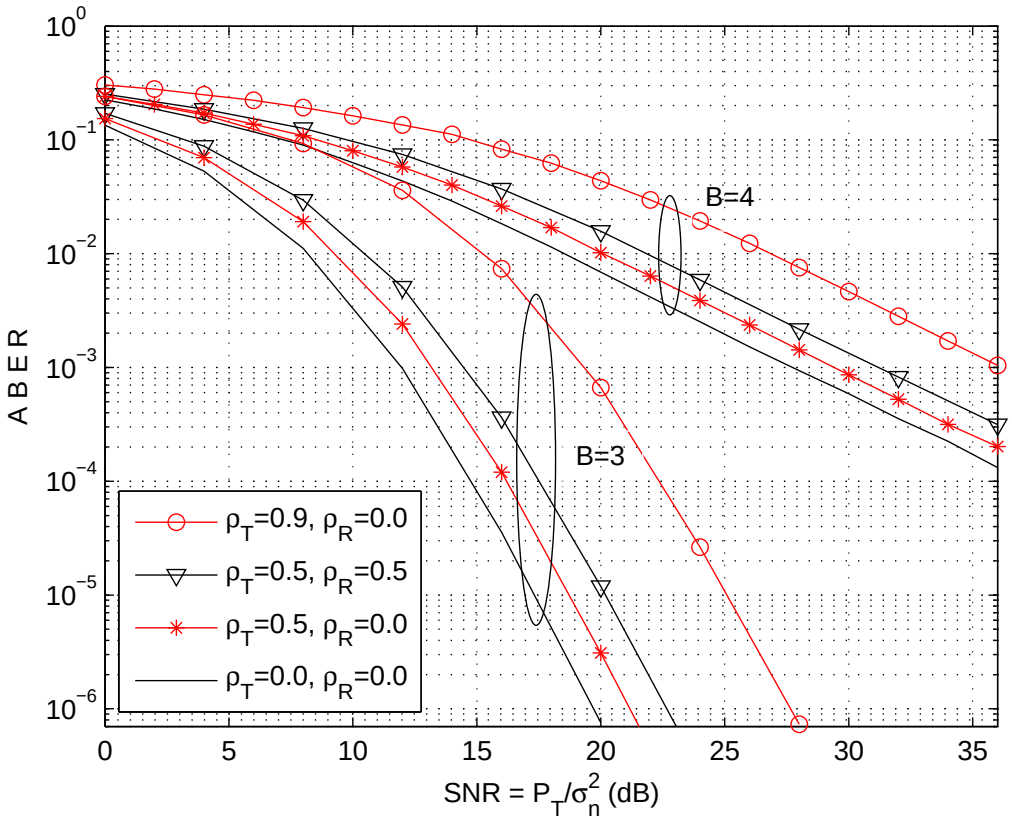

Figure 3.3. The ABER from minimum total MSE design with perfect CSI. $n_T = n_R = 4$, B = 3 or 4. Different amounts of channel correlation are considered: $\rho_T = 0.0, 0.5, 0.9$ and $\rho_R = 0.0, 0.5$.

3. Effects of Channel Estimation Error and Channel Correlation

   Fig. 3.4 shows the ABERs from using the optimum precoder and decoder when the CSI is imperfect.

   Comparing Figs. 3.4 and 3.3, we observe that channel estimation error alone has a tremendously detrimental effect on system ABER performance. Specifically, with $\rho_T = \rho_R = 0$ and $B = 3$, at SNR = 20 dB, the ABER is 7.6×10^{-7} when $\sigma_{ce}^2 = 0$ (see Fig. 3.3). It then increases to 1.4×10^{-5} at the same SNR when $\sigma_{ce}^2 = 0.01$ [corresponding to using $P_{tr}/\sigma_n^2 = 26.016$ dB at the training stage (see Fig. 3.4)]. At medium to high SNR, the performance degradation caused by channel estimation error can be compensated by introducing diversity (i.e., reducing the number of data streams), at the expense of reduced data rate. Also, channel estimation error causes an irreducible error floor at high SNR. High channel correlation further deteriorates system performance. For example, from Fig. 3.4, with $\rho_R = 0$ and $B = 3$, at SNR = 20 dB, when ρ_T increases from 0 to 0.5, the ABER increases from 1.4×10^{-5} to 6.8×10^{-5}, and when ρ_T increases from 0.5 to 0.9, the ABER increases drastically from 6.8×10^{-5} to 8.8×10^{-3}.

4. Optimum Precoder vs. Two Asymptotically Optimum Precoders

   Consider the special case without receive correlation as in Section 3.4. A suboptimum transceiver can be obtained by ignoring the channel correlation information at the transmitter, treating $\hat{\mathbf{H}}$ as if it were the true channel and then applying the results in [85]. In this way, the precoder is restricted to be of the form $\mathbf{F}_{NS} = \mathbf{V}_1 \mathbf{\Lambda}_{FNS}$, where the matrix $\mathbf{V}_1$ consists of the effective eigenvectors (corresponding to the non-zero eigenvalues) of $\hat{\mathbf{H}}^H \hat{\mathbf{H}}$ and $\mathbf{\Lambda}_{FNS}$ is a diagonal matrix for power allocation. The decoder is obtained from (3.25) or (3.45). Based on **Remark 3.1** and **Remark 3.2**, this

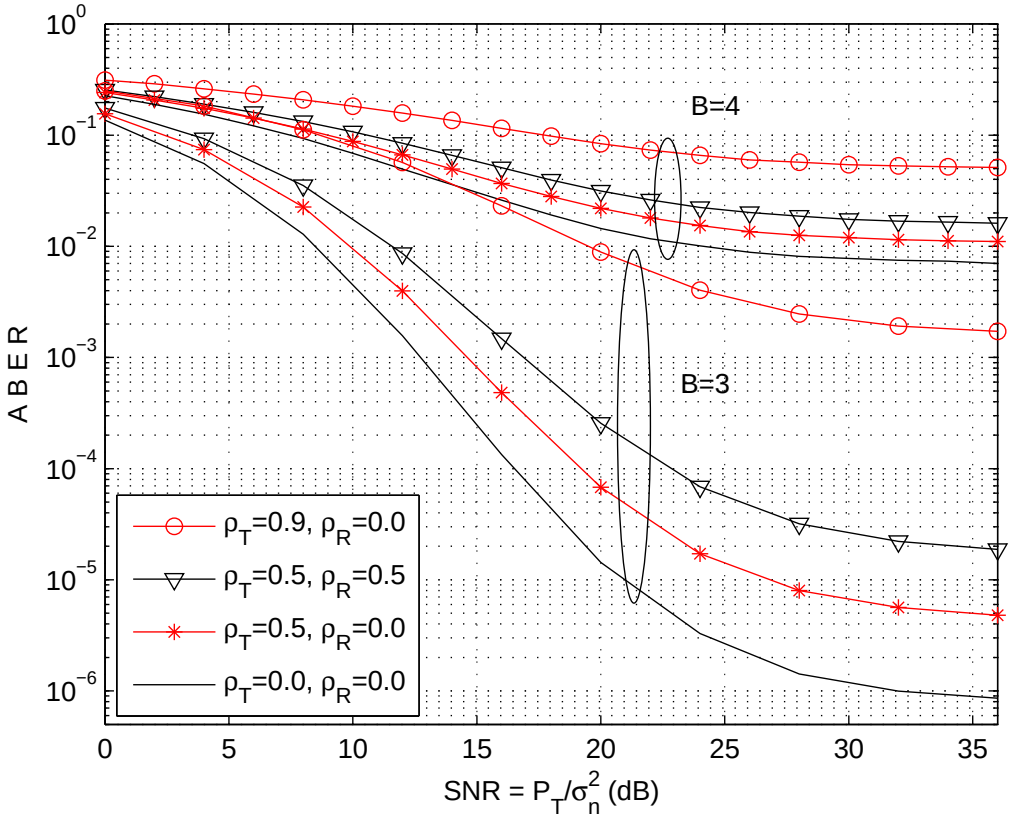

Figure 3.4. The ABER from minimum total MSE design with imperfect CSI. $n_T = n_R = 4$, B = 3 or 4. Different amounts of channel correlation are considered. $P_{tr}/\sigma_n^2 = 26.016$ dB. The values of σ_{ce}^2 are 0.01, 0.015, and 0.0739, for ρ_T = 0.0, 0.5, and 0.9, respectively. Correspondingly, the values of σ_E^2 are 0.0099, 0.0148, and 0.0689, for ρ_T = 0.0, 0.5, and 0.9.

precoder is asymptotically optimum when $\sigma_{ce}^2 \to 0$ (and thus the additive noise is the dominant source of error), or when $\mathbf{R}_T \to \mathbf{I}_{n_T}$. We refer to it as the noise-suppression precoder.

On the other hand, we obtain another transceiver structure by restricting the precoder as $\mathbf{F}_{CC} = \mathbf{R}_T^{-\frac{1}{2}} \mathbf{V}_2 \mathbf{\Lambda}_{FCC}$, where $\mathbf{V}_2$ is composed of the effective eigenvectors of $\hat{\mathbf{H}}_{w0}^H \hat{\mathbf{H}}_{w0}$ and $\mathbf{\Lambda}_{FCC}$ is also a diagonal power allocation matrix. Again, the decoder is determined from (3.45). Based on **Remark 3.2**, this precoder here is asymptotically optimum when P_T/σ_n^2 goes to infinity so that channel estimation error becomes the dominant source of error, or when $\mathbf{R}_T \to \mathbf{I}_{n_T}$. We refer to this as the correlation-cancelation precoder.

It is interesting to compare the optimum precoder in **Theorem 1** and the above two suboptimum ones. The three schemes here have similar computational complexity. Compared to the other two, the noise-suppression precoder does not require correlation information at the transmitter. The performance comparisons shown in Fig. 3.5 remind us of the relationship between the matched filter (the noise-suppression precoder), the zero-forcing filter (the correlation-cancelation precoder), and the optimum linear MMSE filter in multiuser detection [51]. From Fig. 3.5, we observe again the tremendous effect of channel estimation error on system performance.

The noise-suppression precoder represents the direct application of previous results assuming perfect CSI [70, 85, 87] to the case with imperfect CSI. Clearly, this causes a large performance loss at medium to high SNR. We also notice that the correlation-cancelation precoder has close-to-optimum performance at medium to high SNR, since it also utilizes the transmit correlation information. However, inverting the transmit correlation is not optimum at low SNR, and thus the correlation-cancelation structure performs worse than the optimum transmitter in a lower SNR region.

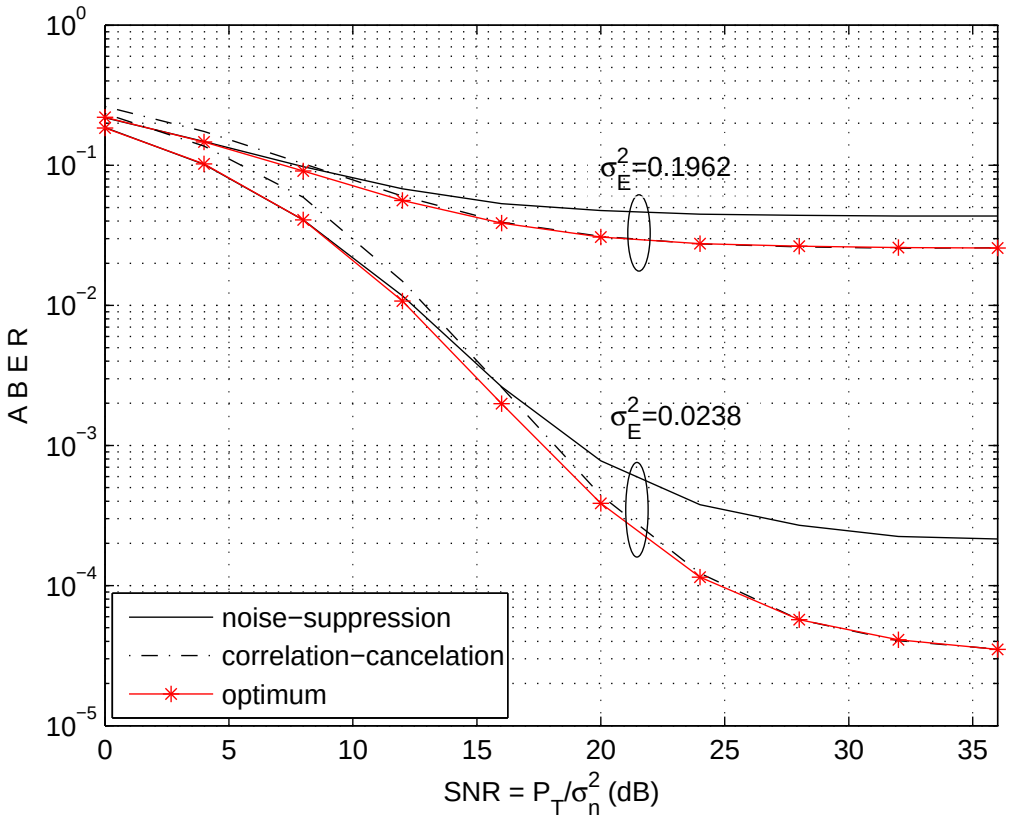

Figure 3.5. Comparison of the optimum and two suboptimum transceivers. $n_T = n_R = 4$, $B = 3$, $\rho_T = 0.7$, $\rho_R = 0.0$. Two values of the training power are used: $P_{tr}/\sigma_n^2 = 26.016$ dB (corresponding to $\sigma_E^2 = 0.0238$), and $P_{tr}/\sigma_n^2 = 16.016$ dB (corresponding to $\sigma_E^2 = 0.1962$).

5. Effect of Transmit Correlation vs. Effect of Receive Correlation

   Fig. 3.6 is a comparison of the effects of transmit and receive correlation. It is clear that the same amount of transmit or receive correlation has exactly the same effect on system performance when the CSI is perfect.

   In the channel estimation described in Section 3.2, the knowledge of $\mathbf{R}_T$ is explicitly used in the training signal design, but the knowledge of $\mathbf{R}_R$ is not. This means the knowledge of $\mathbf{R}_T$ and $\mathbf{R}_R$ is not exploited the same way. Therefore, when there is channel estimation error, the same amount of correlation at the transmitter and the receiver affects system performance differently[3].

6. Effect of Feedback Delay

   We now simulate the effect of feedback delay on the joint precoder/decoder design. Both spatial and temporal channel correlation are considered. At any time instant, the spatial correlation is modeled in the same way as in Subsection 2.1.1. Using the Jakes' model [42], the temporal magnitude correlation of two channel realizations separated Δ seconds apart is given by $\rho_\Delta = J_0^2(2\pi f_d \Delta)$, where $J_0(\cdot)$ denotes the zero-th order Bessel function of the first kind, and f_d is the maximum Doppler frequency. As in [132], we consider the system working at a carrier frequency of $f_c = 2$ GHz. The data rate R_s on each data stream is set to be 400 kilo-symbols per second (ks/s), which implies the symbol duration $T_s = 1/R_s = 2.5 \times 10^{-6}$ s. The terminal speed is v = 30 m/s. Then f_d is calculated to be 200 Hz. We simulate the fading channel according to [73].

[3] As mentioned in Section 3.2, a different CSI model has been used in [66], in which the functions of $\mathbf{R}_T$ and $\mathbf{R}_R$ are symmetric. It is interesting to note that, after applying our analysis with the CSI model used there, the effect of $\mathbf{R}_T$ and $\mathbf{R}_R$ is the same whether there is channel estimation error or not. The same comments also apply to the CSI model used in [128, Section VI].

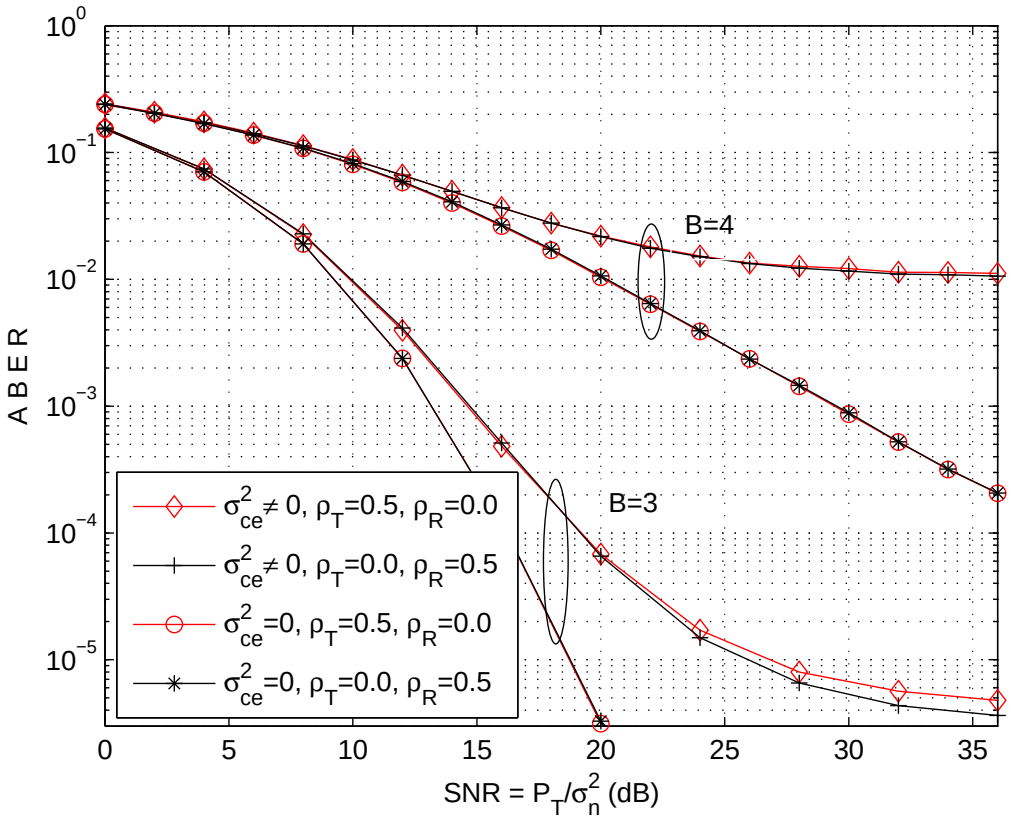

Figure 3.6. Effect of transmit correlation vs. effect of receive correlation. $n_T = n_R = 4$, B = 3 or 4, (ρ_T, ρ_R) = (0.5, 0.0) or (0.0, 0.5), In the case of imperfect CSI, $P_{tr}/\sigma_n^2 = 26.016$ dB. The values of σ_{ce}^2 are 0.01 and 0.015, for ρ_T = 0.0 and 0.5, respectively.

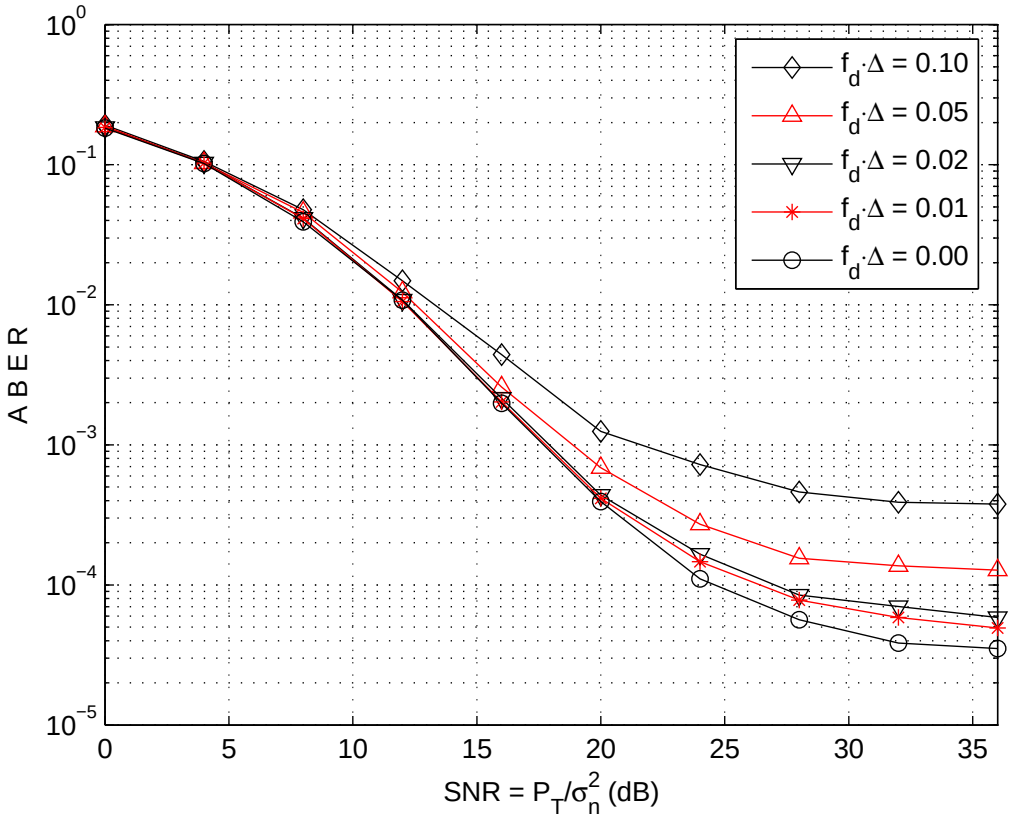

Figure 3.7. The effect of feedback delay on system performance. $n_T = n_R = 4$, B = 3, $\rho_T = 0.7$, $\rho_R = 0.0$, $P_{tr}/\sigma_n^2 = 26.016$ dB (corresponding to σ_E^2 = 0.0238).

At time t, the receiver obtains $\hat{\mathbf{H}}^t$, an estimate of the true channel $\mathbf{H}^t$. Here the superscript denotes the time index, as in Subsection 2.1.1. Due to the feedback delay Δ, the transmitter only knows $\hat{\mathbf{H}}^{t-\Delta}$, i.e., the estimate of $\mathbf{H}^{t-\Delta}$. Therefore, at time t, the precoder $\mathbf{F}$ can only be calculated according to $\hat{\mathbf{H}}^{t-\Delta}$. The decoder $\mathbf{G}$ is calculated from (3.25) or (3.45), and is matched to the precoder. The resulting performances for such a scenario are shown in Fig. 3.7 with different values of Δ.

As shown, as long as the normalized delay $f_d \cdot \Delta$ is smaller than 0.01 (i.e., $\Delta \leq 20\ T_s$ in the example above), the performance degradation is small. Note that $f_d \cdot \Delta = 0.01$

is observed as a critical normalized delay in [19, 132], below which the system can operate satisfactorily. Thus, our system design is robust against reasonably small delays. Similar results can also be observed using other values of system parameters ($\rho_T, P_{tr}/\sigma_n^2, B$, etc.).

3.8 Summary

We have formulated and solved a minimum total MSE transceiver design problem for MIMO systems with channel mean as well as both transmit and receive correlation information at both ends. The structures of the optimum precoder and decoder are obtained. Our results gracefully fit those in the existing literature as channel estimation error diminishes. Simulation results are provided. We have observed that channel estimation error causes an error floor at high SNR and a large performance degradation across the whole SNR range. At medium to high SNR, this degradation can be compensated by introducing diversity. High correlation has a large impact on system performance as well. The same amounts of transmit and receive correlation impact the system performance equivalently under the assumption of perfect channel estimation, whereas under imperfect channel estimation, these two might show different effects on the system performance, depending on the specific channel estimation method employed. The more general minimum weighted MSE design has also been studied, which can be used to assess the performance of some QoS-based designs with imperfect CSI.

3.9 Derivation and Proof Details

3.9.1 Derivations of (3.3) and (3.4)

Perform vectorization operation on (3.2) to obtain

$$vec(\tilde{\mathbf{H}}_w) = vec(\mathbf{H}_w) + (\mathbf{I}_{n_T} \otimes \mathbf{R}_R^{-\frac{1}{2}}) vec(\mathbf{N}_0).$$

Then the minimum MSE (MMSE) estimate of $vec(\mathbf{H}_w)$ is given by [77, p. 156, Eq. (IV.B.53)]

$$\begin{aligned} vec(\hat{\mathbf{H}}_w) &= [\mathbf{I}_{n_T n_R} + \mathbf{I}_{n_T} \otimes \mathbf{R}_R^{-1} \cdot \sigma_{ce}^2]^{-1} vec(\tilde{\mathbf{H}}_w) \\ &= \{\mathbf{I}_{n_T} \otimes [\mathbf{I}_{n_R} + \mathbf{R}_R^{-1} \cdot \sigma_{ce}^2]^{-1}\} vec(\tilde{\mathbf{H}}_w). \end{aligned}$$

Then (3.3) is obtained by converting $vec(\hat{\mathbf{H}}_w)$ back to its matrix version. The resulting estimation error covariance matrix is [77, p. 156, Eq. (IV.B.54)]

$$\begin{aligned} \mathbf{\Psi} &= \mathbb{E}\left\{ \left[vec(\mathbf{H}_w) - vec(\hat{\mathbf{H}}_w)\right] \left[vec(\mathbf{H}_w) - vec(\hat{\mathbf{H}}_w)\right]^H \right\} \\ &= \mathbf{I}_{n_T n_R} - [\mathbf{I}_{n_T n_R} + \sigma_{ce}^2 \cdot (\mathbf{I}_{n_T} \otimes \mathbf{R}_R^{-1})]^{-1} \\ &= \mathbf{I}_{n_T} \otimes [\mathbf{I}_{n_R} - (\mathbf{I}_{n_R} + \sigma_{ce}^2 \mathbf{R}_R^{-1})^{-1}] \\ &= \sigma_{ce}^2 \cdot \underbrace{\mathbf{I}_{n_T} \otimes [\mathbf{R}_R^{-1} (\mathbf{I}_{n_R} + \sigma_{ce}^2 \mathbf{R}_R^{-1})^{-1}]}_{\mathbf{\Psi}_0}. \end{aligned}$$

The estimation error vector can be represented by $\mathbf{\Psi}_0^{\frac{1}{2}} vec(\mathbf{E}_w)$, where $\mathbf{E}_w$ stands for a $n_R \times n_T$ matrix whose entries are i.i.d. $\mathcal{N}_c(0, \sigma_{ce}^2)$ [equivalently, $vec(\mathbf{E}_w) \sim \mathcal{N}_c(0, \sigma_{ce}^2 \cdot \mathbf{I}_{n_T n_R})$]. The matrix version of $\mathbf{\Psi}_0^{\frac{1}{2}} vec(\mathbf{E}_w)$ is given by $\mathbf{R}_R^{-\frac{1}{2}} (\mathbf{I}_{n_R} + \sigma_{ce}^2 \cdot \mathbf{R}_R^{-1})^{-\frac{1}{2}} \mathbf{E}_w$, and (3.4) follows. □

3.9.2 Proof of Existence of a Global Minimum for (3.9)

The problem in (3.9) can be equivalently formulated as [7, p. 130, Section 4.1.3]

$$\min_{\mathbf{F},\ \mathrm{tr}(\mathbf{F}\mathbf{F}^H)\le P_T} \ \min_{\mathbf{G}(\mathbf{F})} \ \mathrm{tr}\left\{MSE\left[\mathbf{F},\mathbf{G}(\mathbf{F})\right]\right\}. \tag{3.44}$$

The minimizing $\mathbf{G}$ for the inner unconstrained minimization is readily shown to be[4]:

$$\mathbf{G} = \mathbf{F}^H\hat{\mathbf{H}}^H\left[\hat{\mathbf{H}}\mathbf{F}\mathbf{F}^H\hat{\mathbf{H}}^H + \sigma_{ce}^2\cdot\mathrm{tr}(\mathbf{R}_T\mathbf{F}\mathbf{F}^H)\cdot\mathbf{R}_{e,R} + \sigma_n^2\cdot\mathbf{I}_{n_R}\right]^{-1}, \tag{3.45}$$

which is the linear MMSE data estimator (Wiener filter) given $\hat{\mathbf{H}}$ and $\mathbf{F}$ [46, Chapter 12] [77]. Substituting (3.45) into (3.44), the problem in (3.9) can be equivalently formulated as

$$\min_{\mathbf{F},\ \mathrm{tr}(\mathbf{F}\mathbf{F}^H)\le P_T} \mathrm{tr}\left[MSE\left(\mathbf{F}\right)\right], \tag{3.46}$$

where

$$MSE\left(\mathbf{F}\right) = \left\{\mathbf{I}_B + \mathbf{F}^H\hat{\mathbf{H}}^H[\sigma_{ce}^2\cdot\mathrm{tr}(\mathbf{R}_T\mathbf{F}\mathbf{F}^H)\cdot\mathbf{R}_{e,R} + \sigma_n^2\cdot\mathbf{I}_{n_R}]^{-1}\hat{\mathbf{H}}\mathbf{F}\right\}^{-1}. \tag{3.47}$$

The feasible set of (3.46) is $\left\{\mathbf{F}|\mathrm{tr}(\mathbf{F}\mathbf{F}^H)\le P_T\right\}$, a (closed and bounded) Frobenius norm ball of radius $\sqrt{P_T}$ [7]. The objective function of (3.46) is continuous at all points of the feasible set. Thus, according to Weierstrass' Theorem [5, p. 654, **Proposition A.8**], there exists a global minimum for the problem given by (3.46). Since (3.9) and (3.46) are equivalent, the same global minimum also exists for (3.9) [7, p. 130, Section 4.1.3]. In addition, the minimizing $\mathbf{F}$ is the same for both problems, while the minimizing $\mathbf{G}$ for (3.9) is calculated according to (3.45). □

3.9.3 Derivations of (3.11)-(3.14)

For partial derivatives of a scalar-valued trace function of complex matrices, one can simply apply the results in [35, Table II]. However, in many cases, it is desirable to have a systematic way of calculating derivatives of more complicated scalar-valued functions with

[4] In fact, the inner optimization problem is a convex quadratic program [7, p. 152].

respective to their matrix arguments. Below we introduce preliminary results on complex matrix differentiation, which are used in this chapter as well as in subsequent chapters.

3.9.3.1 Preliminaries of Complex Matrix Differentials

We first present some complex matrix differential identities, which will be used in subsequent derivations. Here $i = \sqrt{-1}$. Based on derivative operations on real-valued matrices [60] [63, Appendix C, p. 525], we obtain:

$$\frac{\partial \text{ tr}\left[\mathbf{A}\mathbf{Z}^H\right]}{\partial \Re\mathbf{Z}} = \mathbf{A}, \quad i \cdot \frac{\partial \text{tr}\left[\mathbf{A}\mathbf{Z}^H\right]}{\partial \Im\mathbf{Z}} = \mathbf{A},$$
$$\frac{\partial \text{ tr}[\mathbf{B}\mathbf{Z}]}{\partial \Re\mathbf{Z}} = \mathbf{B}^T, \quad i \cdot \frac{\partial \text{ tr}[\mathbf{B}\mathbf{Z}]}{\partial \Im\mathbf{Z}} = -\mathbf{B}^T.$$

The following definition of the generalized complex derivative will be used [8]. Let z be a complex-valued scalar variable.

$$\frac{df(z)}{dz} = \frac{1}{2}\left[\frac{\partial f(z)}{\partial \Re z} - i \cdot \frac{\partial f(z)}{\partial \Im z}\right].$$

The conjugate complex derivative is given by

$$\frac{df(z)}{dz^*} = \frac{1}{2}\left[\frac{\partial f(z)}{\partial \Re z} + i \cdot \frac{\partial f(z)}{\partial \Im z}\right].$$

Furthermore, according to [8] [35, **Theorem** 2], to find a stationary point of the real scalar function $f(\mathbf{Z}, \mathbf{Z}^*)$, it suffices to determine it from *either* of the following:

$$\frac{df(\mathbf{Z}, \mathbf{Z}^*)}{d\mathbf{Z}} = 0, \text{ or } \frac{df(\mathbf{Z}, \mathbf{Z}^*)}{d\mathbf{Z}^*} = 0.$$

Therefore, to derive (3.11)-(3.12) in our case, we only need to consider taking the partial derivatives of $\mathscr{L}_1(\mathbf{F}, \mathbf{G}, \mu_1)$ with respect to $\mathbf{F}^*$ and $\mathbf{G}^*$. In fact, taking the partial derivatives of $\mathscr{L}_1(\mathbf{F}, \mathbf{G}, \mu_1)$ with respect to $\mathbf{F}$ and $\mathbf{G}$ yields the same equations.

3.9.3.2 Derivations of (3.11)-(3.14)

Note that (3.13)-(3.14) follow from the power constraint and the complementary slackness, respectively.

Using the identities presented earlier, we obtain, with respect to $\mathbf{F}$ and $\mathbf{F}^H$,

$$\begin{aligned}
&\partial \mathscr{L}_1(\mathbf{F},\mathbf{G},\mu_1) \\
&= \mathrm{tr}\left[\mathbf{G}\hat{\mathbf{H}}(\partial\mathbf{F})\,\mathbf{F}^H\hat{\mathbf{H}}^H\mathbf{G}^H - \mathbf{G}\hat{\mathbf{H}}(\partial\mathbf{F}) + \mathbf{G}\hat{\mathbf{H}}\mathbf{F}(\partial\mathbf{F}^H)\,\hat{\mathbf{H}}^H\mathbf{G}^H - (\partial\mathbf{F}^H)\,\hat{\mathbf{H}}^H\mathbf{G}^H\right] \\
&\quad + \sigma_E^2\cdot\mathrm{tr}(\mathbf{G}\mathbf{G}^H)\cdot\mathrm{tr}\left[\mathbf{R}_T(\partial\mathbf{F})\mathbf{F}^H + \mathbf{R}_T\mathbf{F}(\partial\mathbf{F}^H)\right] + \mu_1\cdot\mathrm{tr}\left[(\partial\mathbf{F})\mathbf{F}^H + \mathbf{F}(\partial\mathbf{F}^H)\right] \\
&= \mathrm{tr}\left\{\left[\mathbf{F}^H\hat{\mathbf{H}}^H\mathbf{G}^H\mathbf{G}\hat{\mathbf{H}} - \mathbf{G}\hat{\mathbf{H}} + \sigma_E^2\cdot\mathrm{tr}(\mathbf{G}\mathbf{G}^H)\cdot\mathbf{F}^H\mathbf{R}_T + \mu_1\cdot\mathbf{F}^H\right](\partial\mathbf{F})\right\} \\
&\quad + \mathrm{tr}\left\{\left[\hat{\mathbf{H}}^H\mathbf{G}^H\mathbf{G}\hat{\mathbf{H}}\mathbf{F} - \hat{\mathbf{H}}^H\mathbf{G}^H + \sigma_E^2\cdot\mathrm{tr}(\mathbf{G}\mathbf{G}^H)\cdot\mathbf{R}_T\mathbf{F} + \mu_1\cdot\mathbf{F}\right](\partial\mathbf{F}^H)\right\}.
\end{aligned}$$

Therefore,

$$\begin{aligned}
\frac{\partial \mathscr{L}_1(\mathbf{F},\mathbf{G},\mu_1)}{\partial \Re\mathbf{F}} &= \left[\mathbf{F}^H\hat{\mathbf{H}}^H\mathbf{G}^H\mathbf{G}\hat{\mathbf{H}} - \mathbf{G}\hat{\mathbf{H}} + \sigma_E^2\cdot\mathrm{tr}(\mathbf{G}\mathbf{G}^H)\cdot\mathbf{F}^H\mathbf{R}_T + \mu_1\cdot\mathbf{F}^H\right]^T \\
&\quad + \left[\hat{\mathbf{H}}^H\mathbf{G}^H\mathbf{G}\hat{\mathbf{H}}\mathbf{F} - \hat{\mathbf{H}}^H\mathbf{G}^H + \sigma_E^2\cdot\mathrm{tr}(\mathbf{G}\mathbf{G}^H)\cdot\mathbf{R}_T\mathbf{F} + \mu_1\cdot\mathbf{F}\right], \\
i\cdot\frac{\partial \mathscr{L}_1(\mathbf{F},\mathbf{G},\mu_1)}{\partial \Im\mathbf{F}} &= -\left[\mathbf{F}^H\hat{\mathbf{H}}^H\mathbf{G}^H\mathbf{G}\hat{\mathbf{H}} - \mathbf{G}\hat{\mathbf{H}} + \sigma_E^2\cdot\mathrm{tr}(\mathbf{G}\mathbf{G}^H)\cdot\mathbf{F}^H\mathbf{R}_T + \mu_1\cdot\mathbf{F}^H\right]^T \\
&\quad + \left[\hat{\mathbf{H}}^H\mathbf{G}^H\mathbf{G}\hat{\mathbf{H}}\mathbf{F} - \hat{\mathbf{H}}^H\mathbf{G}^H + \sigma_E^2\cdot\mathrm{tr}(\mathbf{G}\mathbf{G}^H)\cdot\mathbf{R}_T\mathbf{F} + \mu_1\cdot\mathbf{F}\right],
\end{aligned}$$

and

$$\begin{aligned}
\frac{\partial \mathscr{L}_1(\mathbf{F},\mathbf{G},\mu_1)}{\partial \mathbf{F}^*} &= \frac{1}{2}\left[\frac{\partial \mathscr{L}_1(\mathbf{F},\mathbf{G},\mu_1)}{\partial \Re\mathbf{F}} + i\cdot\frac{\partial \mathscr{L}_1(\mathbf{F},\mathbf{G},\mu_1)}{\partial \Im\mathbf{F}}\right] \\
&= \hat{\mathbf{H}}^H\mathbf{G}^H\mathbf{G}\hat{\mathbf{H}}\mathbf{F} - \hat{\mathbf{H}}^H\mathbf{G}^H + \sigma_E^2\cdot\mathrm{tr}(\mathbf{G}\mathbf{G}^H)\cdot\mathbf{R}_T\mathbf{F} + \mu_1\cdot\mathbf{F}.
\end{aligned}$$

Similarly, with respect to $\mathbf{G}$ and $\mathbf{G}^H$,

$$\begin{aligned}
&\partial \mathscr{L}_1(\mathbf{F},\mathbf{G},\mu_1) \\
&= \mathrm{tr}\left\{\left[\hat{\mathbf{H}}\mathbf{F}\mathbf{F}^H\hat{\mathbf{H}}^H\mathbf{G}^H - \hat{\mathbf{H}}\mathbf{F} + [\sigma_n^2 + \sigma_E^2\cdot\mathrm{tr}(\mathbf{R}_T\mathbf{F}\mathbf{F}^H)]\cdot\mathbf{G}^H\right](\partial\mathbf{G})\right\} \\
&\quad + \mathrm{tr}\left\{\left[\mathbf{G}\hat{\mathbf{H}}\mathbf{F}\mathbf{F}^H\hat{\mathbf{H}}^H - \mathbf{F}^H\hat{\mathbf{H}}^H + [\sigma_n^2 + \sigma_E^2\cdot\mathrm{tr}(\mathbf{R}_T\mathbf{F}\mathbf{F}^H)]\cdot\mathbf{G}\right](\partial\mathbf{G}^H)\right\}.
\end{aligned}$$

Thus,

$$\begin{aligned}\frac{\partial \mathscr{L}_1(\mathbf{F},\mathbf{G},\mu_1)}{\partial \Re\mathbf{G}} &= \left[\hat{\mathbf{H}}\mathbf{F}\mathbf{F}^H\hat{\mathbf{H}}^H\mathbf{G}^H - \hat{\mathbf{H}}\mathbf{F} + [\sigma_n^2+\sigma_E^2\cdot\mathrm{tr}(\mathbf{R}_T\mathbf{F}\mathbf{F}^H)]\cdot\mathbf{G}^H\right]^T \\ &\quad + \left[\mathbf{G}\hat{\mathbf{H}}\mathbf{F}\mathbf{F}^H\hat{\mathbf{H}}^H - \mathbf{F}^H\hat{\mathbf{H}}^H + [\sigma_n^2+\sigma_E^2\cdot\mathrm{tr}(\mathbf{R}_T\mathbf{F}\mathbf{F}^H)]\cdot\mathbf{G}\right], \\ i\cdot\frac{\partial \mathscr{L}_1(\mathbf{F},\mathbf{G},\mu_1)}{\partial \Im\mathbf{G}} &= -\left[\hat{\mathbf{H}}\mathbf{F}\mathbf{F}^H\hat{\mathbf{H}}^H\mathbf{G}^H - \hat{\mathbf{H}}\mathbf{F} + [\sigma_n^2+\sigma_E^2\cdot\mathrm{tr}(\mathbf{R}_T\mathbf{F}\mathbf{F}^H)]\cdot\mathbf{G}^H\right]^T \\ &\quad + \left[\mathbf{G}\hat{\mathbf{H}}\mathbf{F}\mathbf{F}^H\hat{\mathbf{H}}^H - \mathbf{F}^H\hat{\mathbf{H}}^H + [\sigma_n^2+\sigma_E^2\cdot\mathrm{tr}(\mathbf{R}_T\mathbf{F}\mathbf{F}^H)]\cdot\mathbf{G}\right],\end{aligned}$$

and

$$\begin{aligned}\frac{\partial \mathscr{L}_1(\mathbf{F},\mathbf{G},\mu_1)}{\partial \mathbf{G}^*} &= \frac{1}{2}\left[\frac{\partial \mathscr{L}_1(\mathbf{F},\mathbf{G},\mu_1)}{\partial \Re\mathbf{G}} + i\cdot\frac{\partial \mathscr{L}_1(\mathbf{F},\mathbf{G},\mu_1)}{\partial \Im\mathbf{G}}\right] \\ &= \mathbf{G}\hat{\mathbf{H}}\mathbf{F}\mathbf{F}^H\hat{\mathbf{H}}^H - \mathbf{F}^H\hat{\mathbf{H}}^H + [\sigma_n^2+\sigma_E^2\cdot\mathrm{tr}(\mathbf{R}_T\mathbf{F}\mathbf{F}^H)]\cdot\mathbf{G}.\end{aligned}$$

Set

$$\frac{\partial \mathscr{L}_1(\mathbf{F},\mathbf{G},\mu_1)}{\partial\, \mathbf{F}^*} = 0 \quad \text{and} \quad \frac{\partial \mathscr{L}_1(\mathbf{F},\mathbf{G},\mu_1)}{\partial\, \mathbf{G}^*} = 0,$$

and then we obtain (3.11)-(3.12). This finishes the calculations of (3.11)-(3.14). □

3.9.4 Proof of Lemma 1

Pre-multiplying both sides of (3.11) by **G**, we obtain

$$\mathbf{G}\hat{\mathbf{H}}\mathbf{F}\mathbf{F}^H\hat{\mathbf{H}}^H\mathbf{G}^H + [\sigma_n^2+\sigma_E^2\cdot\mathrm{tr}(\mathbf{R}_T\mathbf{F}\mathbf{F}^H)]\cdot\mathbf{G}\mathbf{G}^H = \mathbf{G}\hat{\mathbf{H}}\mathbf{F}. \tag{3.48}$$

Similarly, post-multiplying both sides of (3.12) by **F**, to get

$$\mathbf{F}^H\hat{\mathbf{H}}^H\mathbf{G}^H\mathbf{G}\hat{\mathbf{H}}\mathbf{F} + \sigma_E^2\cdot\mathrm{tr}(\mathbf{G}\mathbf{G}^H)\cdot\mathbf{F}^H\mathbf{R}_T\mathbf{F} + \mu_1\cdot\mathbf{F}^H\mathbf{F} = \mathbf{G}\hat{\mathbf{H}}\mathbf{F}. \tag{3.49}$$

Clearly, $\mathbf{G}\hat{\mathbf{H}}\mathbf{F}$ must be Hermitian. From (3.48) and (3.49),

$$[\sigma_n^2+\sigma_E^2\cdot\mathrm{tr}(\mathbf{R}_T\mathbf{F}\mathbf{F}^H)]\cdot\mathbf{G}\mathbf{G}^H = \sigma_E^2\cdot\mathrm{tr}(\mathbf{G}\mathbf{G}^H)\cdot\mathbf{F}^H\mathbf{R}_T\mathbf{F} + \mu_1\cdot\mathbf{F}^H\mathbf{F}.$$

Taking the traces at both sides, we obtain $\sigma_n^2\cdot\mathrm{tr}(\mathbf{G}\mathbf{G}^H) = \mu_1\cdot\mathrm{tr}(\mathbf{F}^H\mathbf{F})$. Due to (3.14), if $\mu_1 > 0$, $\mathrm{tr}(\mathbf{F}^H\mathbf{F})$ must be equal to P_T, which yields $\mu_1 = \sigma_n^2\cdot\mathrm{tr}(\mathbf{G}\mathbf{G}^H)/P_T$, the desired

result. Assume $\mathbf{F} \neq 0$ [i.e., $\mathrm{tr}(\mathbf{F}\mathbf{F}^H) > 0$]. Then, if $\mu_1 = 0$, we must have $\mathrm{tr}(\mathbf{G}\mathbf{G}^H) = 0$, and $\mu_1 = \sigma_n^2 \cdot \mathrm{tr}(\mathbf{G}\mathbf{G}^H)/P_T$ is still valid. Finally, it is easy to see that it holds even when $\mathbf{F} = 0$, $\mathbf{G} = 0$ and $\mu_1 = 0$. This concludes the proof of **Lemma 1**. □

3.9.5 Proof of Lemma 2

Assumed $B = r$. Let the matrix $\mathbf{F}$ be expressed as

$$\begin{aligned}\mathbf{F} &= \left[\sigma_E^2 \cdot P_T \cdot \mathbf{R}_T + \sigma_n^2 \cdot \mathbf{I}_{n_T}\right]^{-\frac{1}{2}} [\mathbf{V}\ \ \tilde{\mathbf{V}}][\mathbf{\Lambda}_F^H\ \ \tilde{\mathbf{\Lambda}}_F^H]^H \\ &= \left[\sigma_E^2 \cdot P_T \cdot \mathbf{R}_T + \sigma_n^2 \cdot \mathbf{I}_{n_T}\right]^{-\frac{1}{2}} [\underbrace{\mathbf{V}\mathbf{\Lambda}_F}_{\mathbf{F}_\parallel} + \underbrace{\tilde{\mathbf{V}}\tilde{\mathbf{\Lambda}}_F}_{\mathbf{F}_\perp}],\end{aligned} \tag{3.50}$$

where $\mathbf{V}$ and $\tilde{\mathbf{V}}$ come from (3.16), and $\mathbf{\Lambda}_F$ and $\tilde{\mathbf{\Lambda}}_F$ are arbitrary $r \times r$ and $(n_T - r) \times r$ matrices, respectively. Since $[\sigma_E^2 \cdot P_T \cdot \mathbf{R}_T + \sigma_n^2 \cdot \mathbf{I}_{n_T}]$ is of full rank, $[\mathbf{V}\ \ \tilde{\mathbf{V}}]$ is a $n_T \times n_T$ unitary matrix and $[\mathbf{\Lambda}_F^H\ \ \tilde{\mathbf{\Lambda}}_F^H]^H$ denotes an arbitrary $n_T \times r$ matrix, (3.50) is a general expression for $\mathbf{F}$. Define $\mathbf{F}_\parallel = \mathbf{V}\mathbf{\Lambda}_F$ and $\mathbf{F}_\perp = \tilde{\mathbf{V}}\tilde{\mathbf{\Lambda}}_F$. It can be verified that

$$\mathbf{F}_\perp^H \mathbf{F}_\parallel = 0, \quad \text{and} \quad \mathbf{F}_\parallel^H \mathbf{F}_\perp = 0. \tag{3.51}$$

Furthermore, due to (3.16), we have the following singular value decomposition

$$\hat{\mathbf{H}}\left[\sigma_E^2 \cdot P_T \cdot \mathbf{R}_T + \sigma_n^2 \cdot \mathbf{I}_{n_T}\right]^{-\frac{1}{2}} = \mathbf{U}_1 \mathbf{\Lambda}^{\frac{1}{2}} \mathbf{V}^H,$$

where $\mathbf{U}_1$ is a $n_R \times r$ matrix satisfying $\mathbf{U}_1^H \mathbf{U}_1 = \mathbf{I}_r$ and $\mathbf{V}$ is the same as in (3.16). Then it can be easily seen that

$$\hat{\mathbf{H}}\left[\sigma_E^2 \cdot P_T \cdot \mathbf{R}_T + \sigma_n^2 \cdot \mathbf{I}_{n_T}\right]^{-\frac{1}{2}} \mathbf{F}_\perp = 0. \tag{3.52}$$

By using **Lemma 1**, (3.12) can be rewritten as

$$\mathbf{F}^H \hat{\mathbf{H}}^H \mathbf{G}^H \mathbf{G} \hat{\mathbf{H}} + \frac{\mathrm{tr}(\mathbf{G}\mathbf{G}^H)}{P_T} \cdot \mathbf{F}^H [\sigma_E^2 \cdot P_T \cdot \mathbf{R}_T + \sigma_n^2 \cdot \mathbf{I}_{n_T}] = \mathbf{G}\hat{\mathbf{H}}. \tag{3.53}$$

Post-multiplying both sides of (3.53) by $\left[\sigma_E^2 \cdot P_T \cdot \mathbf{R}_T + \sigma_n^2 \cdot \mathbf{I}_{n_T}\right]^{-\frac{1}{2}} \mathbf{F}_\perp$, using (3.51) and (3.52), we get $\mathbf{F}_\perp^H \mathbf{F}_\perp = 0$, i.e., $\mathbf{F}_\perp = 0$. This means

$$\mathbf{F} = [\sigma_E^2 \cdot P_T \cdot \mathbf{R}_T + \sigma_n^2 \cdot \mathbf{I}_{n_T}]^{-\frac{1}{2}} \mathbf{V} \mathbf{\Lambda}_F,$$

and thus (3.17) holds. Now let $\tau_1 = \sigma_n^2 + \sigma_E^2 \cdot \mathrm{tr}(\mathbf{R}_T \mathbf{F} \mathbf{F}^H)$. The matrix $\mathbf{G}$ satisfying (3.11) is given by

$$\begin{aligned}
\mathbf{G} &= \mathbf{F}^H \hat{\mathbf{H}}^H [\hat{\mathbf{H}} \mathbf{F} \mathbf{F}^H \hat{\mathbf{H}}^H + \tau_1 \cdot \mathbf{I}_{n_R}]^{-1} \\
&= [\mathbf{F}^H \hat{\mathbf{H}}^H \hat{\mathbf{H}} \mathbf{F} + \tau_1 \cdot \mathbf{I}_r]^{-1} \mathbf{F}^H \hat{\mathbf{H}}^H \\
&= \underbrace{[\mathbf{F}^H \hat{\mathbf{H}}^H \hat{\mathbf{H}} \mathbf{F} + \tau_1 \cdot \mathbf{I}_r]^{-1} \mathbf{\Lambda}_F^H}_{\mathbf{J}_1} \mathbf{V}^H \left[\sigma_E^2 \cdot P_T \cdot \mathbf{R}_T + \sigma_n^2 \cdot \mathbf{I}_{n_T}\right]^{-\frac{1}{2}} \hat{\mathbf{H}}^H,
\end{aligned}$$

where the second equation is obtained using the matrix inversion lemma [60], the third equation is obtained by substituting (3.17), and $\mathbf{J}_1 \stackrel{\text{def}}{=} [\mathbf{F}^H \hat{\mathbf{H}}^H \hat{\mathbf{H}} \mathbf{F} + \tau_1 \cdot \mathbf{I}_r]^{-1} \mathbf{\Lambda}_F^H$ is an arbitrary $r \times r$ matrix. Let $\mathbf{\Lambda}_G$ denote an arbitrary $r \times r$ matrix. The general $\mathbf{G}$ satisfying (3.11) can thus be expressed as

$$\mathbf{G} = \mathbf{\Lambda}_G \mathbf{V}^H \left[\sigma_E^2 \cdot P_T \cdot \mathbf{R}_T + \sigma_n^2 \cdot \mathbf{I}_{n_T}\right]^{-\frac{1}{2}} \hat{\mathbf{H}}^H.$$

Therefore, (3.18) holds. □

3.9.6 Deriving (3.19)-(3.24) and Determining k_0 in Theorem 1

Assume $\mathbf{F} \neq 0$. We first show how to obtain (3.19)-(3.24). Post-multiplying both sides of (3.53) [which is from (3.12)] by $\mathbf{F}$, we get

$$\mathbf{F}^H \hat{\mathbf{H}}^H \mathbf{G}^H \mathbf{G} \hat{\mathbf{H}} \mathbf{F} + \frac{\mathrm{tr}(\mathbf{G}\mathbf{G}^H)}{P_T} \cdot \mathbf{F}^H [\sigma_E^2 \cdot P_T \cdot \mathbf{R}_T + \sigma_n^2 \cdot \mathbf{I}_{n_T}] \mathbf{F} = \mathbf{G} \hat{\mathbf{H}} \mathbf{F}. \tag{3.54}$$

Let $\tau_1 = \sigma_n^2 + \sigma_E^2 \cdot \mathrm{tr}(\mathbf{R}_T \mathbf{F}\mathbf{F}^H)$ as in Subsection 3.9.5. Per **Lemma 2**, substituting (3.17) and (3.18) into (3.48) and (3.54), using **Lemma 1**, we obtain the following identities, respectively,

$$\mathbf{\Lambda}_G \mathbf{\Lambda} \mathbf{\Lambda}_F = \mathbf{\Lambda}_G \mathbf{\Lambda} \mathbf{\Lambda}_F \mathbf{\Lambda}_F^H \mathbf{\Lambda} \mathbf{\Lambda}_G^H + \tau_1 \mathbf{\Lambda}_G \mathbf{\Lambda} \mathbf{\Lambda}_G^H,$$
$$\mathbf{\Lambda}_G \mathbf{\Lambda} \mathbf{\Lambda}_F = \mathbf{\Lambda}_F^H \mathbf{\Lambda} \mathbf{\Lambda}_G^H \mathbf{\Lambda}_G \mathbf{\Lambda} \mathbf{\Lambda}_F + (\mu_1/\sigma_n^2) \mathbf{\Lambda}_F^H \mathbf{\Lambda}_F.$$

Based on the above two equations, the optimum $\mathbf{\Lambda}_F$ and $\mathbf{\Lambda}_G$ can be shown to be diagonal without loss of generality as in [85], and are given by $\mathbf{\Lambda}_{Fopt}$ and $\mathbf{\Lambda}_{Gopt}$ in (3.21) and (3.22), respectively. Finally, insert (3.19)-(3.22) into $\mathrm{tr}(\mathbf{F}\mathbf{F}^H) = P_T$ and $\mu_1 = \sigma_n^2 \cdot \mathrm{tr}(\mathbf{G}\mathbf{G}^H)/P_T$, to obtain two equations with τ_1 and μ_1 being the variables. Solving these two equations, we can find τ_1 and μ_1 as given by (3.23) and (3.24), respectively.

An iterative procedure for calculating the number k_0 in **Theorem 1** is described below. Let λ_l be the l-th entry on the main diagonal of $\mathbf{\Lambda}$ ($l = 1, \ldots, B = r$). Recall that the diagonal elements of $\mathbf{\Lambda}$ are arranged in decreasing order. Initialize $k = B$.

1. Calculate τ_1 and μ_1 from (3.23) and (3.24), respectively. If $\mu_1 \leq \lambda_k \sigma_n^2/\tau_1$, stop and set $k_0 = k$; else: go to step 2.

2. Let $\mathbf{\Lambda}_{Fopt,k} := 0$ and $k := k - 1$. Go to step 1.

We now compare the total MSE obtained from the non-zero solutions and the zero solution satisfying the KKT conditions (3.11)-(3.14). The MSE corresponding to the zero solution is simply given by

$$mse_{zero} = \mathrm{tr}\,(\mathbf{I}_B) = B,$$

whereas the MSE corresponding to all non-zero solutions is the same and is given by:

$$mse_{nz} = \mathrm{tr}\left[\left(\mathbf{I}_B + \frac{1}{\tau_1} \cdot \mathbf{F}_{opt}^H \hat{\mathbf{H}}^H \hat{\mathbf{H}} \mathbf{F}_{opt}\right)^{-1}\right].$$

Since it can be verified by direct calculations that $\mathbf{F}_{opt}^H \hat{\mathbf{H}}^H \hat{\mathbf{H}} \mathbf{F}_{opt}$ is positive semidefinite, we have

$$\mathbf{I}_B + \frac{1}{\tau_1} \cdot \mathbf{F}_{opt}^H \hat{\mathbf{H}}^H \hat{\mathbf{H}} \mathbf{F}_{opt} \succeq \mathbf{I}_B.$$

Note that if two positive semidefinite matrices $\mathbf{A}$ and $\mathbf{B}$ satisfy $\mathbf{B} \succeq \mathbf{A}$ (or $\mathbf{A} \preceq \mathbf{B}$), then $\mathbf{B} - \mathbf{A}$ is a positive semidefinite matrix. The above inequality implies

$$\left[\mathbf{I}_B + \frac{1}{\tau_1} \cdot \mathbf{F}_{opt}^H \hat{\mathbf{H}}^H \hat{\mathbf{H}} \mathbf{F}_{opt} \right]^{-1} \preceq \mathbf{I}_B.$$

According to [64, pp. 585-586], if $\mathbf{A}_1 \preceq \mathbf{A}_2$, then $\mathrm{tr}(\mathbf{A}_1) \leq \mathrm{tr}(\mathbf{A}_2)$. Therefore, $mse_{nz} \leq mse_{zero}$. □

3.9.7 Proof of Theorem 2

Assume $B = r_g$. It is easy to identify the zero solution satisfying the KKT conditions (3.25)-(3.28): $\mathbf{F} = 0, \mathbf{G} = 0, \mu_g = 0$. We now focus on finding the non-zero solutions.

First, following the same line in Subsection 3.9.4, based on the KKT conditions (3.25)-(3.28), it can be shown that

$$\mu_g = \sigma_n^2 \cdot \mathrm{tr}\left(\mathbf{G}\mathbf{G}^H\right) / P_T.$$

In general, the matrix $\mathbf{F}$ can be expressed as

$$\mathbf{F} = \left[\tau_2 \cdot \sigma_{ce}^2 \cdot \mathbf{R}_T + \mu_g \cdot \mathbf{I}_{n_T} \right]^{-\frac{1}{2}} \left[\mathbf{V}_g \ \tilde{\mathbf{V}}_g \right] \left[\mathbf{\Lambda}_{F,g}^H \ \tilde{\mathbf{\Lambda}}_{F,g}^H \right]^H,$$

where τ_2 has been defined in (3.30), and $\mathbf{V}_g$ and $\tilde{\mathbf{V}}_g$ have been defined in (3.31). Here $\mathbf{\Lambda}_{F,g}$ and $\tilde{\mathbf{\Lambda}}_{F,g}$ denote $r_g \times r_g$ and $r_g \times (n_T - r_g)$ arbitrary matrices, respectively. Same as in Subsection 3.9.6, we express $\mathbf{F}$ as follows:

$$\mathbf{F} = \left[\tau_2 \cdot \sigma_{ce}^2 \cdot \mathbf{R}_T + \mu_g \cdot \mathbf{I}_{n_T} \right]^{-\frac{1}{2}} \left[\underbrace{\mathbf{V}_g \mathbf{\Lambda}_{F,g}}_{\mathbf{F}_{g,\parallel}} + \underbrace{\tilde{\mathbf{V}}_g \tilde{\mathbf{\Lambda}}_{F,g}}_{\mathbf{F}_{g,\perp}} \right], \tag{3.55}$$

where we have defined $\mathbf{F}_{g,\|} = \mathbf{V}_g \mathbf{\Lambda}_{F,g}$ and $\mathbf{F}_{g,\perp} = \tilde{\mathbf{V}}_g \tilde{\mathbf{\Lambda}}_{F,g}$. Clearly,

$$\mathbf{F}_{g,\perp}^H \mathbf{F}_{g,\|} = 0, \text{ and } \mathbf{F}_{g,\|}^H \mathbf{F}_{g,\perp} = 0. \tag{3.56}$$

Using similar arguments as for (3.52) in Subsection 3.9.5, we can show that

$$\left[\tau_3 \cdot \mathbf{R}_{e,R} + \sigma_n^2 \cdot \mathbf{I}_{n_R}\right]^{-\frac{1}{2}} \hat{\mathbf{H}} \left[\tau_2 \cdot \sigma_{ce}^2 \cdot \mathbf{R}_T + \mu_g \cdot \mathbf{I}_{n_T}\right]^{-\frac{1}{2}} \mathbf{F}_{g,\perp} = 0,$$

where τ_3 has been introduced in (3.30), and then

$$\hat{\mathbf{H}} \left[\tau_2 \cdot \sigma_{ce}^2 \cdot \mathbf{R}_T + \mu_g \cdot \mathbf{I}_{n_T}\right]^{-\frac{1}{2}} \mathbf{F}_{g,\perp} = 0. \tag{3.57}$$

From (3.26),

$$\mathbf{F}^H \hat{\mathbf{H}}^H \mathbf{G}^H \mathbf{G} \hat{\mathbf{H}} + \mathbf{F}^H \left[\tau_2 \cdot \sigma_{ce}^2 \mathbf{R}_T + \mu_g \cdot \mathbf{I}_{n_T}\right] = \mathbf{G} \hat{\mathbf{H}}.$$

Post-multiplying both sides of the above equation by $\left[\tau_2 \cdot \sigma_{ce}^2 \cdot \mathbf{R}_T + \mu_g \cdot \mathbf{I}_{n_T}\right]^{-\frac{1}{2}} \mathbf{F}_{g,\perp}$, using (3.55), (3.56) and (3.57), we obtain $\mathbf{F}_{g,\perp}^H \mathbf{F}_{g,\perp} = 0$, i.e., $\mathbf{F}_{g,\perp} = 0$. Therefore, the general expression of matrix $\mathbf{F}$ satisfying the KKT condition (3.26) can be written as:

$$\mathbf{F} = \left[\tau_2 \cdot \sigma_{ce}^2 \cdot \mathbf{R}_T + \mu_g \cdot \mathbf{I}_{n_T}\right]^{-\frac{1}{2}} \mathbf{V}_g \mathbf{\Lambda}_{F,g}. \tag{3.58}$$

From (3.25),

$$\begin{aligned}
\mathbf{G} &= \mathbf{F}^H \hat{\mathbf{H}}^H \left[\hat{\mathbf{H}} \mathbf{F} \mathbf{F}^H \hat{\mathbf{H}}^H + \tau_3 \cdot \mathbf{R}_{e,R} + \sigma_n^2 \cdot \mathbf{I}_{n_R}\right]^{-1} \\
&= \underbrace{\left\{\mathbf{I}_{r_g} + \mathbf{F}^H \hat{\mathbf{H}}^H \left[\tau_3 \cdot \mathbf{R}_{e,R} + \sigma_n^2 \cdot \mathbf{I}_{n_R}\right]^{-1} \hat{\mathbf{H}} \mathbf{F}\right\}^{-1}}_{\mathbf{J}_g} \mathbf{F}^H \hat{\mathbf{H}}^H \left[\tau_3 \cdot \mathbf{R}_{e,R} + \sigma_n^2 \cdot \mathbf{I}_{n_R}\right]^{-1} \\
&= \mathbf{J}_g \mathbf{\Lambda}_{F,g}^H \mathbf{V}_g^H \left[\tau_2 \cdot \sigma_{ce}^2 \cdot \mathbf{R}_T + \mu_g \cdot \mathbf{I}_{n_T}\right]^{-\frac{1}{2}} \hat{\mathbf{H}}^H \left[\tau_3 \cdot \mathbf{R}_{e,R} + \sigma_n^2 \cdot \mathbf{I}_{n_R}\right]^{-1} \\
&= \mathbf{\Lambda}_{G,g} \mathbf{V}_g^H \left[\tau_2 \cdot \sigma_{ce}^2 \cdot \mathbf{R}_T + \mu_g \cdot \mathbf{I}_{n_T}\right]^{-\frac{1}{2}} \hat{\mathbf{H}}^H \left[\tau_3 \cdot \mathbf{R}_{e,R} + \sigma_n^2 \cdot \mathbf{I}_{n_R}\right]^{-1},
\end{aligned} \tag{3.59}$$

where we have used the matrix inversion lemma [60], (3.58) and have defined $\mathbf{\Lambda}_{G,g} = \mathbf{J}_g \mathbf{\Lambda}_{F,g}^H$. Due to $\mathbf{\Lambda}_{F,g}$, $\mathbf{\Lambda}_{G,g}$ is a corresponding arbitrary $r_g \times r_g$ matrix. Pre-multiplying

(3.25) by **G**, post-multiplying (3.26) by **F**, substituting (3.58) and (3.59) into the resulting two equations, and using (3.31), we get

$$\mathbf{\Lambda}_{G,g}\,\mathbf{\Lambda}_g\,\mathbf{\Lambda}_{F,g} = \mathbf{\Lambda}_{G,g}\,\mathbf{\Lambda}_g\,\mathbf{\Lambda}_{F,g}\,\mathbf{\Lambda}_{F,g}^H\,\mathbf{\Lambda}_g\,\mathbf{\Lambda}_{G,g}^H + \mathbf{\Lambda}_{G,g}\,\mathbf{\Lambda}_g\,\mathbf{\Lambda}_{G,g}^H,$$
$$\mathbf{\Lambda}_{G,g}\,\mathbf{\Lambda}_g\,\mathbf{\Lambda}_{F,g} = \mathbf{\Lambda}_{F,g}^H\,\mathbf{\Lambda}_g\,\mathbf{\Lambda}_{G,g}^H\,\mathbf{\Lambda}_{G,g}\,\mathbf{\Lambda}_g\,\mathbf{\Lambda}_{F,g} + \mathbf{\Lambda}_{F,g}^H\,\mathbf{\Lambda}_{F,g}.$$

Again, applying the method in [85], to obtain $\mathbf{\Lambda}_{F,gopt}$ and $\mathbf{\Lambda}_{G,gopt}$ as given by (3.34) and (3.35), respectively. Replacing $\mathbf{\Lambda}_{F,g}$ and $\mathbf{\Lambda}_{G,g}$ in (3.58) and (3.59), respective, we obtain (3.32) and (3.33).

In the above, we have identified the structures of the non-zero precoder and decoder satisfying the KKT conditions (3.25)-(3.28). All the non-zero solutions lead to the same MSE, denoted as $mse_{nz,g}$ here. Using (3.25), similar to (3.47), we obtain

$$mse_{nz,g} = \mathrm{tr}\left\{\left[\mathbf{I}_B + \mathbf{F}_{gopt}^H\hat{\mathbf{H}}^H(\sigma_{ce}^2\cdot\mathrm{tr}\left(\mathbf{R}_T\mathbf{F}_{gopt}\mathbf{F}_{gopt}^H\right)\cdot\mathbf{R}_{e,R} + \sigma_n^2\cdot\mathbf{I}_{n_R}\right)^{-1}\hat{\mathbf{H}}\mathbf{F}_{gopt}\right]^{-1}\right\}.$$

It remains to compare $mse_{nz,g}$ with the MSE obtained from the zero solution, i.e.,

$$mse_{zero,g} = \mathrm{tr}\left(\mathbf{I}_B\right) = B.$$

Using (3.32), (3.34) and (3.31), it is easy to show that

$$\mathbf{F}_{gopt}^H\hat{\mathbf{H}}^H\left[\sigma_{ce}^2\cdot\mathrm{tr}\left(\mathbf{R}_T\mathbf{F}_{gopt}\mathbf{F}_{gopt}^H\right)\cdot\mathbf{R}_{e,R} + \sigma_n^2\cdot\mathbf{I}_{n_R}\right]^{-1}\hat{\mathbf{H}}\mathbf{F}_{gopt}$$

is positive semidefinite. As in Subsection 3.9.6, it can be shown that $mse_{nz,g} \leq mse_{zero,g}$. This establishes the global optimality of the non-zero solutions. Therefore, **Theorem 2** is proved. □

Chapter 4

Maximum Mutual Information Design with Channel Uncertainty

4.1 Introduction

The mutual information between the input and the output of a channel and the minimum mean-square error (MMSE) in estimating the input given the output are two basic quantities in information theory and estimation theory. In [32, 71], fundamental relationships between the mutual information and the minimum mean-square error have been discovered for discrete-time, continuous-time, scalar and vector channels with Gaussian noise. In particular, it is found in [71] that in vector (MIMO) Gaussian channels[1], the gradient of the mutual information with respect to the channel matrix is equal to the product of the channel matrix and the error covariance matrix of the best estimate of the input given the output (i.e., the MMSE matrix).

In [87], it has been shown that with perfect channel state information (CSI) at both ends,

[1]Here, by vector Gaussian channels, we mean that the channel matrix is fixed and the noise is Gaussian. The input distribution can be arbitrary [71].

the maximum mutual information (capacity) design minimizes the (log) determinant[2] of the MSE matrix, whereas the minimum total MSE design minimizes the trace. The optimum linear transmitters for both designs consist of a diagonal power allocation matrix followed by a general beamforming matrix composed of the effective channel eigenmodes [see Subsection 2.1.4, and Section 3.4 with $\sigma_E^2 = 0$]. The two differ only in the diagonal power allocations. In [85], the minimum weighted MSE design is considered. The minimum total MSE design turns out to be a special case with the weighting matrix being an identity matrix, whereas the maximum mutual information design corresponds to the case when the weighting matrix is equal to the diagonal non-zero eigenvalue matrix.

Two natural questions arise here are: how should one design a MIMO system for maximum mutual information with imperfect CSI? What is the relationship between these two designs in this case?

From Subsection 2.1.4, we have seen the enormous potential of a coherent MIMO system to provide high data rate in a rich-scattering environment. However, the capacity of a single-user MIMO channel depends on the CSI available at both ends. Correspondingly, different transmit strategies should be used with different types of CSI. As we have already known, the case when the fading channel is perfectly known to both ends has been studied in [85, 87, 102]. More recently, the optimum transmit strategies are obtained for the case with perfect CSI at the receiver (CSIR) and with the CSI at the transmitter (CSIT) being the channel mean information (CMI) or channel correlation information (CCI) [38, 40]. In [39, 61], the non-coherent case with no instantaneous CSIT or CSIR has been studied. A comprehensive overview of the capacity results of MIMO channels can be found in [31]. In the above, either a perfect coherent system (perfect CSIR) or a non-coherent system (no

[2] Since the log function is monotonically increasing, minimizing the determinant of a matrix (assumed to be positive) is equivalent to minimizing its log determinant [87].

instantaneous CSIR at all) has been assumed.

In [121], a different MIMO channel scenario is considered, where the CSIR is obtained through channel estimation and thus contains estimation errors (nonideal coherent reception). The CSIT is assumed to be transferred from the receiver via a lossless feedback link, and is thus the same as the CSIR. Under this assumption of CSI, an exact capacity expression is hard to obtain. Instead, tight upper- and lower-bounds on capacity have been proposed for system designs [121], which are generalizations from those for a SISO channel [62]. The case when the CSI at both ends consists of channel estimates and channel correlation has been studied in [66, 122]. In particular, the lower-bound on the MIMO channel ergodic capacity has been formulated and used as the design criterion [66, 122]. A numerical search method has been proposed in [122] to find the optimum transmit covariance matrix for the lower-bound. Unfortunately, so far, the optimum structure of the transmit covariance matrix has not been obtained for the lower-bound. For convenience, we refer to this problem as the capacity lower-bound problem or the maximum mutual information design with channel uncertainty (imperfect CSI).

In this chapter, we will show that a globally optimum transmit covariance matrix exists for the capacity lower-bound with the channel mean (i.e., the channel estimate) and channel correlation information at both ends. We will also present its explicit structure, which can be conveniently determined. For the special case with no receive correlation, the closed-form optimum transmit covariance matrix will be provided. The CSI assumed in this chapter is the same as in that in Chapter 3. In the end, we will be able to answer the question raised earlier: the relation between the maximum mutual information design and the minimum total MSE design in Chapter 3 will be elucidated.

This chapter is unfolded as follows. Section 4.2 describes the design problem at hand. In Section 4.3, the optimum transmit covariance matrix is determined for the capacity

lower-bound when $\mathbf{R}_T \neq \mathbf{I}_{n_T}$ and $\mathbf{R}_R = \mathbf{I}_{n_R}$. Results for the more general case when $\mathbf{R}_T \neq \mathbf{I}_{n_T}$ and $\mathbf{R}_R \neq \mathbf{I}_{n_R}$ are presented in Section 4.4. Section 4.5 discusses the relation between the minimum total MSE design in Chapter 3 and the maximum mutual information in this chapter. Simulation results are provided in Section 4.6, which show that it is appropriate to use the capacity lower-bound as a design criterion with the above assumed CSI, since the upper- and lower-bounds are close to each other. The advantage of using the optimum transmitter is demonstrated. The effect of channel estimation error and channel correlation are also assessed by simulation. A summary of this chapter is given in Section 4.7. Derivation and proof details are collected in Section 4.8.

4.2 Upper- and Lower-bounds on the Mutual Information

Consider a single-user MIMO communication system, described by

$$\mathbf{y} = \mathbf{H}\mathbf{x} + \mathbf{n}.$$

Here $\mathbf{x}$ is the $n_T \times 1$ zero-mean data vector (channel input) with a covariance matrix given by $\mathbf{Q} = \mathbb{E}(\mathbf{x}\mathbf{x}^H)$. The $n_R \times 1$ received signal vector $\mathbf{y}$ denotes the channel output. The $n_R \times 1$ channel noise vector $\mathbf{n}$ is assumed to be independent of both data and channel fades, spatially and temporally white, zero-mean and circularly symmetric complex Gaussian [i.e., distributed according to $\mathcal{N}_c(0, \sigma_n^2 \cdot \mathbf{I}_{n_R})$].

As mentioned in Subsection 2.1.1, the slow-varying flat-fading channel is modeled as $\mathbf{H} = \mathbf{R}_R^{\frac{1}{2}} \mathbf{H}_w \mathbf{R}_T^{\frac{1}{2}}$. Both $\mathbf{R}_T$ and $\mathbf{R}_R$ are assumed to be *full-rank* as in Chapter 3. The imperfect channel state information is modeled in the same way as in Section 3.2. To facilitate the presentation in this chapter, we summarize it here:

$$\mathbf{H} = \hat{\mathbf{H}} + \mathbf{E},\ \hat{\mathbf{H}} = \mathbf{R}_R^{\frac{1}{2}} \hat{\mathbf{H}}_w \mathbf{R}_T^{\frac{1}{2}},\ \mathbf{E} = \mathbf{R}_{e,R}^{\frac{1}{2}} \mathbf{E}_w \mathbf{R}_T^{\frac{1}{2}}, \tag{4.1}$$

where $\hat{\mathbf{H}}_w$ is the estimate of $\mathbf{H}_w$, $\mathbf{R}_{e,R} = [\mathbf{I}_{n_R} + \sigma_{ce}^2 \cdot \mathbf{R}_R^{-1}]^{-1}$, and the entries of the spatially white matrix $\mathbf{E}_w$ are i.i.d. $\mathscr{N}_c(0, \sigma_{ce}^2)$. Furthermore, $\hat{\mathbf{H}}$ is the estimate of $\mathbf{H}$, $\mathbf{E}$ is the overall channel estimation error matrix, and $\sigma_{ce}^2 = \mathrm{tr}(\mathbf{R}_T^{-1}) \cdot \sigma_n^2 / P_{tr}$, where P_{tr} is the power for training. Similar to [66,92,121], we assume the same channel information is made available at the transmitter via an error-free and low-delay feedback link, i.e., CSIT is the same as CSIR. Therefore, $\hat{\mathbf{H}}$, $\mathbf{R}_R$, $\mathbf{R}_T$, σ_{ce}^2 and σ_n^2 represent the CSI known to both ends. Note that this implies knowledge of $\mathbf{R}_{e,R}$.

Under the above channel uncertainty model, the channel output can be written as

$$\mathbf{y} = \hat{\mathbf{H}}\mathbf{x} + \mathbf{E}\mathbf{x} + \mathbf{n}.$$

Here the total noise is given by $\mathbf{n}_{total} \stackrel{\text{def}}{=} \mathbf{E}\mathbf{x} + \mathbf{n}$, with zero mean and a covariance matrix given by

$$\begin{aligned}
\mathbf{R}_{n_{total}} &= \mathbb{E}\left[(\mathbf{E}\mathbf{x} + \mathbf{n})(\mathbf{E}\mathbf{x} + \mathbf{n})^H\right] \\
&= \mathbb{E}\left[\mathbf{R}_{e,R}^{\frac{1}{2}} \mathbf{E}_w \mathbf{R}_T^{\frac{1}{2}} (\mathbf{x}\mathbf{x}^H) \mathbf{R}_T^{\frac{1}{2}} \mathbf{E}_w^H \mathbf{R}_{e,R}^{\frac{1}{2}}\right] + \sigma_n^2 \cdot \mathbf{I}_{n_R} \\
&= \sigma_{ce}^2 \cdot \mathrm{tr}(\mathbf{R}_T \mathbf{Q}) \cdot \mathbf{R}_{e,R} + \sigma_n^2 \cdot \mathbf{I}_{n_R},
\end{aligned}$$

where the expectation is taken over the distributions of $\mathbf{x}$, $\mathbf{n}$ and $\mathbf{E}_w$. Note that here $\mathbf{n}_{total}$ is not a Gaussian noise vector. Therefore, with the imperfect CSI assumed earlier, an exact capacity expression is hard to obtain. For the purpose of system design, tight upper- and lower-bounds on capacity have been proposed. With the above assumed CSI, the mutual information between $\mathbf{y}$ and $\mathbf{x}$ given $\hat{\mathbf{H}}$ is bounded as [62, 66, 121, 122]

$$I_{low} \leq I(\mathbf{x}, \mathbf{y} | \hat{\mathbf{H}}) \leq I_{up},$$

where

$$I_{low} = \log_2 \det\left[\mathbf{I}_{n_R} + \hat{\mathbf{H}}\mathbf{Q}\hat{\mathbf{H}}^H \mathbf{R}_{n_{total}}^{-1}\right], \tag{4.2}$$

$$I_{up} = I_{low} + \log_2 \det[\mathbf{R}_{n_{total}}] - \mathbb{E}\left\{\log_2 \det\left[\sigma_{ce}^2 \cdot \mathrm{tr}(\mathbf{R}_T \mathbf{x}\mathbf{x}^H) \cdot \mathbf{R}_{e,R} + \sigma_n^2 \cdot \mathbf{I}_{n_R}\right]\right\}. \quad (4.3)$$

Here I_{low} and I_{up} denote the lower- and upper-bounds on the actual mutual information, respectively. The expectation in (4.3) is taken over the distribution of $\mathbf{x}$.

For convenience, below we will use the lower-bound as a design criterion [121], whereas the upper-bound will be used for comparison. To obtain the highest data rate from using the lower-bound, we need to solve the following problem [66, 122]

$$I_{low} = \max_{\substack{\mathbf{Q}\succeq 0 \\ \mathrm{tr}\{\mathbf{Q}\}\le P_T}} \log_2 \det\left[\mathbf{I}_{n_R} + \hat{\mathbf{H}}\mathbf{Q}\hat{\mathbf{H}}^H \mathbf{R}_{n_{total}}^{-1}\right]. \quad (4.4)$$

The lower-bound on the ergodic capacity is then given by [121, 122]

$$C_{low} = \mathbb{E}[I_{low}], \quad (4.5)$$

where the expectation is taken over the fading distribution. Note that the power constraint is imposed in the spatial domain. No temporal power allocation is considered.

The problem in (4.4) is referred to as the *maximum mutual information design* with imperfect channel knowledge. This explains the title of this chapter.

In general, (4.4) is a non-convex optimization problem. The special case with $\mathbf{R}_R = \mathbf{I}_{n_R}$ has been studied in [122], where a numerical search method was proposed to find the optimum transmit covariance matrix $\mathbf{Q}$. No closed-form result has been obtained. The general problem (4.4) has been formulated in [66]. Again no closed-form optimum $\mathbf{Q}$ has been reported. Despite the unwieldy looking of the problem in (4.4), the optimum structure of its transmit covariance matrix can be determined, and the closed-form optimum $\mathbf{Q}$ exists for the special case with no receive correlation, as will be shown in subsequent sections.

4.3 A Special Case: $\mathbf{R}_T \neq \mathbf{I}_{n_T}, \mathbf{R}_R = \mathbf{I}_{n_R}$

As in Chapter 3, we begin with the special case with $\mathbf{R}_R = \mathbf{I}_{n_R}$ and then extend our results to the general problem (4.4).

In this case, the CSI is the same as in Section 3.4, which is summarized below:

$$\mathbf{H} = (\hat{\mathbf{H}}_{w0} + \mathbf{E}_{w0})\mathbf{R}_T^{\frac{1}{2}} = \hat{\mathbf{H}} + \mathbf{E},$$

where $\hat{\mathbf{H}} = \hat{\mathbf{H}}_{w0}\mathbf{R}_T^{\frac{1}{2}}$ is the channel mean, and $\mathbf{E} = \mathbf{E}_{w0}\mathbf{R}_T^{\frac{1}{2}}$. The entries of $\hat{\mathbf{H}}_{w0}$ and $\mathbf{E}_{w0}$ are mutually uncorrelated, and are i.i.d. $\mathcal{N}_c(0, 1-\sigma_E^2)$ and $\mathcal{N}_c(0, \sigma_E^2)$, respectively, with $\sigma_E^2 = \sigma_{ce}^2/(1+\sigma_{ce}^2)$. Here $\hat{\mathbf{H}}$, $\mathbf{R}_T$, σ_E^2 and σ_n^2 are assumed to be known to both ends, which has been referred to as the channel mean and transmit correlation information.

The problem in (4.4) becomes

$$I_{low} = \max_{\substack{\mathbf{Q}\succeq 0 \\ \mathrm{tr}\{\mathbf{Q}\}\leq P_T}} \log_2 \det\left[\mathbf{I}_{n_R} + \frac{\hat{\mathbf{H}}\mathbf{Q}\hat{\mathbf{H}}^H}{\sigma_E^2 \cdot \mathrm{tr}(\mathbf{R}_T\mathbf{Q}) + \sigma_n^2}\right], \tag{4.6}$$

which is identical to the problem formulation in [122, Section IV-B].

Our approach to obtain the optimum $\mathbf{Q}$ relies on solving an equivalent problem of (4.6). Toward this end, we introduce a virtual auxiliary precoder-decoder pair $(\mathbf{F}, \mathbf{G})$ in our system model (see Fig. 2.2), where $\mathbf{F}$ and $\mathbf{G}$ are $n_T \times r$ and $r \times n_R$ matrices, respectively, and $r = \mathrm{rank}(\hat{\mathbf{H}})$. The repetitive notation of r (see Section 3.4) will soon be justified [after (4.13)], and the choice of the sizes of $\mathbf{F}$ and $\mathbf{G}$ will be explained in Subsection 4.8.3. Here $\mathbf{x} = \mathbf{F}\mathbf{s}$, and $\mathbf{s}$ is a zero-mean $r \times 1$ data vector whose entries are i.i.d. with unit variances. Thus, $\mathbf{Q} = \mathbb{E}(\mathbf{x}\mathbf{x}^H) = \mathbf{F}\mathbf{F}^H$. We now have

$$\mathbf{y} = \hat{\mathbf{H}}\mathbf{F}\mathbf{s} + \mathbf{E}\mathbf{F}\mathbf{s} + \mathbf{n}.$$

The received vector after the decoder is given by $\mathbf{r} = \mathbf{G}\mathbf{y}$. Define

$$MSE(\mathbf{F}, \mathbf{G}) \stackrel{\text{def}}{=} \mathbb{E}\{(\mathbf{r}-\mathbf{s})(\mathbf{r}-\mathbf{s})^H\}$$

$$
\begin{aligned}
&= \mathbb{E}\{[\mathbf{G}(\hat{\mathbf{H}}+\mathbf{E})\mathbf{F}-\mathbf{I}_r]\,\mathbf{s}\,\mathbf{s}^H[\mathbf{G}(\hat{\mathbf{H}}+\mathbf{E})\mathbf{F}-\mathbf{I}_r]^H\}+\sigma_n^2\cdot\mathbf{G}\mathbf{G}^H \\
&= \mathbf{G}\hat{\mathbf{H}}\mathbf{F}\mathbf{F}^H\hat{\mathbf{H}}^H\mathbf{G}^H-\mathbf{G}\hat{\mathbf{H}}\mathbf{F}-\mathbf{F}^H\hat{\mathbf{H}}^H\mathbf{G}^H+\mathbf{I}_r \\
&\quad +[\sigma_n^2+\sigma_E^2\cdot\mathrm{tr}(\mathbf{R}_T\mathbf{F}\mathbf{F}^H)]\cdot\mathbf{G}\mathbf{G}^H. \qquad (4.7)
\end{aligned}
$$

In the above, the expectation is taken over the distributions of $\mathbf{s},\mathbf{n}$ and $\mathbf{E}_w$. It is easy to see (4.7) is identical to (3.10), except for the difference in the dimension of matrices.

Lemma 3 *The problem (4.6) is equivalent to the following optimization problem*

$$
\min_{\substack{\mathbf{F},\mathbf{G} \\ tr\{\mathbf{F}\mathbf{F}^H\}\le P_T}} \ln\det\left[MSE(\mathbf{F},\mathbf{G})\right], \qquad (4.8)
$$

where $MSE(\mathbf{F},\mathbf{G})$ *is given by (4.7) and* ln *denotes the natural log function. Let the optimum solution for (4.8) be* $(\mathbf{F}_{c,opt},\mathbf{G}_{c,opt})$*. Then the optimum covariance matrix for (4.6) is related to the optimum solution for (4.8) by* $\mathbf{Q}_{opt}=\mathbf{F}_{c,opt}\mathbf{F}_{c,opt}^H$*. A global maximum exists for (4.6) and a global minimum exists for (4.8).*

Proof. See Subsection 4.8.1. ■

Therefore, to solve (4.6), we attempt to solve (4.8) instead. Note that (4.8) is also a non-convex problem. Nevertheless, the objective and constraint functions of (4.8) are continuously differentiable with respect to $\mathbf{F}^*$ and $\mathbf{G}^*$ (or $\mathbf{F}$ and $\mathbf{G}$). There is only one inequality constraint here, so that any feasible solution is regular. Thus, the global minimum (which exists according to **Lemma 3**) should satisfy the first-order KKT necessary conditions associated with (4.8) [5]. Our method is the same as in Section 3.3, i.e., it is to find all the solutions satisfying the KKT conditions and then identify the optimum $(\mathbf{F}_{c,opt},\mathbf{G}_{c,opt})$ among them. Note that if $(\mathbf{F}_{c,opt},\mathbf{G}_{c,opt})$ is optimum, so is $(\mathbf{F}_{c,opt}\mathbf{U},\mathbf{U}^H\mathbf{G}_{c,opt})$, where $\mathbf{U}$ is an arbitrary $r\times r$ unitary matrix. As in Chapter 3, below we refer to $(\mathbf{F}_{c,opt},\mathbf{G}_{c,opt})$ as an optimum solution for (4.8) *up to a unitary transform*. However, the optimum transmit covariance matrix $\mathbf{Q}_{opt}=\mathbf{F}_{c,opt}\mathbf{F}_{c,opt}^H$ is unique.

We can see that the maximum mutual information design here and the minimum total MSE design in Subsection 3.4 are related. The former is to minimize the log determinant of the MSE matrix (4.7), whereas the latter is to minimize its trace. Indeed, the content in this chapter is parallel to that in Chapter 3. We will reveal more of the relationship between these two designs later in Section 4.5. For now, we focus on solving (4.8).

With the MSE matrix given by (4.7), the Lagrangian associated with (4.8) is

$$\mathscr{L}_2(\mathbf{F},\mathbf{G},\mu_2) = \ln\det\left[MSE\left(\mathbf{F},\mathbf{G}\right)\right] + \mu_2 \cdot \left[\mathrm{tr}(\mathbf{F}\mathbf{F}^H) - P_T\right],$$

where μ_2 is the Lagrange multiplier. By taking the derivative of the Lagrangian with respect to $\mathbf{F}^*$ and $\mathbf{G}^*$, respectively, we obtain the KKT conditions for (4.8):

$$\hat{\mathbf{H}}\mathbf{F} = \left[\hat{\mathbf{H}}\mathbf{F}\mathbf{F}^H\hat{\mathbf{H}}^H + \tau_4 \cdot \mathbf{I}_{n_R}\right]\mathbf{G}^H, \tag{4.9}$$

$$\begin{aligned}&\hat{\mathbf{H}}^H\mathbf{G}^H\left[MSE\left(\mathbf{F},\mathbf{G}\right)\right]^{-1}\left(\mathbf{G}\hat{\mathbf{H}}\mathbf{F} - \mathbf{I}_r\right)\\ &\quad + \ \sigma_E^2 \cdot \mathrm{tr}\left\{\left[MSE\left(\mathbf{F},\mathbf{G}\right)\right]^{-1}\mathbf{G}\mathbf{G}^H\right\} \cdot \mathbf{R}_T\mathbf{F} + \mu_2\mathbf{F} = 0,\end{aligned} \tag{4.10}$$

$$\mu_2 \geq 0,\ \mathrm{tr}(\mathbf{F}\mathbf{F}^H) - P_T \leq 0, \tag{4.11}$$

$$\mu_2 \cdot \left[\mathrm{tr}(\mathbf{F}\mathbf{F}^H) - P_T\right] = 0, \tag{4.12}$$

where $\tau_4 = \sigma_n^2 + \sigma_E^2 \cdot \mathrm{tr}(\mathbf{R}_T\mathbf{F}\mathbf{F}^H)$. Detailed derivations are presented in Subsection 4.8.2.

It turns out that, to solve (4.8), we need to consider the following eigenvalue decomposition, which is exactly the same as in (3.16):

$$\begin{aligned}&\left[\sigma_E^2 \cdot P_T \cdot \mathbf{R}_T + \sigma_n^2 \cdot \mathbf{I}_{n_T}\right]^{-\frac{1}{2}}\hat{\mathbf{H}}^H\hat{\mathbf{H}}\left[\sigma_E^2 \cdot P_T \cdot \mathbf{R}_T + \sigma_n^2 \cdot \mathbf{I}_{n_T}\right]^{-\frac{1}{2}}\\ &= \ [\mathbf{V}\ \tilde{\mathbf{V}}]\begin{pmatrix}\mathbf{\Lambda} & 0\\ 0 & \tilde{\mathbf{\Lambda}}\end{pmatrix}[\mathbf{V}\ \tilde{\mathbf{V}}]^H.\end{aligned} \tag{4.13}$$

All the variables involved here are defined in the same way as those in (3.16). In particular, $r = \mathrm{rank}(\hat{\mathbf{H}}) = \mathrm{rank}(\mathbf{\Lambda})$ denotes the number of non-zero channel eigenmodes, as before.

This explains the use of r earlier in this section. Without loss of generality, the entries of the diagonal matrix $\mathbf{\Lambda}$ are arranged in decreasing order.

Theorem 4 *With the MSE matrix given by (4.7), the optimum precoder and decoder for (4.8) are given by*

$$\mathbf{F}_{c,opt} = \left[\sigma_E^2 \cdot P_T \cdot \mathbf{R}_T + \sigma_n^2 \cdot \mathbf{I}_{n_T}\right]^{-\frac{1}{2}} \mathbf{V}\mathbf{\Phi}_{Fopt}, \tag{4.14}$$

$$\mathbf{G}_{c,opt} = \mathbf{\Phi}_{Gopt}\mathbf{V}^H \left[\sigma_E^2 \cdot P_T \cdot \mathbf{R}_T + \sigma_n^2 \cdot \mathbf{I}_{n_T}\right]^{-\frac{1}{2}} \hat{\mathbf{H}}^H, \tag{4.15}$$

respectively, where

$$\mathbf{\Phi}_{Fopt} = \left(\mu_2/\sigma_n^2\right)^{-\frac{1}{2}} \left[\mathbf{I}_r - (\mu_2\tau_4/\sigma_n^2)\cdot\mathbf{\Lambda}^{-1}\right]_+^{\frac{1}{2}}, \tag{4.16}$$

$$\mathbf{\Phi}_{Gopt} = \left(\mu_2/\sigma_n^2\right)^{\frac{1}{2}} \left[\mathbf{I}_r - (\mu_2\tau_4/\sigma_n^2)\cdot\mathbf{\Lambda}^{-1}\right]_+^{\frac{1}{2}} \mathbf{\Lambda}^{-1}. \tag{4.17}$$

The scalars μ_2 and τ_4 are given by

$$\mu_2 = \frac{\sigma_n^2 b_1 P_T + \sigma_n^2 b_1 b_3 - m_0\sigma_n^2 b_2}{P_T(P_T + b_3)}, \tag{4.18}$$

$$\tau_4 = \frac{m_0 P_T}{b_1 P_T + b_1 b_3 - m_0 b_2}, \tag{4.19}$$

where the integer m_0 ($m_0 \leq r$) denotes the non-zero entries of matrix $\mathbf{\Phi}_{Fopt}$. Scalars b_1, b_2 and b_3 are traces of the $m_0 \times m_0$ top-left submatrices of $\mathbf{V}^H \left[\sigma_E^2 \cdot P_T \cdot \mathbf{R}_T + \sigma_n^2 \cdot \mathbf{I}_{n_T}\right]^{-1}\mathbf{V}$, $\mathbf{\Lambda}^{-1}\mathbf{V}^H \left[\sigma_E^2 \cdot P_T \cdot \mathbf{R}_T + \sigma_n^2 \cdot \mathbf{I}_{n_T}\right]^{-1}\mathbf{V}$ and $\mathbf{\Lambda}^{-1}$, respectively. The optimum solution is unique up to a unitary transform.

Proof. See Subsection 4.8.3. The method to determine m_0 is also included there. ■

Corollary 1 *The unique optimum covariance matrix for (4.8) can be written as*

$$\mathbf{Q}_{opt} = [\sigma_E^2 \cdot P_T \cdot \mathbf{R}_T + \sigma_n^2 \cdot \mathbf{I}_{n_T}]^{-\frac{1}{2}} \mathbf{V}\mathbf{\Phi}_Q\mathbf{V}^H [\sigma_E^2 \cdot P_T \cdot \mathbf{R}_T + \sigma_n^2 \cdot \mathbf{I}_{n_T}]^{-\frac{1}{2}},$$

*where $\mathbf{\Phi}_Q = \mathbf{\Phi}_{Fopt}\mathbf{\Phi}_{Fopt}^H$ and $\mathbf{\Phi}_{Fopt}$ is from **Theorem 4**.*

Proof. The result follows immediately from **Lemma 3** and **Theorem 4**. ■

Remark 4.1: When $\sigma_E^2 = 0$, **Corollary 1** reduces to the capacity result obtained in [75, 85, 102] (see Subsection 2.1.4). The explicit structure of the optimum transmitter is the same as the precoder shown in Fig. 3.1, except that $\mathbf{\Lambda_{Fopt}}$ is replaced by $\mathbf{\Phi_{Fopt}}$.

Remark 4.2: In [122, Theorem 5], it has been pointed out that when P_T/σ_n^2 goes to infinity, the optimum transmit strategy is to perform water-filling over the eigenmodes of $\hat{\mathbf{H}}_{w0}$ and then invert the effect of $\mathbf{R}_T$. This agrees with **Corollary 1**.

4.4 The General Case: $\mathbf{R}_T \neq \mathbf{I}_{n_T}, \mathbf{R}_R \neq \mathbf{I}_{n_R}$

The same method for the special case is used here. It is easy to extend the proof of **Lemma 3** to the general case. Our method for solving (4.4) is then to solve an equivalent problem formulated as in (4.8), where, with $\mathbf{R}_T \neq \mathbf{I}_{n_T}$ and $\mathbf{R}_R \neq \mathbf{I}_{n_R}$, the MSE matrix is given by

$$\begin{aligned} MSE(\mathbf{F},\mathbf{G}) = {} & \mathbf{G}\hat{\mathbf{H}}\mathbf{F}\mathbf{F}^H\hat{\mathbf{H}}^H\mathbf{G}^H - \mathbf{G}\hat{\mathbf{H}}\mathbf{F} - \mathbf{F}^H\hat{\mathbf{H}}^H\mathbf{G}^H + \mathbf{I}_{r_{gc}} \\ & + [\sigma_{ce}^2 \cdot \mathrm{tr}(\mathbf{R}_T\mathbf{F}\mathbf{F}^H)] \cdot \mathbf{G}\mathbf{R}_{e,R}\mathbf{G}^H + \sigma_n^2 \cdot \mathbf{G}\mathbf{G}^H. \end{aligned} \tag{4.20}$$

Note that (4.20) is the same as (3.8), except for the difference in the dimension of matrices. Here $r_{gc} = \mathrm{rank}(\hat{\mathbf{H}})$. Define

$$\tau_5 = \mathrm{tr}\left\{\mathbf{G}\mathbf{R}_{e,R}[\sigma_{ce}^2 \cdot \mathrm{tr}(\mathbf{R}_T\mathbf{F}\mathbf{F}^H) \cdot \mathbf{R}_{e,R} + \sigma_n^2 \cdot \mathbf{I}_{n_R}]^{-1}\hat{\mathbf{H}}\mathbf{F}\right\}, \tag{4.21}$$

$$\mu_{gc} = \frac{\sigma_n^2}{P_T} \cdot \mathrm{tr}\left\{\mathbf{G}[\sigma_{ce}^2 \cdot \mathrm{tr}(\mathbf{R}_T\mathbf{F}\mathbf{F}^H) \cdot \mathbf{R}_{e,R} + \sigma_n^2 \cdot \mathbf{I}_{n_R}]^{-1}\hat{\mathbf{H}}\mathbf{F}\right\}, \tag{4.22}$$

$$\tau_6 = \sigma_{ce}^2 \cdot \mathrm{tr}(\mathbf{R}_T\mathbf{F}\mathbf{F}^H). \tag{4.23}$$

The Lagrangian here is

$$\mathscr{L}_{gc}(\mathbf{F},\mathbf{G},\mu_{gc}) = \ln\det[MSE(\mathbf{F},\mathbf{G})] + \mu_{gc} \cdot [\mathrm{tr}(\mathbf{F}\mathbf{F}^H) - P_T],$$

where μ_{gc} is the Lagrangian multiplier here. Similar to Subsection 4.8.2, the KKT conditions in the general case can be obtained, and are given by

$$\hat{\mathbf{H}}\mathbf{F} = \left[\hat{\mathbf{H}}\mathbf{F}\mathbf{F}^H\hat{\mathbf{H}}^H + \sigma_{ce}^2 \cdot \mathrm{tr}(\mathbf{R}_T\mathbf{F}\mathbf{F}^H) \cdot \mathbf{R}_{e,R} + \sigma_n^2 \cdot \mathbf{I}_{n_R}\right]\mathbf{G}^H, \tag{4.24}$$

$$\begin{aligned}&\hat{\mathbf{H}}^H\mathbf{G}^H\left[MSE(\mathbf{F},\mathbf{G})\right]^{-1}\left(\mathbf{G}\hat{\mathbf{H}}\mathbf{F} - \mathbf{I}_{r_{gc}}\right)\\ &\quad + \sigma_{ce}^2 \cdot \mathrm{tr}\left\{\left[MSE(\mathbf{F},\mathbf{G})\right]^{-1}\mathbf{G}\mathbf{R}_{e,R}\mathbf{G}^H\right\} \cdot \mathbf{R}_T\mathbf{F} + \mu_{gc} \cdot \mathbf{F} = 0,\end{aligned} \tag{4.25}$$

$$\mu_{gc} \geq 0, \;\; \mathrm{tr}(\mathbf{F}\mathbf{F}^H) - P_T \leq 0, \tag{4.26}$$

$$\mu_{gc} \cdot [\mathrm{tr}(\mathbf{F}\mathbf{F}^H) - P_T] = 0. \tag{4.27}$$

Consider the following EVD

$$\begin{aligned}&\left[\sigma_{ce}^2\tau_5 \cdot \mathbf{R}_T + \mu_{gc} \cdot \mathbf{I}_{n_T}\right]^{-\frac{1}{2}}\hat{\mathbf{H}}^H\left[\tau_6 \cdot \mathbf{R}_{e,R} + \sigma_n^2 \cdot \mathbf{I}_{n_R}\right]^{-1}\hat{\mathbf{H}}\left[\sigma_{ce}^2\tau_5 \cdot \mathbf{R}_T + \mu_{gc} \cdot \mathbf{I}_{n_T}\right]^{-\frac{1}{2}}\\ &= \left[\mathbf{V}_{gc} \;\; \tilde{\mathbf{V}}_{gc}\right]\begin{pmatrix}\mathbf{\Lambda}_{gc} & 0\\ 0 & \tilde{\mathbf{\Lambda}}_{gc}\end{pmatrix}\left[\mathbf{V}_{gc} \;\; \tilde{\mathbf{V}}_{gc}\right]^H,\end{aligned} \tag{4.28}$$

where $\mathbf{V}_{gc}$, $\tilde{\mathbf{V}}_{gc}$, $\mathbf{\Lambda}_{gc}$ and $\tilde{\mathbf{\Lambda}}_{gc}$ are defined similarly as those in (3.31). Note that $r_{gc} = \mathrm{rank}(\mathbf{\Lambda}_{gc})$. The entries of the diagonal matrix $\mathbf{\Lambda}_{gc}$ are arranged in decreasing order.

Theorem 5 *With the MSE matrix given by (4.20), the optimum precoder and decoder for (4.8) are given by*

$$\mathbf{F}_{c,gopt} = \left[\sigma_{ce}^2 \cdot \tau_5 \cdot \mathbf{R}_T + \mu_{gc} \cdot \mathbf{I}_{n_T}\right]^{-\frac{1}{2}}\mathbf{V}_{gc}\mathbf{\Phi}_{F,gopt}, \tag{4.29}$$

$$\mathbf{G}_{c,gopt} = \mathbf{\Phi}_{G,gopt}\mathbf{V}_{gc}^H\left[\sigma_{ce}^2\tau_5 \cdot \mathbf{R}_T + \mu_{gc} \cdot \mathbf{I}_{n_T}\right]^{-\frac{1}{2}}\hat{\mathbf{H}}^H\left[\tau_6 \cdot \mathbf{R}_{e,R} + \sigma_n^2 \cdot \mathbf{I}_{n_R}\right]^{-1}, \tag{4.30}$$

$$\mathbf{\Phi}_{F,gopt} = \left[\mathbf{I}_{r_{gc}} - \mathbf{\Lambda}_{gc}^{-1}\right]_+^{\frac{1}{2}}, \tag{4.31}$$

$$\mathbf{\Phi}_{G,gopt} = \left[\mathbf{I}_{r_{gc}} - \mathbf{\Lambda}_{gc}^{-1}\right]_+^{\frac{1}{2}}\mathbf{\Lambda}_{gc}^{-1}. \tag{4.32}$$

Inserting (4.29)-(4.32) into (4.21)-(4.23) yields three equations with μ_{gc}, τ_5 and τ_6 being the only three variables. By solving these three equations numerically, μ_{gc}, τ_5 and τ_6 are determined. The optimum solution is unique up to a unitary transform.

Proof. See Subsection 4.8.4. ■

Theorem 5 clearly describes the structure of the optimum precoder and decoder. However, μ_{gc}, τ_5 and τ_6 need to be determined numerically, which is inconvenient. As in Section 3.5, we now provide a KKT-conditions-based iterative algorithm to determine the optimum solution. From (4.52) we obtain

$$\mathbf{F} = \left[\sigma_{ce}^2 \cdot \tau_5 \cdot \mathbf{R}_T + \mu_{gc} \cdot \mathbf{I}_{n_T}\right]^{-1} \hat{\mathbf{H}}^H \mathbf{G}^H. \tag{4.33}$$

The above formula is used in the iterative algorithm given in Table 4.1. This algorithm converges, because the value of the objective function is reduced at each iteration and is bounded from below. Furthermore, as shown in the proof of **Theorem 4**, any non-zero solution to the KKT conditions leads to the same value of the objective function. Thus, starting from a non-zero matrix $\mathbf{F}_0$, the algorithm in Table 4.1 converges and yields the optimum $(\mathbf{F}_{c,gopt}, \mathbf{G}_{c,gopt})$ up to a unitary transform.

The following corollary follows immediately.

Corollary 2 *The unique optimum covariance matrix for (4.4) is given by*

$$\mathbf{Q}_{gopt} = \mathbf{F}_{c,gopt} \mathbf{F}_{c,gopt}^H,$$

where $\mathbf{F}_{c,gopt}$ *is from* ***Theorem 5****.*

4.5 Relation to Minimum Total MSE Design

By now, we have observed much of the parallelism between Chapter 3 and this chapter. In this section, we summarize the connection between these two important designs assuming the same imperfect CSI.

To elucidate their relation, we first delve into how the capacity lower-bound (4.2) is obtained. As mentioned in Section 4.2, with imperfect CSI, the total noise is no longer

Table 4.1. An iterative algorithm for solving (4.8) [with the MSE matrix given by (3.8)]

1)	Initialize $\mathbf{F} = \mathbf{F}_0$; the upper $r_{gc} \times r_{gc}$ sub-matrix of $\mathbf{F}_0$ is chosen be a scaled identity to and to satisfy the power constraint with equality, while the remaining entries of $\mathbf{F}_0$ are set to zero.
2)	Update $\mathbf{G}$ using (4.48) [i.e., (4.24)];
3)	Update μ_{gc} and τ_5 using (4.22) and (4.21), respectively;
4)	Update $\mathbf{F}$ using (4.33);
5)	If the termination condition is met, stop; otherwise, go back to 2).

Gaussian, and it is hard to find the optimum input distribution to maximize

$$I(\mathbf{x};\mathbf{y}|\hat{\mathbf{H}}) = d_h(\mathbf{x}|\hat{\mathbf{H}}) - d_h(\mathbf{x}|\mathbf{y},\hat{\mathbf{H}}), \tag{4.34}$$

where $d_h(\cdot)$ denotes the differential entropy [17, Chapter 9, p. 224]. The lower-bound on the above mutual information is obtained using the following two steps [62, 66, 121]:

- assuming the channel input is Gaussian (although here the Gaussian input may no longer be the mutual information maximizer) and thus fixing the first term in the right-hand side of (4.34);
- upper-bounding the second term in the right-hand side of (4.34) by the differential entropy of a Gaussian random vector whose covariance matrix is equal to the mean-square error matrix from the linear MMSE estimation of $\mathbf{x}$ given $\mathbf{y}$ and $\hat{\mathbf{H}}$.

Therefore, the derivation of (4.2) is related to the linear MMSE data estimation [46, Chapter 12] [77]. Interestingly, with the lower-bound derived using the above approach, the optimum transmitters for both designs still share the same structures with differences mainly in the power allocation, as can be seen from Chapter 3 and this chapter.

Analogous to the perfect CSI case, both transmitters can be derived from the minimum weighted MSE design. In the special case with only transmit correlation, from Sections 3.4, 3.6 and 4.3, it can be seen that the minimum total MSE design is a special case with $\mathbf{W} = \mathbf{I}_B$, whereas the maximum mutual information design corresponds to the case when $\mathbf{W} = \mathbf{\Lambda}$.

4.6 Simulation Results and Discussions

Let $n_T = n_R = 4$. The channel correlation model used here is described in Subsection 2.1.1 (see also Section 3.7, Part 1). Below the ergodic capacity or its bounds will be shown (in bits/channel use), calculated by averaging the instantaneous mutual information (or its bounds) over the fading distribution [similar to (4.5)]. The SNR here is defined as P_T/σ_n^2.

1. Comparison of the Ergodic Capacity Bounds

   Fig. 4.1 shows a comparison between the ergodic capacity upper- and lower-bounds, calculated using (4.3) and (4.2), respectively, and then averaged over the fading distribution.

   Note that CLB and CUB in the figures denote the capacity lower-bound and capacity upper-bound, respectively. The optimum covariance matrix for the lower-bound derived in this chapter is used as the transmit strategy in the calculations of both (4.3) and (4.2). From Fig. 4.1, we observe that the two bounds are very close to each other, especially in the low to medium SNR region ($\leq$ 20 dB), and thus are both tight. This justifies the use of the lower-bound as a design criterion to maximize the mutual information. More asymptotic analysis of the difference between the upper- and lower-bounds can be found in [66, 121].

2. Optimum Transmit Strategy vs. Uniform Power Allocation

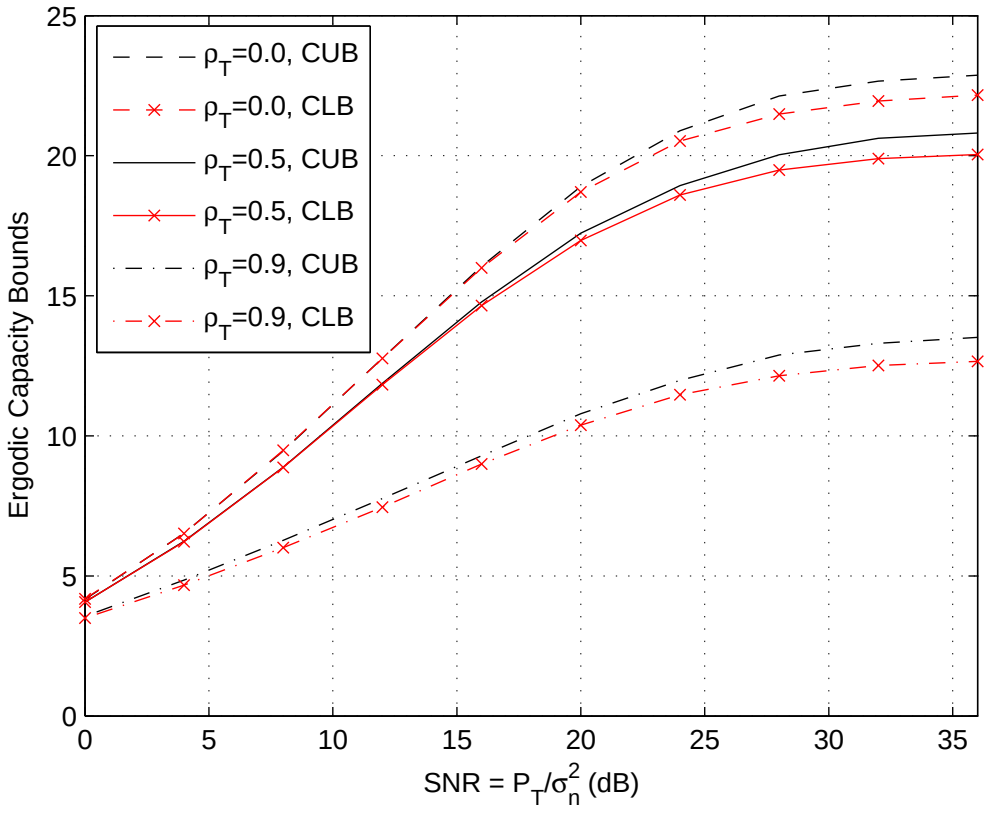

Figure 4.1. Comparison of the capacity upper- and lower-bounds. Both bounds are obtained using the optimum transmit covariance matrix for the lower-bound. $n_T = n_R = 4$, $\rho_R = 0.0$, $P_{tr}/\sigma_n^2 = 26.016$ dB. The values of σ_E^2 are 0.0099, 0.0148, and 0.0689, for ρ_T = 0.0, 0.5, and 0.9, respectively.

In the case of imperfect CSI here, the optimum transmit strategy refers to that for the capacity lower-bound. As mentioned in Subsection 2.1.4, the uniform power allocation scheme distributes the total transmit power evenly among all antennas without requiring any CSI.

As expected (see the discussions in Subsection 2.1.4), from Fig. 4.2, with perfect CSI at both ends, the capacities obtained from using the optimum transmit strategy and uniform power allocation converge at high SNR for our channel model. The case with imperfect CSI is shown in Fig. 4.3. Clearly, with imperfect CSI, the uniform power allocation (used in [66]) performs strictly worse over the entire SNR range when the channel correlation is high. This, in turn, shows the advantage (in terms of accuracy) of using the optimum covariance matrix for the lower-bound.

3. Effects of Channel Estimation Error and Channel Correlation

   Figs. 4.4 and 4.5 give the capacity without channel estimation error, and the capacity lower-bound with imperfect CSI, respectively.

   It is observed that channel estimation error causes a huge loss in ergodic capacity. For example, from Fig. 4.4, with $\rho_T = 0.5$ and $\rho_R = 0$, the ergodic capacity is about 15.9 bits/channel use at SNR = 15 dB. However, if the CSI is obtained from channel estimation with $P_{tr}/\sigma_n^2 = 26.016$ dB, the ergodic capacity shrinks to 14.1 bits/channel use at the same SNR (see Fig. 4.5). From Figs. 4.1 and 4.5, at high SNR, the capacity is saturated due to channel estimation error. Channel correlation can also significantly reduce the ergodic capacity. For instance, from Fig. 4.5, with $\rho_R = 0$, at SNR = 15 dB, the capacity decreases from 14.1 bits/channel use to around 8.75 bits/channel use if ρ_T increases from 0.5 to 0.9. (At SNR = 15 dB, the capacity upper- and lower-bounds are fairly close.)

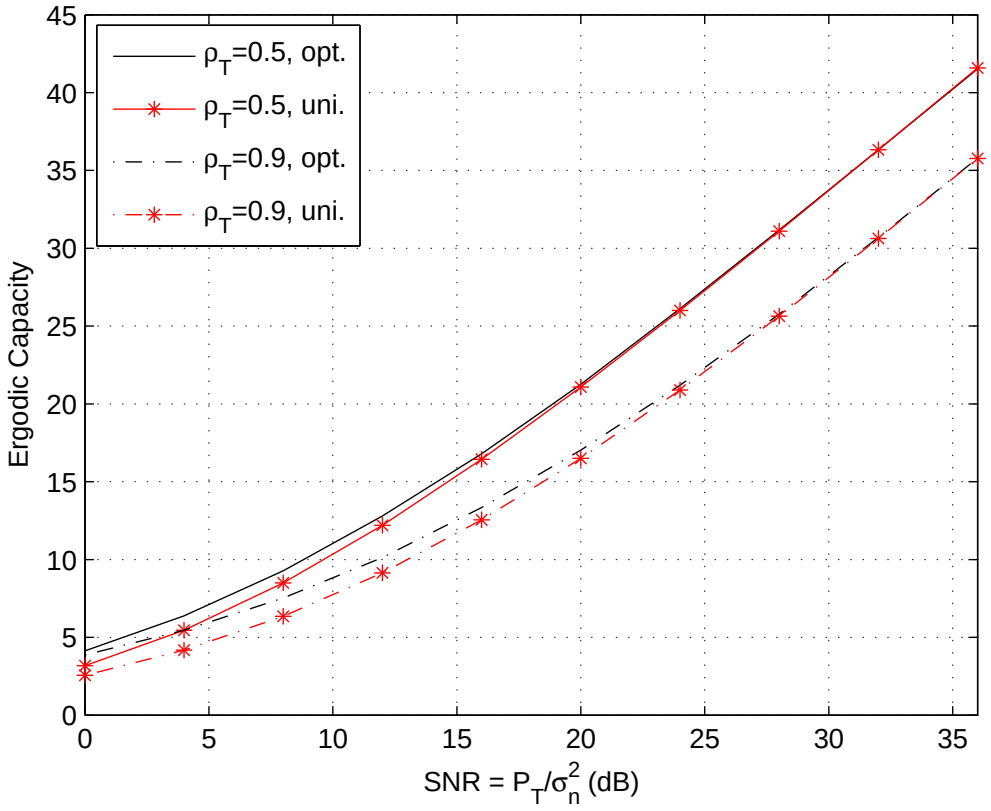

Figure 4.2. Ergodic capacity of a MIMO channel: optimum vs. uniform. $n_T = n_R = 4$, $\rho_R = 0.0$. Perfect CSI at both ends is assumed for the optimum strategy.

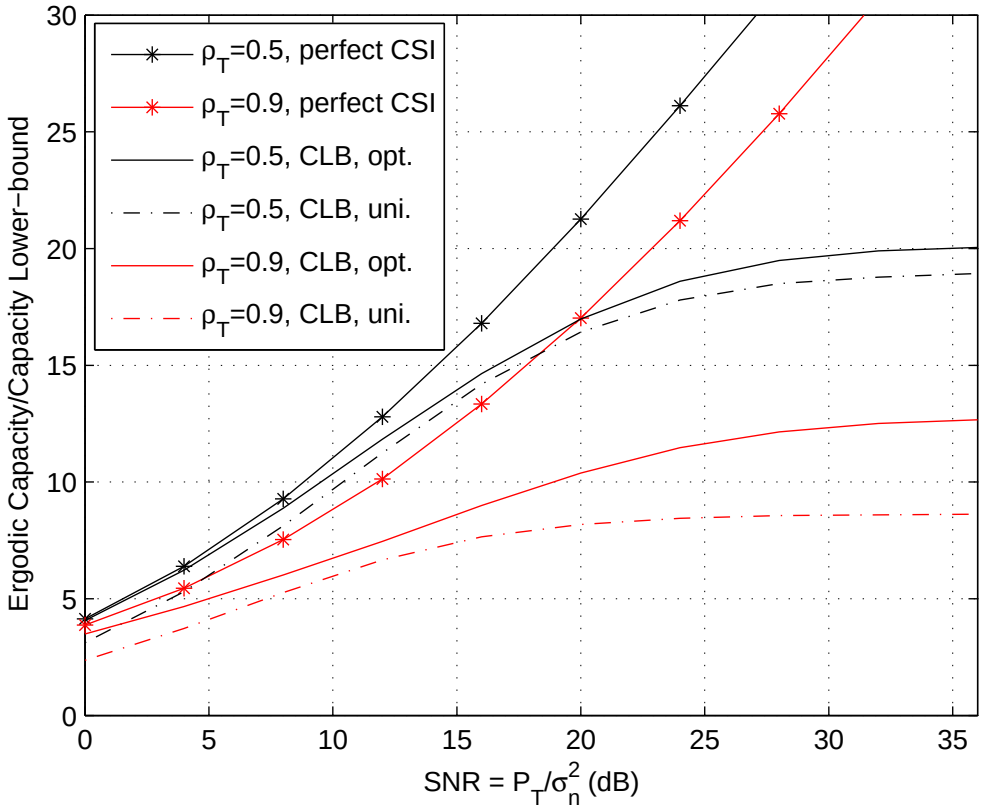

Figure 4.3. Ergodic capacity lower-bound of a MIMO channel: optimum vs. uniform. $n_T = n_R = 4$, $\rho_R = 0.0$, $P_{tr}/\sigma_n^2 = 26.016$ dB. The values of σ_E^2 are 0.0148 and 0.0689, for ρ_T = 0.5 and 0.9, respectively.

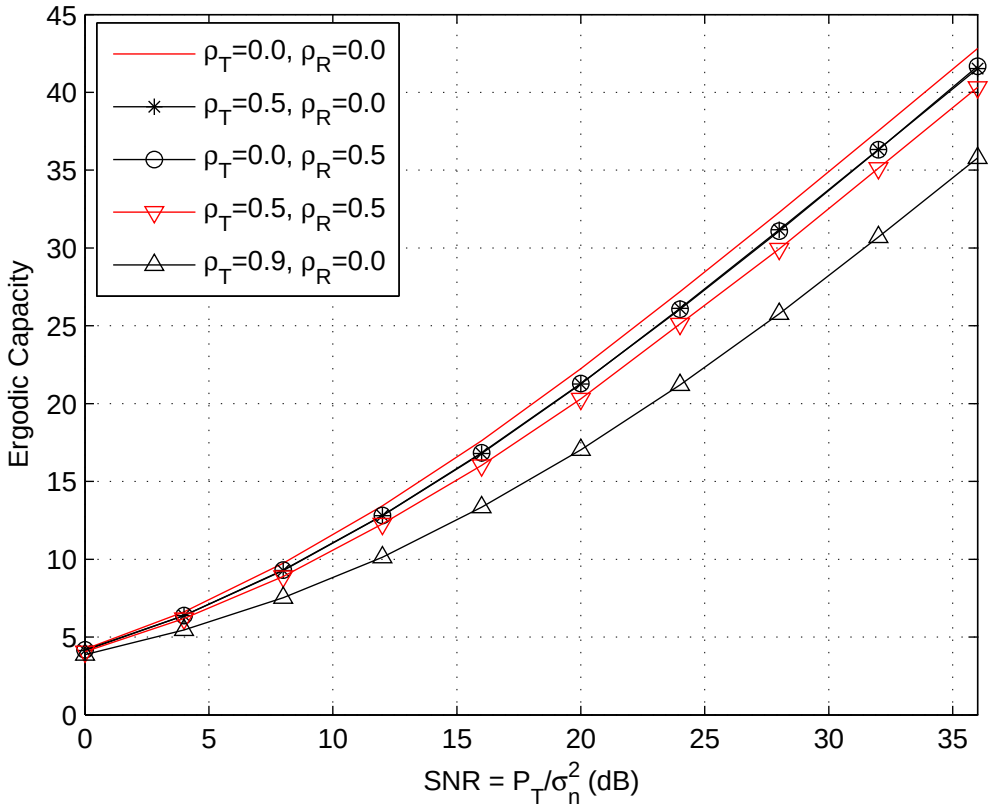

Figure 4.4. Ergodic capacity of a MIMO channel. $n_T = n_R = 4$. The two curves overlap for $(\rho_T, \rho_R) = (0.5, 0.0)$ and $(\rho_T, \rho_R) = (0.0, 0.5)$.

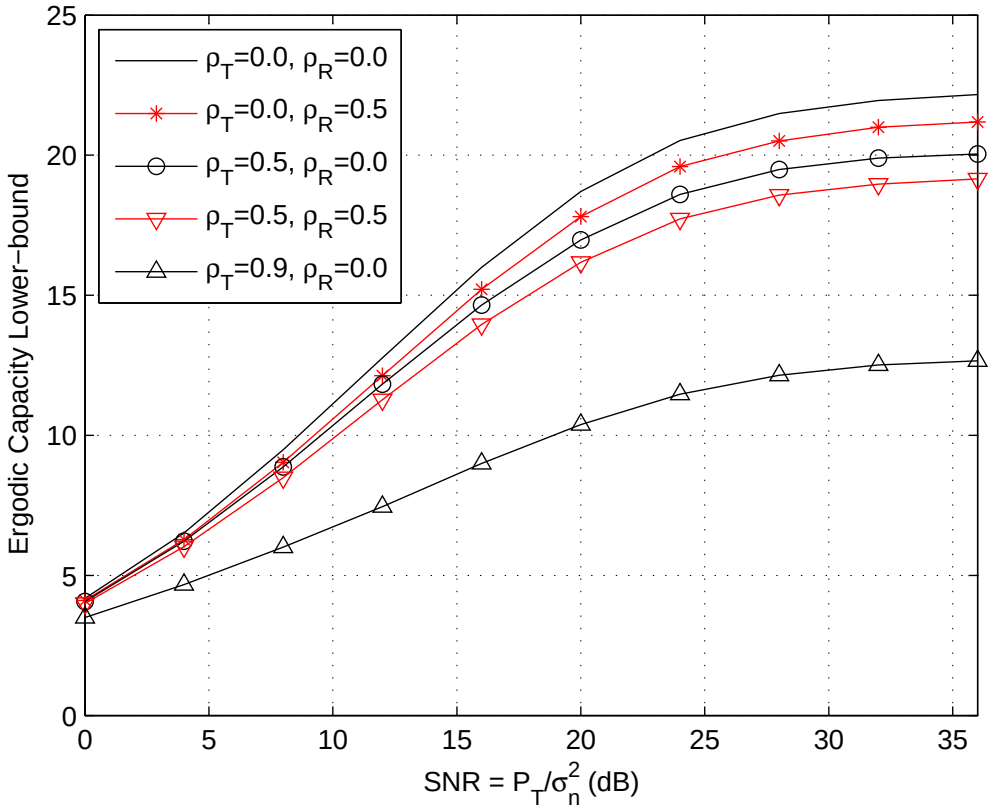

Figure 4.5. Ergodic capacity lower-bound of a MIMO channel using the optimum transmit covariance matrix. $n_T = n_R = 4$, $P_{tr}/\sigma_n^2 = 26.016$ dB. The values of σ_E^2 are 0.0099, 0.0148, and 0.0689, for ρ_T = 0.0, 0.5, and 0.9, respectively. The two curves do not overlap for $(\rho_T, \rho_R) = (0.5, 0.0)$ and $(\rho_T, \rho_R) = (0.0, 0.5)$.

Based on Figs. 4.4 and 4.5, the two curves marked with $(\rho_T, \rho_R) = (0.5, 0.0)$ and $(\rho_T, \rho_R) = (0.0, 0.5)$ overlap with perfect CSI, but they do not overlap with imperfect CSI. Again, this is due to the unsymmetrical use of $\mathbf{R}_T$ and $\mathbf{R}_R$ in our channel estimation.

4. Optimum vs. Two Suboptimum Transmitters with Asymptotic Optimality

   We now consider the special case without receive correlation as in Section 4.3 or in Part 4 of Section 3.7.

   Two suboptimum transmission strategies can be obtained:

   - by ignoring the channel correlation information at the transmitter, treating $\hat{\mathbf{H}}$ as if it were the actual channel,
   - or by a water-filling type of power allocation to the effective channel eigenmodes of $\hat{\mathbf{H}}_{w0}^H \hat{\mathbf{H}}_{w0}$ (see Section 3.4) followed by a cancelation of the effect of $\mathbf{R}_T$.

   We refer to them as the noise-suppression structure and the correlation-cancelation structure, respectively, as in Part 4 of Section 3.7. Fig. 4.6 shows the comparison of the optimum and two suboptimum schemes.

   It is interesting to note that the relation between these three curves is analogous to that observed in Fig. 3.5.

4.7 Summary

In this chapter, we have used a tight capacity lower-bound as the design criterion to maximize the mutual information of a MIMO channel with imperfect channel knowledge at both ends. The tightness of the lower-bound has been shown by simulation. The closed-form

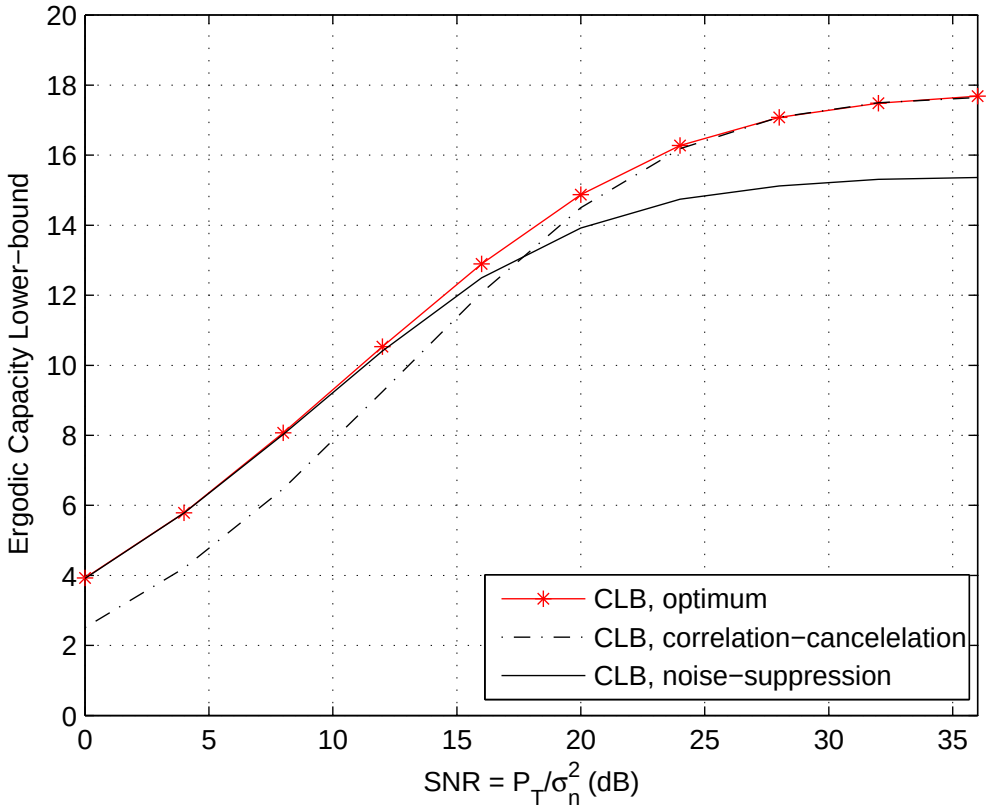

Figure 4.6. Ergodic capacity lower-bound of a MIMO channel: optimum vs. suboptimum transmitters. $n_T = n_R = 4$. $\rho_T = 0.7$, $\rho_R = 0.0$. $P_{tr}/\sigma_n^2 = 26.016$ dB. The value of σ_E^2 is 0.0238 for ρ_T = 0.7.

optimum transmit covariance matrix (or the precoder matrix) for this lower-bound has been determined for the special case with no receive correlation, and the optimum structure of the transmitter has been presented for the general case with correlation at both ends. The optimum transmit covariance matrix is shown to be advantageous over the non-optimum uniform power allocation scheme. The effects of channel estimation error and channel correlation have been assessed. We have also revealed the relationship between the capacity lower-bound problem and the minimum total MSE design.

4.8 Derivation and Proof Details

4.8.1 Proof of Lemma 3

We first equivalently formulate (4.8) as [7, p. 130, Section 4.1.3]

$$\min_{\mathbf{F},\mathrm{tr}(\mathbf{F}\mathbf{F}^H)\le P_T} \min_{\mathbf{G}(\mathbf{F})} \ln\det\left[MSE\left[\mathbf{F},\mathbf{G}(\mathbf{F})\right]\right].$$

The inner minimization is achieved by

$$\mathbf{G} = \mathbf{F}^H\hat{\mathbf{H}}^H\left\{\hat{\mathbf{H}}\mathbf{F}\mathbf{F}^H\hat{\mathbf{H}}^H + \left[\sigma_n^2 + \sigma_E^2\cdot\mathrm{tr}(\mathbf{R}_T\mathbf{F}\mathbf{F}^H)\right]\cdot\mathbf{I}_{n_R}\right\}^{-1}. \tag{4.35}$$

This can be easily shown by taking the derivative of $\ln\det\left[MSE\left(\mathbf{F},\mathbf{G}\right)\right]$ with respect to $\mathbf{G}$ (see Subsection 4.8.2). Substituting this formula into (4.7), (4.8) can then be equivalently formulated as

$$\min_{\mathbf{F},\mathrm{tr}(\mathbf{F}\mathbf{F}^H)\le P_T} -\ln\det\left[\mathbf{I}_{n_R} + \frac{\hat{\mathbf{H}}\mathbf{F}\mathbf{F}^H\hat{\mathbf{H}}^H}{\sigma_n^2 + \sigma_E^2\cdot\mathrm{tr}(\mathbf{R}_T\mathbf{F}\mathbf{F}^H)}\right]. \tag{4.36}$$

In the above, we have used the result $\det[\mathbf{I}+\mathbf{A}\mathbf{B}] = \det[\mathbf{I}+\mathbf{B}\mathbf{A}]$. Define $\mathbf{Q} = \mathbf{F}\mathbf{F}^H$, and then it is obvious that (4.36) is equivalent to (4.6).

The problem (4.36) has a closed and bounded feasible set and its objective function is continuous at all points of the feasible set. Thus, by Weierstrass' Theorem [5, p. 654,

Proposition A.8], a global minimum exists for (4.36). By equivalence [7, p. 130, Section 4.1.3], the same global minimum exists for (4.8). Again, by equivalence, a global maximum exists for (4.6) and the maximizing $\mathbf{Q}_{opt}$ for (4.6) is related to the minimizing $\mathbf{F}_{c,opt}$ for (4.36) or (4.8) as $\mathbf{Q}_{opt} = \mathbf{F}_{c,opt}\mathbf{F}_{c,opt}^H$. This concludes the proof of **Lemma 1**. □

4.8.2 Derivations of (4.9)-(4.12)

Note that (4.11) and (4.12) come from the power constraint and the complementary slackness, respectively. To derive (4.9)-(4.10), the preliminaries presented in Subsection 3.9.3 are needed. As before, we only need to take the partial derivatives of $\mathscr{L}_2(\mathbf{F},\mathbf{G},\mu_2)$ with respect to $\mathbf{F}^*$ and $\mathbf{G}^*$, i.e., we need to find $\partial\mathscr{L}_2/\partial\,\mathbf{F}^*$ and $\partial\mathscr{L}_2/\partial\,\mathbf{G}^*$.

From [60], $\partial\left[\ln\det\mathbf{X}\right] = \mathrm{tr}(\mathbf{X}^{-1}\partial\mathbf{X})$. Therefore, with respect to $\mathbf{F}$ and $\mathbf{F}^H$,

$$
\begin{aligned}
&\partial\mathscr{L}_2(\mathbf{F},\mathbf{G},\mu_2)\\
&= \mathrm{tr}\left\{\left[MSE(\mathbf{F},\mathbf{G})\right]^{-1}\left[\mathbf{G}\hat{\mathbf{H}}(\partial\mathbf{F})\mathbf{F}^H\hat{\mathbf{H}}^H\mathbf{G}^H + \mathbf{G}\hat{\mathbf{H}}\mathbf{F}(\partial\mathbf{F}^H)\hat{\mathbf{H}}^H\mathbf{G}^H\right]\right\}\\
&\quad - \mathrm{tr}\left\{\left[MSE(\mathbf{F},\mathbf{G})\right]^{-1}\left[\mathbf{G}\hat{\mathbf{H}}(\partial\mathbf{F}) + (\partial\mathbf{F}^H)\hat{\mathbf{H}}^H\mathbf{G}^H\right]\right\} + \mu_2\cdot\mathrm{tr}\left[(\partial\mathbf{F})\mathbf{F}^H + \mathbf{F}(\partial\mathbf{F}^H)\right]\\
&\quad + \sigma_E^2\cdot\mathrm{tr}\left\{\left[MSE(\mathbf{F},\mathbf{G})\right]^{-1}\mathbf{G}\mathbf{G}^H\right\}\cdot\mathrm{tr}\left[\mathbf{R}_T(\partial\mathbf{F})\mathbf{F}^H + \mathbf{R}_T\mathbf{F}(\partial\mathbf{F}^H)\right]\\
&= \mathrm{tr}\left\{\left[\left[\mathbf{F}^H\hat{\mathbf{H}}^H\mathbf{G}^H - \mathbf{I}_r\right]\left[MSE(\mathbf{F},\mathbf{G})\right]^{-1}\mathbf{G}\hat{\mathbf{H}} + \mu_2\cdot\mathbf{F}^H\right](\partial\mathbf{F})\right\}\\
&\quad + \mathrm{tr}\left\{\left[\hat{\mathbf{H}}^H\mathbf{G}^H\left[MSE(\mathbf{F},\mathbf{G})\right]^{-1}\left[\mathbf{G}\hat{\mathbf{H}}\mathbf{F} - \mathbf{I}_r\right] + \mu_2\cdot\mathbf{F}\right](\partial\mathbf{F}^H)\right\}\\
&\quad + \sigma_E^2\cdot\mathrm{tr}\left\{\left[MSE(\mathbf{F},\mathbf{G})\right]^{-1}\mathbf{G}\mathbf{G}^H\right\}\cdot\mathrm{tr}\left[\mathbf{F}^H\mathbf{R}_T(\partial\mathbf{F}) + \mathbf{R}_T\mathbf{F}(\partial\mathbf{F}^H)\right].
\end{aligned}
$$

Using the identities in Subsection 3.9.3,

$$
\begin{aligned}
\frac{\partial\mathscr{L}_2(\mathbf{F},\mathbf{G},\mu_2)}{\partial\Re\mathbf{F}} &= \left\{\left[\mathbf{F}^H\hat{\mathbf{H}}^H\mathbf{G}^H - \mathbf{I}_r\right]\left[MSE(\mathbf{F},\mathbf{G})\right]^{-1}\mathbf{G}\hat{\mathbf{H}} + \mu_2\cdot\mathbf{F}^H\right\}^T\\
&\quad + \hat{\mathbf{H}}^H\mathbf{G}^H\left[MSE(\mathbf{F},\mathbf{G})\right]^{-1}\left(\mathbf{G}\hat{\mathbf{H}}\mathbf{F} - \mathbf{I}_r\right) + \mu_2\cdot\mathbf{F}\\
&\quad + \sigma_E^2\cdot\mathrm{tr}\left\{\left[MSE(\mathbf{F},\mathbf{G})\right]^{-1}\mathbf{G}\mathbf{G}^H\right\}\cdot\left[\left(\mathbf{F}^H\mathbf{R}_T\right)^T + \mathbf{R}_T\mathbf{F}\right],\\
i\cdot\frac{\partial\mathscr{L}_c(\mathbf{F},\mathbf{G},\mu_c)}{\partial\Im\mathbf{F}} &= -\left\{\left[\mathbf{F}^H\hat{\mathbf{H}}^H\mathbf{G}^H - \mathbf{I}_r\right]\left[MSE(\mathbf{F},\mathbf{G})\right]^{-1}\mathbf{G}\hat{\mathbf{H}} + \mu_2\cdot\mathbf{F}^H\right\}^T
\end{aligned}
$$

$$+\hat{\mathbf{H}}^H\mathbf{G}^H[MSE(\mathbf{F},\mathbf{G})]^{-1}\left(\mathbf{G}\hat{\mathbf{H}}\mathbf{F}-\mathbf{I}_r\right)+\mu_2\cdot\mathbf{F}$$
$$+\sigma_E^2\cdot\mathrm{tr}\left\{[MSE(\mathbf{F},\mathbf{G})]^{-1}\mathbf{G}\mathbf{G}^H\right\}\cdot\left[-\left(\mathbf{F}^H\mathbf{R}_T\right)^T+\mathbf{R}_T\mathbf{F}\right].$$

Therefore,

$$\begin{aligned}\frac{\partial\mathscr{L}_2(\mathbf{F},\mathbf{G},\mu_2)}{\partial\mathbf{F}^*}&=\frac{1}{2}\left[\frac{\partial\mathscr{L}_2(\mathbf{F},\mathbf{G},\mu_2)}{\partial\Re\mathbf{F}}+i\cdot\frac{\partial\mathscr{L}_2(\mathbf{F},\mathbf{G},\mu_2)}{\partial\Im\mathbf{F}}\right]\\&=\hat{\mathbf{H}}^H\mathbf{G}^H[MSE(\mathbf{F},\mathbf{G})]^{-1}(\mathbf{G}\hat{\mathbf{H}}\mathbf{F}-\mathbf{I}_r)+\mu_2\cdot\mathbf{F}\\&\quad+\sigma_E^2\cdot\mathrm{tr}\left\{[MSE(\mathbf{F},\mathbf{G})]^{-1}\mathbf{G}\mathbf{G}^H\right\}\cdot\mathbf{R}_T\mathbf{F}.\end{aligned}$$

Similarly, with respect to $\mathbf{G}$ and $\mathbf{G}^H$,

$$\begin{aligned}\partial\mathscr{L}_2(\mathbf{F},\mathbf{G},\mu_2)&=\mathrm{tr}\left\{\left[\hat{\mathbf{H}}\mathbf{F}(\mathbf{F}^H\hat{\mathbf{H}}^H\mathbf{G}^H-\mathbf{I}_r)+\tau_4\cdot\mathbf{G}^H\right][MSE(\mathbf{F},\mathbf{G})]^{-1}(\partial\mathbf{G})\right\}\\&\quad+\mathrm{tr}\left\{[MSE(\mathbf{F},\mathbf{G})]^{-1}\left[(\mathbf{G}\hat{\mathbf{H}}\mathbf{F}-\mathbf{I}_r)\mathbf{F}^H\hat{\mathbf{H}}^H+\tau_4\cdot\mathbf{G}\right](\partial\mathbf{G}^H)\right\},\end{aligned}$$

where $\tau_4=\sigma_n^2+\sigma_E^2\cdot\mathrm{tr}(\mathbf{R}_T\mathbf{F}\mathbf{F}^H)$, as defined in Section 4.3, and

$$\begin{aligned}\frac{\partial\mathscr{L}_2(\mathbf{F},\mathbf{G},\mu_2)}{\partial\Re\mathbf{G}}&=\left\{\left[\hat{\mathbf{H}}\mathbf{F}(\mathbf{F}^H\hat{\mathbf{H}}^H\mathbf{G}^H-\mathbf{I}_r)+\tau_4\cdot\mathbf{G}^H\right][MSE(\mathbf{F},\mathbf{G})]^{-1}\right\}^T\\&\quad+[MSE(\mathbf{F},\mathbf{G})]^{-1}\left[(\mathbf{G}\hat{\mathbf{H}}\mathbf{F}-\mathbf{I}_r)\cdot\mathbf{F}^H\hat{\mathbf{H}}^H+\tau_4\cdot\mathbf{G}\right],\\i\cdot\frac{\partial\mathscr{L}_2(\mathbf{F},\mathbf{G},\mu_2)}{\partial\Im\mathbf{G}}&=-\left\{\left[\hat{\mathbf{H}}\mathbf{F}(\mathbf{F}^H\hat{\mathbf{H}}^H\mathbf{G}^H-\mathbf{I}_r)+\tau_4\cdot\mathbf{G}^H\right][MSE(\mathbf{F},\mathbf{G})]^{-1}\right\}^T\\&\quad+[MSE(\mathbf{F},\mathbf{G})]^{-1}\left[(\mathbf{G}\hat{\mathbf{H}}\mathbf{F}-\mathbf{I}_r)\cdot\mathbf{F}^H\hat{\mathbf{H}}^H+\tau_4\cdot\mathbf{G}\right].\end{aligned}$$

Therefore,

$$\begin{aligned}\frac{\partial\mathscr{L}_2(\mathbf{F},\mathbf{G},\mu_2)}{\partial\mathbf{G}^*}&=\frac{1}{2}\left[\frac{\partial\mathscr{L}_2(\mathbf{F},\mathbf{G},\mu_2)}{\partial\Re\mathbf{G}}+i\cdot\frac{\partial\mathscr{L}_2(\mathbf{F},\mathbf{G},\mu_2)}{\partial\Im\mathbf{G}}\right]\\&=[MSE(\mathbf{F},\mathbf{G})]^{-1}\left[\mathbf{G}(\hat{\mathbf{H}}\mathbf{F}\mathbf{F}^H\hat{\mathbf{H}}^H+\tau_4\cdot\mathbf{I}_{n_R})-\mathbf{F}^H\hat{\mathbf{H}}^H\right].\end{aligned}$$

Set

$$\frac{\partial\mathscr{L}_2(\mathbf{F},\mathbf{G},\mu_2)}{\partial\,\mathbf{F}^*}=0\quad\text{and}\quad\frac{\partial\mathscr{L}_2(\mathbf{F},\mathbf{G},\mu_2)}{\partial\,\mathbf{G}^*}=0.$$

Using the fact that $MSE(\mathbf{F},\mathbf{G})$ is full-rank, we obtain (4.9)-(4.10). This finishes the derivation of (4.9)-(4.12). □

4.8.3 Proof of Theorem 4

As outlined in Section 4.3, our method is to find all the solutions satisfying the KKT conditions (4.9)-(4.12) and then identify the optimum solution. An obvious solution that satisfies the conditions is $\mathbf{F} = 0, \mathbf{G} = 0, \mu_2 = 0$. Clearly, this solution is of no practical use, except that it will be used for comparison later. For now, we consider the case where $\mathbf{F} \neq 0$.

From (4.9), we can express $\mathbf{G}$ in terms of $\mathbf{F}$ as in (4.35). Substituting (4.35) into (4.7), using the matrix inversion lemma [60], we obtain

$$\begin{aligned} MSE(\mathbf{F},\mathbf{G}) &= \mathbf{I}_r - \mathbf{G}\hat{\mathbf{H}}\mathbf{F} && (4.37)\\ &= \tau_4 \cdot \left[\mathbf{F}^H\hat{\mathbf{H}}^H\hat{\mathbf{H}}\mathbf{F} + \tau_4 \cdot \mathbf{I}_r\right]^{-1}, && (4.38)\\ \mathbf{G} &= \left[\mathbf{F}^H\hat{\mathbf{H}}^H\hat{\mathbf{H}}\mathbf{F} + \tau_4 \cdot \mathbf{I}_r\right]^{-1}\mathbf{F}^H\hat{\mathbf{H}}^H. && (4.39) \end{aligned}$$

Clearly, here $\mathbf{G}\hat{\mathbf{H}}\mathbf{F}$ is a Hermitian matrix, i.e., $\mathbf{G}\hat{\mathbf{H}}\mathbf{F} = \mathbf{F}^H\hat{\mathbf{H}}^H\mathbf{G}^H$. Based on (4.37), (4.38) and (4.39),

$$\begin{aligned} \mathrm{tr}\left\{\left[MSE(\mathbf{F},\mathbf{G})\right]^{-1}\mathbf{G}\mathbf{G}^H\right\} &= \mathrm{tr}\left(\mathbf{F}^H\hat{\mathbf{H}}^H\mathbf{G}^H\right)/\tau_4,\\ &= \mathrm{tr}\left(\mathbf{G}\hat{\mathbf{H}}\mathbf{F}\right)/\tau_4. && (4.40) \end{aligned}$$

Using (4.37) and (4.40), (4.10) can be simplified as

$$\hat{\mathbf{H}}^H\mathbf{G}^H = \left\{\mu_2 \cdot \mathbf{I}_{n_T} + [\mathrm{tr}(\mathbf{G}\hat{\mathbf{H}}\mathbf{F})/\tau_4] \cdot \sigma_E^2 \cdot \mathbf{R}_T\right\}\mathbf{F}. \quad (4.41)$$

First pre-multiplying both sides of (4.41) by $\mathbf{F}^H$ and then taking the trace of both sides, using the fact that $\mathbf{G}\hat{\mathbf{H}}\mathbf{F}$ is Hermitian, we obtain

$$\tau_4 \cdot \mathrm{tr}\left(\mathbf{G}\hat{\mathbf{H}}\mathbf{F}\right) = \mu_2\tau_4 \cdot \mathrm{tr}\left(\mathbf{F}\mathbf{F}^H\right) + \mathrm{tr}\left(\mathbf{G}\hat{\mathbf{H}}\mathbf{F}\right) \cdot \sigma_E^2 \cdot \mathrm{tr}\left(\mathbf{R}_T\mathbf{F}\mathbf{F}^H\right).$$

Using the definition of τ_4, we obtain

$$\mu_2 \cdot \tau_4 \cdot \mathrm{tr}\left(\mathbf{F}\mathbf{F}^H\right) = \sigma_n^2 \cdot \mathrm{tr}\left(\mathbf{G}\hat{\mathbf{H}}\mathbf{F}\right).$$

Due to (4.12), if $\mu_2 > 0$, $\mathrm{tr}(\mathbf{F}\mathbf{F}^H)$ must be equal to P_T, which yields

$$\mu_2 = \sigma_n^2 \cdot \mathrm{tr}\left(\mathbf{G}\hat{\mathbf{H}}\mathbf{F}\right)/(\tau_4 \cdot P_T). \tag{4.42}$$

Assume $\mathbf{F} \neq 0$ [i.e., $\mathrm{tr}(\mathbf{F}\mathbf{F}^H) > 0$]. Then if $\mu_2 = 0$, we must have $\mathrm{tr}\left(\mathbf{G}\hat{\mathbf{H}}\mathbf{F}\right) = 0$, and (4.42) is still valid. Furthermore, (4.42) holds even when $\mathbf{F} = 0, \mathbf{G} = 0, \mu_2 = 0$.

Using (4.42), (4.41) can be rewritten as

$$(\mu_2/\sigma_n^2)\mathbf{F}^H\left[\sigma_E^2 \cdot P_T \cdot \mathbf{R}_T + \sigma_n^2 \cdot \mathbf{I}_{n_T}\right] = \mathbf{G}\hat{\mathbf{H}}. \tag{4.43}$$

In general, the matrix $\mathbf{F}$ can be expressed as

$$\begin{aligned}\mathbf{F} &= \left[\sigma_E^2 \cdot P_T \cdot \mathbf{R}_T + \sigma_n^2 \cdot \mathbf{I}_{n_T}\right]^{-\frac{1}{2}}\left[\mathbf{V}\ \ \tilde{\mathbf{V}}\right]\left[\mathbf{\Phi}_F^H\ \ \tilde{\mathbf{\Phi}}_F^H\right]^H \\ &= \left[\sigma_E^2 \cdot P_T \cdot \mathbf{R}_T + \sigma_n^2 \cdot \mathbf{I}_{n_T}\right]^{-\frac{1}{2}}\left[\underbrace{\mathbf{V}\mathbf{\Phi}_F}_{\mathbf{F}_{c,\|}} + \underbrace{\tilde{\mathbf{V}}\tilde{\mathbf{\Phi}}_F}_{\mathbf{F}_{c,\perp}}\right],\end{aligned}$$

where $\mathbf{V}$ and $\tilde{\mathbf{V}}$ have been defined in (4.13), $\mathbf{\Phi}_F$ and $\tilde{\mathbf{\Phi}}_F$ are $r \times B$ and $(n_T - r) \times B$ arbitrary matrices, respectively ($r \leq B \leq n_T$). As in Subsection 3.9.5, it can be verified that

$$\mathbf{F}_{c,\|}^H\mathbf{F}_{c,\perp} = 0,\ \ \mathbf{F}_{c,\perp}^H\mathbf{F}_{c,\|} = 0,\ \text{ and }\ \hat{\mathbf{H}}\left[\sigma_E^2 \cdot P_T \cdot \mathbf{R}_T + \sigma_n^2 \cdot \mathbf{I}_{n_T}\right]^{-\frac{1}{2}}\mathbf{F}_{c,\perp} = 0.$$

Post-multiplying (4.43) by $\left[\sigma_E^2 \cdot P_T \cdot \mathbf{R}_T + \sigma_n^2 \cdot \mathbf{I}_{n_T}\right]^{-\frac{1}{2}}\mathbf{F}_{c,\perp}$, using the above identities, we obtain $\mathbf{F}_{c,\perp} = 0$. Thus, the $\mathbf{F}$ matrix satisfying the KKT conditions can be expressed as

$$\mathbf{F} = \left[\sigma_E^2 \cdot P_T \cdot \mathbf{R}_T + \sigma_n^2 \cdot \mathbf{I}_{n_T}\right]^{-\frac{1}{2}}\mathbf{V}\mathbf{\Phi}_F. \tag{4.44}$$

Furthermore, based on (4.9), using a method similar to that in Subsection 3.9.5, we can show that the $\mathbf{G}$ matrix satisfying the KKT conditions can be expressed as

$$\mathbf{G} = \mathbf{\Phi}_G\mathbf{V}^H\left[\sigma_E^2 \cdot P_T \cdot \mathbf{R}_T + \sigma_n^2 \cdot \mathbf{I}_{n_T}\right]^{-\frac{1}{2}}\hat{\mathbf{H}}^H, \tag{4.45}$$

where $\mathbf{\Phi}_G$ is an arbitrary $B \times r$ matrix corresponding to $\mathbf{\Phi}_F$.

Up to now, $\mathbf{\Phi}_F$ and $\mathbf{\Phi}_G$ are arbitrary $r \times B$ and $B \times r$ matrices, respectively, where B can be any integer satisfying $r \leq B \leq n_T$. Since our ultimate goal is to determine $\mathbf{Q}$, which is given by $\mathbf{Q} = \mathbf{F}\mathbf{F}^H$, the quantity of interest is the $r \times r$ matrix $\mathbf{\Phi}_F \mathbf{\Phi}_F^H$. We can then safely choose $B = r$ without incurring any loss of generality for our problem. This explains why we have chosen the size of the precoder matrix $\mathbf{F}$ to be $n_T \times r$ in Section 4.3.

Assume $\mathbf{F} \neq 0$. Post-multiply both sides of (4.43) by $\mathbf{F}$ and pre-multiply both sides of (4.9) by $\mathbf{G}$. Substitute (4.14) and (4.15) into the resulting formulas, to obtain

$$\mathbf{\Phi}_G \mathbf{\Lambda} \mathbf{\Phi}_F = \mathbf{\Phi}_G \mathbf{\Lambda} \mathbf{\Phi}_F \mathbf{\Phi}_F^H \mathbf{\Lambda} \mathbf{\Phi}_G^H + \tau_4 \cdot \mathbf{\Phi}_G \mathbf{\Lambda} \mathbf{\Phi}_G^H, \tag{4.46}$$

$$\mathbf{\Phi}_G \mathbf{\Lambda} \mathbf{\Phi}_F = (\mu_2/\sigma_n^2) \cdot \mathbf{\Phi}_F^H \mathbf{\Phi}_F. \tag{4.47}$$

Based on the above two formulas, using the method in [85], the optimum $\mathbf{\Phi}_{Fopt}$ (up to a unitary transform from the right-hand side) and $\mathbf{\Phi}_{Gopt}$ (up to a unitary transform from the left-hand side) can be shown to be diagonal without loss of generality and are given by (4.16) and (4.17), respectively. Inserting (4.14), (4.15), (4.16) and (4.17) into the expression for μ_2 and the power constraint $\mathrm{tr}(\mathbf{F}_{c,opt}\mathbf{F}_{c,opt}^H) = P_T$, we can obtain two equations. By solving them, we obtain μ_2 and τ_4 as given by (4.18) and (4.19), respectively.

An iterative procedure is used to determine the number m_0 in the expressions of (4.18) and (4.19). Let λ_l be the l-th element of $\mathbf{\Lambda}$ ($1 \leq l \leq r$). Initialize $m = r$.

1. Calculate τ_4 and μ_2 from (4.19) and (4.18). If $\mu_2 \leq \lambda_m \sigma_n^2/\tau_4$, stop and set $m_0 = m$; else: go to step 2.

2. Let $\mathbf{\Phi}_{Fopt,m} := 0$ and $m := m - 1$. Go to step 1).

So far, we have shown that all the solutions satisfying the KKT conditions (4.9)-(4.12) with $\mathbf{F} \neq 0$ are given by (4.14)-(4.19), up to a unitary transform. All these solutions differ only in a unitary transform, and thus lead to the same value of the objective function in

(4.8), which, based on (4.9), can be shown to be

$$-\ln\det\left[\mathbf{I}_r+\frac{1}{\tau_4}\mathbf{F}_{c,opt}^H\hat{\mathbf{H}}^H\hat{\mathbf{H}}\mathbf{F}_{c,opt}\right].$$

Since $\mathbf{F}_{c,opt}^H\hat{\mathbf{H}}^H\hat{\mathbf{H}}\mathbf{F}_{c,opt}$ is positive semidefinite, it is easy to see that the above is lower than the value of the objective function from ($\mathbf{F}=0,\mathbf{G}=0,\mu_2=0$). Therefore, we conclude that **Theorem 4** holds. □

4.8.4 Proof of Theorem 5

As in Subsection 4.8.3, we start from the KKT conditions (4.24)-(4.27).

The zero solution satisfying these conditions, i.e., $\mathbf{F}=0,\mathbf{G}=0,\mu_{gc}=0$, is immediately identified, and is left aside for now. We go on to find out the non-zero solutions.

From (4.24), using the matrix inversion lemma [60], we obtain

$$\mathbf{G}=\mathbf{F}^H\hat{\mathbf{H}}^H\left[\hat{\mathbf{H}}\mathbf{F}\mathbf{F}^H\hat{\mathbf{H}}^H+\sigma_{ce}^2\cdot\mathrm{tr}\left(\mathbf{R}_T\mathbf{F}\mathbf{F}^H\right)\cdot\mathbf{R}_{e,R}+\sigma_n^2\cdot\mathbf{I}_{n_R}\right]^{-1} \tag{4.48}$$

$$=\left\{\mathbf{I}_{r_{gc}}+\mathbf{F}^H\hat{\mathbf{H}}^H\left[\sigma_{ce}^2\cdot\mathrm{tr}\left(\mathbf{R}_T\mathbf{F}\mathbf{F}^H\right)\cdot\mathbf{R}_{e,R}+\sigma_n^2\cdot\mathbf{I}_{n_R}\right]^{-1}\hat{\mathbf{H}}\mathbf{F}\right\}^{-1}$$
$$\cdot\mathbf{F}^H\hat{\mathbf{H}}^H\left[\sigma_{ce}^2\cdot\mathrm{tr}\left(\mathbf{R}_T\mathbf{F}\mathbf{F}^H\right)\cdot\mathbf{R}_{e,R}+\sigma_n^2\cdot\mathbf{I}_{n_R}\right]^{-1}. \tag{4.49}$$

Based on (4.48) and the matrix inversion lemma, the following holds:

$$MSE(\mathbf{F},\mathbf{G})=\mathbf{I}_{r_{gc}}-\mathbf{G}\hat{\mathbf{H}}\mathbf{F}$$
$$=\left\{\mathbf{I}_{r_{gc}}+\mathbf{F}^H\hat{\mathbf{H}}^H\left[\sigma_{ce}^2\cdot\mathrm{tr}\left(\mathbf{R}_T\mathbf{F}\mathbf{F}^H\right)\cdot\mathbf{R}_{e,R}+\sigma_n^2\cdot\mathbf{I}_{n_R}\right]^{-1}\hat{\mathbf{H}}\mathbf{F}\right\}^{-1}. \tag{4.50}$$

From (4.49) and (4.50),

$$\mathbf{G}\mathbf{R}_{e,R}\mathbf{G}^H\left[MSE\left(\mathbf{F},\mathbf{G}\right)\right]^{-1}$$
$$=\mathbf{G}\mathbf{R}_{e,R}\left[\sigma_{ce}^2\cdot\mathrm{tr}\left(\mathbf{R}_T\mathbf{F}\mathbf{F}^H\right)\cdot\mathbf{R}_{e,R}+\sigma_n^2\cdot\mathbf{I}_{n_R}\right]^{-1}\hat{\mathbf{H}}\mathbf{F},$$
$$\mathrm{tr}\left\{\left[MSE\left(\mathbf{F},\mathbf{G}\right)\right]^{-1}\mathbf{G}\mathbf{R}_{e,R}\mathbf{G}^H\right\}$$

$$= \underbrace{\mathrm{tr}\left\{\mathbf{G}\mathbf{R}_{e,R}\left[\sigma_{ce}^2 \cdot \mathrm{tr}\left(\mathbf{R}_T\mathbf{F}\mathbf{F}^H\right)\cdot\mathbf{R}_{e,R} + \sigma_n^2\cdot\mathbf{I}_{n_R}\right]^{-1}\hat{\mathbf{H}}\mathbf{F}\right\}}_{\tau_5,\ \text{as defined in (4.21)}}. \tag{4.51}$$

From (4.51), (4.25) and the first equation in (4.50), we can show that

$$\begin{aligned}
&\hat{\mathbf{H}}^H\mathbf{G}^H[MSE(\mathbf{F},\mathbf{G})]^{-1}[\mathbf{G}\hat{\mathbf{H}}\mathbf{F} - \mathbf{I}_{r_{gc}}] + \left[\sigma_{ce}^2\mathrm{tr}\{[MSE(\mathbf{F},\mathbf{G})]^{-1}\mathbf{G}\mathbf{R}_{e,R}\mathbf{G}^H\}\mathbf{R}_T + \mu_{gc}\mathbf{I}_{n_T}\right]\mathbf{F}\\
&= -\hat{\mathbf{H}}^H\mathbf{G}^H + \left[\sigma_{ce}^2\cdot\tau_5\cdot\mathbf{R}_T + \mu_{gc}\cdot\mathbf{I}_{n_T}\right]\mathbf{F}\\
&= 0,
\end{aligned}$$

i.e.,

$$\mathbf{G}\hat{\mathbf{H}} = \mathbf{F}^H\left[\sigma_{ce}^2\cdot\tau_5\cdot\mathbf{R}_T + \mu_{gc}\cdot\mathbf{I}_{n_T}\right]. \tag{4.52}$$

From (4.51),

$$\begin{aligned}
\tau_5 &= \mathrm{tr}\left\{\mathbf{G}\mathbf{R}_{e,R}[\sigma_{ce}^2\cdot\mathrm{tr}(\mathbf{R}_T\mathbf{F}\mathbf{F}^H)\cdot\mathbf{R}_{e,R} + \sigma_n^2\cdot\mathbf{I}_{n_R}]^{-1}\hat{\mathbf{H}}\mathbf{F}\right\}\\
&= \frac{\mathrm{tr}\left\{\mathbf{G}[\sigma_{ce}^2\mathrm{tr}(\mathbf{R}_T\mathbf{F}\mathbf{F}^H)\cdot\mathbf{R}_{e,R} + \sigma_n^2\mathbf{I}_{n_R} - \sigma_n^2\mathbf{I}_{n_R}][\sigma_{ce}^2\mathrm{tr}(\mathbf{R}_T\mathbf{F}\mathbf{F}^H)\cdot\mathbf{R}_{e,R} + \sigma_n^2\mathbf{I}_{n_R}]^{-1}\hat{\mathbf{H}}\mathbf{F}\right\}}{\sigma_{ce}^2\cdot\mathrm{tr}(\mathbf{R}_T\mathbf{F}\mathbf{F}^H)}\\
&= \frac{\mathrm{tr}\left(\mathbf{G}\hat{\mathbf{H}}\mathbf{F}\right) - \sigma_n^2\cdot\mathrm{tr}\left\{\mathbf{G}[\sigma_{ce}^2\cdot\mathrm{tr}(\mathbf{R}_T\mathbf{F}\mathbf{F}^H)\cdot\mathbf{R}_{e,R} + \sigma_n^2\cdot\mathbf{I}_{n_R}]^{-1}\hat{\mathbf{H}}\mathbf{F}\right\}}{\sigma_{ce}^2\cdot\mathrm{tr}(\mathbf{R}_T\mathbf{F}\mathbf{F}^H)}.
\end{aligned} \tag{4.53}$$

On the other hand, from (4.52),

$$\mathrm{tr}\left\{\mathbf{F}^H\hat{\mathbf{H}}^H\mathbf{G}^H\right\} = \tau_5\cdot\sigma_{ce}^2\cdot\mathrm{tr}(\mathbf{F}^H\mathbf{R}_T\mathbf{F}) + \mu_{gc}\cdot\mathrm{tr}(\mathbf{F}\mathbf{F}^H). \tag{4.54}$$

From (4.53) and (4.54), using the fact that $\mathbf{G}\hat{\mathbf{H}}\mathbf{F}$ is Hermitian, it is clear that

$$\mu_{gc}\cdot\mathrm{tr}(\mathbf{F}\mathbf{F}^H) = \sigma_n^2\cdot\mathrm{tr}\left\{\mathbf{G}[\sigma_{ce}^2\cdot\mathrm{tr}(\mathbf{R}_T\mathbf{F}\mathbf{F}^H)\cdot\mathbf{R}_{e,R} + \sigma_n^2\cdot\mathbf{I}_{n_R}]^{-1}\hat{\mathbf{H}}\mathbf{F}\right\}. \tag{4.55}$$

Due to (4.27), if $\mu_{gc} > 0$, $\mathrm{tr}(\mathbf{F}\mathbf{F}^H)$ must be equal to P_T, which yields

$$\mu_{gc} = \frac{\sigma_n^2}{P_T}\mathrm{tr}\left\{\mathbf{G}[\sigma_{ce}^2\cdot\mathrm{tr}(\mathbf{R}_T\mathbf{F}\mathbf{F}^H)\cdot\mathbf{R}_{e,R} + \sigma_n^2\cdot\mathbf{I}_{n_R}]^{-1}\hat{\mathbf{H}}\mathbf{F}\right\},$$

i.e., (4.22). Assume $\mathbf{F} \neq 0$ [i.e., $\mathrm{tr}(\mathbf{F}\mathbf{F}^H) > 0$]. Then if $\mu_{gc} = 0$, the right-hand side of (4.55) must be zero and the above identity is still valid. Furthermore, (4.22) holds even when $\mathbf{F} = 0, \mathbf{G} = 0, \mu_{gc} = 0$.

From (4.52), using the method used for deriving (4.44) and (4.45) in Subsection 4.8.3 as well as the method used in Subsection 3.9.7, it can be shown that the precoder and decoder matrix satisfying (4.24)-(4.27) can be expressed as

$$\mathbf{F} = \left[\sigma_{ce}^2 \cdot \tau_5 \cdot \mathbf{R}_T + \mu_{gc} \cdot \mathbf{I}_{n_T}\right]^{-\frac{1}{2}} \mathbf{V}_{gc} \mathbf{\Phi}_{F,g}, \tag{4.56}$$

$$\mathbf{G} = \mathbf{\Phi}_{G,g} \mathbf{V}_{gc}^H \left[\sigma_{ce}^2 \cdot \tau_5 \cdot \mathbf{R}_T + \mu_{gc} \cdot \mathbf{I}_{n_T}\right]^{-\frac{1}{2}} \hat{\mathbf{H}}^H \left[\tau_6 \cdot \mathbf{R}_{e,R} + \sigma_n^2 \cdot \mathbf{I}_{n_R}\right]^{-1}, \tag{4.57}$$

where $\tau_6 = \sigma_{ce}^2 \cdot \mathrm{tr}(\mathbf{R}_T \mathbf{F}\mathbf{F}^H)$, as in (4.23).

Pre-multiply (4.24) by $\mathbf{G}$, and post-multiply (4.52) by $\mathbf{F}$ to obtain two equations. Substituting (4.56) and (4.57) into these two equations, we get

$$\mathbf{\Phi}_{G,g} \mathbf{\Lambda}_{gc} \mathbf{\Phi}_{F,g} = \mathbf{\Phi}_{F,g}^H \mathbf{\Phi}_{F,g},$$

$$\mathbf{\Phi}_{G,g} \mathbf{\Lambda}_{gc} \mathbf{\Phi}_{F,g} = \mathbf{\Phi}_{G,g} \mathbf{\Lambda}_{gc} \mathbf{\Phi}_{F,g} \mathbf{\Phi}_{F,g}^H \mathbf{\Lambda}_{gc} \mathbf{\Phi}_{G,g}^H + \mathbf{\Phi}_{G,g} \mathbf{\Lambda}_{gc} \mathbf{\Phi}_{G,g}^H.$$

Once again applying the method in [85], we obtain (4.31) and (4.32). The constants involved here, i.e., τ_5, μ_{gc} and τ_6 can be determined numerically. Therefore, we have determined the non-zero solutions to (4.4), as given by (4.29)-(4.32), up to a unitary transform.

Finally, as in Subsection 4.8.3, by comparing the values of the objective function from using the non-zero solutions and from using the zero solution, it is easy to verify that the non-zero solutions are all optimum. This concludes the proof for **Theorem 5**. □

Chapter 5

Minimum Sum MSE Transceiver Optimization for Multiuser MIMO Systems with Imperfect Channel Knowledge

5.1 Introduction

In Subsection 2.2.3, minimum sum mean-square error (MSMSE) linear transceiver designs under sum power constraints for multiuser MIMO systems have been introduced as a low-complexity and effective signal processing technique to manage both inter-stream and multiuser interferences as well as to offer diversity and high data rate.

The MSMSE linear precoding/decoding design has been studied for the uplink in [91], and for the downlink in [47, 89, 103, 125]. Most of previous work on this design has assumed perfect channel state information (CSI). In this chapter, the imperfectness of channel knowledge is taken into account [22, 23]. Two sum MSE minimization problems are formulated for the uplink and the downlink, respectively, subject to sum power constraints and under imperfect CSI. Iterative algorithms based on the Karush-Kuhn-Tucker (KKT) conditions are proposed for both the uplink and the downlink optimizations. Since the

KKT-conditions-based algorithm is not guaranteed to achieve the globally optimum solution, a sequential semidefinite programming (SDP) method is also proposed for the uplink optimization, which not only represents a feasible method to find the solution, but also serves a way to check the performance of the KKT-conditions-based algorithm.

As mentioned in Subsection 2.2.2, from the information-theoretic point of view, the multiple access channel (MAC, uplink) is better understood than the broadcast channel (BC, downlink), due to their differences in interference and cooperation [17, 31]. From the viewpoint of signal processing, the uplink is also easier to deal with than the downlink [82, 83, 88, 108]. Thus, the uplink–downlink duality is an important tool to simplify the downlink system design (see Subsections 2.2.2 and 2.2.3). To be specific, in a multiuser system with multiple antennas at the base station (BS) and with single-antenna users, under perfect channel knowledge, with the same sum power, the achievable signal-to-interference-plus-noise ratio (SINR) regions and normalized MSE regions for both links are the same, when noise variances are identical at all receivers [82, 94, 110]. Because of duality, beamforming problems in the downlink can be solved by forming and solving a dual uplink problem [82, 88, 108]. The same idea has been applied to the linear precoder-decoder designs *when both the BS and mobile stations (MSs) are equipped with multiple antennas* [47, 89], the scenario considered in this chapter.

Here in the context of joint linear precoder-decoder designs with sum power constraints, the uplink–downlink duality in average sum MSE is proved with imperfect CSI. Based on this duality, the minimum sum MSEs in both links are the same. Any uplink MSMSE design satisfying the associated KKT conditions can be translated for application to the downlink. Unlike the methods in [21, 89, 93] that show the duality by direct calculations of the MSEs or SINRs of all users, our proof here is solely based on the associated KKT conditions and thus provides an interesting new perspective to the relation of the dual links.

In Section 5.2, we describe the two design problems mathematically. Section 5.3 presents two KKT-conditions-based iterative algorithms for both the uplink and the downlink. The duality in sum MSE is presented in Section 5.4. The sequential SDP method for the uplink design is proposed in Section 5.5. Simulation results in Section 5.6 corroborate our analysis and show the effect of imperfect CSI. We supply all the derivation and proof details in Section 5.8.

5.2 Uplink and Downlink System Designs with Imperfect Channel Knowledge

Consider the multiuser MIMO system model with linear precoding/decoding in Fig. 2.3. It is assumed that the channels arising from the antennas at each MS are spatially uncorrelated due to the presence of sufficient local scattering. Therefore, the uplink channel model is given by [95] (see also Subsection 2.1.1):

$$\mathbf{H}_i = \mathbf{\Sigma}_i^{\frac{1}{2}} \mathbf{H}_{wi},$$

where $\mathbf{\Sigma}_i$ is the normalized channel correlation matrix at the BS (with unit diagonal entries) seen by user i, $i = 1, \ldots, K$. The entries of $\mathbf{H}_{wi}$ are independent and identically-distributed (i.i.d.) $\mathcal{N}_c(0,1)$, $\forall i$. The dual downlink channel model is given by

$$\mathbf{H}_i^H = \mathbf{H}_{wi}^H \mathbf{\Sigma}_i^{\frac{1}{2}}, i = 1, \ldots, K.$$

In practice, CSI is obtained through channel estimation. As mentioned earlier, the downlink is more likely to become the bottleneck in data transfer than the uplink [4]. Therefore, we put more emphasis on the downlink, and assume that the channel estimation is performed there. A common training signal matrix can be broadcast to all users for

them to obtain the channel estimates. More generally, to account for different QoS requirements of individual users, separate training signal matrices can be employed to obtained channel estimates for different users. In the latter case, for each user, the channel estimation process is exactly the same as described in Section 3.2 and Section 3.4. Therefore, the downlink CSI model is given by

$$\mathbf{H}_i^H = \hat{\mathbf{H}}_i^H + \mathbf{E}_i^H,\ \hat{\mathbf{H}}_i^H = \hat{\mathbf{H}}_{wi}^H \boldsymbol{\Sigma}_i^{\frac{1}{2}},\ \text{and}\ \mathbf{E}_i^H = \mathbf{E}_{wi}^H \boldsymbol{\Sigma}_i^{\frac{1}{2}},\ i = 1, \ldots, K.$$

The entries of $\hat{\mathbf{H}}_{wi}^H$ and $\mathbf{E}_{wi}^H$ are i.i.d. $\mathcal{N}_c(0, 1-\sigma_{Ei}^2)$ and $\mathcal{N}_c(0, \sigma_{Ei}^2)$, respectively, where σ_{Ei}^2 is the channel estimation error variance for user i, $i = 1, \ldots, K$. It is assumed that the channel estimation errors are independent of the data and channel noises. Denote the power of the training signal matrix for user i as $P_{tr,i}$, $\forall i$. Then, as explained in Section 3.4,

$$\sigma_{Ei}^2 = \frac{\mathrm{tr}(\boldsymbol{\Sigma}_i^{-1}) \cdot \sigma_n^2 / P_{tr,i}}{1 + \left[\mathrm{tr}(\boldsymbol{\Sigma}_i^{-1}) \cdot \sigma_n^2 / P_{tr,i}\right]},\ \forall i.$$

The dual uplink CSI model at the BS can be expressed as:

$$\mathbf{H}_i = \hat{\mathbf{H}}_i + \mathbf{E}_i, i = 1, \ldots, K.$$

In the downlink, to make the transmitter aware of the channel state, the channel estimates are fed back to the BS from the MSs. Thus, we assume that the estimated channel matrices $\{\hat{\mathbf{H}}_i\}_{i=1}^K$ (or, equivalently, $\{\hat{\mathbf{H}}_i^H\}_{i=1}^K$), the channel estimation error variances $\{\sigma_{Ei}^2\}_{i=1}^K$, the noise variance σ_n^2, and the channel correlation matrices $\{\boldsymbol{\Sigma}_i\}_{i=1}^K$ are available at the BS. As in [91], it is assumed that the joint optimizations are performed at the BS, and then the optimum filters (i.e., precoders/decoders) for the users are sent to the MSs.

5.2.1 The Uplink Design

With the above CSI model,

$$\mathbf{y}_{ul} = \sum_{i=1}^{K} (\hat{\mathbf{H}}_i + \mathbf{E}_i)\, \mathbf{F}_i\, \mathbf{s}_{ul,i} + \mathbf{n}_{ul}.$$

The MSE matrix for user j, $j = 1, \ldots, K$, is given by

$$\begin{aligned} MSE_{ul,j} &= \mathbb{E}\left[(\mathbf{r}_{ul,j} - \mathbf{s}_{ul,j})(\mathbf{r}_{ul,j} - \mathbf{s}_{ul,j})^H\right] \\ &= \mathbf{G}_j \left\{ \left[\sum_{i=1}^{K} \hat{\mathbf{H}}_i \mathbf{F}_i \mathbf{F}_i^H \hat{\mathbf{H}}_i^H \right] + \sigma_n^2 \cdot \mathbf{I}_M \right\} \mathbf{G}_j^H - \mathbf{G}_j \hat{\mathbf{H}}_j \mathbf{F}_j - \mathbf{F}_j^H \hat{\mathbf{H}}_j^H \mathbf{G}_j^H + \mathbf{I}_{l_j} \\ &\quad + \mathbf{G}_j \left[\sum_{i=1}^{K} \sigma_{Ei}^2 \cdot \mathrm{tr}(\mathbf{F}_i \mathbf{F}_i^H) \cdot \mathbf{\Sigma}_i \right] \mathbf{G}_j^H. \end{aligned} \tag{5.1}$$

The detailed derivation of (5.1) is given in Subsection 5.8.1. The sum MSE from all users is then given by

$$mse_{ul,t} = \sum_{j=1}^{K} \mathrm{tr}(MSE_{ul,j}).$$

The uplink problem is to minimize the sum MSE from all users subject to a sum power constraint P_S, i.e.,

$$\begin{aligned} &\min_{\{(\mathbf{F}_j, \mathbf{G}_j)\}_{j=1}^{K}} mse_{ul,t} \\ &\text{subject to } \sum_{j=1}^{K} \mathrm{tr}(\mathbf{F}_j \mathbf{F}_j^H) \leq P_S. \end{aligned} \tag{5.2}$$

5.2.2 The Downlink Design

With imperfect CSI, for each j, $j = 1, \ldots, K$,

$$\mathbf{y}_{dl,j} = (\hat{\mathbf{H}}_j^H + \mathbf{E}_j^H) \left[\sum_{i=1}^{K} \mathbf{T}_i \, \mathbf{s}_{dl,i} \right] + \mathbf{n}_{dl,j}.$$

Similar to the uplink case, the MSE matrix for user j is calculated as

$$\begin{aligned} MSE_{dl,j} &= \mathbb{E}\left[(\mathbf{r}_{dl,j} - \mathbf{s}_{dl,j})(\mathbf{r}_{dl,j} - \mathbf{s}_{dl,j})^H\right] \\ &= \mathbf{R}_j \left\{ \hat{\mathbf{H}}_j^H \left[\sum_{i=1}^{K} \mathbf{T}_i \mathbf{T}_i^H \right] \hat{\mathbf{H}}_j + \sigma_n^2 \cdot \mathbf{I}_{N_j} \right\} \mathbf{R}_j^H - \mathbf{R}_j \hat{\mathbf{H}}_j^H \mathbf{T}_j - \mathbf{T}_j^H \hat{\mathbf{H}}_j \mathbf{R}_j^H + \mathbf{I}_{l_j} \\ &\quad + \sigma_{Ej}^2 \cdot \mathrm{tr}\left\{ \mathbf{\Sigma}_j \left[\sum_{i=1}^{K} \mathbf{T}_i \mathbf{T}_i^H \right] \right\} \cdot \mathbf{R}_j \mathbf{R}_j^H. \end{aligned} \tag{5.3}$$

Detailed calculations of (5.3) are presented in Subsection 5.8.2. The sum MSE for the downlink can be expressed as

$$mse_{dl,t} = \sum_{j=1}^{K} \mathrm{tr}(MSE_{dl,j}).$$

The downlink problem is formulated as

$$\begin{aligned} &\min_{\{(\mathbf{T}_j,\mathbf{R}_j)\}_{j=1}^K} mse_{dl,t} \\ &\text{subject to } \sum_{j=1}^{K} \mathrm{tr}(\mathbf{T}_j\mathbf{T}_j^H) \le P_S. \end{aligned} \tag{5.4}$$

5.3 Iterative Algorithms Based on the KKT Conditions

5.3.1 The KKT Conditions

Consider the uplink problem (5.2). We first formulate the associated Lagrangian:

$$\mathscr{L}_{ul}\left[\left\{(\mathbf{F}_j,\mathbf{G}_j)\right\}_{j=1}^K,\mu_{ul}\right] = mse_{ul,t} + \mu_{ul}\cdot\left\{\left[\sum_{j=1}^{K}\mathrm{tr}(\mathbf{F}_j\mathbf{F}_j^H)\right] - P_S\right\},$$

where μ_{ul} is the Lagrange multiplier associated with the uplink sum power constraint. The associated KKT conditions can be obtained using the same method as in Subsection 3.9.3, and are given by (5.5)-(5.8).

$$\mathbf{F}_k^H\hat{\mathbf{H}}_k^H = \mathbf{G}_k\left[\sum_{j=1}^{K}\hat{\mathbf{H}}_j\mathbf{F}_j\mathbf{F}_j^H\hat{\mathbf{H}}_j^H + \sigma_n^2\cdot\mathbf{I}_M + \sum_{j=1}^{K}\sigma_{Ej}^2\cdot\mathrm{tr}(\mathbf{F}_j\mathbf{F}_j^H)\cdot\mathbf{\Sigma}_j\right], \tag{5.5}$$

$$\hat{\mathbf{H}}_k^H\mathbf{G}_k^H = \left\{\hat{\mathbf{H}}_k^H\left[\sum_{j=1}^{K}\mathbf{G}_j^H\mathbf{G}_j\right]\hat{\mathbf{H}}_k + \mu_{ul}\cdot\mathbf{I}_{N_k} + \sigma_{Ek}^2\cdot\left[\sum_{j=1}^{K}\mathrm{tr}(\mathbf{G}_j\mathbf{\Sigma}_k\mathbf{G}_j^H)\right]\cdot\mathbf{I}_{N_k}\right\}\mathbf{F}_k, \tag{5.6}$$

$$k = 1,\ldots,K,$$

$$\mu_{ul} \ge 0,\ \sum_{j=1}^{K}\mathrm{tr}(\mathbf{F}_j\mathbf{F}_j^H) \le P_S, \tag{5.7}$$

$$\mu_{ul}\cdot\left[\sum_{j=1}^{K}\mathrm{tr}(\mathbf{F}_j\mathbf{F}_j^H) - P_S\right] = 0. \tag{5.8}$$

Similarly, for the downlink problem (5.4), the Lagrangian is given by

$$\mathscr{L}_{dl}\left[\left\{(\mathbf{T}_j,\mathbf{R}_j)\right\}_{j=1}^{K},\mu_{dl}\right] = mse_{dl,t} + \mu_{dl}\cdot\left\{\left[\sum_{j=1}^{K}\mathrm{tr}(\mathbf{T}_j\mathbf{T}_j^H)\right] - P_S\right\},$$

where μ_{dl} is the Lagrange multiplier. The associated KKT conditions for (5.4) are obtained similarly as in the uplink case, and are given by (5.9)-(5.12).

$$\hat{\mathbf{H}}_k\mathbf{R}_k^H = \left\{\sum_{j=1}^{K}\hat{\mathbf{H}}_j\mathbf{R}_j^H\mathbf{R}_j\hat{\mathbf{H}}_j^H + \mu_{dl}\cdot\mathbf{I}_M + \sum_{j=1}^{K}\sigma_{Ej}^2\cdot\mathrm{tr}(\mathbf{R}_j\mathbf{R}_j^H)\cdot\mathbf{\Sigma}_j\right\}\mathbf{T}_k, \tag{5.9}$$

$$\mathbf{T}_k^H\hat{\mathbf{H}}_k = \mathbf{R}_k\left\{\hat{\mathbf{H}}_k^H\left[\sum_{j=1}^{K}\mathbf{T}_j\mathbf{T}_j^H\right]\hat{\mathbf{H}}_k + \sigma_n^2\cdot\mathbf{I}_{N_k} + \sigma_{Ek}^2\cdot\sum_{j=1}^{K}\mathrm{tr}(\mathbf{T}_j^H\mathbf{\Sigma}_k\mathbf{T}_j)\cdot\mathbf{I}_{N_k}\right\}, \tag{5.10}$$

$$k = 1,\ldots,K,$$

$$\mu_{dl}\geq 0,\ \sum_{k=1}^{K}\mathrm{tr}(\mathbf{T}_k\mathbf{T}_k^H)\leq P_S, \tag{5.11}$$

$$\mu_{dl}\cdot\left[\sum_{k=1}^{K}\mathrm{tr}(\mathbf{T}_k\mathbf{T}_k^H) - P_S\right] = 0. \tag{5.12}$$

5.3.2 Relation between the Lagrange Multipliers and the Decoders

Lemma 4 *[Relation between the Lagrange multipliers and the receive filters (decoders)]*

For any solutions satisfying the KKT conditions, the following identities hold:

$$\mu_{ul} = (\sigma_n^2/P_S)\cdot\sum_{k=1}^{K}tr(\mathbf{G}_k\mathbf{G}_k^H), \tag{5.13}$$

$$\mu_{dl} = (\sigma_n^2/P_S)\cdot\sum_{k=1}^{K}tr(\mathbf{R}_k\mathbf{R}_k^H). \tag{5.14}$$

Proof. See Subsection 5.8.3. ■

5.3.3 Iterative Algorithms Based on KKT Conditions

The problems (5.2) and (5.4) are not convex. However, it can be shown that a global minimum exists for both (5.2) and (5.4) (see Subsection 5.8.4). The objective and constraint

functions for both problems are *continuously differentiable*. Furthermore, since there is only one inequality constraint here, any feasible solution is regular. With these properties, we conclude that the KKT conditions are necessary for local minimums (including the global minimums) [5]. Therefore, we now propose two algorithms developed from the KKT conditions [(5.5)-(5.8) and (5.9)-(5.12)], as given in Tables 5.1 and 5.2, for solving both problems.

Table 5.1. The KKT-based iterative algorithm for solving (5.2)

1) Initialize $\mathbf{F}_k,\ k = 1,\ldots,K$, which are non-zero and satisfy the power constraint with equality.
2) Update $\mathbf{G}_k$ using (5.5), $k = 1,\ldots,K$;
   $\mathbf{G}_k = \mathbf{F}_k^H \hat{\mathbf{H}}_k^H [\sum_{j=1}^K \hat{\mathbf{H}}_j \mathbf{F}_j \mathbf{F}_j^H \hat{\mathbf{H}}_j^H + \sigma_n^2 \cdot \mathbf{I}_M + \sum_{j=1}^K \sigma_{Ej}^2 \cdot \mathrm{tr}(\mathbf{F}_j \mathbf{F}_j^H) \cdot \mathbf{\Sigma}_j]^{-1}$;
3) Update μ_{ul} using (5.13);
4) Update $\mathbf{F}_k$ using (5.6), $k = 1,\ldots,K$;
   $\mathbf{F}_k = [\hat{\mathbf{H}}_k^H (\sum_{j=1}^K \mathbf{G}_j^H \mathbf{G}_j) \hat{\mathbf{H}}_k + \mu_{ul} \cdot \mathbf{I}_{N_k} + \sigma_{Ek}^2 \cdot \sum_{j=1}^K \mathrm{tr}(\mathbf{G}_j \mathbf{\Sigma}_k \mathbf{G}_j^H) \cdot \mathbf{I}_{N_k}]^{-1} \hat{\mathbf{H}}_k^H \mathbf{G}_k^H$;
5) If the termination condition is met, stop; otherwise, go back to 2).

Table 5.2. The KKT-based iterative algorithm for solving (5.4)

1) Initialize $\mathbf{T}_k,\ k = 1,\ldots,K$, which are non-zero and satisfy the power constraint with equality.
2) Update $\mathbf{R}_k$ using (5.10), $k = 1,\ldots,K$;
   $\mathbf{R}_k = \mathbf{T}_k^H \hat{\mathbf{H}}_k [\hat{\mathbf{H}}_k^H (\sum_{j=1}^K \mathbf{T}_j \mathbf{T}_j^H) \hat{\mathbf{H}}_k + \sigma_n^2 \cdot \mathbf{I}_{N_k} + \sigma_{Ek}^2 \cdot \sum_{j=1}^K \mathrm{tr}(\mathbf{T}_j^H \mathbf{\Sigma}_k \mathbf{T}_j) \cdot \mathbf{I}_{N_k}]^{-1}$;
3) Update μ_{dl} using (5.14);
4) Update $\mathbf{T}_k$ using (5.9), $k = 1,\ldots,K$;
   $\mathbf{T}_k = [\sum_{j=1}^K \hat{\mathbf{H}}_j \mathbf{R}_j^H \mathbf{R}_j \hat{\mathbf{H}}_j^H + \mu_{dl} \cdot \mathbf{I}_M + \sum_{j=1}^K \sigma_{Ej}^2 \cdot \mathrm{tr}(\mathbf{R}_j \mathbf{R}_j^H) \cdot \mathbf{\Sigma}_k]^{-1} \hat{\mathbf{H}}_k \mathbf{R}_k^H$;
5) If the termination condition is met, stop; otherwise, go back to 2).

Similar algorithms have been used in [91, 125] with perfect CSI. However, here the update of the Lagrange multipliers is based on (5.13) and (5.14), which is simpler and more accurate than the method in [91, 125], as the latter requires eigenvalue decompositions and

a solution to a non-linear equation for each update of the Lagrange multiplier. This will be demonstrated by an example in Part 2 of Section 5.6.

As in [47,91,125], we cannot show that the iterative algorithm in Table 5.1 or Table 5.2 is guaranteed to achieve the globally optimum solution (except when $K = 1$ [20]), despite the fact that the global minimum exists, since the objective function in (5.2) or (5.4) are not convex in $\{\mathbf{F}_i, \mathbf{G}_i\}_{i=1}^K$ or $\{\mathbf{T}_i, \mathbf{R}_i\}_{i=1}^K$[1]. However, as indicated by the simulations in Section 5.6, starting from a set of non-zero $\{\mathbf{F}_i\}_{i=1}^K$, the algorithms yield reasonable results, consistent with those obtained from alternative algorithms.

5.4 Uplink–Downlink Duality in Average Sum MSE with Imperfect Channel Knowledge Via KKT Conditions

Theorem 6 *(Uplink–downlink duality in average sum MSE)*

Let $\{\mathbf{F}_k, \mathbf{G}_k\}_{k=1}^K$ denote an admissible set of precoder-decoder pairs for the uplink average sum MSE performance that satisfies the KKT conditions (5.5)-(5.8). Let $\mathbf{T}_k = \sqrt{\sigma_n^2/\mu_{ul}} \cdot \mathbf{G}_k^H$, and let $\mathbf{R}_k$ satisfy (5.10), $k = 1, \ldots, K$. Then under the same sum power constraint, the average sum MSE achieved in the uplink by using $\{\mathbf{F}_k, \mathbf{G}_k\}_{k=1}^K$ can be achieved by $\{\mathbf{T}_k, \mathbf{R}_k\}_{k=1}^K$, which satisfies the KKT conditions for the downlink problem. Conversely, assume that $\{\mathbf{T}_j, \mathbf{R}_j\}_{j=1}^K$ is an admissible set for the downlink sum MSE performance that satisfies the KKT conditions (5.9)-(5.12). Let $\mathbf{F}_j = \sqrt{\sigma_n^2/\mu_{dl}} \cdot \mathbf{R}_j^H$, and let $\mathbf{G}_j$ satisfy (5.5), $j = 1, \ldots, K$. Then under the same sum power constraint, the average sum MSE achieved in the downlink by $\{\mathbf{T}_j, \mathbf{R}_j\}_{j=1}^K$ can be achieved by $\{\mathbf{F}_j, \mathbf{G}_j\}_{j=1}^K$, which satisfies the KKT conditions for the uplink problem.

[1] Note that in (5.2) and (5.4), the objective function is non-convex in $\{\mathbf{F}_i, \mathbf{G}_i\}_{i=1}^K$ or $\{\mathbf{T}_i, \mathbf{R}_i\}_{i=1}^K$ even when $\sigma_{Ei}^2 = 0, \forall i$.

Proof. See Subsection 5.8.5. ■

We have shown that if a solution satisfying the uplink KKT conditions achieves a certain average sum MSE, this sum MSE can also be achieved by a solution satisfying the downlink KKT conditions, and vice versa.

As mentioned in Subsection 5.3.3, here the KKT conditions are only necessary for local minimums in both links. However, by **Theorem 6**, every possible local minimum (satisfying the KKT conditions) of the uplink sum MSE corresponds to a same local minimum in the downlink. We then conclude that the globally minimum sum MSEs for the uplink and downlink must be the same (under the same sum power constraint and the same imperfect CSI).

According to the proof of **Theorem 6** in Subsection 5.8.5, at each local optimum (including the global optimum), each user's average MSEs in both links are the same, not just the average sum MSEs. See (5.37)-(5.38) and (5.40)-(5.41).

Theorem 6 matches the duality results in [47,89,93] when $\sigma_{E_j}^2 = 0$ and generalizes the sum MSE duality results when $\sigma_{E_j}^2 > 0, \forall j$. It reveals the underlying connection between the uplink and downlink joint MSMSE linear precoder-decoder designs based on the KKT conditions, whereas previous duality results were obtained by calculating the individual SINRs or MSEs for each user in both links [21,47,89,93].

Remark 5.1: According to the uplink–downlink duality with imperfect CSI, when we need to solve a linear MSMSE transceiver optimization problem with imperfect CSI for *the downlink*, we can first formulate a dual uplink problem, find the $\{\mathbf{F}_i, \mathbf{G}_i\}_{i=1}^K$ for the dual link using the above method, and then translate the transceiver pairs for application in the downlink.

5.5 Alternative Method for Uplink Optimization

In this section, we assume that the number of data streams is equal to the number of transmit antennas for each user, i.e., $l_i = N_i, i = 1,\ldots,K$. We intend to solve (5.2) by solving an equivalent problem. Since the KKT-conditions-based algorithm is not guaranteed to yield the globally optimum solution, here we propose another method for uplink optimization. In general, this alternative method is not guaranteed to obtain the global minimum, either. However, it is still of great importance, not only as an actual way of finding the uplink transceiver pairs, but also as an effective way to check how the KKT-based algorithm performs.

The uplink problem (5.2) can be equivalently formulated as

$$\min_{\{\mathbf{F}_i\}_{i=1}^K,\ \sum_{i=1}^K \mathrm{tr}(\mathbf{F}_i\mathbf{F}_i^H)\le P_S}\ \min_{\{\mathbf{G}_i\}_{i=1}^K} mse_{ul,t}.$$

It turns out that the inner minimization is achieved when (5.5) is satisfied for all k. Then it can be shown that

$$mse_{ul,t} = \mathrm{tr}\left\{\check{\mathbf{X}}\left[\sigma_n^2\mathbf{I}_M + \sum_{j=1}^K \sigma_{Ej}^2\cdot\mathrm{tr}(\mathbf{Q}_j)\cdot\mathbf{\Sigma}_j\right]\right\} + const,$$

where *const* denotes a constant that equals $\left[\sum_{j=1}^K \mathrm{tr}\left(\mathbf{I}_{l_j}\right) - \mathrm{tr}\left(\mathbf{I}_M\right)\right]$, $\mathbf{Q}_j \overset{\text{def}}{=} \mathbf{F}_j\mathbf{F}_j^H, \forall j$, and

$$\check{\mathbf{X}} \overset{\text{def}}{=} \left[\sum_{j=1}^K \hat{\mathbf{H}}_j\mathbf{Q}_j\hat{\mathbf{H}}_j^H + \sum_{j=1}^K \sigma_{Ej}^2\cdot\mathrm{tr}(\mathbf{Q}_j)\cdot\mathbf{\Sigma}_j + \sigma_n^2\cdot\mathbf{I}_M\right]^{-1}. \tag{5.15}$$

Therefore, instead of solving (5.2) directly, we attempt to solve its equivalent problem, as shown below:

$$\min_{\check{\mathbf{X}};\ \{\mathbf{Q}_j\}_{j=1}^K}\ \mathrm{tr}\left\{\check{\mathbf{X}}\left[\sum_{j=1}^K \sigma_{Ej}^2\cdot\mathrm{tr}(\mathbf{Q}_j)\cdot\mathbf{\Sigma}_j + \sigma_n^2\cdot\mathbf{I}_M\right]\right\}, \tag{5.16}$$

$$\text{subject to}\ \sum_{j=1}^K \mathrm{tr}(\mathbf{Q}_j) \le P_S, \tag{5.17}$$

$$\check{\mathbf{X}} \text{ as given in (5.15)}, \tag{5.18}$$

$$\mathbf{Q}_j \succeq 0, j = 1, \ldots, K. \tag{5.19}$$

We first present the following theorem for a special case.

Theorem 7 *When $\sigma_{E\,j}^2 = \tilde{\sigma}_E^2$ and $\mathbf{\Sigma}_j = \mathbf{\Sigma}_{BS}, j = 1, \ldots, K$, the problem given by (5.16)-(5.19) is equivalent to the following semidefinite program (SDP):*

$$\begin{aligned}
&\min_{\check{\mathbf{X}};\, \{\mathbf{Q}_j\}_{j=1}^K} \; tr\left\{\check{\mathbf{X}} \cdot \left[\sigma_n^2 \cdot \mathbf{I}_M + \tilde{\sigma}_E^2 \cdot P_S \cdot \mathbf{\Sigma}_{BS}\right]\right\}, \\
&\textit{subject to} \;\; \sum_{j=1}^{K} tr(\mathbf{Q}_j) \leq P_S, \\
&\qquad \begin{pmatrix} \check{\mathbf{X}} & \mathbf{I}_M \\ \mathbf{I}_M & \sum_{j=1}^K \hat{\mathbf{H}}_j \mathbf{Q}_j \hat{\mathbf{H}}_j^H + \tilde{\sigma}_E^2 P_S \cdot \mathbf{\Sigma}_{BS} + \sigma_n^2 \cdot \mathbf{I}_M \end{pmatrix} \succeq 0, \\
&\qquad \mathbf{Q}_j \succeq 0, j = 1, \ldots, K.
\end{aligned}$$

Proof. The proof is an extension of that in [59]. Details are given in Subsection 5.8.6.

A SDP is a convex optimization problem [7] and can be solved using SDP software [97]. A globally optimum solution is guaranteed.

Once the globally optimum solution for the SDP is obtained, $\{\mathbf{F}_j\}_{j=1}^K$ can be obtained by performing Cholesky factorizations of $\{\mathbf{Q}_j\}_{j=1}^K$ [59], due to the assumption that $l_j = N_j, j = 1, \ldots, K$. The corresponding $\{\mathbf{G}_j\}_{j=1}^K$ can be obtained using (5.5).

Note that if $\{\mathbf{F}_j\}_{j=1}^K$ is an optimum set in terms of sum MSE, then $\{\mathbf{F}_j \mathbf{U}_j\}_{j=1}^K$ is also an optimum set, where $\{\mathbf{U}_j\}_{j=1}^K$ is any set of unitary matrices of proper size.

Clearly, the result in **Theorem 7** itself has very limited application, because of the conditions required ($\sigma_{E\,j}^2 = \tilde{\sigma}_E^2$ and $\mathbf{\Sigma}_j = \mathbf{\Sigma}_{BS}, \forall j$).

In general, the equivalent problem given by (5.16)-(5.19) is not a SDP, because the objective function in (5.16) is not convex. However, **Theorem 7** provides a basis to find a

solution to the equivalent problem. Specifically, we have a SDP-based iterative algorithm given in Table 5.3.

Table 5.3. The SDP-based iterative algorithm for solving (5.2) [the sequential SDP method]

1) Initialize $\mathbf{Q}_j = [P_S/(KN_j)] \cdot \mathbf{I}_{N_j}, \forall j$. Calculate the value of the objective function f^{old} using (5.15) and (5.16), given $\{\mathbf{Q}_j\}_{j=1}^K$.
2) Given $\{\mathbf{Q}_j\}_{j=1}^K$, calculate $\check{\mathbf{Z}} = \sum_{j=1}^K \sigma_{Ej}^2 \cdot \mathrm{tr}(\mathbf{Q}_j) \cdot \mathbf{\Sigma}_j + \sigma_n^2 \cdot \mathbf{I}_M$.
3) Solve the SDP given by (5.20)-(5.23) to obtain a new set of $\{\mathbf{Q}_j\}_{j=1}^K$. Calculate the value of the objective function f^{new}, i.e., the value of (5.20).
4) If $|f^{new} - f^{old}| \leq \varepsilon$, stop; otherwise, set $f^{old} := f^{new}$, and go back to 2).

During each iteration, the matrix $\check{\mathbf{Z}}$ (see Table 5.3) is fixed and thus the problem given by (5.20)-(5.23) is a SDP:

$$\min_{\check{\mathbf{X}};\, \{\mathbf{Q}_j\}_{j=1}^K} \quad \mathrm{tr}\left\{\check{\mathbf{X}}\check{\mathbf{Z}}\right\} \tag{5.20}$$

$$\text{subject to} \quad \sum_{j=1}^K \mathrm{tr}(\mathbf{Q}_j) \leq P_S, \tag{5.21}$$

$$\begin{pmatrix} \check{\mathbf{X}} & \mathbf{I}_M \\ \mathbf{I}_M & \sum_{j=1}^K \hat{\mathbf{H}}_j \mathbf{Q}_j \hat{\mathbf{H}}_j^H + \check{\mathbf{Z}} \end{pmatrix} \succeq 0, \tag{5.22}$$

$$\mathbf{Q}_j \succeq 0, j = 1, \ldots, K. \tag{5.23}$$

Essentially, the algorithm in Table 5.3 approaches the solution by solving a sequence of SDPs which approximate and converge to that given by (5.16)-(5.19). Therefore, it is also referred to the sequential semidefinite programming method.

After obtaining $\{\mathbf{Q}_j\}_{j=1}^K$, we can obtain $\{\mathbf{F}_j, \mathbf{G}_j\}_{j=1}^K$ as mentioned earlier.

5.6 Simulation Results and Discussions

1. Simulation Setup

As in previous chapters, the exponential model is used to describe the correlation of the channels arising from the BS antennas: $\mathbf{\Sigma}_{i,pq} = \rho_i^{|p-q|}$, where $0 \leq \rho_i < 1$, $p,q \in \{1,\ldots,M\}$ and $i = 1,\ldots,K$. When simulating the ABER performance, we assume that 4-QAM is used in each user's data streams. Here the SNR is defined as SNR $= P_S/\sigma_n^2$, which should not be confused with that defined in Chapter 3 or in Chapter 4. In the following simulations, the number of users K is assumed to be 3, and the number of BS antennas M is either 6 or 8. The number of antennas of each user equals the number of data streams, both equal to 2 (i.e., $N_i = l_i = 2, \forall i$). Unless otherwise stated, the correlation exponents, training powers and channel estimation error variances are given in Tables 5.4 and 5.5 (with the only exception in Fig. 5.2).

Table 5.4. Channel correlation exponents and estimation error variances ($M = 6$)

	correlation exponents and error variances
$P_{tr,i}/\sigma_n^2 = 30$ dB, $\forall i$	higher $\rho's$: $\rho_1 = 0.8, \rho_2 = 0.7, \rho_3 = 0.5$; $\sigma_{E1}^2 = 0.0238, \sigma_{E2}^2 = 0.0156, \sigma_{E3}^2 = 0.0093$
	lower $\rho's$: $\rho_1 = 0.5, \rho_2 = 0.3, \rho_3 = 0.2$; $\sigma_{E1}^2 = 0.0093, \sigma_{E2}^2 = 0.0070, \sigma_{E3}^2 = 0.0064$
$P_{tr,i}/\sigma_n^2 = 25$ dB, $\forall i$	higher $\rho's$: $\rho_1 = 0.8, \rho_2 = 0.7, \rho_3 = 0.5$; $\sigma_{E1}^2 = 0.0752, \sigma_{E2}^2 = 0.0494, \sigma_{E3}^2 = 0.0295$
	lower $\rho's$: $\rho_1 = 0.5, \rho_2 = 0.3, \rho_3 = 0.2$; $\sigma_{E1}^2 = 0.0295, \sigma_{E2}^2 = 0.0221, \sigma_{E3}^2 = 0.0203$

2. Comparison of the KKT-based Algorithm and the SDP-based Algorithm for the Uplink Problem (5.2)

Table 5.5. Channel correlation exponents and estimation error variances ($M = 8$)

$P_{tr,i}/\sigma_n^2 = 30$ dB, $\forall i$	correlation exponents and error variances
higher $\rho's$	$\rho_1 = 0.8, \rho_2 = 0.7, \rho_3 = 0.5$; $\sigma_{E1}^2 = 0.0329, \sigma_{E2}^2 = 0.0215, \sigma_{E3}^2 = 0.0127$
lower $\rho's$	$\rho_1 = 0.5, \rho_2 = 0.3, \rho_3 = 0.2$; $\sigma_{E1}^2 = 0.0127, \sigma_{E2}^2 = 0.0094, \sigma_{E3}^2 = 0.0086$

Here we provide a concrete example to show the equivalence of average sum MSEs obtained from the two algorithms in Tables 5.1 and 5.3. Let $K = 3$, $M = 6$ and $N_i = l_i = 2, \forall i$. Assume $P_{tr,i}/\sigma_n^2$ = 30 dB, $\forall i$. The channel correlation exponents are given by $\rho_1 = 0.8, \rho_2 = 0.7, \rho_3 = 0.5$ (the higher $\rho's$), and the corresponding estimation error variances can be found in Table 5.4. We set the SNR (P_S/σ_n^2) to be 20 dB.

Using the channel estimation method in Section 5.2, the following channel estimates are obtained for a specific channel realization:

$$\hat{\mathbf{H}}_1 = \begin{pmatrix} -0.6707 + 0.0949i & -0.1160 - 0.1406i \\ -0.7679 + 0.4335i & -0.0944 - 0.3061i \\ -0.5513 - 0.3191i & 0.0039 + 0.0052i \\ -0.3205 - 0.6796i & -0.3382 - 0.0634i \\ -0.8113 - 0.2604i & -0.2913 - 0.5147i \\ -0.9751 - 0.5906i & -0.3598 - 1.1833i \end{pmatrix},$$

Table 5.6. A comparison of the two algorithms given in Tables 5.1 and 5.3

	SDP-based	KKT-based
achieved sum MSE	0.9953	0.9941
average computation time (seconds)	8.0061	0.0771

$$\hat{\mathbf{H}}_2 = \begin{pmatrix} 0.4579 - 0.0463i & -0.9577 + 0.5081i \\ 0.9834 + 0.3877i & -0.9878 - 0.1083i \\ 0.5648 + 0.6865i & -0.3627 - 0.4536i \\ -0.6043 + 0.9826i & -0.4557 + 0.3526i \\ -0.3226 - 0.4818i & -0.2589 + 1.0222i \\ -0.5015 - 0.6484i & -0.3455 + 0.7778i \end{pmatrix},$$

$$\hat{\mathbf{H}}_3 = \begin{pmatrix} 1.5141 - 0.3107i & 0.6366 - 0.8878i \\ 0.9365 - 1.3479i & -0.4525 - 1.7763i \\ 1.2987 - 0.5662i & 0.2079 - 1.0612i \\ -0.0272 + 0.1190i & -0.3041 + 0.3201i \\ -0.6847 - 0.0002i & 0.0914 + 0.0215i \\ -0.2971 + 0.7746i & -0.6777 + 0.2412i \end{pmatrix}.$$

The comparison of the two algorithms is given in Table 5.6.

Although neither is guaranteed to achieve the globally optimum solution, the two algorithms have been found to converge after only several iterations and yield equivalent results as shown in Table 5.6. Note that the complexity of the SDP-based algorithm is much higher than that of the KKT-based algorithm, where complexity is measured by the computation time required for both algorithms to converge (at the

same required data precision). Both algorithms are run on the same hardware using the same version of MATLAB. It is also worth mentioning that if in the KKT-based algorithm the Lagrange multiplier is updated using the method in [91] , then the average computation time is 0.6728 seconds, which is 8.7 times that required from using (5.13).

Similar comparison results (as in Table 5.6) can also be observed for different channel realizations and with different system parameters. Fig. 5.1 shows more comparisons of these two algorithms with different values of P_S/σ_n^2 and with different amounts of channel correlation. Each point on the curve is obtained by averaging the sum MSE from 10,000 channel realizations.

When $\sigma_{Ei}^2 = \tilde{\sigma}_E^2$ and $\rho_i = \rho, \forall i$ (i.e., $\mathbf{\Sigma}_i = \mathbf{\Sigma}_{BS}, \forall i$), the KKT-based algorithm also yields the equivalent average sum MSE as that from solving a single SDP (see **Theorem 7**). Fig. 5.2 shows an example of the comparisons, where $P_{tr,i}/\sigma_n^2 = 29.66$ dB, $\forall i$, $\tilde{\sigma}_E^2 = 0.01$, $\rho = 0.5$, $K = 3, M = 6, N_i = l_i = 2, \forall i$.

We can see that the results obtained using the KKT-based algorithm are consistent with those from the SDP-based algorithm as given by Table 5.3, or from solving a single SDP in the case specified by **Theorem 7**. Therefore, below we investigate the effects of channel estimation error and channel correlation in the uplink based on the $\{\mathbf{F}_i, \mathbf{G}_i\}_{i=1}^K$ obtained from the KKT-based algorithm in Table 5.1, since it is less complex.

3. Effects of Channel Estimation Errors and Channel Correlation on the Uplink Performance

   Fig. 5.3 shows the effect of channel estimation errors as well as that of channel correlation.

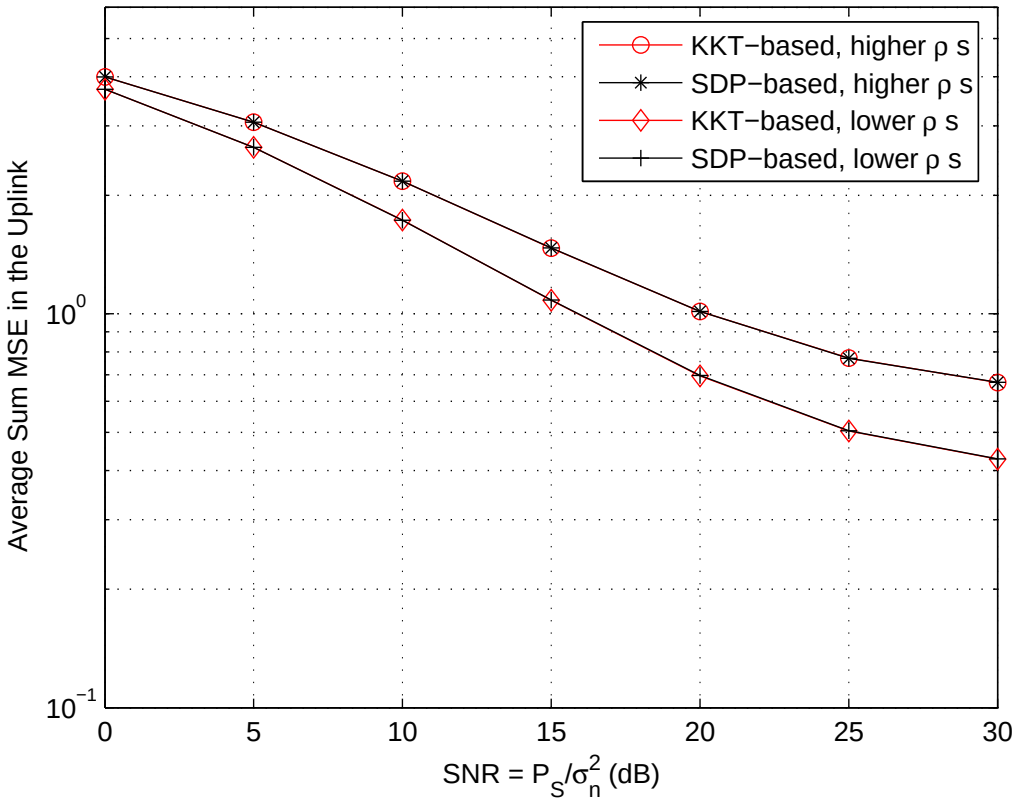

Figure 5.1. A comparison of the average sum MSEs obtained from the two algorithms in Tables 5.1 and 5.3. $K = 3$, $M = 6$, $N_i = l_i = 2$, $P_{tr,i}/\sigma_n^2 = 30$ dB, $\forall i$. Channel correlation exponents and channel estimation error variances are given in Table 5.4.

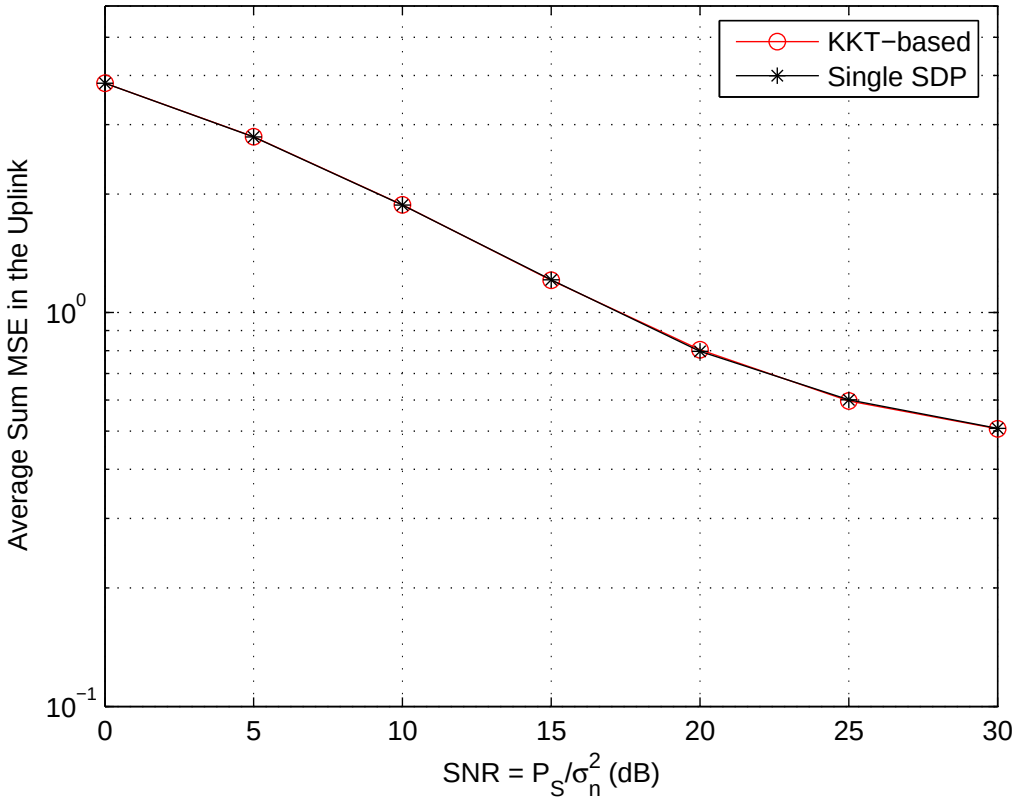

Figure 5.2. A comparison between the average sum MSEs obtained from the KKT-based algorithm and from solving a single SDP as described in **Theorem 7**. $K = 3$, $M = 6$, $N_i = l_i = 2$; $P_{tr,i}/\sigma_n^2 = 29.66$ dB, $\rho_i = \rho = 0.5$, $\sigma_{Ei}^2 = \tilde{\sigma}_E^2 = 0.01$, $\forall i$.

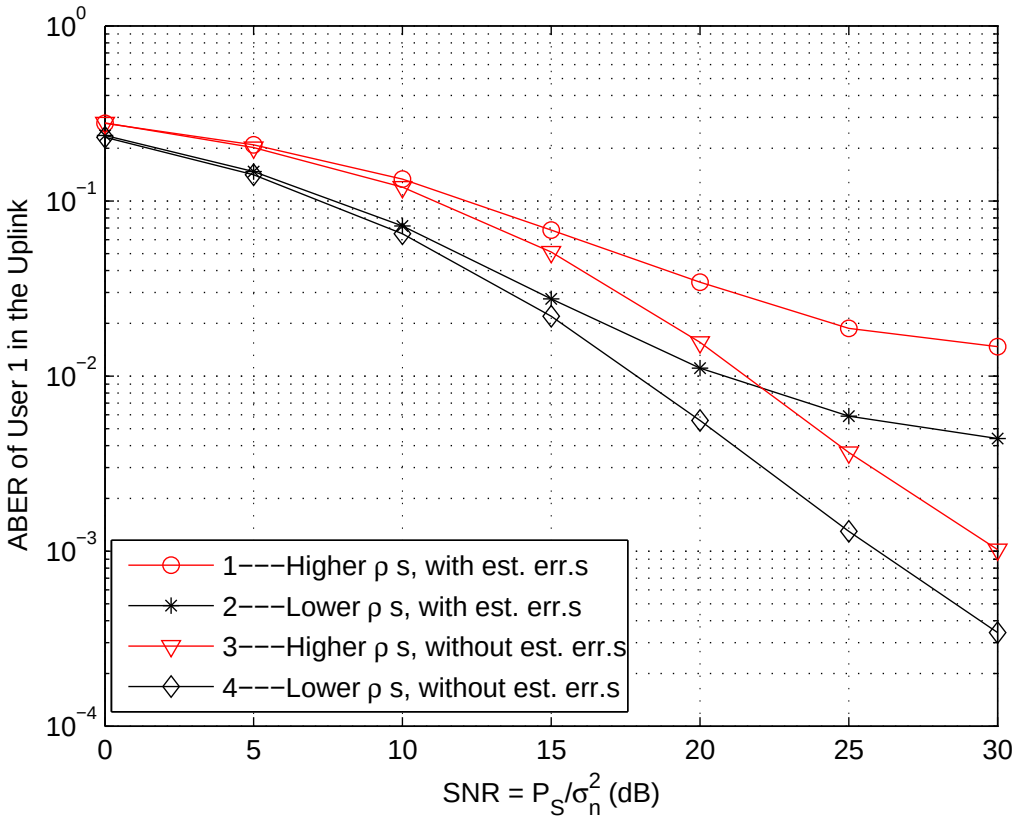

Figure 5.3. Comparison of the ABERs of User 1 in the uplink with or without channel estimation errors and with different amounts of channel correlation. With imperfect CSI, the following parameters are used for this figure: $M = 6, K = 3, N_i = l_i = 2$. $P_{tr,i}/\sigma_n^2 = 30$ dB, $\forall i$.

In the case of imperfect CSI, the training power for each user is 30 dB. Different amounts of channel correlation have been considered. Comparing curves 1 and 3 or curves 2 and 4, we can see that channel estimation errors cause a large performance degradation on the ABER of User 1. Comparing curves 1 and 2 or curves 3 and 4, we can see that channel correlation also has a significant impact on system performance. For example, in the case of perfect CSI, from curves 3 and 4, the performance degradation is about 3.75 dB when (ρ_1, ρ_2, ρ_3) changes from $(0.5, 0.3, 0.2)$ to $(0.8, 0.7, 0.5)$. In the case of imperfect CSI, the performance degradation caused by channel correlation is even larger. Similar observations can be made from Fig. 5.4, where the training power for each user is 25 dB in the case of imperfect channel estimation.

Fig. 5.5 shows the ABER results of User 1, when the number of BS antennas, M, increases from 6 to 8. Increasing M implies introducing more antenna diversity. Therefore, from curves 1 and 3 or curves 2 and 4 there, we can see that the effect of channel estimation errors can be compensated by introducing diversity. Note that one can also introduce diversity by transmitting fewer data streams (i.e., reducing $l_i, \forall i$).

4. Duality in Average MSE with Imperfect Channel Knowledge

In Fig. 5.6, the curve of average sum MSE in the uplink is obtained using Table 5.1. One of the curves for the downlink is obtained by using **Theorem 6**, the other is directly obtained from Table 5.2. The three curves overlap with both perfect and imperfect channel estimation. Therefore, the results in Fig. 5.6 agree with **Theorem 6**. The average sum MSE curves obtained here also agree with those in Fig. 5.1 with same parameters.

The duality in average sum MSE can also be observed in Fig. 5.7 under different

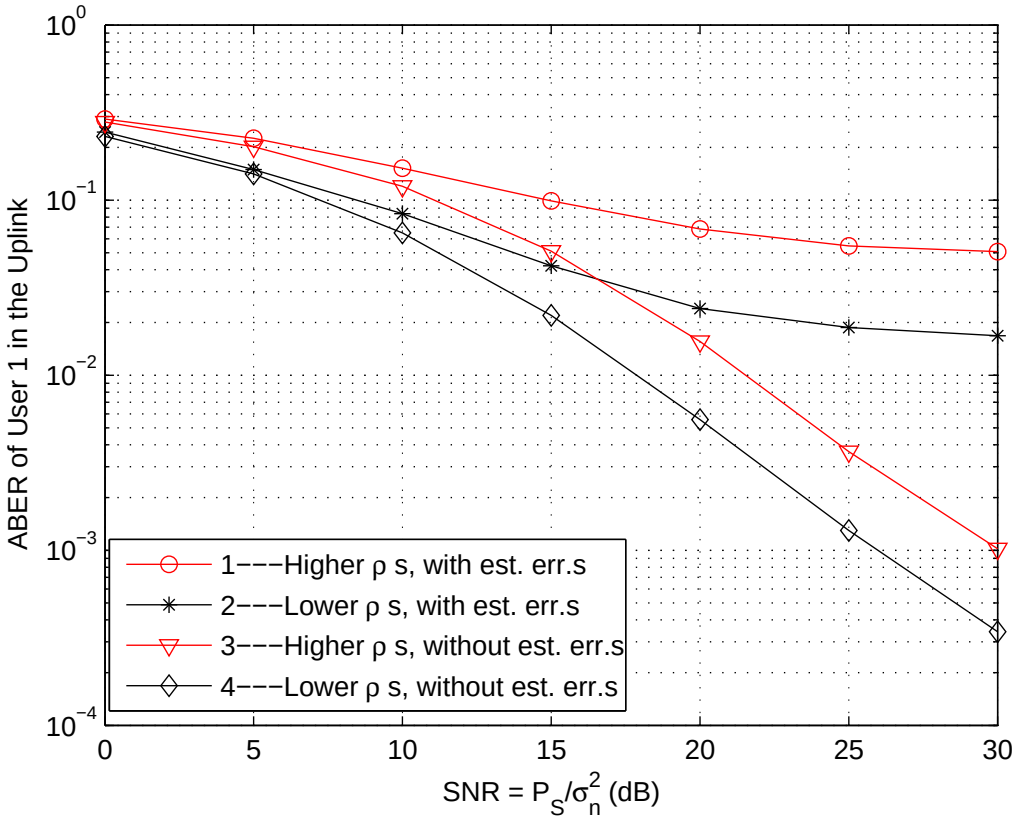

Figure 5.4. Comparison of the ABERs of User 1 in the uplink with or without channel estimation errors and with different amounts of channel correlation. With imperfect CSI, the following parameters are used for this figure: $K = 3$, $M = 6$, $N_i = l_i = 2$, $P_{tr,i}/\sigma_n^2 = 25$ dB, $i = 1, \ldots, K$.

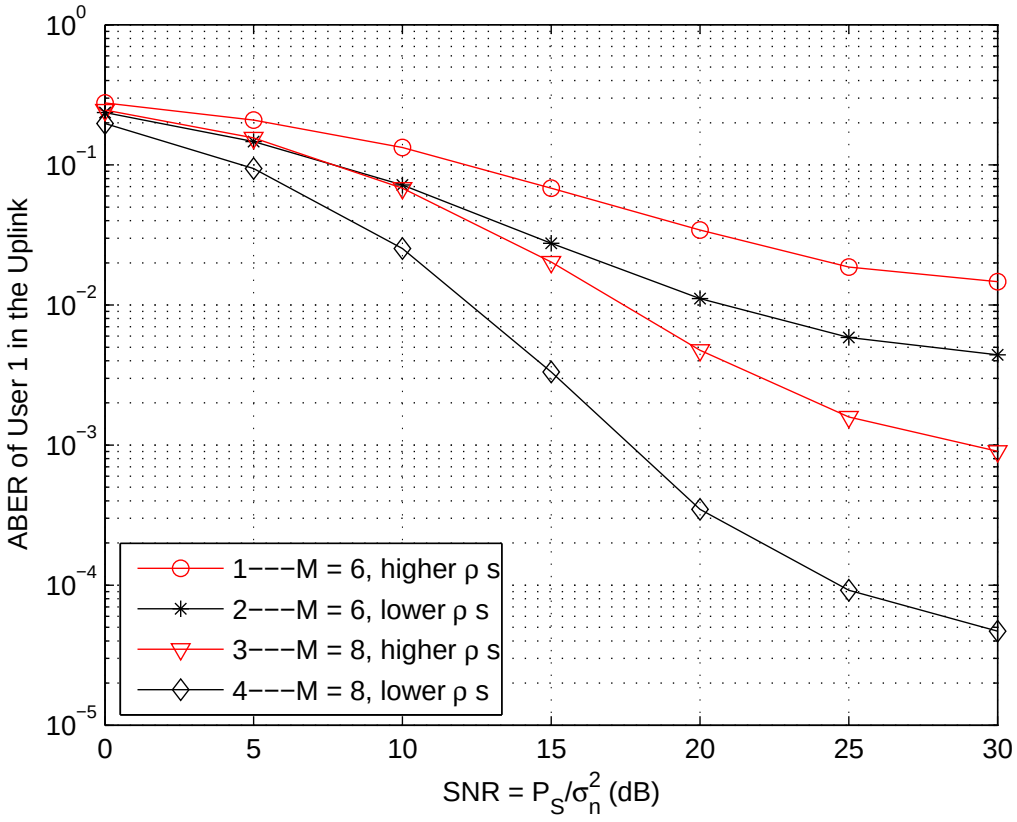

Figure 5.5. Comparison of the ABERs of User 1 with channel estimation errors and different amounts of antenna diversity. $K = 3, N_i = l_i = 2, P_{tr,i}/\sigma_n^2 = 30$ dB, $\forall i$. $M = 6$ or 8. The corresponding correlation exponents and estimation error variances are given in Tables 5.4 and 5.5.

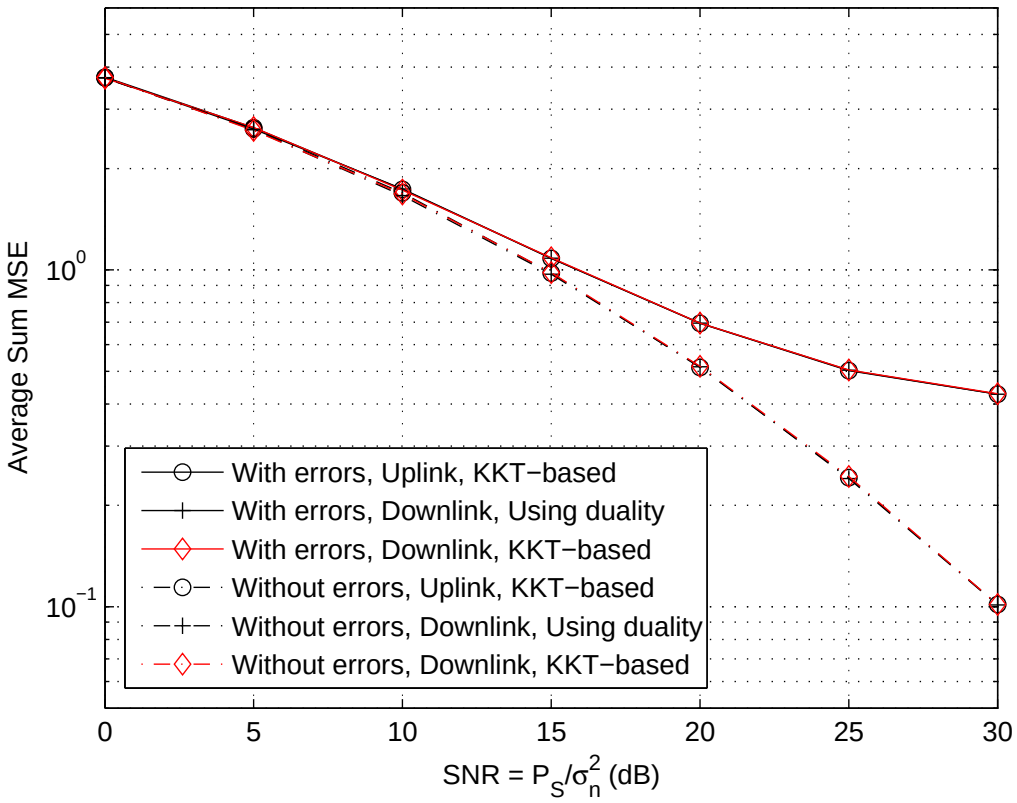

Figure 5.6. Duality in average sum MSE. $K = 3$, $M = 6$, $N_i = l_i = 2$, $i = 1,\ldots,K$. The lower $\rho's$ are used: $\rho_1 = 0.5$, $\rho_2 = 0.3$, $\rho_3 = 0.2$. $P_{tr,i}/\sigma_n^2 = 30$ dB, $\forall i$.

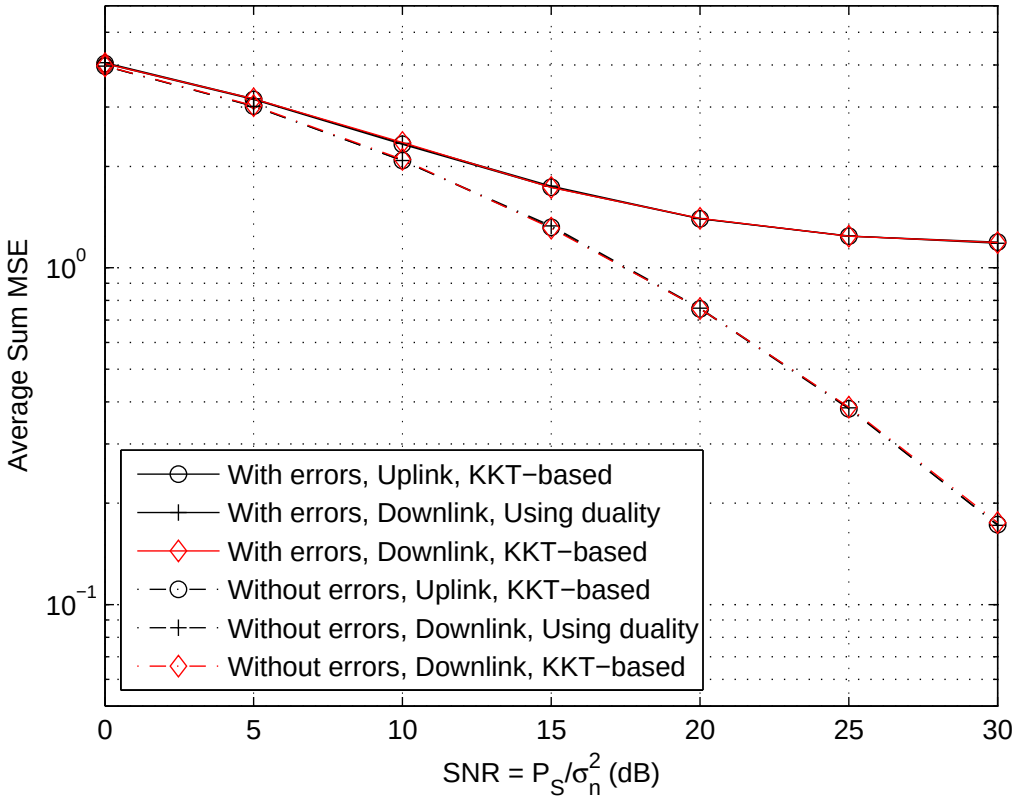

Figure 5.7. Duality in average sum MSE. $K = 3$, $M = 6$, $N_i = l_i = 2$, $i = 1,\ldots,K$. The higher $\rho's$ are used: $\rho_1 = 0.8$, $\rho_2 = 0.7$, $\rho_3 = 0.5$. $P_{tr,i}/\sigma_n^2 = 25$ dB, $\forall i$.

system parameters.

As mentioned in Section 5.4, at the local or global optimum, each user's average MSEs in both links are the same. This is shown in Fig. 5.8.

5. Effects of Channel Estimation Errors and Channel Correlation on the Downlink Performance

Figs. 5.9 and 5.10 demonstrate the effects of channel estimation errors and channel correlation on the downlink system performance, which are similar to those observed

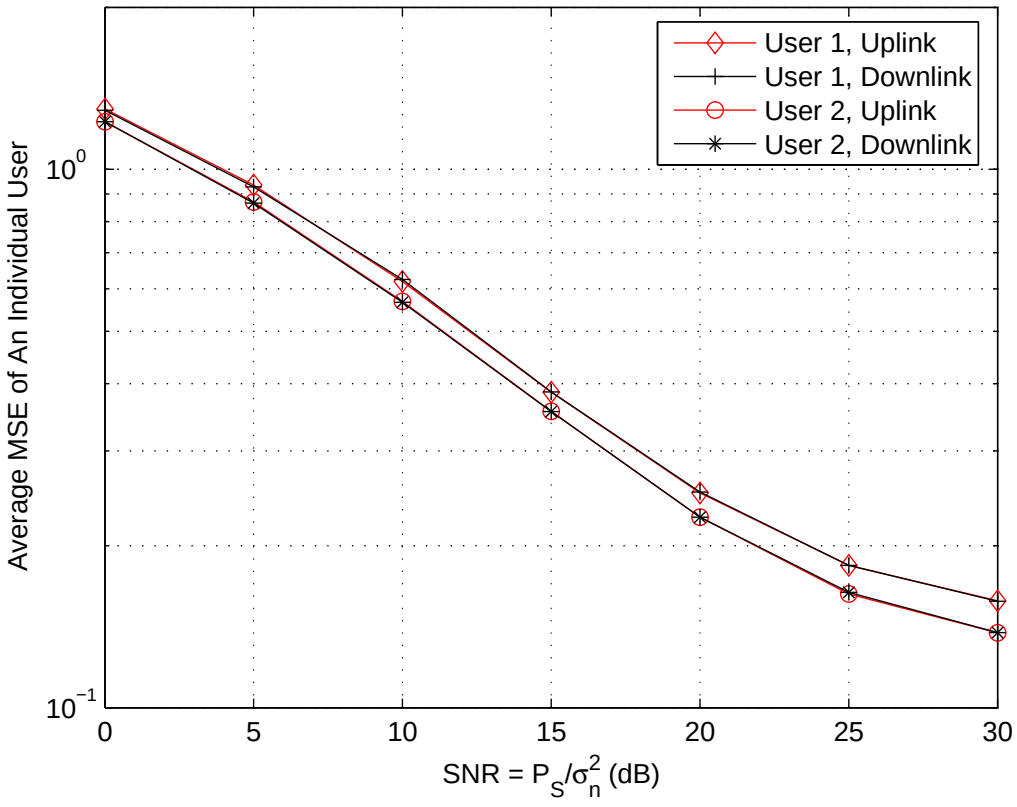

Figure 5.8. Duality in individual users' MSEs. $K = 3$, $M = 6$, $N_i = l_i = 2$, $P_{tr,i}/\sigma_n^2 = 30$ dB, $\forall i$. The lower $\rho's$ are used: $\rho_1 = 0.5$, $\rho_2 = 0.3$, $\rho_3 = 0.2$. For each user, curves for the uplink and the downlink overlap.

in the uplink.

We also compare the ABERs of User 1 in both links with or without channel estimation errors. See Figs. 5.11 and 5.12. We observe that without channel estimation errors, the ABERs in both links seem to be the same. However, this is not true with imperfect CSI. Thus, in case of imperfect CSI, the duality holds in average MSE, but not in ABER. Similar results have been observed in [21, 114] in the case when the BS is mounted with multiple antennas and the MSs are each equipped with a single antenna.

We now provide more insight into the results shown in Figs. 5.8, 5.11 and 5.12. From previous sections, we can see that the derivations of average individual or sum MSEs depend largely on the first-order and second-order statistics of the transmitter signal, channel fades, channel noises and channel estimation errors, which are the same for the dual links. Thus, it is expected that the duality in average MSE holds. On the other hand, the BERs depend on the interference-plus-noise distributions, which vary with the relative strengths of the interferences[2]. When there are channel estimation errors, the interference strengths depend on P_S in different ways for the uplink and the downlink [see (5.1) and (5.3)]. Therefore, the BERs in both links become noticeably unequal when P_S is relatively large (and thus channel estimation errors become dominant).

While the ABERs in both links are not identical, they are of the same order of magnitude. If we have used the duality to obtain the transceiver pairs for the downlink from the dual uplink, we should take into account the ABER performance difference between the dual links at high SNR and use some extra margins based on Figs. 5.11

[2]Here the interferences include the inter-stream interferences from the same user, the multiuser interferences, as well as those caused by channel estimation errors.

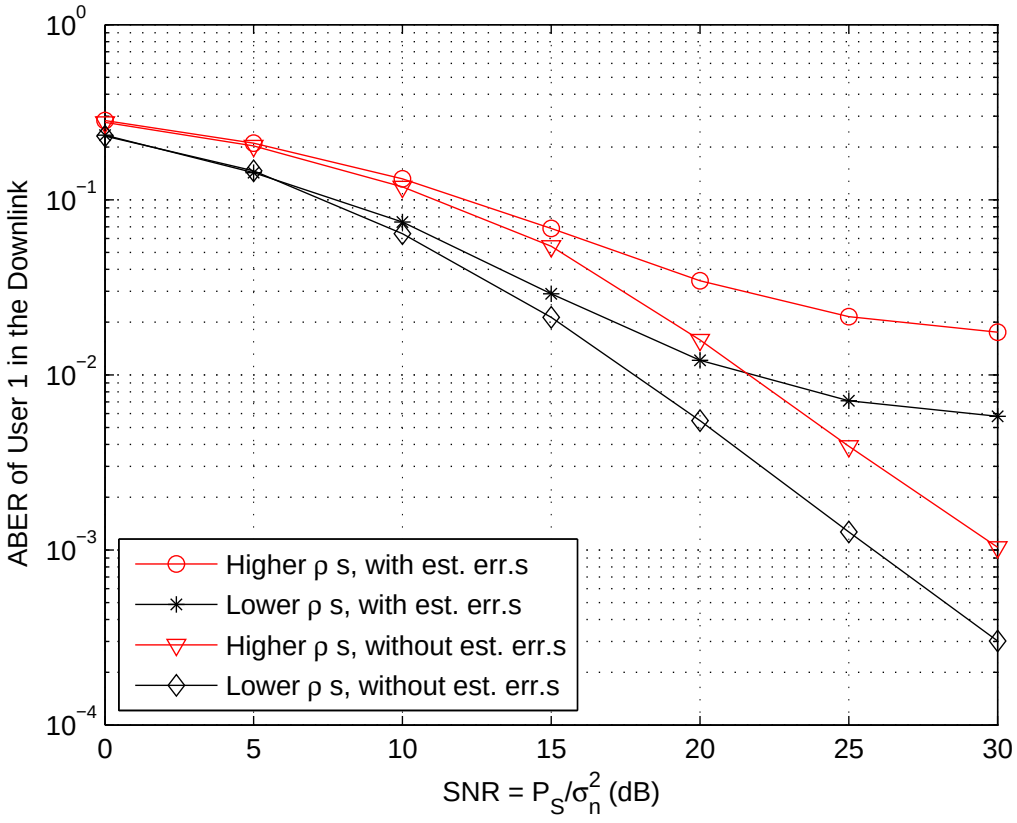

Figure 5.9. Comparison of the ABERs of User 1 in the downlink with or without channel estimation errors and with different amounts of channel correlation. $K = 3$, $M = 6$, $N_i = l_i = 2, \forall i$. With imperfect CSI, $P_{tr,i}/\sigma_n^2 = 30$ dB, $\forall i$. The corresponding correlation exponents and estimation error variances are given in Table 5.4.

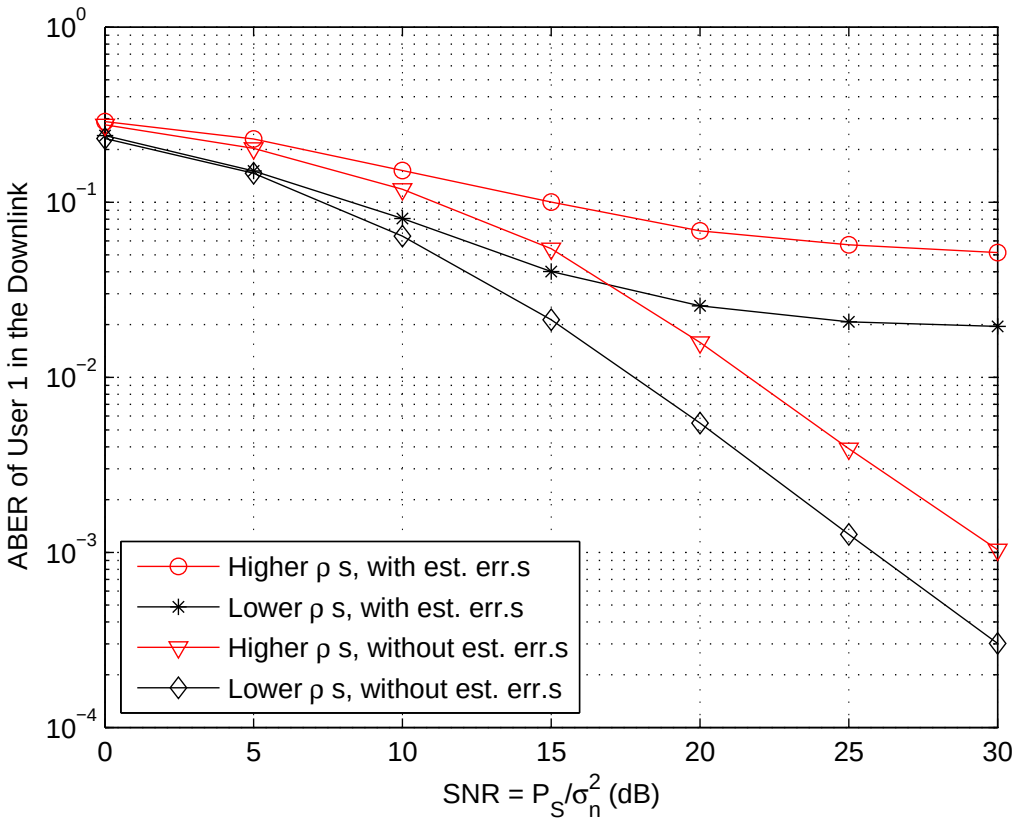

Figure 5.10. Comparison of the ABERs of User 1 in the downlink with or without channel estimation errors and with different amounts of channel correlation. $K = 3$, $M = 6$, $N_i = l_i = 2, \forall i$. With imperfect CSI, $P_{tr,i}/\sigma_n^2 = 25$ dB, $\forall i$.

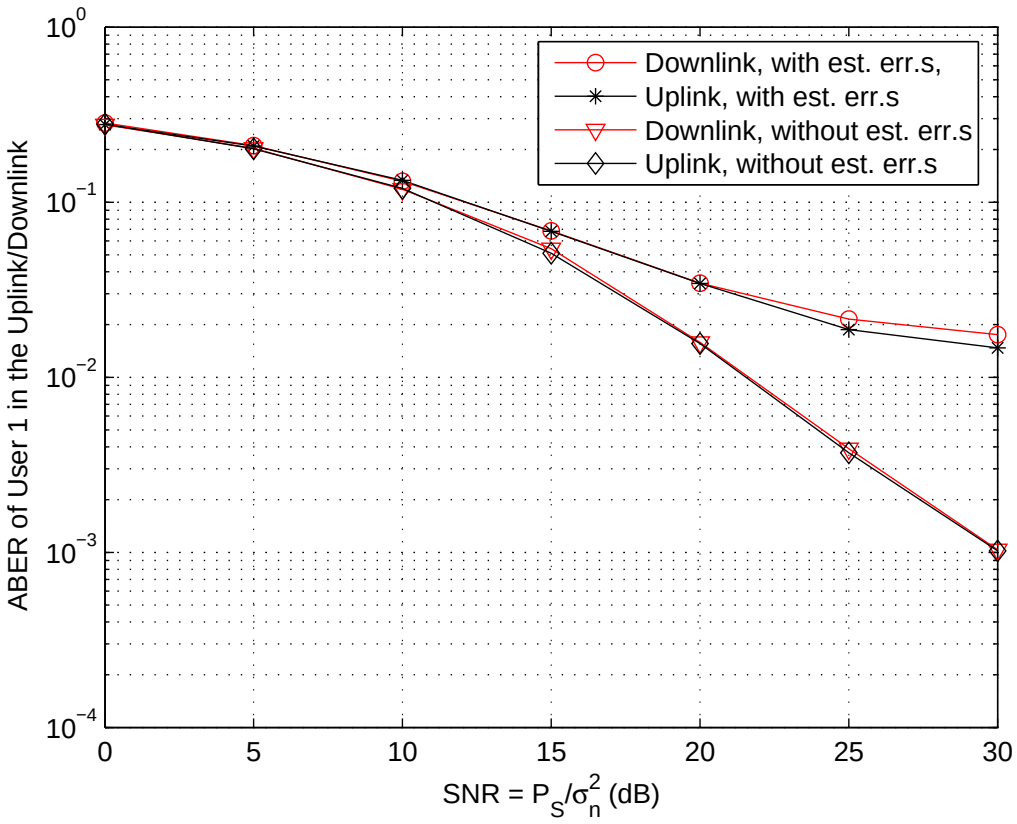

Figure 5.11. Comparison of the ABERs of User 1 in the uplink and in the downlink with or without channel estimation errors. $K = 3$, $M = 6$, $N_i = l_i = 2, \forall i$. With imperfect CSI, $P_{tr,i}/\sigma_n^2 = 30$ dB, $\forall i$. The higher $\rho's$ are used: $\rho_1 = 0.8$, $\rho_2 = 0.7$, $\rho_3 = 0.5$.

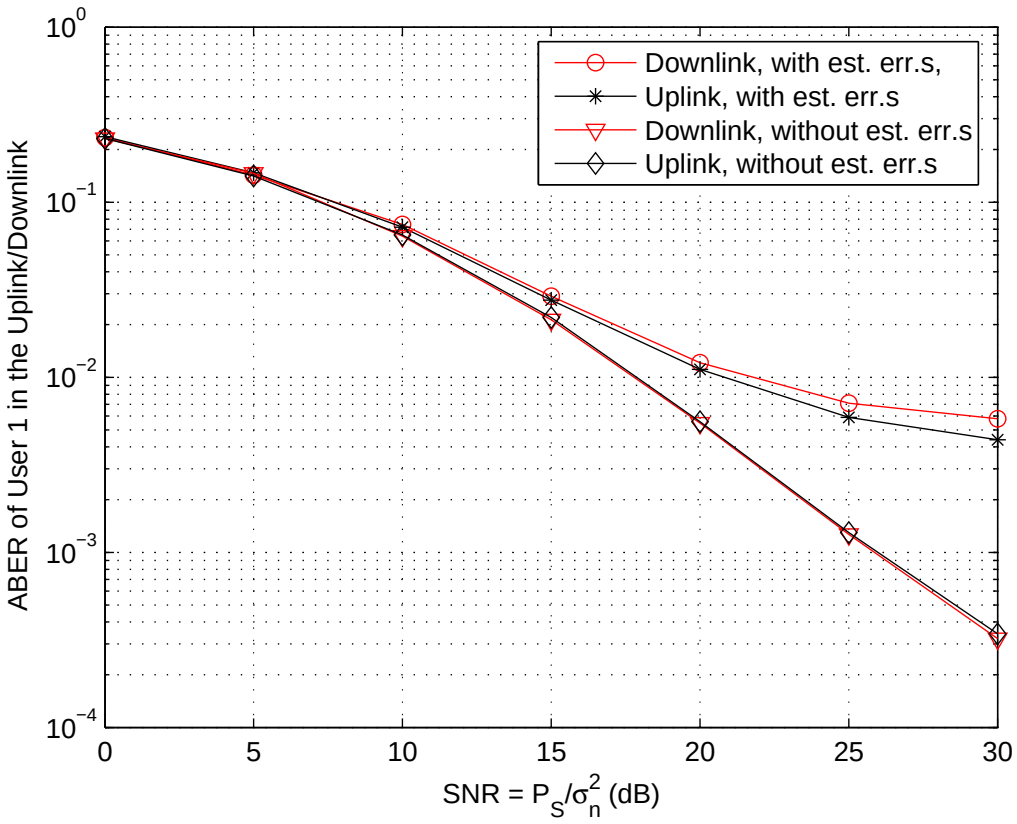

Figure 5.12. Comparison of the ABERs of User 1 in the uplink and in the downlink with or without channel estimation errors. $K = 3$, $M = 6$, $N_i = l_i = 2, \forall i$. With imperfect CSI, $P_{tr,i}/\sigma_n^2 = 30$ dB, $\forall i$. The lower $\rho's$ are used: $\rho_1 = 0.5$, $\rho_2 = 0.3$, $\rho_3 = 0.2$.

and 5.12. Specific values of these margins can be obtained from simulations.

5.7 Summary

Minimum sum MSE linear transceiver design problems are formulated for multiuser MIMO uplink and downlink assuming imperfect CSI. A duality in average sum MSE between these two designs has been proved based on the associated KKT conditions. Furthermore, when the minimum average sum MSE is achieved, each user's individual average MSEs in both links are also the same. Simulation results agree with the analytical duality results. The KKT-conditions-based algorithms are proposed for both designs. For the uplink, we have also proposed a sequential SDP method. By simulation, the two algorithms are shown to obtain consistent sum MSE results.

Based on the optimized transceiver pairs, we have assessed the the effects of channel estimation errors and channel correlation at the BS. It has been noted that while the individual users' average MSEs in both links are the same, their average BERs are not the same, due to different interference structures.

5.8 Derivation and Proof Details

5.8.1 Detailed Calculations of (5.1)

From Section 5.2, $\mathbf{r}_{ul,j} = \mathbf{G}_j \cdot \mathbf{y}_{ul} = \mathbf{G}_j(\sum_{i=1}^{K} \hat{\mathbf{H}}_i \mathbf{F}_i \mathbf{s}_{ul,i} + \sum_{i=1}^{K} \mathbf{E}_i \mathbf{F}_i \mathbf{s}_{ul,i} + \mathbf{n}_{ul})$.

Define $\mathbf{y}_{ul,eff} = \sum_{i=1}^{K} \hat{\mathbf{H}}_i \mathbf{F}_i \mathbf{s}_{ul,i}$, and $\mathbf{e}_{ul,ch} = \sum_{i=1}^{K} \mathbf{E}_i \mathbf{F}_i \mathbf{s}_{ul,i}$. Then,

$$
\begin{aligned}
& MSE_{ul,j} \\
&= \mathbb{E}\left[\left(\mathbf{r}_{ul,j} - \mathbf{s}_{ul,j} \right) \left(\mathbf{r}_{ul,j} - \mathbf{s}_{ul,j} \right)^H \right]
\end{aligned}
$$

$$= \mathbb{E}\left[\left(\mathbf{G}_j\mathbf{y}_{ul,eff} + \mathbf{G}_j\mathbf{e}_{ul,ch} + \mathbf{G}_j\mathbf{n}_{ul} - \mathbf{s}_{ul,j}\right)\left(\mathbf{G}_j\mathbf{y}_{ul,eff} + \mathbf{G}_j\mathbf{e}_{ul,ch} + \mathbf{G}_j\mathbf{n}_{ul} - \mathbf{s}_{ul,j}\right)^H\right]. \tag{5.24}$$

Here the expectation is taken over the distributions of data vectors, channel noise and channel estimation error matrices. Using the assumptions made in Subsection 2.2.3,

$$\mathbb{E}(\mathbf{s}_{ul,j}\mathbf{s}_{ul,j}^H) = \mathbf{I}_{l_j},\ \mathbb{E}(\mathbf{s}_{ul,i}\mathbf{s}_{ul,j}^H) = 0, \forall i,j, i \neq j,\ \mathbb{E}[\mathbf{G}_j\mathbf{n}_{ul}\mathbf{n}_{ul}^H\mathbf{G}_j^H] = \sigma_n^2 \cdot \mathbf{G}_j\mathbf{G}_j^H. \tag{5.25}$$

Furthermore, using the assumptions made in Subsection 2.2.3 as well as in Section 5.2,

$$\begin{aligned}
\mathbb{E}\left[\mathbf{G}_j\mathbf{y}_{ul,eff}\mathbf{y}_{ul,eff}^H\mathbf{G}_j^H\right] &= \mathbb{E}\left[\mathbf{G}_j\left(\sum_{i=1}^{K}\sum_{k=1}^{K}\hat{\mathbf{H}}_i\mathbf{F}_i\mathbf{s}_{ul,i}\mathbf{s}_{ul,k}^H\mathbf{F}_k^H\hat{\mathbf{H}}_k^H\right)\mathbf{G}_j^H\right] \\
&= \mathbf{G}_j\left[\sum_{i=1}^{K}\sum_{k=1}^{K}\hat{\mathbf{H}}_i\mathbf{F}_i\mathbb{E}\left(\mathbf{s}_{ul,i}\mathbf{s}_{ul,k}^H\right)\mathbf{F}_k^H\hat{\mathbf{H}}_k^H\right]\mathbf{G}_j^H \\
&= \mathbf{G}_j\left[\sum_{i=1}^{K}\hat{\mathbf{H}}_i\mathbf{F}_i\mathbf{F}_i^H\hat{\mathbf{H}}_i^H\right]\mathbf{G}_j^H, \qquad (5.26) \\
\mathbb{E}\left[\mathbf{G}_j\mathbf{e}_{ul,ch}\mathbf{e}_{ul,ch}^H\mathbf{G}_j^H\right] &= \mathbb{E}\left[\mathbf{G}_j\left(\sum_{i=1}^{K}\sum_{k=1}^{K}\mathbf{E}_i\mathbf{F}_i\mathbf{s}_{ul,i}\mathbf{s}_{ul,k}^H\mathbf{F}_k^H\mathbf{E}_k^H\right)\mathbf{G}_j^H\right] \\
&= \mathbf{G}_j\cdot\mathbb{E}\left[\sum_{i=1}^{K}\sum_{k=1}^{K}\mathbf{E}_i\mathbf{F}_i\mathbb{E}\left(\mathbf{s}_{ul,i}\mathbf{s}_{ul,k}^H\right)\mathbf{F}_k^H\mathbf{E}_k^H\right]\cdot\mathbf{G}_j^H \\
&= \mathbf{G}_j\left[\sum_{i=1}^{K}\mathbf{\Sigma}_i^{\frac{1}{2}}\mathbb{E}\left(\mathbf{E}_{wi}\mathbf{F}_i\mathbf{F}_i^H\mathbf{E}_{wi}^H\right)\mathbf{\Sigma}_i^{\frac{1}{2}}\right]\mathbf{G}_j^H \\
&= \mathbf{G}_j\left[\sum_{i=1}^{K}\sigma_{Ei}^2\cdot\mathrm{tr}\left(\mathbf{F}_i\mathbf{F}_i^H\right)\cdot\mathbf{\Sigma}_i\right]\mathbf{G}_j^H, \qquad (5.27)
\end{aligned}$$

where in the second line of (5.27), the outer expectation is with respect to the distributions of channel estimation error matrices and the inner one is with respect to those of data vectors. In addition, using the independence between data vectors from different users, data vectors and noise vectors, data vectors and channel estimation errors as well as between noise vectors and channel estimation errors, it is easy to verify that

$$\mathbb{E}\left[\mathbf{G}_j\mathbf{y}_{ul,eff}\mathbf{e}_{ul,ch}^H\mathbf{G}_j^H\right] = 0,\ \mathbb{E}\left[\mathbf{G}_j\mathbf{y}_{ul,eff}\mathbf{n}_{ul}^H\mathbf{G}_j^H\right] = 0,$$

$$\mathbb{E}\left[\mathbf{G}_j\mathbf{e}_{ul,ch}\mathbf{n}_{ul}^H\mathbf{G}_j^H\right]=0, \qquad \mathbb{E}\left[\mathbf{G}_j\mathbf{y}_{ul,eff}\mathbf{s}_{ul,j}^H\right]=\mathbf{G}_j\hat{\mathbf{H}}_j\mathbf{F}_j,$$
$$\mathbb{E}\left[\mathbf{G}_j\mathbf{e}_{ul,ch}\mathbf{s}_{ul,j}^H\right]=0, \qquad \mathbb{E}\left[\mathbf{G}_j\mathbf{n}_{ul}\mathbf{s}_{ul,j}^H\right]=0. \tag{5.28}$$

Expanding (5.24) and using (5.25)-(5.28), we can then obtain (5.1).

5.8.2 Detailed Calculations of (5.3)

From Section 5.2,

$$\mathbf{r}_{dl,j}=\mathbf{R}_j\mathbf{y}_{dl,j}=\mathbf{R}_j\left[\left(\hat{\mathbf{H}}_j^H+\mathbf{E}_j^H\right)\left(\sum_{i=1}^{K}\mathbf{T}_i\mathbf{s}_{dl,i}\right)+\mathbf{n}_{dl,j}\right].$$

Define $\mathbf{y}_{dl,eff,j}=\hat{\mathbf{H}}_j^H\left(\sum_{i=1}^{K}\mathbf{T}_i\mathbf{s}_{dl,i}\right)$, and $\mathbf{e}_{dl,ch,j}=\mathbf{E}_j^H\left(\sum_{i=1}^{K}\mathbf{T}_i\mathbf{s}_{dl,i}\right)$. Then,

$$\begin{aligned}
&MSE_{dl,j}\\
&=\mathbb{E}\left[\left(\mathbf{r}_{dl,j}-\mathbf{s}_{dl,j}\right)\left(\mathbf{r}_{dl,j}-\mathbf{s}_{dl,j}\right)^H\right]\\
&=\mathbb{E}\left\{\left[\mathbf{R}_j\left(\mathbf{y}_{dl,eff,j}+\mathbf{e}_{dl,ch,j}+\mathbf{n}_{dl,j}\right)-\mathbf{s}_{dl,j}\right]\left[\mathbf{R}_j\left(\mathbf{y}_{dl,eff,j}+\mathbf{e}_{dl,ch,j}+\mathbf{n}_{dl,j}\right)-\mathbf{s}_{dl,j}\right]^H\right\}.
\end{aligned} \tag{5.29}$$

Clearly, by assumptions made in Subsection 2.2.3,

$$\mathbb{E}[\mathbf{s}_{dl,j}\mathbf{s}_{dl,j}^H]=\mathbf{I}_{l_j},\mathbb{E}[\mathbf{s}_{dl,i}\mathbf{s}_{dl,j}^H]=0,\forall i,j,i\neq j;\ \text{and}\ \mathbb{E}[\mathbf{R}_j\mathbf{n}_{dl,j}\mathbf{n}_{dl,j}^H\mathbf{R}_j^H]=\sigma_n^2\cdot\mathbf{R}_j\mathbf{R}_j^H.$$

Using the assumptions of independence between data vectors from different users, data vectors and noise vectors, data vectors and channel estimation errors as well as between noise vectors and estimation errors, we obtain

$$\begin{aligned}
\mathbb{E}\left[\mathbf{R}_j\mathbf{y}_{dl,eff,j}\mathbf{y}_{dl,eff,j}^H\mathbf{R}_j^H\right]&=\mathbf{R}_j\hat{\mathbf{H}}_j^H\left[\sum_{i=1}^{K}\sum_{k=1}^{K}\mathbf{T}_i\mathbb{E}\left(\mathbf{s}_{dl,i}\mathbf{s}_{dl,k}^H\right)\mathbf{T}_k^H\right]\hat{\mathbf{H}}_j\mathbf{R}_j^H\\
&=\mathbf{R}_j\hat{\mathbf{H}}_j^H\left(\sum_{i=1}^{K}\mathbf{T}_i\mathbf{T}_i^H\right)\hat{\mathbf{H}}_j\mathbf{R}_j^H,
\end{aligned} \tag{5.30}$$

$$\mathbb{E}\left[\mathbf{R}_j\mathbf{e}_{dl,ch,j}\mathbf{e}_{dl,ch,j}^H\mathbf{R}_j^H\right]=\mathbb{E}\left[\mathbf{R}_j\mathbf{E}_j^H\left(\sum_{i=1}^{K}\sum_{k=1}^{K}\mathbf{T}_i\mathbf{s}_{dl,i}\mathbf{s}_{dl,k}^H\mathbf{T}_k^H\right)\mathbf{E}_j\mathbf{R}_j^H\right]$$

$$
\begin{aligned}
&= \mathbb{E}\left[\mathbf{R}_j \mathbf{E}_{wj}^H \boldsymbol{\Sigma}_j^{\frac{1}{2}} \left(\sum_{i=1}^{K} \mathbf{T}_i \mathbf{T}_i^H\right) \boldsymbol{\Sigma}_j^{\frac{1}{2}} \mathbf{E}_{wj} \mathbf{R}_j^H\right] \\
&= \sigma_{Ej}^2 \cdot \mathrm{tr}\left[\boldsymbol{\Sigma}_j^{\frac{1}{2}} \left(\sum_{i=1}^{K} \mathbf{T}_i \mathbf{T}_i^H\right) \boldsymbol{\Sigma}_j^{\frac{1}{2}}\right] \cdot \mathbf{R}_j \mathbf{R}_j^H \\
&= \sigma_{Ej}^2 \cdot \mathrm{tr}\left[\boldsymbol{\Sigma}_j \left(\sum_{i=1}^{K} \mathbf{T}_i \mathbf{T}_i^H\right)\right] \cdot \mathbf{R}_j \mathbf{R}_j^H. \qquad (5.31)
\end{aligned}
$$

In addition,

$$
\begin{aligned}
&\mathbb{E}\left[\mathbf{R}_j \mathbf{y}_{dl,eff,j} \mathbf{e}_{dl,ch,j}^H \mathbf{R}_j^H\right] = 0, \;\; \mathbb{E}\left[\mathbf{R}_j \mathbf{y}_{dl,eff,j} \mathbf{n}_{dl,j}^H \mathbf{R}_j^H\right] = 0, \\
&\mathbb{E}\left[\mathbf{R}_j \mathbf{e}_{dl,ch,j} \mathbf{n}_{dl,j}^H \mathbf{R}_j^H\right] = 0, \qquad \mathbb{E}\left[\mathbf{R}_j \mathbf{y}_{dl,eff,j} \mathbf{s}_{dl,j}^H\right] = \mathbf{R}_j \hat{\mathbf{H}}_j^H \mathbf{T}_j, \\
&\mathbb{E}\left[\mathbf{R}_j \mathbf{n}_{dl,j} \mathbf{s}_{dl,j}^H\right] = 0, \qquad \mathbb{E}\left[\mathbf{R}_j \mathbf{e}_{dl,ch,j} \mathbf{s}_{dl,j}^H\right] = 0. \qquad (5.32)
\end{aligned}
$$

Expanding (5.29) and using (5.30)-(5.32), we obtain (5.3).

5.8.3 Proof of Lemma 4

We will only show (5.13). Post-multiplying both sides of (5.5), for $k = 1, \ldots, K$, to obtain

$$
\mathbf{F}_k^H \hat{\mathbf{H}}_k^H \mathbf{G}_k^H = \mathbf{G}_k \left[\sum_{j=1}^{K} \hat{\mathbf{H}}_j \mathbf{F}_j \mathbf{F}_j^H \hat{\mathbf{H}}_j^H + \sigma_n^2 \cdot \mathbf{I}_M + \sum_{j=1}^{K} \sigma_{Ej}^2 \cdot \mathrm{tr}(\mathbf{F}_j \mathbf{F}_j^H) \cdot \boldsymbol{\Sigma}_j\right] \mathbf{G}_k^H, \; \forall k.
$$

Taking the trace of both sides and summing over k, to get

$$
\begin{aligned}
\sum_{k=1}^{K} \mathrm{tr}\left(\mathbf{F}_k^H \hat{\mathbf{H}}_k^H \mathbf{G}_k^H\right) = \mathrm{tr}&\left[\left(\sum_{k=1}^{K} \mathbf{G}_k^H \mathbf{G}_k\right)\left(\sum_{j=1}^{K} \hat{\mathbf{H}}_j \mathbf{F}_j \mathbf{F}_j^H \hat{\mathbf{H}}_j^H\right)\right] + \sigma_n^2 \cdot \sum_{k=1}^{K} \mathrm{tr}\left(\mathbf{G}_k \mathbf{G}_k^H\right) \\
&+ \sum_{j=1}^{K} \sigma_{Ej}^2 \cdot \mathrm{tr}(\mathbf{F}_j \mathbf{F}_j^H) \cdot \left[\sum_{k=1}^{K} \mathrm{tr}\left(\mathbf{G}_k \boldsymbol{\Sigma}_j \mathbf{G}_k^H\right)\right]. \qquad (5.33)
\end{aligned}
$$

Pre-multiplying both sides of (5.6), for $k = 1, \ldots, K$, to obtain

$$
\mathbf{F}_k^H \hat{\mathbf{H}}_k^H \mathbf{G}_k^H = \mathbf{F}_k^H \left\{\hat{\mathbf{H}}_k^H \left[\sum_{j=1}^{K} \mathbf{G}_j^H \mathbf{G}_j\right] \hat{\mathbf{H}}_k + \left[\mu_{ul} + \sigma_{Ek}^2 \cdot \sum_{j=1}^{K} \mathrm{tr}(\mathbf{G}_j \boldsymbol{\Sigma}_k \mathbf{G}_j^H)\right] \cdot \mathbf{I}_{N_k}\right\} \mathbf{F}_k, \; \forall k.
$$

Therefore,

$$
\sum_{k=1}^{K} \mathrm{tr}\left(\mathbf{F}_k^H \hat{\mathbf{H}}_k^H \mathbf{G}_k^H\right) = \mathrm{tr}\left[\left(\sum_{k=1}^{K} \hat{\mathbf{H}}_k \mathbf{F}_k \mathbf{F}_k^H \hat{\mathbf{H}}_k^H\right)\left(\sum_{j=1}^{K} \mathbf{G}_j^H \mathbf{G}_j\right)\right] + \mu_{ul} \cdot \sum_{k=1}^{K} \mathrm{tr}\left(\mathbf{F}_k \mathbf{F}_k^H\right)
$$

$$+\sum_{k=1}^{K}\sigma_{Ek}^2\cdot\mathrm{tr}(\mathbf{F}_k\mathbf{F}_k^H)\cdot\left[\sum_{j=1}^{K}\mathrm{tr}\left(\mathbf{G}_j\boldsymbol{\Sigma}_k\mathbf{G}_j^H\right)\right]. \tag{5.34}$$

Simply by comparing (5.33) and (5.34), it is easy to see that

$$\sigma_n^2\cdot\sum_{k=1}^{K}\mathrm{tr}\left(\mathbf{G}_k\mathbf{G}_k^H\right)=\mu_{ul}\cdot\sum_{k=1}^{K}\mathrm{tr}\left(\mathbf{F}_k\mathbf{F}_k^H\right).$$

According to (5.8), if $\mu_{ul}>0$, then $\sum_{k=1}^{K}\mathrm{tr}\left(\mathbf{F}_k\mathbf{F}_k^H\right)=P_S$ and (5.13) follows immediately. If $\mu_{ul}=0$, using the above equality, one must have $\sigma_n^2\cdot\sum_{k=1}^{K}\mathrm{tr}\left(\mathbf{G}_k\mathbf{G}_k^H\right)=0$ and (5.13) still holds. The proof for (5.14) is similar, and is omitted for brevity. This concludes the proof of **Lemma 4**.

5.8.4 Proof of Existence of Global Minimums for (5.2) and (5.4)

The uplink problem (5.2) can be equivalently formulated as

$$\min_{\{\mathbf{F}_i\}_{i=1}^K,\ \sum_{i=1}^K\mathrm{tr}(\mathbf{F}_i\mathbf{F}_i^H)\le P_S}\ \min_{\{\mathbf{G}_i\}_{i=1}^K} mse_{ul,t}.$$

It is easy to show that the inner minimization is achieved when (5.5) is satisfied for all k.

Define

$$\mathbf{J}_2=\sigma_n^2\cdot\mathbf{I}_M+\sum_{j=1}^{K}\sigma_{Ej}^2\cdot\mathrm{tr}\left(\mathbf{F}_j\mathbf{F}_j^H\right)\cdot\boldsymbol{\Sigma}_j.$$

Using (5.5) for all k, the average sum MSE can be expressed as:

$$mse_{ul,t}=\sum_{j=1}^{K}\mathrm{tr}\left(\mathbf{I}_{l_j}\right)-\mathrm{tr}\left(\mathbf{I}_M\right)+\mathrm{tr}\left\{\left[\sum_{j=1}^{K}\hat{\mathbf{H}}_j\mathbf{F}_j\mathbf{F}_j^H\hat{\mathbf{H}}_j^H+\mathbf{J}_2\right]^{-1}\mathbf{J}_2\right\}, \tag{5.35}$$

and (5.2) is equivalent to

$$\begin{aligned}&\min_{\{\mathbf{F}_i\}_{i=1}^K}\ mse_{ul,t}\ \ [\text{as in (5.35)}]\\ &\text{subject to }\sum_{i=1}^{K}\mathrm{tr}(\mathbf{F}_i\mathbf{F}_i^H)\le P_S.\end{aligned} \tag{5.36}$$

Let $\tilde{\mathbf{F}} = \text{diag}\{\mathbf{F}_1, \ldots, \mathbf{F}_K\}$. Then the constraint in (5.36) can be written as $\text{tr}\left(\tilde{\mathbf{F}}\tilde{\mathbf{F}}^H\right) \leq P_S$. Thus, the feasible set of (5.36) is a subset of the (closed and bounded) Frobenius norm ball of radius $\sqrt{P_S}$. It can be shown that this set itself is closed and bounded. As can be seen from (5.35), $mse_{ul,t}$ as a function of $\{\mathbf{F}_j\}_{j=1}^K$ is continuous at all points of the feasible set. Invoking Weierstrass' Theorem [5, p. 654, **Proposition A.8**], we conclude that a global minimum exists for (5.36). Since (5.2) and (5.36) are equivalent, the same global minimum also exists for (5.2) [7, p. 130, Section 4.1.3].

The proof of existence of a global minimum for (5.4) is similar and is omitted for brevity. □

5.8.5 Proof of Theorem 6

We begin with the forward part. Suppose that we are given $\{\mathbf{F}_k, \mathbf{G}_k\}_{k=1}^K$, a set of precoder-decoder pairs for the uplink that satisfies the KKT conditions (5.5)-(5.8). Then using (5.5) for $k = 1, \ldots, K$, we obtain

$$mse_{ul,t} = \sum_{i=1}^{K} \text{tr}(\mathbf{I}_{l_i}) - \sum_{i=1}^{K} \text{tr}\left(\hat{\mathbf{H}}_i^H \mathbf{G}_i^H \mathbf{F}_i^H\right).$$

Define

$$\mathbf{J}_{A,i} = \hat{\mathbf{H}}_i^H \mathbf{G}_i^H \mathbf{G}_i \hat{\mathbf{H}}_i,\ \mathbf{J}_{B,i,k} = \hat{\mathbf{H}}_i^H \mathbf{G}_k^H \mathbf{G}_k \hat{\mathbf{H}}_i,\ \text{and}\ c_{i,k} = \text{tr}(\mathbf{G}_k \mathbf{\Sigma}_i \mathbf{G}_k^H), i, k = 1, \ldots, K.$$

Using (5.6), it can be shown that

$$\hat{\mathbf{H}}_i^H \mathbf{G}_i^H \mathbf{F}_i^H = \hat{\mathbf{H}}_i^H \mathbf{G}_i^H \mathbf{G}_i \hat{\mathbf{H}}_i \left\{ \hat{\mathbf{H}}_i^H \left(\sum_{k=1}^{K} \mathbf{G}_k^H \mathbf{G}_k \right) \hat{\mathbf{H}}_i + \left[\mu_{ul} + \sigma_{Ei}^2 \cdot \sum_{k=1}^{K} \text{tr}\left(\mathbf{G}_k \mathbf{\Sigma}_i \mathbf{G}_k^H\right) \right] \mathbf{I}_{N_i} \right\}^{-1},$$

and thus

$$mse_{ul,t} = \sum_{i=1}^{K} \text{tr}\left(\mathbf{I}_{l_i}\right) - \sum_{i=1}^{K} \text{tr}\left(\mathbf{D}_i\right), \tag{5.37}$$

where

$$\mathbf{D}_i = \mathbf{J}_{A,i}\left[\sum_{k=1}^{K}\mathbf{J}_{B,i,k} + \left(\mu_{ul} + \sigma_{Ei}^2 \cdot \sum_{k=1}^{K} c_{i,k}\right)\cdot \mathbf{I}_{N_i}\right]^{-1}. \tag{5.38}$$

In the downlink, let

$$\mathbf{T}_k = \alpha_k \cdot \mathbf{G}_k^H, \tag{5.39}$$

where α_k is a scalar whose choice will be discussed later, $\forall k$. Let $\mathbf{R}_k$ be related to $\mathbf{T}_k$ as given by (5.10), $k = 1,\ldots,K$, and then

$$mse_{dl,t} = \sum_{j=1}^{K}\mathrm{tr}(\mathbf{I}_{l_j}) - \sum_{j=1}^{K}\mathrm{tr}(\hat{\mathbf{H}}_j^H\mathbf{T}_j\mathbf{R}_j).$$

Since $\mathbf{R}_j$ is related to $\mathbf{T}_j$ through (5.10),

$$\hat{\mathbf{H}}_j^H\mathbf{T}_j\mathbf{R}_j = \hat{\mathbf{H}}_j^H\mathbf{T}_j\mathbf{T}_j^H\hat{\mathbf{H}}_j\left\{\hat{\mathbf{H}}_j^H\left[\sum_{k=1}^{K}\mathbf{T}_k\mathbf{T}_k^H\right]\hat{\mathbf{H}}_j + \left[\sigma_n^2 + \sigma_{Ej}^2\sum_{k=1}^{K}\mathrm{tr}\left(\mathbf{T}_k^H\boldsymbol{\Sigma}_j\mathbf{T}_k\right)\right]\mathbf{I}_{N_j}\right\}^{-1},$$

$\forall j$. Using (5.39), we can express $mse_{dl,t}$ in terms of $\{\mathbf{G}_k\}_{k=1}^K$ as follows:

$$mse_{dl,t} = \sum_{j=1}^{K}\mathrm{tr}(\mathbf{I}_{l_j}) - \sum_{j=1}^{K}\mathrm{tr}(\tilde{\mathbf{D}}_j), \tag{5.40}$$

where

$$\tilde{\mathbf{D}}_j = \mathbf{J}_{A,j}\left[\sum_{k=1}^{K}\frac{|\alpha_k|^2}{|\alpha_j|^2}\mathbf{J}_{B,j,k} + \left(\frac{\sigma_n^2}{|\alpha_j|^2} + \sigma_{Ej}^2\cdot\sum_{k=1}^{K}\frac{|\alpha_k|^2 c_{j,k}}{|\alpha_j|^2}\right)\cdot\mathbf{I}_{N_j}\right]^{-1}. \tag{5.41}$$

Note that the choice of $\{\alpha_k\}_{k=1}^K$ should satisfy the sum power constraint for the downlink, i.e.,

$$\sum_{k=1}^{K}\mathrm{tr}(\mathbf{T}_k\mathbf{T}_k^H) = \sum_{k=1}^{K}|\alpha_k|^2\mathrm{tr}(\mathbf{G}_k^H\mathbf{G}_k) \le P_S. \tag{5.42}$$

On the other hand, from (5.13),

$$\sum_{k=1}^{K}\frac{\sigma_n^2}{\mu_{ul}}\mathrm{tr}(\mathbf{G}_k^H\mathbf{G}_k) = P_S.$$

If we choose $\alpha_k = \sqrt{\sigma_n^2/\mu_{ul}}$, $\forall k$, from (5.38) and (5.41), the sum MSE for both links will be identical while (5.42) is satisfied with equality. In the remaining proof, we will use this choice of $\{\alpha_k\}_{k=1}^K$.

To complete the forward part, we need to show that $\{\mathbf{T}_k, \mathbf{R}_k\}_{k=1}^K$ chosen here satisfies the downlink KKT conditions, i.e., we need to establish (5.9), (5.11) and (5.12). Note that

$$\begin{aligned}
\mathbf{R}_k &\overset{(5.10)}{=} \mathbf{T}_k^H \hat{\mathbf{H}}_k \left\{ \hat{\mathbf{H}}_k^H \left[\sum_{j=1}^K \mathbf{T}_j \mathbf{T}_j^H \right] \hat{\mathbf{H}}_k + \left[\sigma_n^2 + \sigma_{Ek}^2 \cdot \sum_{j=1}^K \mathrm{tr}(\mathbf{T}_j^H \boldsymbol{\Sigma}_k \mathbf{T}_j) \right] \cdot \mathbf{I}_{N_k} \right\}^{-1} \\
&\overset{(5.39)}{=} \sqrt{\mu_{ul}/\sigma_n^2} \cdot \mathbf{G}_k \hat{\mathbf{H}}_k \left\{ \hat{\mathbf{H}}_k^H \left[\sum_{j=1}^K \mathbf{G}_j^H \mathbf{G}_j \right] \hat{\mathbf{H}}_k + \left[\mu_{ul} + \sigma_{Ek}^2 \sum_{j=1}^K \mathrm{tr}(\mathbf{G}_j \boldsymbol{\Sigma}_k \mathbf{G}_j^H) \right] \cdot \mathbf{I}_{N_k} \right\}^{-1} \\
&= \sqrt{\mu_{ul}/\sigma_n^2} \cdot \mathbf{F}_k^H, \\
\mathbf{F}_k &= \sqrt{\sigma_n^2/\mu_{ul}} \cdot \mathbf{R}_k^H, \ \forall k. \qquad (5.43)
\end{aligned}$$

Then, from (5.39), (5.5) and (5.43), it can be shown that

$$\begin{aligned}
\mathbf{T}_k &\overset{(5.39)}{=} \sqrt{\sigma_n^2/\mu_{ul}} \cdot \mathbf{G}_k^H \\
&\overset{(5.5)}{=} \sqrt{\frac{\sigma_n^2}{\mu_{ul}}} \cdot \left[\sum_{j=1}^K \hat{\mathbf{H}}_j \mathbf{F}_j \mathbf{F}_j^H \hat{\mathbf{H}}_j^H + \sigma_n^2 \cdot \mathbf{I}_M + \sum_{j=1}^K \sigma_{Ej}^2 \cdot \mathrm{tr}(\mathbf{F}_j \mathbf{F}_j^H) \cdot \boldsymbol{\Sigma}_j \right]^{-1} \hat{\mathbf{H}}_k \mathbf{F}_k \\
&\overset{(5.43)}{=} \left[\sum_{j=1}^K \hat{\mathbf{H}}_j \mathbf{R}_j^H \mathbf{R}_j \hat{\mathbf{H}}_j^H + \mu_{ul} \cdot \mathbf{I}_M + \sum_{j=1}^K \sigma_{Ej}^2 \cdot \mathrm{tr}(\mathbf{R}_j^H \mathbf{R}_j) \cdot \boldsymbol{\Sigma}_j \right]^{-1} \hat{\mathbf{H}}_k \mathbf{R}_k^H. \qquad (5.44)
\end{aligned}$$

Let $\mu_{dl} = \mu_{ul}$, and then (5.44) is the same as (5.9). Furthermore, (5.11) and (5.12) are also all satisfied. Therefore, from the set $\{\mathbf{F}_k, \mathbf{G}_k\}_{k=1}^K$ satisfying the uplink KKT conditions, we have found a set $\{\mathbf{T}_k, \mathbf{R}_k\}_{k=1}^K$ which achieves the same sum MSE and satisfies the downlink KKT conditions. This concludes the forward part. Using similar arguments, we can prove the converse part, which is omitted to avoid repetition. This is the end of the proof of **Theorem 6**.

5.8.6 Proof of Theorem 7

Assume $\sigma_{Ej}^2 = \tilde{\sigma}_E^2$ and $\boldsymbol{\Sigma}_j = \boldsymbol{\Sigma}_{BS}$, $\forall j$. If the inequality sum power constraint in the problem given by (5.16)-(5.19) is replaced by an equality constraint, then the resultant problem is

equivalent to

$$\min_{\check{\mathbf{X}};\, \mathbf{Q}_j, j=1,\ldots,K} \operatorname{tr}\left[\check{\mathbf{X}}\left(\sigma_n^2 \cdot \mathbf{I}_M + \tilde{\sigma}_E^2 \cdot P_S \cdot \boldsymbol{\Sigma}_{BS}\right)\right], \tag{5.45}$$

$$\text{subject to} \quad \sum_{j=1}^{K} \operatorname{tr}(\mathbf{Q}_j) = P_S, \tag{5.46}$$

$$\begin{pmatrix} \check{\mathbf{X}} & \mathbf{I}_M \\ \mathbf{I}_M & \sum_{j=1}^{K} \hat{\mathbf{H}}_j \mathbf{Q}_j \hat{\mathbf{H}}_j^H + \tilde{\sigma}_E^2 \cdot P_S \cdot \boldsymbol{\Sigma}_{BS} + \sigma_n^2 \cdot \mathbf{I}_M \end{pmatrix} \succeq 0, \tag{5.47}$$

$$\mathbf{Q}_j \succeq 0, j = 1, \ldots, K. \tag{5.48}$$

Note that (5.45)-(5.48) follow from two steps:

1. According to [7, p. 130, Section 4.1.3], a substitution of the equality power constraint into the objective function and other related inequality constraints preserves the equivalence.

2. After the substitution, (5.18) [i.e., (5.15)] becomes

$$\check{\mathbf{X}} = \left[\sum_{j=1}^{K} \hat{\mathbf{H}}_j \mathbf{Q}_j \hat{\mathbf{H}}_j^H + \tilde{\sigma}_E^2 \cdot P_S \cdot \boldsymbol{\Sigma}_{BS} + \sigma_n^2 \cdot \mathbf{I}_M\right]^{-1},$$

   which can be replaced by

$$\check{\mathbf{X}} \succeq \left[\sum_{j=1}^{K} \hat{\mathbf{H}}_j \mathbf{Q}_j \hat{\mathbf{H}}_j^H + \tilde{\sigma}_E^2 \cdot P_S \cdot \boldsymbol{\Sigma}_{BS} + \sigma_n^2 \cdot \mathbf{I}_M\right]^{-1}$$

   under a monotonicity argument. Then (5.47) follows using Schur's complement [7, Section A.5.5, p. 651] [59].

Now, to show **Theorem 7**, we only need to show that the minimum value of the objective function of the problem in [(5.45)-(5.48)] is a non-increasing function of P_S, i.e. (5.46) can be replaced by an inequality constraint. Let $f(P_{S1})$ and $f(P_{S2})$ be the minimum values of the objective function corresponding to the sum power P_{S1} and P_{S2}, respectively, where

$P_{S1} \leq P_{S2}$. Let $\check{\mathbf{X}}_1, \{\mathbf{Q}_{1j}\}_{j=1}^K$ denote the matrices achieving $f(P_{S1})$, i.e.,

$$\check{\mathbf{X}}_1 = \left(\sum_{j=1}^{K} \hat{\mathbf{H}}_j \mathbf{Q}_{1j} \hat{\mathbf{H}}_j^H + \sigma_E^2 \cdot P_{S1} \cdot \mathbf{\Sigma}_{BS} + \sigma_n^2 \cdot \mathbf{I}_M \right)^{-1},$$

and $\sum_{j=1}^K \mathrm{tr}(\mathbf{Q}_{1j}) = P_{S1}$. Let $\tilde{\mathbf{Q}}_{2j} = \frac{P_{S2}}{P_{S1}} \cdot \mathbf{Q}_{1j}$, $j = 1, \ldots, K$, and then $\sum_{j=1}^K \mathrm{tr}(\tilde{\mathbf{Q}}_{2j}) = P_{S2}$. Let

$$\begin{aligned}
\tilde{\mathbf{X}}_2 &= \left(\sum_{j=1}^{K} \hat{\mathbf{H}}_j \tilde{\mathbf{Q}}_{2j} \hat{\mathbf{H}}_j^H + \tilde{\sigma}_E^2 \cdot P_{S2} \cdot \mathbf{\Sigma}_{BS} + \sigma_n^2 \cdot \mathbf{I}_M \right)^{-1} \\
&= \frac{P_{S1}}{P_{S2}} \left(\sum_{j=1}^{K} \hat{\mathbf{H}}_j \mathbf{Q}_{1j} \hat{\mathbf{H}}_j^H + \tilde{\sigma}_E^2 \cdot P_{S1} \cdot \mathbf{\Sigma}_{BS} + \frac{\sigma_n^2 P_{S1}}{P_{S2}} \cdot \mathbf{I}_M \right)^{-1}.
\end{aligned}$$

Define

$$\mathbf{J}_3 = \sum_{j=1}^{K} \hat{\mathbf{H}}_j \mathbf{Q}_{1j} \hat{\mathbf{H}}_j^H + \tilde{\sigma}_E^2 \cdot P_{S1} \cdot \mathbf{\Sigma}_{BS},$$

and we get

$$\begin{aligned}
&\mathrm{tr}\left[\tilde{\mathbf{X}}_2 \left(\sigma_n^2 \cdot \mathbf{I}_M + \tilde{\sigma}_E^2 \cdot P_{S2} \cdot \mathbf{\Sigma}_{BS} \right) \right] \\
&= \mathrm{tr}\left(\mathbf{I}_M \right) - \mathrm{tr}\left[\left(\mathbf{J}_3 + \frac{\sigma_n^2 P_{S1}}{P_{S2}} \mathbf{I}_M \right)^{-1} \left(\sum_{j=1}^{K} \hat{\mathbf{H}}_j \mathbf{Q}_{1j} \hat{\mathbf{H}}_j^H \right) \right] \\
&\leq \mathrm{tr}\left(\mathbf{I}_M \right) - \mathrm{tr}\left[\left(\mathbf{J}_3 + \sigma_n^2 \mathbf{I}_M \right)^{-1} \left(\sum_{j=1}^{K} \hat{\mathbf{H}}_j \mathbf{Q}_{1j} \hat{\mathbf{H}}_j^H \right) \right] \\
&= f(P_{S1}).
\end{aligned}$$

The above inequality is based on the following result. Let $\mathbf{A}$ denote a positive semidefinite matrix. Let $\mathbf{B}_1$ and $\mathbf{B}_2$ be two positive definite matrices, and $\mathbf{B}_2 \succ \mathbf{B}_1$, which means $(\mathbf{B}_2 - \mathbf{B}_1)$ is positive definite. Then $\mathbf{B}_1^{-1} \succ \mathbf{B}_2^{-1}$, and $\mathrm{tr}(\mathbf{B}_1^{-1}\mathbf{A}) \geq \mathrm{tr}(\mathbf{B}_2^{-1}\mathbf{A})$ [64, pp. 585-586]. Since the matrices $[\tilde{\mathbf{X}}_2, \{\tilde{\mathbf{Q}}_{2j}\}_{j=1}^K]$ chosen here with sum power P_{S2} are not necessarily the optimum-achieving ones, we have

$$f(P_{S2}) \leq \mathrm{tr}\left\{ \tilde{\mathbf{X}}_2 \left[\sigma_n^2 \cdot \mathbf{I}_M + \tilde{\sigma}_E^2 \cdot P_{S2} \cdot \mathbf{\Sigma}_{BS} \right] \right\} \leq f(P_{S1}),$$

for $P_{S2} \geq P_{S1}$. Therefore, the minimum value of the objective function of the problem given by (5.45)-(5.48) is a non-increasing function of P_S, and (5.46) can be replaced by an inequality constraint. **Theorem 7** follows immediately. □

Chapter 6

Conclusions and Future Work

In this chapter, we summarize the major contributions in this thesis, and suggest possible future directions based on the research presented.

6.1 Conclusions

In previous chapters, we have studied the optimum linear precoding/decoding designs for single-user and multiuser spatial multiplexing with imperfect channel knowledge in slow, flat, Rayleigh fading.

In Chapter 3, a detailed modeling of imperfect channel estimation with correlation at both ends of a single-user MIMO link is presented. Then the minimum total MSE design with the same imperfect CSI at both ends is formulated as an optimization problem, subject to a total power constraint. Based on the general methodology for non-convex optimization, the optimum structures of the precoder and decoder are derived, which show the coupling effect of channel estimation error and channel correlation. It turns out that compared to the perfect CSI case, linear filters are added to the transceiver to balance the suppression of the channel noise and the additional noise induced from channel estimation error. The linear precoder and decoder diagonalize an equivalent matrix channel into a set of parallel

scalar channels. The analysis is further extended to the minimum weighted MSE design. Based on the optimized precoder/decoder, the significant impacts of channel estimation error and correlation are quantified by simulation. For example, in a 4×4 MIMO system where $B = 3$ data streams are transmitted, at $P_T/\sigma_n^2 = 20$ dB, the ABER is 7.6×10^{-7} when there is perfect CSI at both ends and there is no channel correlation. However, when there is channel estimation error, with P_{tr}/σ_n^2 fixed at 26.016 dB, the ABER increases to 1.4×10^{-5}. When there is transmit correlation with $\rho_T = 0.5$, the ABER increases to 6.8×10^{-5}. Furthermore, when ρ_T increases from 0.5 to 0.9, the ABER increases from 6.8×10^{-5} to 8.8×10^{-3}. The advantage from using the optimum design over suboptimum designs is demonstrated. Simulation results also indicate that the effects of the same amount of transmit and receive correlation might be different, depending on how the knowledge of channel correlation is exploited.

In Chapter 4, the maximum mutual information design for a single-user MIMO system is studied. With the same imperfect CSI as modeled in Chapter 3, the exact capacity expression is hard to obtain. Alternatively, a capacity lower-bound is used for system design. For the special case without receive correlation, the closed-form optimum transmit covariance matrix is derived for determining the lower-bound, whereas in the literature, a numerical search method has been proposed. For the more general case with both transmit and receive correlation, the structure of the optimum transmit covariance matrix for the lower-bound has been obtained, which provides insight on how the imperfect channel estimation and channel correlation jointly affect the actual mutual information. The method employed here to determine the optimum transmit covariance matrix reveals the close relation between the maximum mutual information design and the minimum total MSE design. It is found that under the same imperfect CSI, the two designs lead to similar transceiver structures that are different mainly in transmit power allocation. Simulation results have

shown the tightness of the lower-bound. The accuracy of using the optimum transmit strategy for the lower-bound is also demonstrated through comparison with the uniform power allocation. The effects of channel estimation error and channel correlation are investigated based on capacity bounds. For a 4×4 MIMO channel with $\rho_T = 0.5, \rho_R = 0$, the ergodic capacity is about 15.9 bits/channel use at $P_T/\sigma_n^2 = 15$ dB. However, with imperfect CSI at $P_{tr}/\sigma_n^2 = 26.016$ dB, it drops to 14.1 bits/channel use. The capacity further decreases from 14.1 bits/channel use to around 8.75 bits/channel use when ρ_T increases from 0.5 to 0.9 (with $\rho_R = 0$ and $P_T/\sigma_n^2 = 15$ dB).

Chapter 5 focuses on joint linear precoding/decoding to minimize the average sum MSE from all users for multiuser MIMO systems. Unlike previous designs, here channel estimation errors and channel correlation at the BS have been considered. Two optimization problems are formulated, for the uplink and the downlink, respectively. Iterative algorithms based on the KKT conditions are proposed for solving both problems. A duality in average sum MSE has been proved based on the KKT conditions. It is also shown that when the same minimum average sum MSEs are achieved in both links, the individual users' MSEs in both links are also equal. For the uplink design, we also propose a method that solves a sequence of SDPs. The consistency in the average sum MSE results obtained from different algorithms confirms the duality and corroborates our analysis. By simulation, we have assessed the impact of channel estimation errors and channel correlation at the BS on uplink and downlink system error rate performances. We have found that in multiuser MIMO, while the duality in each user's average MSE holds with imperfect CSI, there is no duality in individual users' ABERs, due to the differences in the structure of the interference in both links.

6.2 Future Directions

In this section, we discuss some issues that remain to be explored, as well as possible future research topics motivated by the results in this thesis.

- Effect of Erroneous Feedback

  In our designs in Chapters 3 and 4, we have assumed that the feedback link is instantaneous and error-free. While the assumption of instantaneous feedback has been partially justified by the insensitivity of system performance to reasonably small delays, the errors in the feedback link need to be modeled and considered. This also motivates the limited feedback design with imperfect CSIR. For these advanced designs, our results can be used for comparison.

- Probability-constrained Transceiver Optimization

  Throughout this thesis, we have used the average performance as the design criterion. In a nutshell, we have studied only stochastic robust design. While the worst-case robust design is often pessimistic, a new approach called the *probability-constrained optimization* is likely to better suit some practical applications [112]. The key idea of this approach is to account for only those channel estimation errors that occur with high probability, instead of addressing all possible error patterns. Furthermore, this approach is applicable to Gaussian channel estimation errors. Therefore, it remains to be determined if this approach can be applied to MIMO transceiver designs.

- Joint Channel Estimation, Feedback and Transceiver Design

  In our thesis, we have taken a modular approach to system design. In fact, we first obtain channel estimates, and then based on these, we consider the feedback and the optimization of the transceiver. However, the transceiver design is tightly coupled

with channel estimation and feedback [65, 98]. It might be worth modeling the joint design and investigating whether a joint design of these three parts will yield performance gain for spatially multiplexed MIMO systems with linear processors. The results obtained in this thesis may be used for comparison.

- MSE-related Designs for Cooperative Communications

  This thesis has focused on designs for systems equipped with co-located multiple antennas. Recently, cooperative communications through distributed single-antenna terminals have been extensively studied for improved signal quality and better coverage without using co-located antenna arrays [52, 67, 90]. Traditionally, in a cooperative network, each node is equipped with one antenna. The source node broadcasts information to a set of relay nodes. Then the relay nodes transmit to the destination. The distributed relay nodes (terminals) can be regarded as forming a virtual antenna array. Two protocols, i.e., the amplify-and-forward and decode-and-forward protocols, have been proposed for signal processing at the relays. As can be seen from [67], the designs for distributed and co-located antenna arrays are different, but also closely related. In [48], a MMSE beamforming has been proposed for cooperative systems using the amplify-and-forward protocol. In [79], deploying multiple antennas at some nodes (source, relays, destination) has been proposed. It would be interesting to see whether the MSE-related designs are applicable to this scenario and to determine the relationship between the maximum mutual information design and the minimum total MSE design in this case.

Bibliography

[1] J. Akhtar and D. Gesbert, "Spatial multiplexing over correlated MIMO channels with a closed-form precoder," *IEEE Trans. Wireless Commun.*, vol. 4, no. 5, pp. 2400–2409, Sept. 2005.

[2] S. M. Alamouti, "A simple transmit diversity technique for wireless communications," *IEEE J. Select. Areas Commun.*, vol. 16, no. 8, pp. 1451–1458, Oct. 1998.

[3] J. B. Andersen, "Array gain and capacity for known random channels with multiple element arrays at both ends," *IEEE J. Select. Areas Commun.*, vol. 18, no. 11, pp. 2172–2178, Nov. 2000.

[4] P. Bender, P. Black, M. Grob, R. Padovani, N. Sindhushayana, and S. Viterbi, "CDMA/HDR: a bandwidth-efficient high-speed wireless data service for nomadic users," *IEEE Commun. Mag.*, vol. 38, no. 7, pp. 70–77, July 2000.

[5] D. P. Bertsekas, *Nonlinear Programming*. Belmont, MA: Athena Scientific, 1999.

[6] S. Bhashyam, A. Sabharwal, and B. Aazhang, "Feedback gain in multiple antenna systems," *IEEE Trans. Commun.*, vol. 50, no. 5, pp. 785–798, May 2002.

[7] S. Boyd and L. Vandenberghe, *Convex Optimization*. New York, NY: Cambridge University Press, 2004.

[8] D. H. Brandwood, “A complex gradient operator and its application in adaptive array theory,” *IEE Proc., Pts. F and H*, vol. 130, no. 1, pp. 11–16, Feb. 1983.

[9] D. G. Brennan, “Linear diversity combining techniques,” *Proc. IRE*, pp. 1075–1102, Feb. 1959.

[10] J. Brewer, “Kronecker products and matrix calculus in system theory,” *IEEE Trans. Circuits and Systems*, vol. 25, no. 9, pp. 772–781, Sept. 1978.

[11] G. Caire and S. Shamai, “On the achievable throughput of a multiantenna gaussian broadcast channel,” *IEEE Trans. Info. Theory*, vol. 49, no. 7, pp. 1691–1706, July 2003.

[12] D. Chizhik, J. Ling, P. W. Wolniansky, R. A. Valenzuela, N. Costa, and K. Huber, “Multiple-input-multiple-output measurements and modeling in Manhattan,” *IEEE J. Select. Areas Commun.*, vol. 21, no. 3, pp. 321–331, Apr. 2003.

[13] L.-U. Choi and R. D. Murch, “A transmit preprocessing technique for multiuser MIMO systems using a decomposition approach,” *IEEE Trans. Wireless Commun.*, vol. 3, no. 1, pp. 20–24, Jan. 2004.

[14] L. Collin, O. Berder, P. Rostaing, and G. Burel, “Optimal minimum distance-based precoder for MIMO spatial multiplexing systems,” *IEEE Trans. Signal Processing*, vol. 52, no. 3, pp. 617–627, Mar. 2004.

[15] M. Costa, “Writing on dirty paper,” *IEEE Trans. Info. Theory*, vol. 29, no. 3, pp. 439–441, May 1983.

[16] T. M. Cover, “Broadcast channels,” *IEEE Trans. Info. Theory*, vol. 18, no. 1, pp. 2–14, Jan. 1972.

[17] T. M. Cover and J. A. Thomas, *Elements of Information Theory*. New York, NY: John Wiley and Sons, 1991.

[18] M. Ding and S. D. Blostein, "MIMO minimum total MSE transceiver design with imperfect CSI at both ends," *IEEE Trans. Signal Processing (revised in Jan. and Jun. 2008, submitted in Apr. 2007)*.

[19] ——, "Low-feedback adaptive-rate MIMO spatial multiplexing with zero-forcing detection," in *Proc. Canadian Workshop on Information Theory*, Montreal, Quebec, Canada, 2005.

[20] ——, "MIMO LMMSE transceiver design with imperfect CSI at both ends," in *Proc. IEEE Int. Conf. Commun.*, Glasgow, Scotland, 2007, pp. 4369–4374.

[21] ——, "Uplink–downlink duality in normalized MSE or SINR under imperfect channel knowledge," in *Proc. IEEE Global Telecommun. Conf.*, Washington D.C., USA, 2007, pp. 3786–3790.

[22] ——, "Joint optimization for multiuser MIMO uplink systems with imperfect CSI," in *Proc. 24th Queen's Biennial Symposium on Communications*, Kingston, Ontario, Canada, 2008, pp. 191–195.

[23] ——, "Relation between joint optimizations for multiuser MIMO uplink and downlink with imperfect CSI," in *Proc. IEEE Int. Conf. Acoustic, Speech and Signal Processing*, 2008, pp. 3149–3152.

[24] A. El Gamal and T. M. Cover, "Multiuser information theory," *Proc. IEEE*, vol. 68, no. 12, pp. 1466–1483, Dec. 1980.

[25] A. Forenza, D. J. Love, and R. W. Heath, "Simplified spatial correlation models for clustered MIMO channels with different array configurations," *IEEE Trans. Veh. Technol.*, vol. 56, no. 4, pp. 1924–1934, July 2007.

[26] G. J. Foschini, "Layered space-time architecture for wireless communication in a fading environment when using multi-element antennas," *Bell Labs Tech. J.*, pp. 41–59, 1996.

[27] G. J. Foschini, D. Chizhik, M. J. Gans, C. Papadias, and R. A. Valenzuela, "Analysis and performance of some basic space-time architectures," *IEEE J. Select. Areas Commun.*, vol. 21, no. 3, pp. 303–320, Apr. 2003.

[28] G. J. Foschini and M. J. Gans, "On limits of wireless communications in a fading environment when using multiple antennas," *Wireless Personal Commun.*, vol. 6, no. 3, pp. 311–335, Mar. 1998.

[29] G. J. Foschini, G. D. Golden, R. A. Valenzuela, and P. W. Wolniansky, "Simplified processing for high spectral efficiency wireless communication employing multi-element arrays," *IEEE J. Select. Areas Commun.*, vol. 17, no. 11, pp. 1841–1852, Nov. 1999.

[30] A. B. Gershman and N. Sidiropoulos, *Space-Time Processing for MIMO Communications*. New York, NY: John Wiley and Sons, 2005.

[31] A. Goldsmith, S. A. Jafar, N. Jindal, and S. Vishwanath, "Capacity limits of MIMO channels," *IEEE J. Select. Areas Commun.*, vol. 21, no. 5, pp. 684–702, June 2003.

[32] D. Guo, S. Shamai, and S. Verdú, "Mutual information and minimum mean-square error in Gaussian channels," *IEEE Trans. Info. Theory*, vol. 51, no. 4, pp. 1261–1282, Apr. 2005.

[33] Y. Guo and B. C. Levy, "Worst-case MSE precoder design for imperfectly known MIMO communications channels," *IEEE Trans. Signal Processing*, vol. 53, no. 8, pp. 2918–2930, Aug. 2005.

[34] B. Hassibi and B. M. Hochwald, "How much training is needed in multiple-antenna wireless links?" *IEEE Trans. Info. Theory*, vol. 49, no. 4, pp. 951–963, Apr. 2003.

[35] A. Hjørungnes, D. Gesbert, and D. P. Palomar, "Unified theory of complex-valued matrix differentiation," in *Proc. IEEE Int. Conf. Acoustic, Speech and Signal Processing*, vol. 3, Honolulu, Hawaii, 2007, pp. 345–348.

[36] B. M. Hochwald, C. B. Peel, and A. L. Swindlehurst, "A vector-perturbation technique for near-capacity multiantenna multiuser communication—Part II: perturbation," *IEEE Trans. Commun.*, vol. 53, no. 3, pp. 537–544, Mar. 2005.

[37] R. A. Horn and C. R. Johnson, *Matrix Analysis*. New York, NY: Cambridge University Press, 1999.

[38] S. A. Jafar and A. Goldsmith, "Transmitter optimization and optimality of beamforming for multiple antenna systems," *IEEE Trans. Wireless Commun.*, vol. 3, no. 4, pp. 1165–1175, July 2004.

[39] ——, "Multi-antenna capacity in Rayleigh fading channels with covaraince information," *IEEE Trans. Wireless Commun.*, vol. 4, no. 3, pp. 990–997, May 2005.

[40] S. A. Jafar, S. Vishwanath, and A. Goldsmith, "Channel capacity and beamforming for multiple transmit and receive antennas with covariance feedback," in *Proc. IEEE Int. Conf. Commun.*, vol. 7, Helsinki, Finland, 2001, pp. 2266–2270.

[41] H. Jafarkhani, "A quasi-orthogonal space-time block code," *IEEE Trans. Commun.*, vol. 49, no. 1, pp. 1–4, Jan. 2001.

[42] W. C. Jakes, *Microwave Mobile Communications*. New York, NY: John Wiley and Sons, 1974.

[43] M. Joham, W. Utschick, and J. A. Nossek, "Linear transmit processing in MIMO communications systems," *IEEE Trans. Signal Processing*, vol. 53, no. 8, pp. 2700–2712, Aug. 2005.

[44] G. Jöngren, M. Skoglund, and B. Ottersten, "Combining bemforming and orthogonal space-time block coding," *IEEE Trans. Info. Theory*, vol. 48, no. 3, pp. 611–627, Mar. 2002.

[45] E. A. Jorswieck and H. Boche, "Transmission strategies for the MIMO MAC with MMSE receiver: average MSE optimization and achievable individual MSE region," *IEEE Trans. Signal Processing*, vol. 51, no. 11, pp. 2872–2881, Nov. 2003.

[46] S. M. Kay, *Fundamentals of Statistical Processing, Volume I: Estimation Theory*. Englewood Cliffs, NJ: Prentice Hall, 1993.

[47] A. Khachan and R. S. Adve, "Linear processing for the downlink in multiuser MIMO systems with multiple data streams," in *Proc. IEEE Int. Conf. Commun.*, Istanbul, Turkey, 2006, pp. 4113–4118.

[48] N. Khajehnouri and A. H. Sayed, "Distributed MMSE relay strategies for wireless sensor networks," *IEEE Trans. Signal Processing*, vol. 55, no. 7, pp. 3336–3348, July 2007.

[49] N. Khaled, G. Leus, C. Desset, and H. D. Man, "A robust joint linear precoder and decoder MMSE design for slowly time-varying MIMO channels," in *Proc. IEEE Int. Conf. Acoustic, Speech and Signal Processing*, vol. 4, 2004, pp. 485–488.

[50] N. Khaled, S. Thoen, and L. Deneire, “Optimizing the joint transmit and receive MMSE design using mode selection,” *IEEE Trans. Commun.*, vol. 53, no. 4, pp. 730–737, Apr. 2005.

[51] A. Klein, G. K. Kaleh, and P. W. Baier, “Zero forcing and minimum mean-square-error equalization for multiuser detection in code-division multiple-access channels,” *IEEE Trans. Veh. Technol.*, vol. 45, no. 2, pp. 276–287, May 1996.

[52] J. N. Laneman, D. N. C. Tse, and G. W. Wornell, “Cooperative diversity in wireless networks: efficient protocols and outage bahavior,” *IEEE Trans. Info. Theory*, vol. 50, no. 12, pp. 3062–3080, Dec. 2004.

[53] E. G. Larsson and P. Stoica, *Space-Time Block Coding for Wireless Communications*. Cambridge University Press, 2003.

[54] V. Lau, Y. Liu, and T.-A. Chen, “The role of transmit diversity on wireless communications—reverse link analysis with partial feedback,” *IEEE Trans. Commun.*, vol. 50, no. 12, pp. 2082–2090, Dec. 2002.

[55] ——, “On the design of MIMO block-fading channels with feedback-link capacity constraint,” *IEEE Trans. Commun.*, vol. 52, no. 1, pp. 62–69, Jan. 2004.

[56] T. Lo, “Maximal ratio transmission,” *IEEE Trans. Commun.*, vol. 47, no. 10, pp. 1458–1461, Oct. 1999.

[57] D. Love, R. Heath, W. Santipach, and M. Honig, “What is the value of limited feedback for MIMO channels,” *IEEE Commun. Mag.*, vol. 42, no. 10, pp. 54–59, Oct. 2004.

[58] D. J. Love and R. W. Heath, "Limited feedback precoding for spatial multiplexing systems," in *Proc. IEEE Global Telecommun. Conf.*, vol. 4, San Francisco, CA, 2003, pp. 1857–1861.

[59] Z.-Q. Luo, T. N. Davidson, G. B. Giannakis, and K. M. Wong, "Transceiver optimization for block-based multiple access through ISI channels," *IEEE Trans. Signal Processing*, vol. 52, no. 4, pp. 1037–1052, Nov. 2004.

[60] H. Lutkepohl, *Handbook of Matrices*. New York, NY: John Wiley and Sons, 1996.

[61] T. L. Marzetta and B. M. Hochwald, "Capacity of a mobile multiple-antenna communication link in Rayleigh flat fading," *IEEE Trans. Info. Theory*, vol. 45, no. 1, pp. 139–157, Jan. 1999.

[62] M. Medard, "The effect upon channel capacity in wireless communications of perfect and imperfect knowledge of the channel," *IEEE Trans. Info. Theory*, vol. 46, no. 3, pp. 933–946, May 2000.

[63] R. A. Monzingo and T. W. Miller, *Introduction to Adaptive Arrays*. New York, NY: John Wiley and Sons, 1980.

[64] R. J. Muirhead, *Aspects of Multivariate Statistical Theory*. New York, NY: John Wiley and Sons, 1982.

[65] K. K. Mullavilli, A. Sabharwal, E. Erkip, and B. Aazhang, "On beamforming with finite rate feedback in multiple-antenna systems," *IEEE Trans. Info. Theory*, vol. 49, no. 10, pp. 2662–2679, Oct. 2003.

[66] L. Musavian, M. R. Nakhai, M. Dohler, and A. H. Aghvami, "Effect of channel uncertainty on the mutual information of MIMO fading channels," *IEEE Trans. Veh. Technol.*, vol. 56, no. 5, pp. 2798–2806, Sept. 2007.

[67] R. U. Nabar, H. Bolcskei, and F. W. Kneubuhler, "Fading relay channels: performance limits and space-time signal design," *IEEE J. Select. Areas Commun.*, vol. 22, no. 6, pp. 1099–1109, Aug. 2004.

[68] A. Narula, M. J. Lopez, M. D. Trott, and G. W. Wornell, "Efficient use of side information in multiple-antenna data transmission over fading channels," *IEEE J. Select. Areas Commun.*, vol. 16, no. 8, pp. 1423–1436, Oct. 1998.

[69] D. P. Palomar, "*A Unified Framework for Communications through MIMO Channels*," Ph.D. dissertation, Universitat Politècnica de Catalunya (UPC), Barcelona, Spain, 2003.

[70] D. P. Palomar, J. M. Cioffi, and M. A. Lagunas, "Joint Tx-Rx beamforming design for multicarrier MIMO channels: a unified framework for convex optimization," *IEEE Trans. Signal Processing*, vol. 51, no. 9, pp. 2381–2401, Sept. 2003.

[71] D. P. Palomar and S. Verdú, "Gradient of mutual information in linear vector Gaussian channels," *IEEE Trans. Info. Theory*, vol. 52, no. 1, pp. 141–154, Jan. 2006.

[72] A. Pascual-Iserte, D. P. Palomar, A. I. Pérez-Neira, and M. A. Lagunas, "A robust maximin approach for MIMO communications with imperfect channel state information based on convex optimization," *IEEE Trans. Signal Processing*, vol. 54, no. 1, pp. 346–360, Jan. 2006.

[73] M. Pätzold, U. Killat, and F. Laue, "A deterministic digital simulation model for Suzuki processes with application to a shadowed Rayleigh land mobile radio channel," *IEEE Trans. Veh. Technol.*, vol. 45, no. 2, pp. 318–331, May 1996.

[74] A. Paulraj, D. Gore, R. Nabar, and H. Bölcskel, "An overview of MIMO communications—a key to gigabit wireless," *Proc. IEEE*, vol. 92, no. 2, pp. 198–218, Feb. 2004.

[75] A. Paulraj, R. Nabar, and D. Gore, *Introduction to Space-Time Wireless Communications*. New York, NY: Cambridge University Press, 2003.

[76] C. B. Peel, B. M. Hochwald, and A. L. Swindlehurst, "A vector-perturbation technique for near-capacity multiantenna multiuser communication—Part I: channel inversion and regularization," *IEEE Trans. Commun.*, vol. 53, no. 1, pp. 195–202, Jan 2005.

[77] H. V. Poor, *Introduction to Signal Detection and Estimation*, 2nd ed. New York, NY: Springer-Verlag, 1994.

[78] J. G. Proakis, *Digital Communications*, 4th ed. New York, NY: McGraw-Hill, 2001.

[79] R. Rajagopalan, D. Reynolds, M. C. Valenti, and B. D. Woerner, "The impact of an antenna array in a relay network," in *Proc. IEEE Int. Conf. Commun.*, Glasgow, Scotland, 2007, pp. 4058–4063.

[80] G. G. Raleigh and J. M. Cioffi, "Spatio-temporal coding for wireless communications," *IEEE Trans. Commun.*, vol. 46, no. 3, pp. 357–366, Mar. 1998.

[81] T. S. Rappaport, *Wireless Communications: Principles and Practice*. Englewood Cliffs, NJ: Prentice Hall, 1996.

[82] F. Rashid-Farrokhi, K. Liu, and L. Tassiulas, "Transmit beamforming and power control for cellular wireless systems," *IEEE J. Select. Areas Commun.*, vol. 16, no. 8, pp. 1437–1450, Oct. 1998.

[83] F. Rashid-Farrokhi, L. Tassiulas, and K. Liu, "Joint optimal power control and beamforming in wireless network using antenna arrays," *IEEE Trans. Commun.*, vol. 46, no. 10, pp. 1313–1324, Oct. 1998.

[84] H. Sampath and A. Paulraj, "Linear precoding for space-time coded systems with known fading correlations," in *Proc. Asilomar Conf. on Signals, Systems and Computers*, Pacific Grove, CA, 2001, pp. 246–251.

[85] H. Sampath, P. Stoica, and A. Paulraj, "Generalized linear precoder and decoder design for MIMO channels using the weighted MMSE criterion," *IEEE Trans. Commun.*, vol. 49, no. 12, pp. 2198–2206, Dec. 2001.

[86] A. Scaglione, G. B. Giannakis, and S. Barbarossa, "Redundant filterbank precoders and equalizers—Part 1. Unification and optimal designs," *IEEE Trans. Signal Processing*, vol. 47, no. 7, pp. 1988–2006, July 1999.

[87] A. Scaglione, P. Stoica, S. Barbarossa, G. B. Giannakis, and H. Sampath, "Optimal designs for space-time linear precoders and equalizers," *IEEE Trans. Signal Processing*, vol. 50, no. 5, pp. 1051–1064, May 2002.

[88] M. Schubert and H. Boche, "Solution of the multiuser downlink beamforming problem with individual SINR constraint," *IEEE Trans. Veh. Technol.*, vol. 53, no. 1, pp. 18–28, Jan 2004.

[89] M. Schubert, S. Shi, E. A. Jorswieck, and H. Boche, "Downlink sum-MSE transceiver optimization for linear multi-user MIMO systems," in *Proc. Asilomar Conf. on Signals, Systems and Computers*, Pacific Grove, CA, 2005, pp. 1424–1428.

[90] A. Sendonaris, E. Erkip, and B. Aazhang, "User cooperative diversity—Part I: system description," *IEEE Trans. Commun.*, vol. 51, no. 11, pp. 1927–1938, Nov. 2003.

[91] S. Serbetli and A. Yener, “Transceiver optimization for multiuser MIMO systems,” *IEEE Trans. Signal Processing*, vol. 52, no. 1, pp. 214–226, Jan. 2004.

[92] ——, “MMSE transmitter design for correlated MIMO systems with imperfect channel estimates: power allocation trade-offs,” *IEEE Trans. Wireless Commun.*, vol. 5, no. 8, pp. 2295–2304, Aug. 2006.

[93] M. B. Shenouda and T. N. Davidson, “Statistically robust transceiver design for broadcast channels with uncertainty,” in *Proc. Canadian Conf. on Electrical and Computer Engineering*, 2007, pp. 320–323.

[94] S. Shi and M. Schubert, “MMSE transmit optimization for multi-user multi-antenna systems,” in *Proc. IEEE Int. Conf. Acoustic, Speech and Signal Processing*, vol. 3, 2005, pp. 409–412.

[95] D. Shiu, G. J. Foschini, M. J. Gans, and J. M. Kahn, “Fading correlation and its effect on the capacity of multielement antenna systems,” *IEEE Trans. Commun.*, vol. 48, no. 3, pp. 502–513, Mar. 2000.

[96] Q. H. Spencer, A. L. Swindlehurst, and M. Haardt, “Zero-forcing methods for downlink spatial multiplexing in multiuser MIMO channels,” *IEEE Trans. Signal Processing*, vol. 52, no. 2, pp. 461–471, Feb. 2004.

[97] J. F. Sturm, “Using SeDuMi 1.02, a MATLAB toolbox for optimization over symmetric cones,” *Optimization Methods and Software*, vol. 11-12, pp. 625–653, 1999.

[98] G. Taricco and E. Biglieri, “Space-time decoding with imperfect channel estimation,” *IEEE Trans. Wireless Commun.*, vol. 4, no. 4, pp. 1874–1888, July 2005.

[99] V. Tarokh, H. Jafarkhani, and A. R. Calderbank, "Space-time block codes from orthogonal designs," *IEEE Trans. Info. Theory*, vol. 45, no. 5, pp. 1456–1467, July 1999.

[100] ——, "Space-time block coding for wireless communications: performance results," *IEEE J. Select. Areas Commun.*, vol. 17, no. 3, pp. 451–459, Mar. 1999.

[101] V. Tarokh, N. Seshadri, and A. Calderbank, "Space-time codes for high data rate wireless communication: performance criterion and code construction," *IEEE Trans. Info. Theory*, vol. 44, no. 2, pp. 744–765, Mar. 1998.

[102] E. Telatar, "Capacity of multi-antenna Gaussian channels," *European Trans. Telecommun.*, vol. 10, no. 6, pp. 585–595, Nov./Dec. 1999.

[103] A. Tenenbaum and R. S. Adve, "Joint multiuser transmit-receive optimization using linear processing," in *Proc. IEEE Int. Conf. Commun.*, Paris, France, 2004, pp. 588–592.

[104] D. Tse and P. Viswanath, *Fundamentals of Wireless Communication*. Cambridge University Press, 2005.

[105] D. Tse, P. Viswanath, and L. Zheng, "Diversity-multiplexing tradeoff in multiple access channels," *IEEE Trans. Info. Theory*, vol. 50, no. 9, pp. 1859–1874, Sept. 2004.

[106] J.-J. van de Beek, O. Edfors, M. Sandell, S. K. Wilson, and P. O. Borjesson, "On channel estimation in OFDM systems," in *Proc. IEEE Veh. Technol. Conf.*, vol. 2, 1995, pp. 815–819.

[107] S. Vishwanath, N. Jindal, and A. Goldsmith, "Duality, achievable rates, and sum-rate capacity of Gaussian MIMO broadcast channels," *IEEE Trans. Info. Theory*, vol. 49, no. 10, pp. 2658–2668, Oct. 2003.

[108] E. Visotsky and U. Madhow, "Optimum beamforming using transmit antenna arrays," in *Proc. IEEE Veh. Technol. Conf.*, 1999, pp. 851–856.

[109] ——, "Space-time transmit precoding with imperfect feedback," *IEEE Trans. Info. Theory*, vol. 47, no. 6, pp. 2632–2639, Sept. 2001.

[110] P. Viswanath and D. Tse, "Sum capacity of the vector Gaussian broadcast channel and uplink–downlink duality," *IEEE Trans. Info. Theory*, vol. 49, no. 8, pp. 1912–1921, Aug. 2003.

[111] S. A. Vorobyov, A. B. Gershman, and Z.-Q. Luo, "Robust adaptive beamforming using worst-case performance optimization: a solution to the signal mismatch problem," *IEEE Trans. Signal Processing*, vol. 51, no. 2, pp. 313–324, Feb. 2003.

[112] S. A. Vorobyov, A. B. Gershman, and Y. Rong, "On the relationship between the worst-case optimization-based and probability-constrained approaches to robust adaptive beamforming," in *Proc. IEEE Int. Conf. Acoustic, Speech and Signal Processing*, vol. 2, Honolulu, Hawaii, 2007, pp. 977–980.

[113] N. Wang, "*Transmit Optimization for Multicarrier and Multiple-Input Multiple-Output Wireless Communications*," Ph.D. dissertation, Dept. of Electrical and Computer Engineering, Queen's University, 2005.

[114] T. Weber, A. Sklavos, and M. Meurer, "Imperfect channel state information in MIMO transmission," *IEEE Trans. Commun.*, vol. 54, no. 3, pp. 543–552, Mar. 2006.

[115] H. Weingarten, Y. Steinberg, and S. Shamai, "The capacity region of the Gaussian multiple-input multiple-output broadcast channel," *IEEE Trans. Info. Theory*, vol. 52, no. 9, pp. 3936–3964, Sept. 2006.

[116] A. Wittneben, "Basestation modulation diversity for digital SIMULCAST," in *Proc. IEEE Veh. Technol. Conf.*, St. Louis, Missouri, 1991, pp. 848–853.

[117] P. W. Wolniansky, G. J. Foschini, G. D. Golden, and R. A. Valenzuela, "V-BLAST: an architecture for realizing very high data rates over the rich-scattering wireless channel," in *Proc. URSI Int. Symposium on Signals, Systems, and Electronics*, Pisa, Italy, 1998, pp. 295–300.

[118] P. Xia and G. B. Giannakis, "Design and analysis of transmit beamforming based on limited-rate feedback," in *Proc. IEEE Veh. Technol. Conf. (fall)*, Los Angeles, California, 2004, pp. 1653–1657.

[119] Z. Yan, K. M. Wong, and Z.-Q. Luo, "Optimal diagonal precoder for multiantenna communication systems," *IEEE Trans. Signal Processing*, vol. 53, no. 6, pp. 2089–2100, June 2005.

[120] J. Yang and S. Roy, "On joint transmitter and receiver optimization for multiple-input-multiple-output (MIMO) transmission systems," *IEEE Trans. Commun.*, vol. 42, no. 12, pp. 3221–3231, Dec. 1994.

[121] T. Yoo and A. Goldsmith, "Capacity and power allocation for fading MIMO channels with channel estimation error," *IEEE Trans. Info. Theory*, vol. 52, no. 5, pp. 2203–2214, May 2006.

[122] T. Yoo, E. Yoon, and A. Goldsmith, "MIMO capacity with channel uncertainty: Does feedback help?" in *Proc. IEEE Global Telecommun. Conf.*, vol. 1, Dallas, Texas, 2004, pp. 96–100.

[123] W. Yu and J. M. Cioffi, "Trellis precoding for the broadcast channel," in *Proc. IEEE Global Telecommun. Conf.*, 2001, pp. 1344–1348.

[124] ——, "Iterative water-filling for Gaussian vector multiple-access channels," *IEEE Trans. Info. Theory*, vol. 50, no. 1, pp. 145–152, Jan. 2004.

[125] J. Zhang, Y. Wu, S. Zhou, and J. Wang, "Joint linear transmitter and receiver design for the downlink of multiuser MIMO systems," *IEEE Commun. Letters*, vol. 9, no. 11, pp. 991–993, Nov. 2005.

[126] X. Zhang, D. P. Palomar, and B. Ottersten, "Robust design of linear MIMO transceiver for low SNR," in *Proc. Asilomar Conf. on Signals, Systems and Computers*, Pacific Grove, CA, 2005, pp. 398–402.

[127] ——, "Robust design of linear MIMO transceiver under channel uncertainty," in *Proc. IEEE Int. Conf. Acoustic, Speech and Signal Processing*, vol. 4, 2006, pp. 77–80.

[128] ——, "Statistically robust design of linear MIMO transceivers," *IEEE Trans. Signal Processing*, in press. [Online]. Available: http://www.ece.ust.hk/~palomar/publications.html

[129] L. Zheng and D. Tse, "Diversity and multiplexing: a fundamental tradeoff in multiple antenna channels," *IEEE Trans. Info. Theory*, vol. 49, no. 5, pp. 1073–1096, May 2003.

[130] S. Zhou and G. B. Giannakis, "Optimal transmitter eigen-beamforming and space-time block coding based on channel mean feedback," *IEEE Trans. Signal Processing*, vol. 50, no. 10, pp. 2599–2613, Oct. 2002.

[131] ——, "Optimal transmitter eigen-beamforming and space-time block coding based on channel correlations," *IEEE Trans. Info. Theory*, vol. 49, no. 7, pp. 1673–1690, July 2003.

[132] ——, "How accurate channel prediction needs to be for transmit-beamforming with adaptive modulation over Rayleigh MIMO channels?" *IEEE Trans. Wireless Commun.*, vol. 3, no. 4, pp. 1285–1294, July 2004.